A SYSTEMS APPROACH TO RENAL DIALYSIS

Ranjeet Jashan Uttamsingh

Thesis submitted for the degree of Doctor of Philosophy

The City University

Department of Systems Science

February 1981

TABLE OF CONTENTS.

Acknowledgements.

I am grateful to Dr. Ewart Carson, whose advice and encouragement played a vital role in this research programme. The computing facilities at the Royal College Of Surgeons Of England, which were made available to me by Dr. John Bushman, proved to be very useful during the execution of this research. I wish to thank Dr. D. Thompson for the medical information and clinical data used in this work. I also wish to thank Professor L. Finklestein for his helpful guidance. I am grateful for the financial support recieved from the Science Research Council. And finally, this work would not have been possible without the encouragement and painstaking devotion of my wife.

ABSTRACT.

The objective of this research programme is the development of a comprehensive mathematical model of the patient - artificial kidney machine system consisting of several interconnected sub-systems of the human organism. The model is based on current general physiological knowledge, but can be tailored to simulate individual patients by adjusting model parameters. Model parameters for individual patients may be obtained by using a parameter identification technique and available past data of the patient. The model is designed to be used in an interactive mode by the renal clinician. Using the model as a predictive instrument, the clinician would be aided in the selection of optimal therapeutic procedures for individual patients.

The model can also be used to represent the renal - body fluid system of a normal, healthy human. As such, it may be used as a vehicle with which to test hypotheses concerning the functioning of the complex and poorly understood control mechanisms of this system.

Validation of the model was performed using pattern recognition feature comparison and classical least squares techniques.

CHAPTER 1

INTRODUCTION.

The benefits which accrue from the application of systems engineering to the fields of medicine and health care are beginning to be recognised. The exchange of ideas between engineers and clinicians over the past decade or so has resulted in considerable advances in medical instrumentation and in the use of artificial limbs and organs. The application of computers in hospitals as an information storage and retrieval system is now commercially available on a turn-key basis. However, the usefulness of the application of the tools and methods at the disposal of the systems engineer to further physiological knowledge and to aid in patient management is still to be fully accepted.

One of the principal tools used by the biomedical systems engineer in health care is the mathematical model. The first step in developing a mathematical model is to form the functional description of the system of interest in systems' notation. This, in itself, is of great value to the physiologist, since the mechanisms of the overall system are easier to comprehend when described in this fashion rather than in the verbal form of description traditionally used by physiologist.

Areas of weak knowledge in the physiology of the system are then highlighted when the mathematical description of the system is derived from the functional model. These areas may be filled in one of two ways. The first is to attempt to determine the unknown relationships by direct measurement on the system. Although the uncertain relationships sometimes can be inferred from measurements of related variables, or derived from experiments on laboratory animals, the accuracy and even the possibility of determining the relationships depends, largely, on the availability of suitable instrumentation.

The second method entails using the mathematical model as a vehicle for testing hypotheses. Candidate mathematical hypotheses are inserted in the model for the uncertain

relationships until the variables of the model behave in a manner, similar to those of the real system under the same conditions. When the model mimics the aspects of the behaviour of the real system with the accuracy necessary to accomplish the purposes of model-building, then the model is said to be valid. Since this process depends on the elimination of a certain number of hypotheses, a resulting valid model may not be unique; that is, more than one of the candidate hypotheses could result in the model being observed as valid. It is also possible that the set of candidate hypotheses may be exhausted without a single being able to satisfy the conditions of validity set for the model.

In spite of the above limitations, the effect that mathematical modelling of biological systems has had on the advancement of knowledge in various areas in the field of human physiology may be found in the following references:- Guyton (1971), Kitney (1974), Blesser (1969), Cooney (1976).

An obvious advantage of this form of research is that the results of different internal or external environments (therapies, for instance) can be tested on a valid mathematical model as opposed to on the actual system or on animal models. Examples of this are the testing of the effects of drugs on the cardiovascular system (Pullen, 1976), optimizing dialysis therapy (Frost and Kerr, 1977) and the study of the effects of pesticides on plant growth.

A further potential benefit is that by rigorous mathematical analysis of the most complex piece of machinery known to man - man, himself - the structure of biological controllers may be determined and adapted for technological uses. If, for instance, the structure of the internal temperature homeostatis mechanism of the human body could be determined and adapted for use in industry, advantages such as better behaved large scale chemical reactions might be forthcoming.

The original purpose of biological systems modelling was to aid in the advancement of knowledge of human physiology by the methods suggested above. The models produced for this purpose were generally of a single organ or metabolic system. These were as isomorphic with the system being modelled as permitted by the extent of the knowledge of the relevant

physiology, and by the available computer facilities at that time. Although the benefits of this form of modelling were considerable, they did not have any immediate impact upon the vast majority of the medical profession whose assistance for the purpose of supplying data is invaluable . For this reason, biological modelling came under criticism of having little more purpose than that of occupying the time of otherwise bored mathematicians.

The modeller, armed with ever-improving computer facilities, responded to this crtiticism by producing models of medical situations designed, for instance, to aid the clinicians in the decision making process in patient management. These models, often incorporating models of several of the subsystems of the human organism, did not have to provide a comprehensive description of the actual physiological mechanisms being modelled; instead the accuracy of response was of prime importance. Hence, empirical or 'black-box' modelling techniques came into use.

The work described here, however, attempts to utilize current knowledge as far as is practical to arrive at a structural model of the patient-artificial kidney machine system. The aim is that the model should be used in a renal unit by the clinician in order that he may be aided in the selection of parameters for the dialysis therapy so that the patient may be maintained in an optimal state.

The need for this work arose due to the observations by the clinician that an alarming number of dialysis patients complained of feeling worse after dialysis than before. Specifically, some patients suffered from nausea and vomiting during and just after dialysis, and occasionally the blood pressure of patients deviated from normal to such an extent that it would have been dangerous not to terminate dialysis prematurely. The causes for these conditions are unknown at present, although it has been suggested that perhaps the feeling of nausea is due to the disequilibriation syndrome (Abbrecht and Prodany, 1971), when the intracellular concentration of urea does not fall as rapidly as the extracellular concentration, and that the circulatory problems arise because of a similar effect on body potassium, which, in

turn, affects the pumping ability of the heart. Due to the limitations of instrumentation , it is not possible to test these or similar hypotheses by direct measurement. However, relevant data are readily available from a valid mathematical model for the purpose of such testing.

It has been casually observed (Thompson, 1976) that the above mentioned problems which occur during dialysis are generally accompanied by deviation in the core and surface temperatures of the patient. Statistical analysis of the data generated by the model suitably linked to a thermo-regulatory model would confirm that the temperature deviations are expected in these conditions, and investigation of the structure of the model may reveal the reasons for this phenomenon. This may throw more light on the reasons for the occurrance of the complications during dialysis. Also, it may be possible that by monitoring the temperature of the patient, early warning of circulatory problems may be obtained, provided that the deviation in temperature is not a direct result of the change in blood flow patterns.

In the majority of cases, there is little pre-dialysis monitoring of patients due to measurement difficulties. During the course of dialysis, blood pressure and pulse rate are generally the only variables monitored. Hence the dialysis therapy selected may not be optimal as far as the end-state of the patient is concerned. In addition, since there is a drastic shortage of renal units and their resources, compared with the need for this service, minimization of time on dialysis for each patient is extremely desirable.

The objectives of the work described in this thesis are hence as follows:-

(1) To produce and validate a comprehensive, strutural model of the patient-artificial kidney machine system, including as many of the subsystems of the human body whose variables are of interest to the clinician.

(2) To adapt the above model so that it may be used in the renal unit to predict continuously with time the future (during dialysis and post-dialysis) states of

the patient, given the present (pre-dialysis) state and proposed therapy so that the clinician, by repeating this procedure for different therapies, may be aided in the selection of the therapy that would produce an optimal end-state for the patient. The model should also be capable of predicting the state of the patient for up to several days after dialysis so that the clinician may obtain an indication of any complications that might occur in between dialyses when the patient may be away from clinical supervision, and also an indication as to when the next dialysis should be performed.

(3) To utilize the model, adapted to represent the subsystems with normal renal functions, as an instrument with which to test current hypotheses concerning the renal-body fluid regulating system.

(4) To statistically analyse the data generated by the model linked to a thermoregulatory system model in order to establish the dependance, if any, of the temperature variables to the patients condition during dialysis. This may give more information on the causes of the abnormal conditions seen to occur during dialysis.

Apart from the benefits to patient management and medical science mentioned previously, this work has several contributions to make to systems science:-

(1) The model developed for this work consists of models of several subsystems linked by their common variables. Previous biological models have been developed mainly to represent a single subsystem of the human organism.

(2) Although biological system models for the purpose of patient management have been developed in recent years, these are generally of a rather empirical nature. This work shows that a structural model may be applied successfully in the health care situation, having the advantage that the unmeasureable

system variables of interest may be obtained from the model.

(3) The lack of any formalised approach to the problem of validation of biological models has resulted in many models being presented without sufficient validation. Several validation techniques, including a feature comparison technique were used on the model presented here, so that the effectiveness, advantages and disadvantages of the different techniques may be compared.

The description, in systems terminology of the health care process to be modelled is presented in Chapter 2. The functions of the normal kidneys are outlined first. This is followed by a description of the abnormal states which arise from renal failure; and finally the dialysis process is explained.

A review of past work on the modelling of relevant biological systems is presented in Chapter 3. Since the model produced in this work consists of several sub-models, past work on each of the subsystems incorporated is examined in turn. Chapter 3 concludes with a review of past models with an emphasis on dialysis patient management

The detailed description of the mathematical model is presented in Chapter 4.

Relevant experiments on humans are simulated using modifications of the basic model, and the results are presented in Chapter 5. The capabilities and limitations of the model, as well as results using the hypothesis testing facility of the model are also discussed here.

The results of tests of the validity of the model of the patient-artificial kidney machine are presented in Chapter 6. A feature comparison technique is used in order to utilize available measurement data gathered during the dialysis of patients in a renal unit.

For improved predictive performance, certain parameters of the model need to be 'tuned' so that the individual patient is represented more accurately by the model. A description of the application of a parameter estimation routine for this purpose, and the improvement in simulation

accuracy thus obtained, is presented in Chapter 7.

A description of how the model may be used interactively in the renal unit to aid in optimal therapy selection is presented in Chapter 8.

Chapter 9 concludes the thesis and discusses the lines along which further research could progress to further benefit the dialysis patient.

CHAPTER 2

MEDICAL PROCESS TO BE MODELLED.

The first stage in the development of a mathematical model of a complex system is the formulation of a functional description of the system. In addition, it is necessary for this functional description to be relevant to the objectives underlying the model formulation process. Therefore, a description of the current concepts of the physiology of the renal - body fluid system and the related functional model, in the form of block diagrams, are presented in this chapter. The first section of this chapter presents an overall description of the renal - body fluid system; and the second section examines certain components of this system in greater detail. Section 2.3 briefly describes the causes and effects of renal failure, and the final section describes the process of renal haemodialysis, which is used to compensate for the lost kidney function, and thus, sustain the life of the patient suffering from renal failure. The material presented in this chapter, thus forms the basis for the formulation of a major portion of the mathematical model, described in Chapter 4.

2.1. Overall Description Of The Renal - Body Fluid System.

The primary role of the kidneys is the excretion of waste materials generated in the body. This function is accomplished in the following manner. First, a large volume of blood (approximately 1500 litres per day)* is filtered in the kidneys, such that approximately one ninth of this volume is forced across the two million glomerular filtration membranes into their associated tubules. (Figure 2.1 depicts a functional diagram of a nephron). The chemical composition of the glomerular filtrate is very similar to that of plasma, except that the

* All quantities quoted in this chapter are average values for a normal 70 kg. male, cited from Cooney (1976), Guyton (1971) and Maude (1977).

concentration of protein in the filtrate is negligible. The glomerular filtrate therefore, contains the waste products to be excreted and, in addition, large quantities of vital substances such as water, electrolytes, amino acids and glucose. It is then the function of the tubules to cause the reabsorption, back into the bloodstream, of these vital substances to the extent required for the correct functioning of the body. The remaining fluid, containing the wastes, is then collected in the bladder and is periodically released from the body as urine at a rate of approximately 1.3 litres per day.

Quantitatively, the most important substances of the tubular reabsorbate are water and sodium salts. Hence the secondary, but nevertheless extremely important task of the kidneys is the regulation of the volume and composition of the body fluids.

The functions of the kidneys, in relation to the other organs of the body, are made apparent by considering the majot body fluid compartments and their important influx and efflux pathways, as shown in Figure 2.2.

The two channels representing influxes to the body are ingestion via the gastrointestinal tract (2.3 litres of water and 7.0 grammes of NaCl per day) and the metabolic generation of wastes and water (30 grammes of urea, 0.6 grammes of creatinine, and 0.3 litres of water per day).

The plasma (3.2 litres in volume), circulating throughout the body, acts as a medium for the transport of substances from the influx to the efflux channels. In addition, filtration of protein - free plasma across the capillary membranes provides a two way exchange of substances with the largely stationary interstitial fluid compartment (8.4 litres in volume). Although the one way fluxes are very large, the nett two way fluxes of water and electrolytes in the steady state are zero. The plasma and interstitial fluid compartments, together with other minor fluid compartments comprise the extracellular fluid compartment (15 litres in volume). Extremely rapid two way exchange of water and slight exchange of electrolytes by diffusion and active transport take place across the cell walls between the interstitial compartment and intracellular compartment (25 litres in volume approximately). But in the steady state, the nett

movement of water and electrolytes is zero.

The waste products are generated as a result of metabolism in the cells. Hence diffusion of these substances occurs from the intracellular, through the interstitial, to the plasma compartment, from where they are removed by the kidneys (or in the case of a patient with kidney failure, by the artificial kidney machine). Along with these wastes, the kidneys (artificial kidney machine) cause the excretion of water (normally 1.3 litres per day) and electrolytes (normally 6.2 grammes of NaCl per day). There is also some loss of water via the respiratory tract, and some loss of water and electrolytes through the faeces and the skin (sum of non-renal losses is 1.3 litres of water and 0.8 grammes of NaCl per day).

In the steady state, in addition to the three major fluid compartments being in dynamic equilibrium, the total influx of any substance is equal to the total efflux from the body. However, any change in influx or non-renal change in efflux from the body constitutes a disturbance to the system. Apart from a change in the metabolic rate, all other influxes and effluxes will immediately affect the plasma compartment. The rapid rate of transport of substances between the three compartments, however, brings about a large degree of compensation to the effects of the disturbance almost immediately. However, the renal efflux is internally adjusted, so that the kidneys are the ultimate controllers of the volumes and composition of the body fluid compartments.

2.2. Normal Functions Of The Renal System.

Figure 2.3 presents a simplified schematic diagram of the internal variables affecting renal efflux. The variables, apart from the renin-angiotensin-aldosterone feedback system, are seen to originate from the cardiovascular system, although some are affected via the neuroendocrine systems of the body.

Basically, the cardiovascular system consists of the heart in a closed circuit of blood vassels and capillaries. The heart mechanically pumps the blood, containing fluid and nutrients absorbed from the gastrointestinal system, to the various tissues and organs of the body, including the neuroendocrine and renal

systems. The variables of the cardiovascular system, shown as outputs in Figure 2.3, are renal blood flow, RBF, blood volume, BV, and blood osmolality, $[Os]_p$.

The neuroendocrine system, consisting of the hypothalamus-pituitary system and the adrenal gland, monitors the blood volume and osmolality, and also the plasma level of angiotensin II, $[Ang]_p$, which is an output of the renin-angiotensin system. Changes in blood volume or osmolality alter the rate of release of antidiuretic hormone (ADH) and hence its plasma concentration, $[ADH]_p$; and changes in the plasma level of angiotensin II alter the rates of synthesis and release of aldosterone from the adrenal cortex, and hence its plasma concentration, $[Ald]_p$.

The rate of excretion of water, electrolytes and metabolic waste are determined primarily by the renal blood flow rate; however, the rates of excretion of water and electrolytes are modified by the effects of the concentration of ADH and aldosterone respectively.

A deeper understanding of the regulatory function of the kidneys may be obtained by considering in detail the mechanisms involved in (a) the renal system, and (b) the neuroendocrine system.

2.2.1. The Renal System.

The functional diagram of Figure 2.4 represents the mechanisms of the renal system. The upper portion depicts the four major components of the nephron.

The variables seen as outputs from the cardiovascular system are mean arterial pressure, P_{AS}, and renal blood flow, RBF. The rate of renal blood flow is maintained at a relatively constant value by the renal vascular resistance.

There is a pressure drop across the renal vasculature, and hence, the pressure forcing fluid across the glomerular capillary membranes, P_f, is the difference between the resulting pressure in the glomerular capillaries, π_g, and the pressure outside the glomerular capillaries in the Bowman's capsule, P_B. The rate of fluid filtration, GFR, is proportional to the nett filtration pressure, P_f.

In the proximal tubule, approximately three quarters of the filtered sodium, and a corresponding volume of water, are iso-osmotically reabsorbed. The phenomenon that a constant fraction of the filtered load of sodium is actively reabsorbed in the proximal tubule for a wide range of values of glomerular filtration rate, is known as the glomerular-tubular balance. However, it has been shown that the glomerular-tubular balance is upset by certain factors (De Wardener, 1973), the most important for fluid balance being changes in the concentration of sodium in the intraluminal fluid.

The fluid emerging from the proximal tubule, V_{PT}, with osmolality, $[Os]_{PT}$, enters the loop of Henle, where a similar effect is responsible for the control of the ratio of sodium chloride reabsorbed in this section of the nephron. In addition, the filtrate volume and osmolality undergo considerable modification, within the loop of Henle, consistent with the operation of the countercurrent multiplication process (Guyton, 1971). Changes in the final sodium concentration or load in the filtrate, as it emerges from the loop of Henle, NA_{MD}, are monitored by the macula densa cells of the juxtaglomerular apparatus. It is believed that these cells are responsible for the negative feedback control of glomerular filtration rate (Thurau et al. 1967). The theories are discussed in a later section in this chapter.

The filtrate emerging from the loop of Henle, with volume, V_{LH}, and osmolality, $[Os]_{LH}$, undergoes its final changes in volume and composition in the distal tubules and collecting ducts by the effects of the levels of ADH and alsodterone in the circulating interstitium. Increases in the levels of ADH and aldosterone promote increases in the reabsorption of water and sodium respectively. The mechanisms are outlined in the relevant sections in this chapter.

The final filtrate emerging from the collecting ducts, with volume, V_U, and osmolality, $[Os]_U$, is stored in the bladder for periodical excretion as urine; whereas the substances reabsorbed by the tubules are returned to the renal venous blood stream. In this manner, control of the volume and composition of the blood, and indirectly, the interstitial and intracellular fluid compartments is established. The major controlling factors are seen to be the arterial pressure, which is dependant on circulating blood

volume, and ADH and aldosterone levels. Other important factors are described in Chapter 4.

2.2.2. The Neuroendocrine System.

The two major neuroendocrine systems affecting renal function, and hence control of the volume and osmolality of the body fluids, are (i) the antidiuretic hormone (ADH) system, and (ii) the renin-angiotensin-aldosterone (RAA) system. The ADH system influences the rate of water excretion by the kidneys, and hence it affects firstly, the osmolality, and secondly, the volume of the extracellular fluid compartment. Aldosterone influences the rate of sodium excretion by the kidneys, and hence controls the fluid volumes of the body.

However, since a disturbance in fluid volume will affect fluid osmolality and a disturbance in fluid osmolality will cause an ADH - induced effect on fluid volume, the question arises as to how the volume and the osmolality controlling mechanisms interact to bring the fluid systems back to the normal steady state.

(i) The ADH System.

A detailed account of the mechanisms involved in the ADH system may be found in the reviews by Handler and Orloff (1973), Moses and Miller (1974) and Share (1974). The salient features are described below and in Figure 2.5.

Changes in the plasma level of ADH are dependant on the balance between its secretion rate and the rate of its removal from the blood by the liver and kidneys. The secretion rate appears to be largely dependant on blood osmolality and volume.

The major role of ADH is to adjust the water permeability of the cells of the distal and collecting tubular membranes, such that an increase in the level of ADH will lead to an increase, and a decrease will cause a decrease, in the rate of water reabsorption through the membranes of these tubules. In this manner, the osmolality and volume of the fluid leaving the body, and hence, of the body fluids themselves are regulated.

The osmoreceptor theory of ADH secretion, first proposed by Verney (1947), suggests that changes in plasma osmolality, $[Os]_p$, are monitored by osmoreceptors in the supraoptic nucleus of the hypothalamus, which, on an increase in osmolality would increase the frequency of neural discharge, f_o. This would lead to increases in the rates of synthesis and release of ADH from the hypothalamus-pituitary system into the blood, and hence to an increase in its plasma concentration. A decrease in osmolality, however, would lead to the converse effects - a fall in the rate of release and, hence, concentration of ADH.

Volume or stretch receptors for the control of ADH release rate have been located at three sites in the vascular system. Receptors in the left atrium, also known as low-pressure venous vascular bed receptors, measure the distention of the left atrium. Receptors located in the carotid sinus and in the aortic arch monitor the arterial pressure. The receptors at these two sites are also known as the high-pressure arterial vascular bed receptors.

Experiments conducted by Johnson and associates (1969), give evidence to support the theory that receptors in the left atrium monitor the volume of blood, BV, returning to the left ventricle, and for an increase in left atrial pressure (caused by an increase in blood volume), there is an increase in the frequency of impulses in the vagal afferents, f_v, to the hypothalamic centres. There is considerable evidence (Gauer et al., 1970) that the vagal impulses inhibit the synthesis and release of ADH, hence lower its plasma concentration and so reduce the fluid volume by reducing the rate of water reabsorption from the distal and collecting tubules of the kidneys. A decrease in left atrial pressure would give rise to the opposite effects.

The carotid sinus and aortic baroreceptors monitor changes in arterial pressure, P_{AS}, such that an increase in arterial pressure stimulates these receptors to increase their rate of firing impulses, f_b. The impulses then enter the vasomotor centre where they inhibit sympathetic, and stimulate parasympathetic, outflow, f_s, to (among other sites) the kidneys and the hypothalamic-pituitary system. The reduced sympathetic stimulation causes a fall in the renal vascular resistance, and therefore, an increase in glomerular filtration rate; it also causes the

inhibition of the release of ADH from the hypothalamus, which leads to increased fluid excretion and hence a reduction in body fluid volume, and thus also in arterial pressure. Converse effects would occur with a fall in arterial pressure.

The left atrial stretch receptors, rather than the carotid and aortic baroreceptors, appear to be the more important first line of defence against a change in blood volume. Changes in blood volume in excess of ten per cent will cause a change in arterial pressure and hence activate the baroreceptors, whereas smaller changes in blood volume will alter the distention of the left atrium. However, following the experiments of Johnson and associates (1970), the conclusion was reached that the stimuli to release ADH, caused by a change in fluid volume and by a change in fluid osmolality are additive. The relative potency of each of the stimuli are examined in more detail in the development of the model presented in Chapter 4.

(ii) The Renin-Angiotensin-Aldosterone System.

The volume of the extracellular fluid compartment, and hence the blood compartment, is dependant on the total sodium in the extracellular compartment. Normally, only the efflux of sodium is subject to internal variation by the kidneys, and an important factor influencing changes in the rate of efflux of sodium is the renin-angiotensin-aldosterone system, via the effects of aldosterone on the distal and collecting tubules of the nephron. An outline of the components and mechanisms involved in this system is presented here, but a more detailed account may be found in the review by Laragh and Sealey (1973).

Renin is an enzyme produced primarily by the granular cells of the juxtaglomerular apparatus of the kidneys in response to a variety of stimuli. These include a reduction in renal perfusion pressure, a reduction in sodium load at the mascula densa cells and an increase in the sodium concentration at the mascula densa cells of the juxtaglomerular apparatus.

Based on the findings of experiments by Tobian and associates (1959), the intrarenal vascular receptor theory for renin release was proposed. This theory suggests that the granular cells of the juxtaglomerular apparatus, located in the media of the afferent arteriole, are sensitive to changes in stretch in the wall of

this vessel. The degree of stretch is dependant on the renal perfusion pressure, which, in turn, is related to the systemic arterial pressure. Thus, any factor which decreases the renal perfusion pressure tends to reduce the stretch of the afferent arteriole and increase the granularity of the cells, and thereby increase the rate of renin release. An increase in renal perfusion pressure would give rise to the opposite effects. There exists much experimental evidence in support of this theory (Lee, 1969; Blaine et al.,1971), although the exact mechanisms and quantitative relationships between the variables are still to be determined.

Goormaghtigh (1945) first proposed that the macula densa cells of the juxtaglomerular apparatus were involved in a negative feedback loop controlling glomerular filtration rate. The experiments of Vander and Miller (1964) led to the proposal of the macula densa sodium load theory for renin release. This theory states that an increase in sodium load at the macula densa cells inhibits sodium sensitive tubular receptors, thereby decreasing the rate of renin release from the juxtaglomerular cells. However, much controversy exists over this theory, since experiments such as those of Lee (1969) have shown that administration of natriuretic agents in man and dog, which presumably cause an elevation of the tubular sodium load at the macula densa cells, cause an increase, and not a derease, in plasma renin levels. To resolve this apparent discrepancy, Vander and Luciano (1967), through their experimental results, suggested there was more than one mechanism involved in the control of the release of renin in these experiments. However, the controversy over the validity of this theory still exists.

Another theory, the macula densa intraluminal sodium concentration theory proposed by Thurau and associates (1967), has received wider acceptance. The theory suggests that it is the concentration of sodium at the macula densa cells which stimulates the granular cells to increase the release rate of renin into the afferent arteriolar blood. This renin is converted into angiotensin II, a vasopressor substance, which causes the constriction of the afferent arteriole, thereby reducing the glomerular filtration rate. This in turn reduces the sodium load and concentrations reaching the macula densa cells and thereby closes the

feedback loop. There exists much evidence in support of this theory (Meyer et al., 1968; Cooke et al., 1970; Thurau et al., 1972), but it is contested by Vander and Carlson (1969).

To summarize, the three theories regarding the intrarenal control of the release of renin have been outlined above. The mechanisms involved in each of these theories are not clearly understood, but, as shown in Figure 2.6, the stretch of the afferent arteriole and sodium sensitive macula densa cells have been implicated as receptors to control the granulation and thereby the rate of release of renin from the granular cells of the juxtaglomerular apparatus. The release of renin appears to be controlled by other factors as well, possibly mediated via the mechanisms suggested above. These factors include posture (Gordon et al., 1967), the dynamics of sodium (Nash et al., 1968) and potassium (Vander, 1970), sympathetic simulation (Taquini et al.,1964), ADH and angiotensin levels (Shade et al., 1973).

The plasma renin level is determined by the dynamic balance between its rate of release into, and rate of inactivation from, the circulation. Experiments (Heacox et al., 1967) have shown that the liver is the major site for renin inactivation, and that the clearance rate of renin is a function of hepatic blood flow.

It appears that renin has only one physiological effect - to liberate angiotensin I from renin substrate (Skeggs et al., 1964). Conclusions from a study by Sealey and associates (1972) suggest that the substrate concentration in human plasma is far in excess of that needed to maintain a normal plasma level of angiotensin II, and hence renin substrate is not a rate limiting factor in the renin-angiotensin system.

Angiotensin I is split by enzymes found mainly in the lungs and kidneys to yield angiotensin II, a pressor substance (Ng and Vane, 1968). It has been shown that the plasma concentration of angiotensin II is directly related to the plasma level of renin, and inversely related to the degree of sodium depletion (Gocke et al.,1969), and that it is rapidly removed from the circulation by angiotensinase in the liver and kidneys (Ng and Vane, 1968; Biron et al ., 1968). Angiotensin II has two major physiological effects: firstly, it causes vasoconstriction of the arterioles in the circulation; and secondly it acts on the adrenal cortex causing an increase in the rate of secretion of aldosterone.

The rate of aldosterone secretion is also affected by the states of sodium and potassium balances, such that chronic sodium loading or potassium depletion inhibits, and chronic sodium depletion or potassium loading enhances, the secretion of aldosterone (Müller, 1971). The roles of aldosterone are to control the secretion of potassium electrolytes, and the reabsorption of a small fraction (2 - 3%) of the filtered load of sodium remaining in the distal and collecting tubules of the nephrons.

These concepts are summarized in the diagram of Figure 2.7. In addition, we may consider how the renin-angiotensin-aldosterone system affects feedback control on variables which determine the volumes of the two major fluid compartments. Since sodium is the major electrolyte in extracellular fluid, and potassium is the major electrolyte in intracellular fluid, the volumes of the extracellular and intracellular compartments are largely determined by the total body sodium and potassium, respectively. The rate of renin release is stimulated primarily by, firstly, a fall in arterial pressure, brought about, possibly, by a drop in extracellular fluid volume, and secondly, a rise in total body sodium via increased sodium concentration at the macula densa cells of the juxtaglomerular apparatus. The rate at which angiotensin II is produced in the plasma compartment is primarily dependant on the plasma renin level. Elevation of the level of angiotensin II, $[Ang]_p$, increases firstly, the vasoconstriction of circulatory arterioles, thereby returning the arterial pressure towards its normal level, secondly, the renal vascular resistance, and hence lowers glomerular filtration rate which probably removes the stimulus to the sodium - sensitive tubular receptors to release renin, and thirdly, the production rate of aldosterone. The rate of aldosterone production is also increased by hyperkalemia and low plasma sodium concentration. High levels of aldosterone, $[Ald]_p$, promote firstly, tubular secretion and urinary excretion of potassium electrolytes, thereby reducing the body potassium content and controlling the intracellular fluid volume, and secondly, tubular reabsorption of sodium electrolytes, thereby increasing extracellular fluid volume and hence arterial pressure.

Based on the physiological and functional concepts above, a brief description of how various classes of renal disease

affect the normal functions of the kidneys is presented in the next section. There then follows a section describing dialysis therapy which is used to combat the effects of renal failure.

2.3 Renal Failure.

Renal failure represents the terminal stage of certain renal and non-renal diseases. The pathophysiology and etiology may be found in detail in (Maude, 1977). The symptoms of renal failure, in general, are the impairment of the renal functions to various degrees; the extreme case is the complete shut-down of urine flow. Renal failure is described as acute when the onset of this condition is rapid, and is potentially reversible. Chronic renal failure results from a progressive reduction in the number of functioning nephrons over a period of, perhaps, years. Renal failure can be brought about by many factors which fall into the general categories of pre-renal, renal, or post-renal.

2.3.1. Pre-renal Factors.

Pre-renal factors leading to acute renal failure include hypotension, heart failure, haemorrhage, dehydration, burns and shock. Chronic renal failure can be brought about by such pre-renal factors as reduced liver function in cirrhosis of the liver. The common underlying mechanism in all pre-renal factors is the reduction of renal blood flow, leading to renal ischaemia and tubular necrosis.

2.3.2. Renal Factors.

Renal factors are by far the most common causes of renal failure. Acute renal failure may occur as a result of glomerularnephritis (morphological changes to the glomerular membrane resulting in increased membrane permeability, decreased glomerular filtration rate and urine flow), pyelonephritis (infection of the tubules resulting in reduced glomerular filtration rate,

urine flow and some urinary loss of protein), and toxic nephropathy (destruction of nephrons as a result of intake of a toxic material such as a heavy metal). Glomerularnephritis and toxic necropathy are two of the renal factors that could also lead to chronic renal failure. Abnormalities, primarily affecting the kidneys and leading to renal failure, are categorized as renal factors.

2.3.3. Post-renal Factors.

Post-renal factors leading to acute or chronic renal failure are those associated with the obstruction of the flow of urine in the urinary tract, such as obstructive uropathy.

2.3.4. Summary.

The primary symptom of acute renal failure is the sudden drastic reduction in urine output, known as oliguria, such that it is insufficient to excrete waste products, such as urea and creatinine, at a rate needed to prevent the development of uraemia. The onset of chronic renal failure, strangely enough, is marked by an increase of up to three times the normal urine output, known as polyuria. This is followed by a gradual decrease to zero urine output as the number of functioning nephrons diminish. The total cessation of urine output is known as anuria. Other symptoms associated with renal failure are oedema, hypertension, disturbances in the sodium and fluid balance system, hyperkalemia and anaemia.

Clinical management of renal failure patients (apart from attempting to remove the underlying causes of the failure) depends on the severity of the attack. In the initial stages of failure, and if the failure is not severe, control of protein, salt and water intake may be sufficient therapy to counteract the effects of renal failure. When this strategy proves to be ineffective, the kidney functions must be performed artificially by means of peritonial dialysis or haemodialysis. In the limiting case, when hypertension is not controlled by dialysis, renal transplant represents the ultimate therapy.

2.4. Renal Dialysis.

Haemodialysis is the most commonly used method of artificially performing the functions of the kidneys, and thus, of alleviating the patient suffering from renal failure of its associated symptoms. Haemodialysis is a process where the patient is attached to the dialysis machine for periods varying from four to seven hours, two or more times per week, depending on the needs of the patient. The mechanisms of the process are described below and are shown in the diagram of Figure 2.8.

Blood from an artery of the uraemic patient is caused to flow into the artificial kidney machine on one side of a semi-permeable membrane, and an electrolytic solution, the dialysate, is passed on the other side. The electrolytic composition of the dialysate is the same as that of normal plasma, except for the absence of potassium from the dialysate. However, the composition of the dialysate is generally altered, to suit the needs of the individual patient. Electrolytes and waste products then diffuse through the membrane (at rates dependant on the differences in the concentrations of the particular substances) across the membrane. The rate of diffusion of a particular substance through the membrane is also dependant on the surface area of the membrane, and the relative size of the pores of the membrane compared with the size of the molecules of the substance. Fluid is forced through the membrane at a rate dependant on the controllable ultrafiltration pressure across the membrane.

The 'cleaned' blood is then returned, via a vein, to the vascular compartment of the patient, where it equilibriates with the body fluids of the patient. Thus, continuous passage of blood through the artificial kidney machine removes excess water and some of the waste products, and alters the concentrations of the electrolytes to more normal levels in the extracellular and intracellular fluid compartments of the patient.

After dialysis, the patient is free to live a near - normal life, apart from the restriction of a controlled diet, until it is necessary for him to be dialysed again, when the above procedure is repeated.

The above description of the mechanical aspects of haemodialysis gives little indication of the problems associated with

the administrations of this form of therapy. A discussion of these problems, in conjunction with the objectives of the work described in this thesis, was presented in the previous chapter.

2.5. Summary.

The functional description of the renal - body fluid system, the consequences of the various classes of renal failure and the mechanisms of haemodialysis, presented in previous sections of this chapter form the basis from which the mathematical description of the patient - artificial kidney machine system is derived. However, as is evident from the foregoing discussions, certain aspects of renal physiology are, as yet, poorly understood.

One of the objectives of this work, as discussed in the previous chapter, is to produce a model which may be used to test hypotheses regarding these areas of weak knowledge. In the development of the mathematical model, the specific regions of uncertainty are highlighted; and subsequent simulation of the model, as described in Chapter 5, serves to test the validity of assumptions and hypotheses associated with these uncertainties.

However, preceding the chapters presenting the discussions concerning the development and simulation of the model, previous relevant biological models are reviewed in the following chapter in order to facilitate the transition from the verbal to the mathematical description of the system being considered in this work.

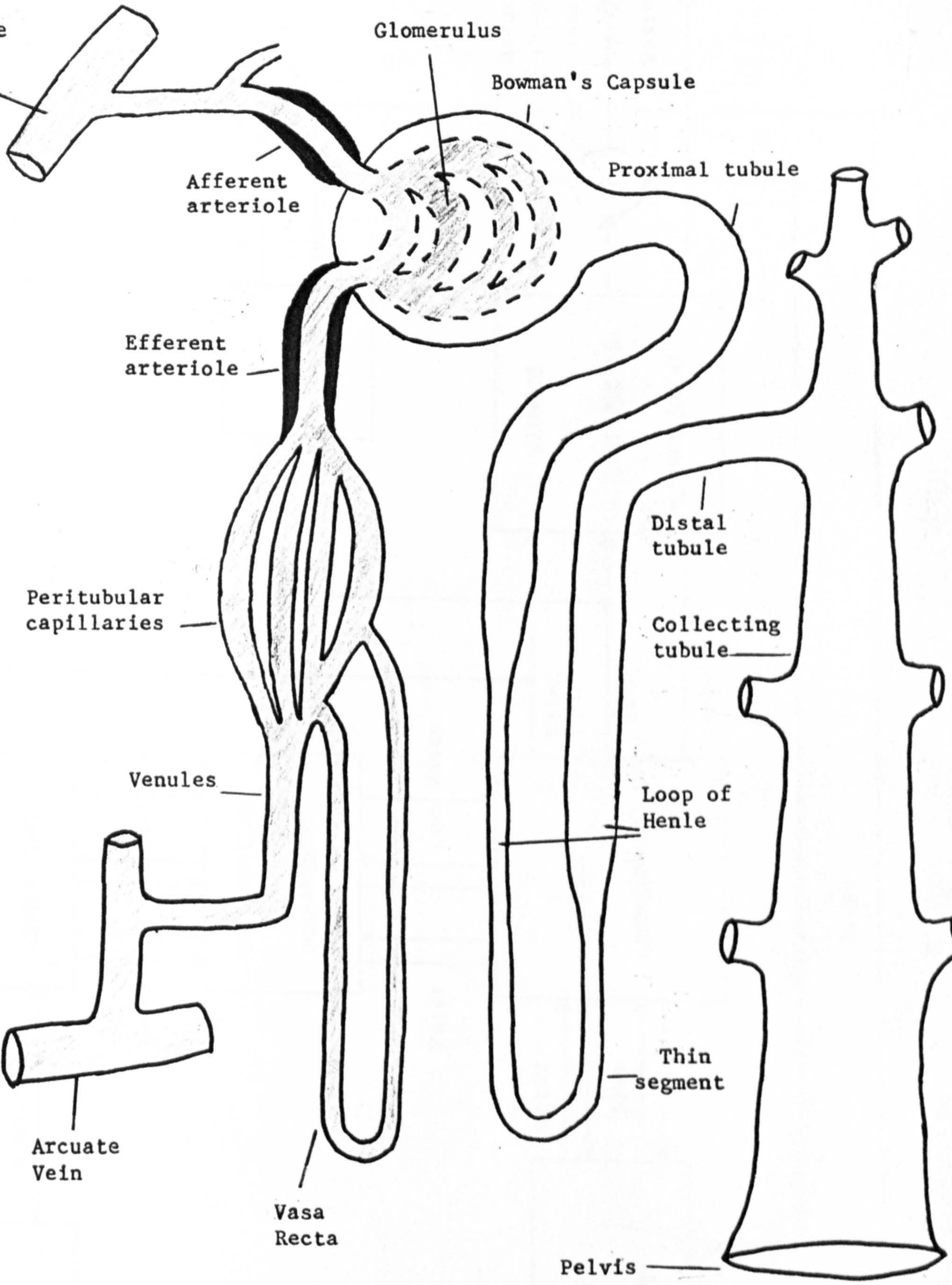

Figure 2.1. The Functional Nephron.

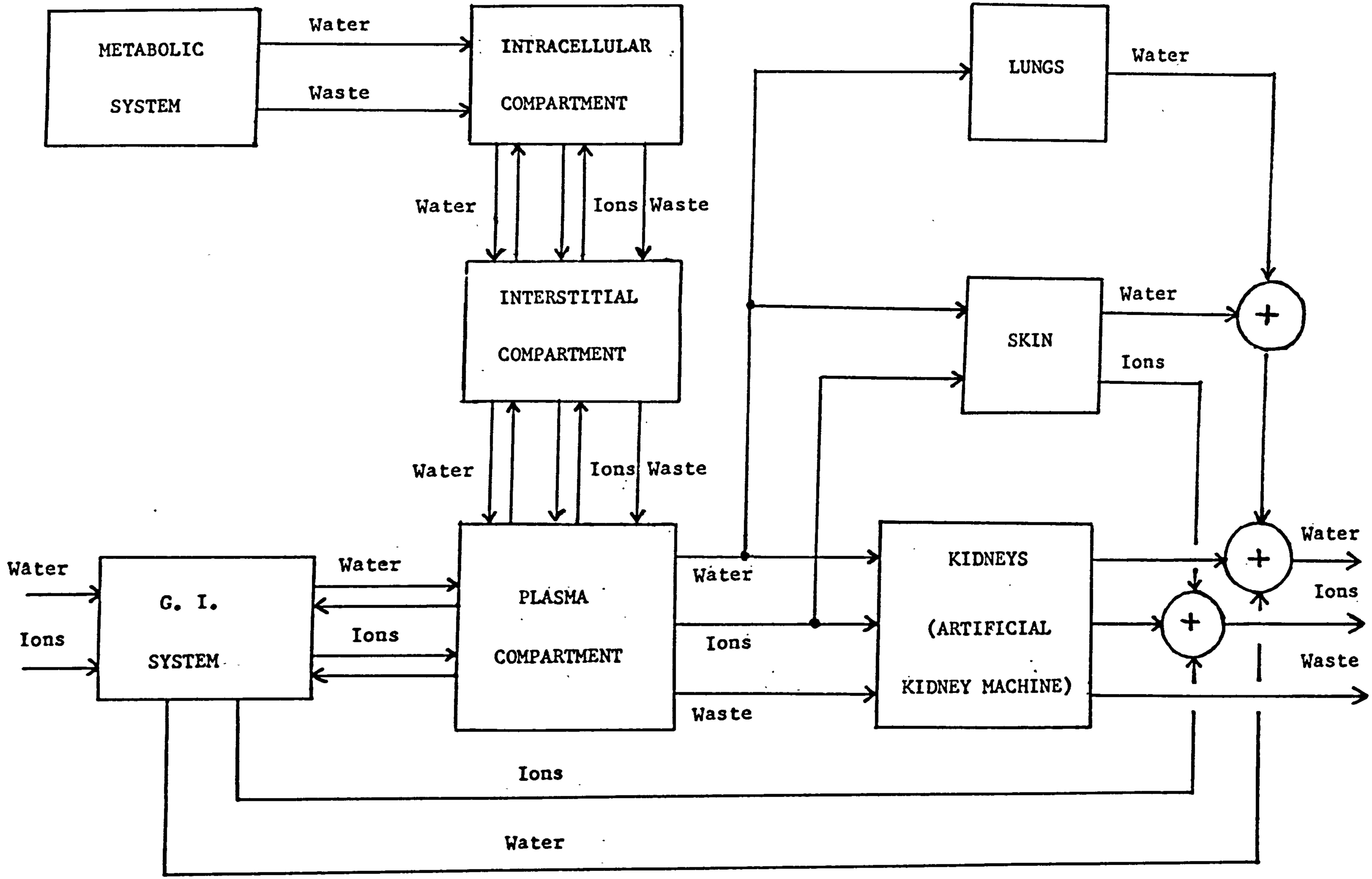

Figure 2.2. Flow diagram of the renal - body fluid system.

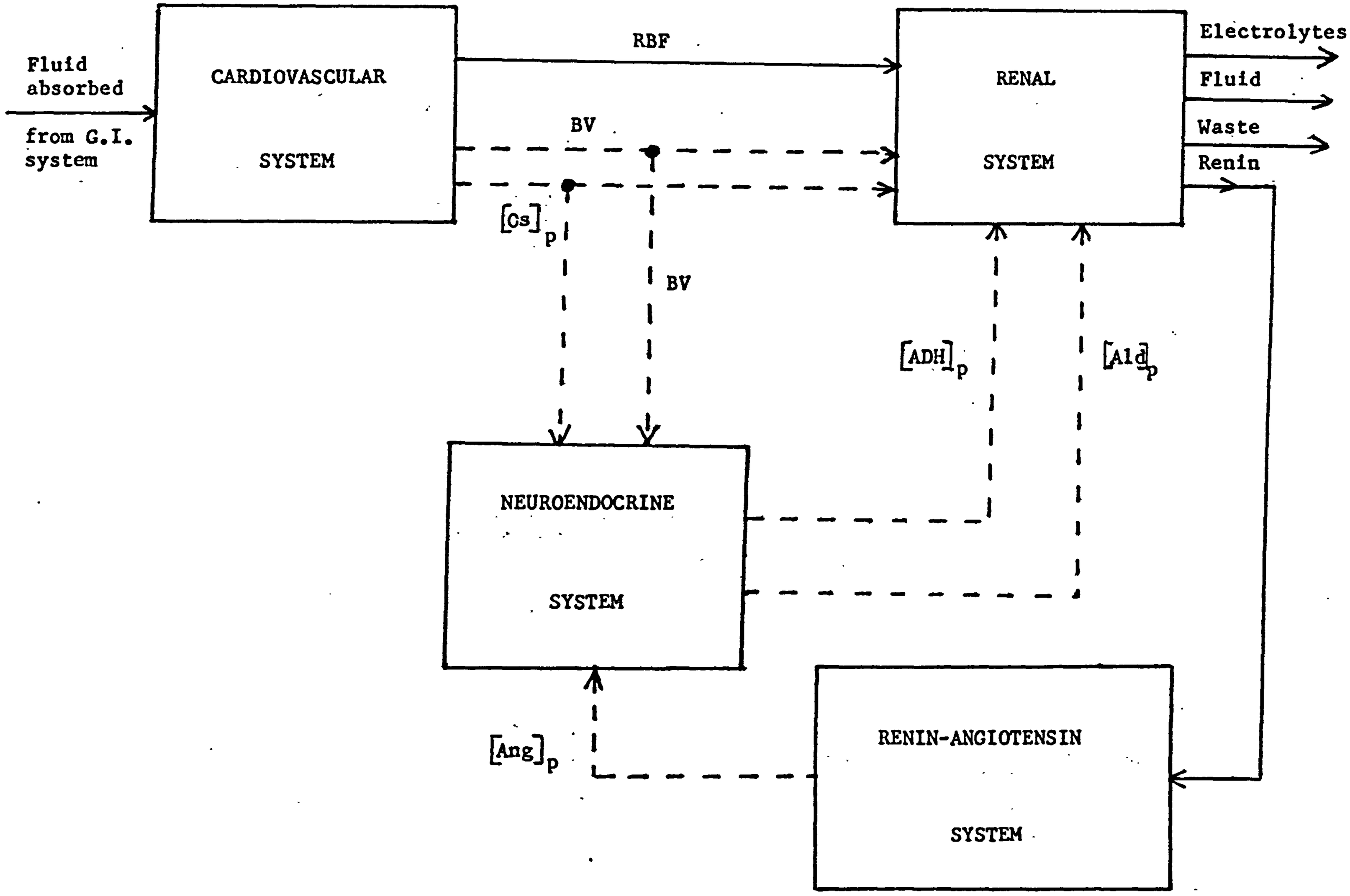

Figure 2.3. Simplified functional diagram of the major components of the renal - body fluid system.

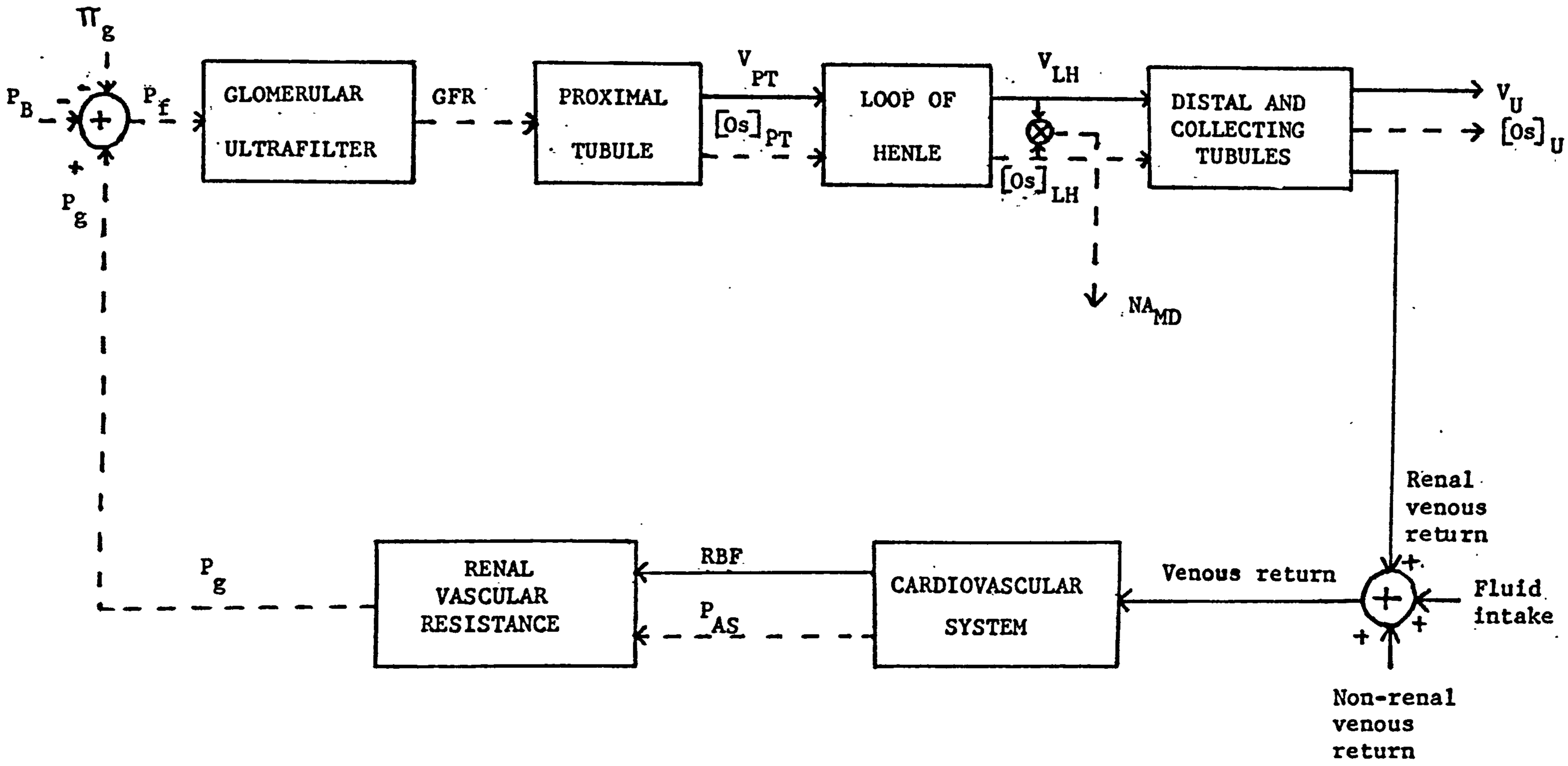

Figure 2.4. Functional diagram of the renal system.

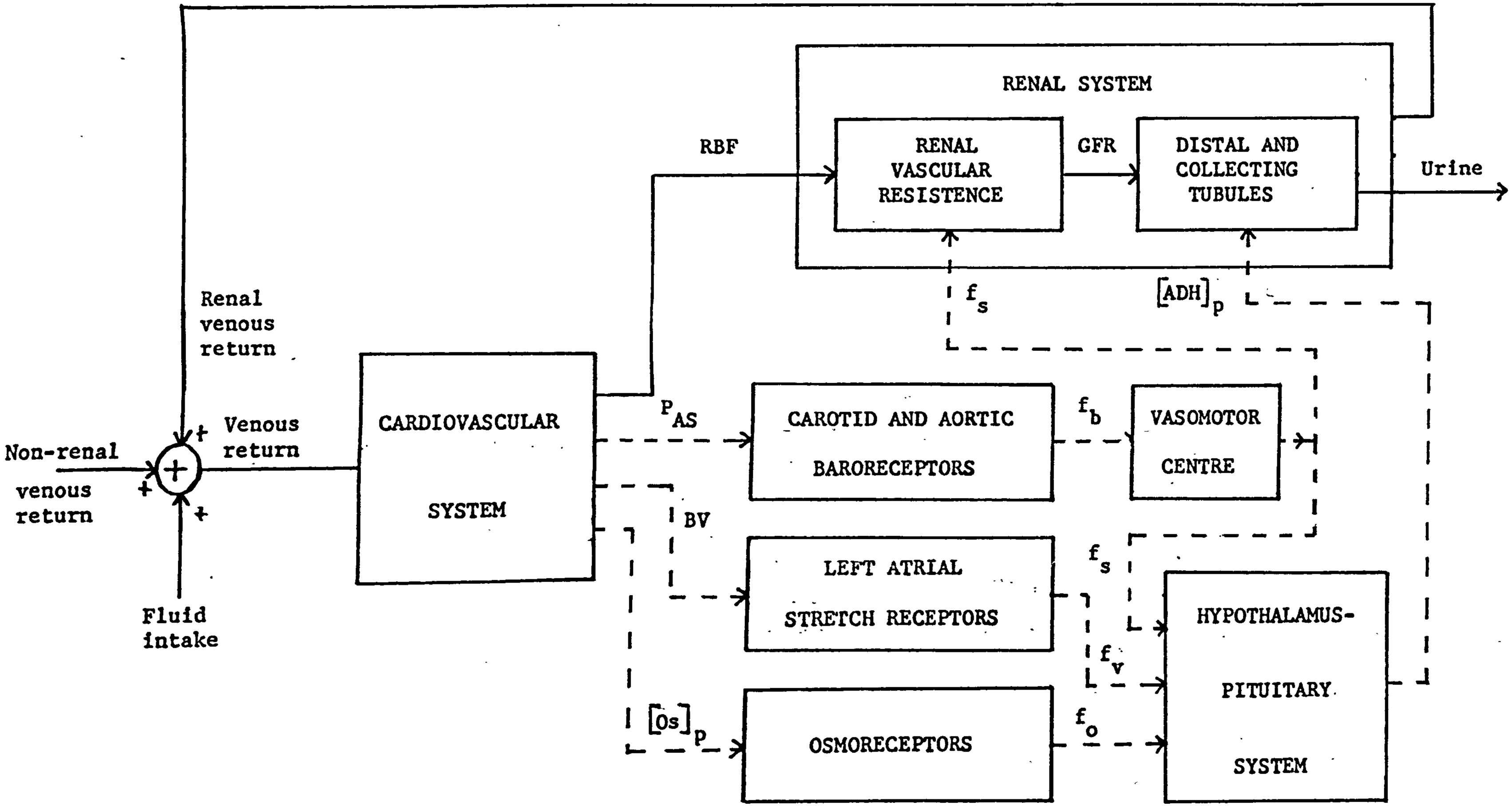

Figure 2.5. Functional diagram of the ADH system.

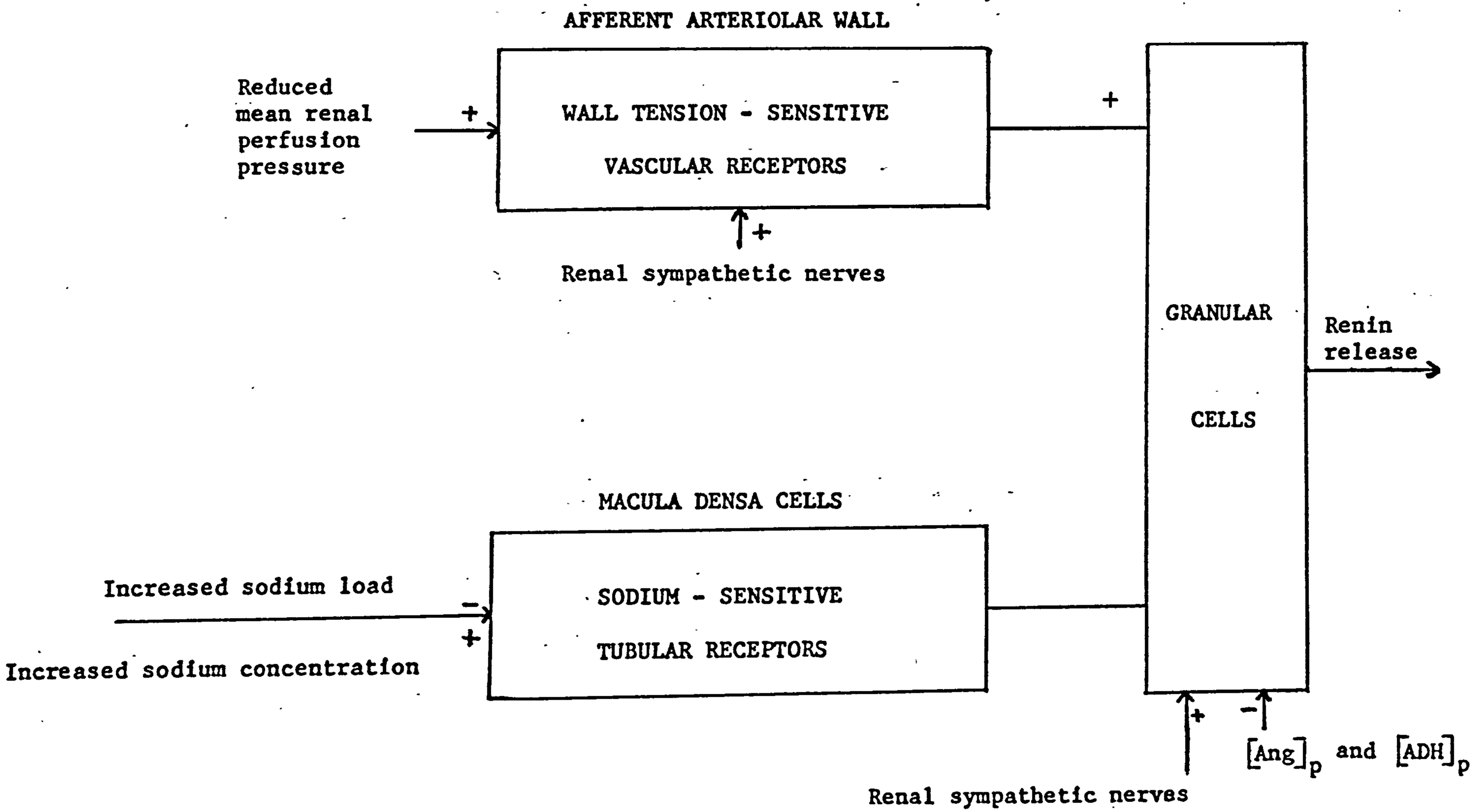

Figure 2.6. Functional diagram of intrarenal control of renin release.

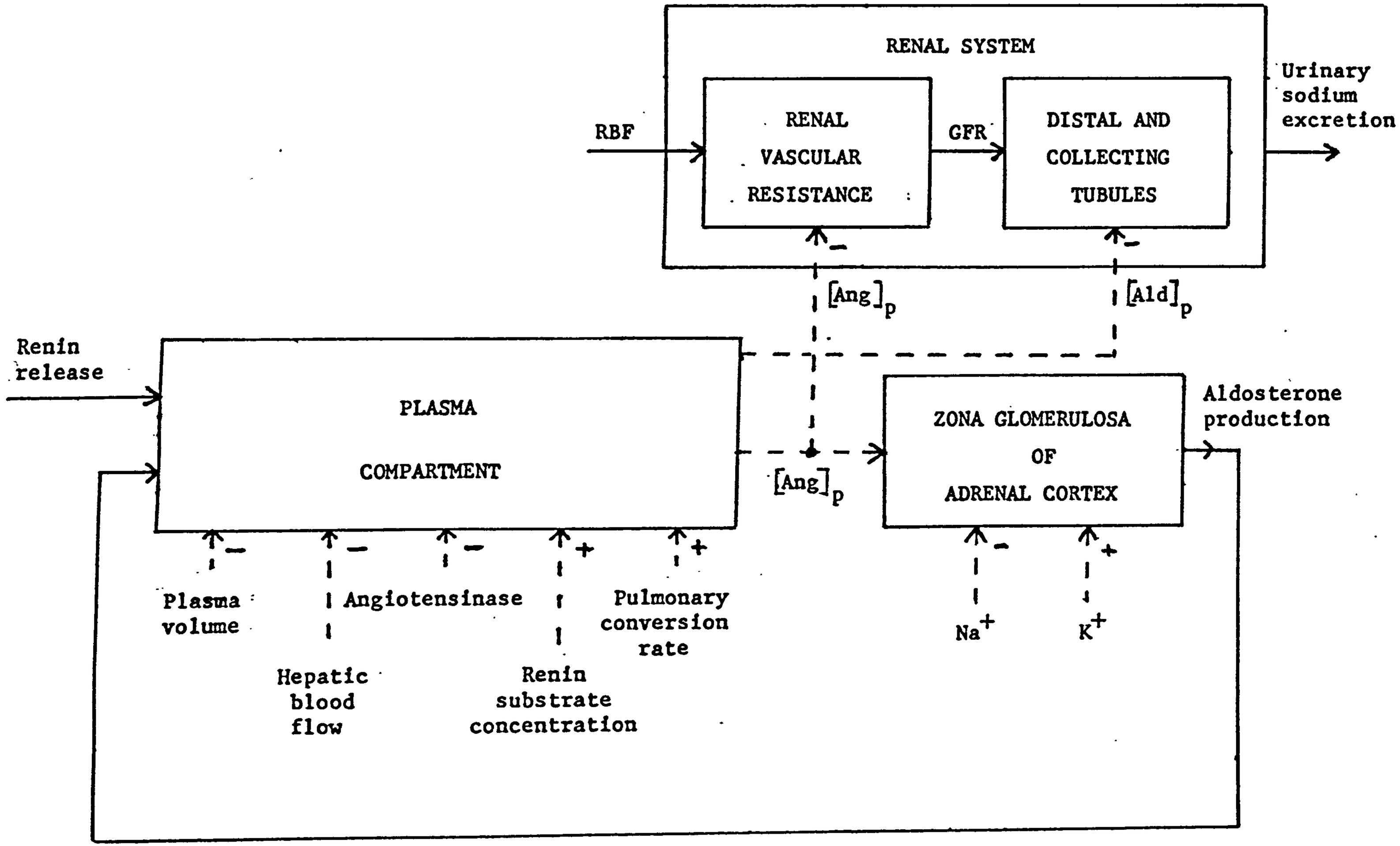

Figure 2.7. Functional diagram of the control of aldosterone release and the renal excretion of sodium.

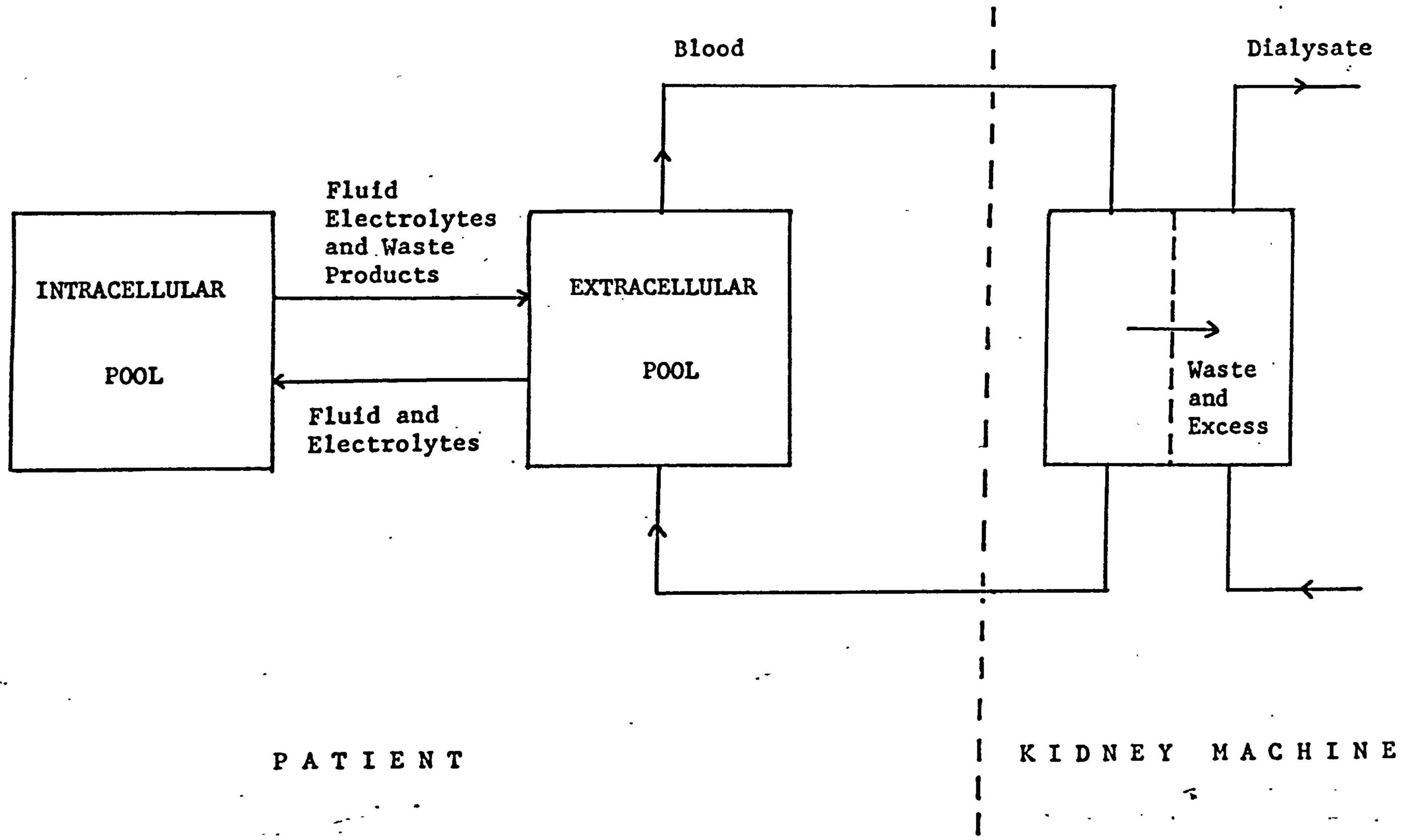

Figure 2.8. Schematic diagram of the patient - artificial kidney machine system.

CHAPTER 3

REVIEW OF PAST BIOLOGICAL MODELS.

Existing biological models relevant to this work are briefly described and examined in this chapter. The purposes for this are as follows:

(1) The various methods of model formulation are made apparent.
(2) The capabilities and limitations of different models are brought to light, and the need for definite purposes for model building is emphasized.
(3) Comparison of certain aspects, such as method of formulation, level of modelling and the potential capabilities of satisfying the objectives of model building, can be made between this work and others.
(4) Aspects of current knowledge of the subsystems to be modelled may be gained by consideration of existing models.

Models describing the individual subsystems incorporated in this work are examined in the first section of this chapter; models built to improve the health care of renal dialysis patients are described in the second section; and in the summarizing section, a comparison is made of the model formulation techniques revealed by this survey in the light of the objectives of the work described in this thesis.

3.1 Individual Subsystem Models.

Brief descriptions of models of the human thermoregulatory system, cardiovascular system and renal functions are given in this section. Since the number of existing biological models relevant to each system is so large, representative models, which demonstrate the range of modelling techniques, are discussed for each of the above subsystems.

3.1.1 Thermoregulatory System Models.

(1) Wyndham and Atkins (1960):

Wyndham and Atkins developed a model, in which they made the simplifying assumption that the human body is represented as a single cylinder whose elements are thin concentric shells about the axis of the cylinder. They also assumed that the temperature is uniform throughout a single element, and that the rate of heat transfer between two adjacent elements is proportional to the temperature difference between them. Hence, using the terminology of Table 3.1, the equation representing the system is:

$$\rho \times C_p \times \frac{\partial T}{\partial t} = \frac{1}{r}\left[\frac{\partial}{\partial r}\left(Kr \times \frac{\partial T}{\partial r}\right)\right] + h_m \qquad (3.1)$$

where the rate of accumulation of heat (left hand side of equation) is given as the sum of the rate of heat conduction and the metabolic heat generation rate.

The boundary conditions for the solution of (3.1) are:

(1) The temperature gradient at the centre of the cylinder is zero.

(2) At the surface, the rate of heat loss to the environment, q_s, is equal to the sum of the heat lost due to convection, q_c, radiation, q_r, and evaporation, q_e.

Radiative heat loss from the surface of the body to the environment is given by the Stefan-Boltzman equation:

$$q_r = K_1 \times A_r \times \left(\bar{T}_s^{\,4} - \bar{T}_w^{\,4}\right) \qquad (3.2)$$

Convection of heat from the surface of the body with air velocity between 10 and 1000 ft/min parallel to the axis of the cylinder is given by:

$$q_c = 0.5 \times A_c \times v_l^{\,0.5} \times \left(T_s - T_e\right) \qquad (3.3)$$

TABLE 3.1. Variables Of The Model By Wyndham And Atkins (1960).

C_p	Specific heat.
ρ	Density of blood.
T	Tissue temperature.
r	Radial distance from axis of cylinder.
K	Thermal conductivity.
h_m	Rate of tissue heat generation by metabolic reaction.
q_r	Heat loss by radiation.
K_1	Universal radiation constant (4.92×10^{-8} cals/m^2/h).
A_r	Effective radiation area.
T_s	Mean radiation absolute temperature of the body surface.
T_w	Mean radiant absolute temperature of the environment.
q_c	Heat loss by convection.
A_c	Effective area of the body creating convection losses.
v_1	Velocity of surrounding air.
T_s	Mean skin temperature.
T_e	Effective environmental temperature.
q_e	Heat loss by evaporation.
A_e	Effective area of body creating evaporative heat losses.
VP_s	Partial pressure of water at skin temperature, T_s.
VP_a	Partial pressure of moisture in air at temperature, T_e.
K_e	Evaporation conductance.

$$q_c = 1.04 \times A_c \times v_1^{\ 0.5} \times (T_s - T_e) \qquad (3.4)$$

Evaporative heat exchange from saturated skin is given by:

$$q_e = 1.4 \times v_1^{\ 0.4} \times A_e \times (VP_s - VP_a) \qquad (3.5)$$

Evaporative heat loss from unsaturated skin is given by:

$$q_e = K_e \times V_1^{0.4} \times A_e \times (VP_s - VP_a) \qquad (3.6)$$

(2) Wissler (1963):

Wissler extended the work of Wyndham and Atkins (1960), whereby the body is assumed to be represented by six interconnected cylinders (head, torso, two arms and two legs), each cylinder assumed to be a homogeneous mixture of bone and tissue, covered with a layer of fat and skin. In addition, this model assumes that the tissues of each cylinder are uniformly perfused with blood. Hence neglecting longitudinal heat transfer and using the terminology of Table 3.2, the heat balance for the i^{th} cylinder is given by:

$$\rho \times C_p \times \frac{\partial T_i}{\partial t} = K \times \left(\frac{\partial^2 T_i}{\partial r^2} + \frac{1}{r} \times \frac{\partial T_i}{\partial r} \right) + h_{mi} + (V_1 \times \rho \times C_p)_i \times (T_{ai} - T_i) \qquad (3.7)$$

This equation is similar to that of a single cylinder, (3.1), except for the additional term on the right hand side to account for heat transfer due to circulating blood.

The system equations, (3.7), are solved, given the initial temperature distribution, and the boundary conditions that the rate of heat transfer to the skin from the tissue layer immediately below is equal to the rate of heat transfer from the skin to the environment.

Blood is assumed to take the temperature of the tissue surrounding it, so that the cylinders are interconnected by the thermal balance equations for blood flowing between the cylinders and the heart.

(3) Stolwijk and Hardy (1966):

The model developed by Stolwijk and Hardy considers the human body as three cylinders and a blood compartment. Each cylinder consists of two or three concentric layers to represent the head (core and skin), trunk (core, muscle and

TABLE 3.2. Variables Of The Model By Wissler (1963).

ρ	Density of blood.
C_p	Specific heat.
T_i	Temperature in the i^{th} cylinder.
K	Thermal conductivity.
r	Radial distance from axis of cylinder.
h_{mi}	Metabolic heat generation rate in the i^{th} cylinder.
V_l	Volume of blood flowing in capillary bed.
T_a	Temperature of blood entering capillary bed.

skin), and extremities (core and skin). Each of these elements is characterized by anatomical, thermal and blood flow rate parameters needed to describe it for the purpose of the model. Mathematical representations of the physiological thermoregulatory mechanisms are also incorporated.

An element of the system exchanges heat with the adjacent layer in the same cylinder by conduction, and with the blood compartment by convection; in addition the skin elements lose heat to the environment by conduction, convection, radiation and evaporation. The passive system is then described by heat balance equations for each of the elements including the blood compartment. As an example, the heat balance relationship for the skin of the cylinder representing the head is given below:

$$C_{HS} \times \frac{dT_{HS}}{dt} = K_{HCHS} \times (T_{HC} - T_{HS}) + M_{OHS} - 0.09Ev_{OHS} - 0.09Ev + \alpha_{HS} \cdot \rho c \times 0.138SBF.(T_{CB} - T_{HS}) - A_{HS} \times h_0 \times (T_{HS} - T_A) \quad (3.8)$$

Equation (3.8) states that the rate of accumulation of heat in the skin of the head is equal to the algebraic sum of the rates of heat gain and heat loss factors. The heat gain factors are heat conduction rate from the core of the head, the metabolic

TABLE 3.3. Variables Of The Model By Stolwijk And Hardy (1966).

C_{HS}	Thermal capacitance of the skin of the head (0.27 kcals./^{o}C.).
T_{HS}	Temperature of the skin of the head.
K_{HCHS}	Thermal conductunce between the core and skin of the head (2.63 kcals./hr./^{o}C.).
T_{HC}	Temperature of the core of the head.
M_{OHS}	Basal metabolic rate of skin of the head (0.12 kcals./hr.).
$0.09Ev_{OHS}$	Assigned fraction of insensible evaporative heat loss (0.8 kcals./hr.).
0.09Ev	Assigned fraction of thermal evaporative heat loss.
α_{HS}	Factor for countercurrent heat exchange.
ρc	Product of density and specific heat of blood (0.92 kcals./^{o}C.).
0.138SBF	Assigned fraction of total skin blood flow.
T_{CB}	Temperature of blood.
$A_{HS} \cdot h_{O}$	Product of area of the skin of the head and the environmental heat transfer coefficient (0.165 x 6.0 kcals./hr./^{o}C.).
T_{A}	Temperature of the environment.
$\bar{T}_{S}$	Average skin temperature.
T_{M}	Muscle temperature.

heat generation rate in the skin of the head and the heat delivered by the fraction of the skin blood flow assigned to the skin of the head. The heat loss factors are the fractions, assigned to the skin of the head, of the total evaporation, convection, radiation and conduction heat loss rates from the skin to the environment.

The controlling system is a mathematical description of the set-point theory of thermoregulation (Hammel et al, 1963). In the model the vasoconstriction and shivering heat gain

is the control of peripheral circulation by the adjustment of vasomotor tone. It is proposed that if this manoeuvre is insufficient to prevent a deviation of core temperature, then the gross second line of defence, namely the shivering and sweating mechanisms, comes into effect.

Analysis of digit blood flow waveforms in response to thermal disturbance has led Burton and Taylor (1940) to isolate spontaneous components, which they associate with vasomotor activity. Further power spectral analysis of digit blood flow by Minorsky (1962) demonstrated that the vasomotor control system could be entrained by a square wave thermal stimulus ($18^{o}C$ - $46^{o}C$) of a period of twenty seconds. This suggests the presence of a nonlinear component in the thermally induced vasomotor control of blood flow, which was considered to be of the 'bang - bang' type.

Kitney rejected the set point temperature controller on the grounds that it produced instabilities in the system response within a certain range of environmental temperatures. Instead, he proposed a set point thermal gradient controller for the system, the set point value having been empirically derived from the responses of the system to variations in skin temperature and vasomotor tone. He reports that analysis of the responses of the complete model to the thermal disturbances led to the power spectra of digit blood flow very similar to those described by Minorsky (1962).

Discussion On Thermoregulatory System Models.

The descriptions of the four preceeding models demonstrate the changes with time in the approach to the problem of mathematically describing the human thermoregulatory system. It is seen that increasing emphasis is placed on the effects of the thermoregulatory controller mechanisms on the thermal dynamics of the human body. In particular, it appears that the control of peripheral blood flow in response to thermal stress plays a major regulatory role, at least within a normal range of body temperatures.

The model by Wyndham and Atkins (1960), incorporating detailed equations for the heat loss mechanisms from the surface, yields a continuous temperature gradient from the

centre to the surface of a cylinder representing the human body. No account is taken of the effects of blood flow or of any form of temperature regulation on the temperature distribution. The model also suffers from the disadvantage that there is the need to specify the distribution of the metabolic heat generation rate with respect to the distance from the centre of the cylinder.

The model by Wissler (1963) utilizes blood flow to convect heat between the six cylinders representing the human body. However, the rate of blood flow is not thermally regulated, and no form of thermoregulatory control is incorporated in the model. In addition, the surface boundary condition imposes a condition of constant surface temperature.

The classic model by Stolwijk and Hardy (1966), describes the human body, thermally, in terms of eight cylindrical elements, with a uniform temperature in each. This model, therefore, does not yield continuous temperature gradients as do the previous two distributed models. However, the control of metabolic heat production, heat loss through evaporation and peripheral blood flow are incorporated by the empirical representation of the set point temperature theory of thermoregulation.

The purpose of the thermoregulatory model of the human forearm by Kitney (1974) was to analyse the thermoregulatory control of blood flow, in particular the nonlinear elements which give rise to the observed oscillatory behaviour of digit blood flow. In his analysis, Kitney rejects the set point temperature theory in favour of a set point temperature gradient theory of thermoregulation. In recent years, the set point temperature gradient theory appears to be gaining recognition, and as a result more distributed parameter thermoregulatory system models incorporating this theory may be forthcoming in order to explain observed thermal phenomena.

The limitations in the accuracy with which the passive system can mathematically be described is dependant on the accuracies with which the thermal and anatomical parameters of the human body are known. However, little is yet known in detail about the mechanisms by which the body maintains control of its temperature. It is the opinion of the author,

however, that the detail with which the thermoregulatory controller needs to be modelled depends on the purpose for which the model is to be used.

3.1.2 Cardiovascular System Models.

(1) Beneken and DeWit (1967):

The model developed by Beneken and DeWit deals with the cardiovascular system as a mechanical system, consisting of the four chambers of the heart acting as pumps; these supply blood to the systemic and pulmonary blood vessels, which are lumped, so that the cardiovascular circuit is represented by fifteen arterial and venous segments and four heart chambers appropriately connected. Haemodynamic relationships of each of the nineteen segments represent the passive system, which is influenced by mathematical representations of certain control mechanisms of the cardiovascular system.

The equations, using the symbols of Table 3.4, relating pressure, flow and volume for a typical segment are:

$$P_0 - P_1 = R_1 \times F_{01} + L_1 \times \frac{dF_{01}}{dt} \qquad (3.11)$$

$$V_1 = V_{01} + \int (F_{01} - F_{12})dt \qquad (3.12)$$

$$P_1 = \frac{1}{C_1} \times (V_1 - V_{u1}) + R'_1 \times \frac{dV_1}{dt} \qquad (3.13)$$

The ventricles and atria are made pulsatile by incorporating time-varying periodic compliances in the pressure - volume relationships of equation (3.13). In addition, the effects of ventricular shape and heart muscle properties on the volumes and pressures of each heart chamber are mathematically represented.

This passive system is under the influence of the controllers such as heart rate controller, peripheral resistance controller, and blood volume adjustment by capillary fluid shift. In addition, nonlinearities due to collapsing veins at low pressures and the influence of variations in coronary blood flow on heart

TABLE 3.4. Variables Of The Model By Beneken And DeWit (1967).

P_0, P_1	Pressures in two adjacent segments.
R_1	Resistance to blood flow in segment 1.
F_{01}	Total flow of blood into segment 1.
L_1	Inertia of blood in segment 1.
V_1	Volume of segment 1.
V_{01}	Initial volume of segment 1.
F_{12}	Total flow of blood out of segment 1.
C_1	Compliance of segment 1.
V_{u1}	Unstressed volume of segment 1.
R_1	Viscosity coefficient of wall material of segment 1.

performance are also incorporated.

Beneken and DeWit report that simulation results of Valsalva manoeuvres, and changes in blood volume by bleeding and reinfusion compare reasonably well with experimental results, although further improvement of simulation response may be afforded with the inclusion of representations of other cardiovascular control systems in the model.

(2) Guyton and Coleman (1967).

The model produced by Guyton and Coleman (1967) was built to represent the long term response of the circulatory system to stresses. Therefore the mechanical aspects of the cardiovascular system, which are important in the short term effects of the circulation, are not modelled. Instead factors which affect body fluid volumes, hence the circulation in the long term, are considered.

The block diagram of figure 3.1 shows the relationships between the important variables of the basic cardiovascular system model. The empirical relationships have been derived mainly from animal experiments. The basic structure represents a feedback loop such that an initial increase in arterial pressure causes an increase in urinary output of fluid, hence a

TABLE 3.5. Variables Of The Model By Guyton And Coleman (1967).

AP	Arterial pressure.
UO	Urine outflow rate.
$\frac{dE}{dt}$	Rate of change of fluid volume.
ECFV	Extracellular fluid volume.
BV	Blood Volume.
MSP	Mean systemic pressure.
RAP	Right atrial pressure.
RVR	Resistance to venous return.
CO	Cardiac output.
VR	Venous return.
TPR	Total peripheral resistance.

decrease in the volumes of body fluids, leading to a reduction in cardiac output and arterial pressure. This simple model was reported to be capable of reproducing the actual variations in arterial pressure, cardiac output and blood volume which occurred due to changes in peripheral resistance in animal experiments.

Structures representing the effects of long term autoregulation (collateral circulation), the autonomic reflexes and limitations in heart performance on circulatory response were added to the basic model. Simulations of experiments, such as reducing renal mass and increasing sodium and fluid intake, reducing heart performance, and applying a Goldblatt clamp to a renal artery, reproduced many of the features of response observed in actual experimental data.

The model was completed with the addition of a circuit representing the long term regulation of interstitial fluid and its effects on the circulation.

(3) Guyton, Coleman And Granger (1972):

This model, developed by Guyton and co-workers, is an extensive lumped parameter, non-pulsatile model of the circulation incorporating many of the physiological systems which interact, both in the short term and the long term, with the circulation. The model, presented in block diagram form (Guyton et al, 1972), consists of 354 blocks, each of which defines a relationship between two or more variables. These relationships, in the main, have been derived from experiments. The diagram is partitioned into eighteen major systems representing the dynamics of the various body fluid compartments, hormonal and kidney control mechanisms, blood flow and oxygen delivery control, and others.

The time constants of the system vary from 0.005 minutes to 57,000minutes. Hence, at the start of the simulation of any stress, it is necessary to integrate with a small time step until the rapid time constant factors reach steady state; the integration interval step is then increased so that the whole system model attains steady state without consuming excessive computer time.

Simulations described include the development of hypertension in a salt loaded renal deficient patient, heart failure, nephrosis, and the effects of severe muscle exercise on the circulation. It is reported that many of the features of the simulation responses are in agreement with those which are observed in studies on animals.

Discussion On Cardiovascular System Models.

Comparison of the model of Beneken and DeWit (1967) and of Guyton and Coleman (1967) demonstrates the two extreme approaches to cardiovascular system modelling. The first model, based on consideration of the mechanical aspects of the circulation, is designed to simulate the cardiovascular system in the short term; the second model relies on empirical descriptions, based on animal experiments, to explain the long term phenomena of the circulation. The third model (Guyton et al, 1972), though empirical in the main, combines both short term and long term effects, but the resulting model is so detailed that it would be found to be unwieldy in use. However, the

model demonstrates the usefulness of the systems analysis approach in the understanding of biological systems.

3.1.3. Renal Function Models.

(1) Cage, Carson And Britton (1977):

A model of the renal medulla was developed by Cage and associates using mass balance equations to describe the flow of water, electrolytes and urea through the loops of Henle of the cortical and the juxtamedullary nephrons, the collecting ducts, vasa recta and medullary interstitium. The primary aim for the development of this model was to examine possible mechanisms which create the concentration gradient for the operation of the countercurrent multiplier.

Figure 3.2 represents the n^{th} segment of a tubule of length, Δx, in a segment of the medulla at time, t. The flux equation for water passing through all the tubule segemnts in the n^{th} segment of the interstitium, using the symbols described in Table 3.6, is:

$$Q(n,t) = Q(n-1,t) - (2\pi R_j \Delta x B_j) \times J(n,t) \qquad (3.14)$$

Equation (3.14) States that the rate of water flow out of all the tubule segments in the n^{th} segment of the interstitium is equal to the difference between the total rate of water flow into the tubules and the rate of water flux through the tubule walls into the intersitium. The fact that the number of nephrons decreases with depth into the medulla from the cortex is taken into account by representing the number of nephrons, B, as a function of distance into the medullary region.

The equation describing mass balance for solutes in the tubule segments of the n^{th} segment of the interstitium is:

$$(\pi R_j^2 \Delta x B_j) \times \frac{dC_i(n,t)}{dt} = C_i(n-1,t) \times Q(n-1,t) - C_i(n,t) \times Q(n,t) - (2\pi R_j \Delta x B_j) \times N_i(n,t) \qquad (3.15)$$

TABLE 3.6. Variables Of The Model By Cage, Carson And Britton (1977).

Q	Flow rate of water.
R_j	Inner radius of tubule type, j.
Δx	Length of segment.
B_j	Number of tubules of type, j, in segment of interstitium.
J	Water efflux rate per unit area.
C_i	Concentration of solute, i.
N_i	Molar flux of solute, i.

Equation (3.15) states that the rate of accumulation of solute, i, in all the tubule segments of the n^{th} segment of the interstitium is equal to the difference between the rates at which the solute, i, enters and leaves the tubule segments minus the rate at which the solute passes through the walls of the tubule segments into the interstitium.

Appropriate equations are written for other phenomena in the system. The quantities of water and solutes entering the interstitium from the tubules are determined by the relative concentrations of solutes according to the laws of osmosis and Fick's law. A factor is included, wherever appropriate, to represent the flux of electrolytes due to active transport mechanisms.

The vasa recta are assumed to have the same concentration of solutes as plasma, and thus the ascending limb acts as a sink. Hence excess water in the interstitium passes freely into the ascending limb of the vasa recta, and solutes pass from the interstitium according to Fick's law. The descending limb is assumed to be impermeable to water and solutes.

The tubule segments are characterized by appropriate parameters representing dimensions and transfer coefficients for solutes and water. The effects of antidiuretic hormone and aldosterone are represented by the adjustment of the appropriate transfer coefficients.

The model is used to simulate the effects of diuresis and antidiuresis. The variations of urinary urea excretion with

variation of the state of diuresis or antidiuresis compares well with clinical data, and this comparison serves as a test of the validity of the model.

(2) Cameron (1977).

A simple representation of kidney function, together with some of the factors which affect renal function, form a closed system model developed by Cameron. This model forms the basis for the testing of hypotheses concerned with the mechanisms of body fluid homeostatis. The framework of the model is similar to that of Guyton et al (1972), though it differs considerably in the extent of detail incorporated.

The renal dynamics are described by a set of empirical algebraic equations. The symbols used are described in Table 3.7. Afferent arteriolar resistance is represented as a function of blood viscosity and a feedback signal from the macula densa:

$$AAR = \frac{95}{3} \times RBV \times RANR \times MDAM / FKR \qquad (3.16)$$

Post afferent renal resistance is simply related to blood viscosity:

$$PAR = \frac{155}{3} \times RBV / FKR \qquad (3.17)$$

The total renal resistance is the sum of these two resistances:

$$RR = AAR + PAR \qquad (3.18)$$

The renal blood flow is calculated from arterial pressure:

$$RBF = AP / RR \qquad (3.19)$$

Nephron blood flow is dependant on the number of functioning nephrons:

$$FNBF = FFN \times RBF \qquad (3.20)$$

TABLE 3.7. Variables Of The Model By Cameron (1977).

AAR	Afferent arteriolar resistance.
RBV	Relative blood viscosity.
RANR	Renal autonomic nervous response.
MDAM	Macula densa autoregulatory multiplier.
FKR	Fraction of kidneys remaining.
PAR	Post afferent resistance.
RR	Renal resistance.
RBF	Renal blood flow.
AP	Arterial pressure.
FNBC	Functional nephron blood flow.
FFN	Fraction of functioning nephrons.
APD	Afferent pressure drop.
PDGF	Pressure driving glomerular filtration.
PCOP	Plasma colloid oncotic pressure.
GFR	Glomerular filtration rate.
TRR	Total tubular reabsorption rate.
ALM	Aldosterone multiplier.
ADHM	Antidiuretic hormone multiplier.
UFR	Urine flow rate.
NER	Sodium excretion rate.
ENC	Extracellular sodium concentration.

The afferent arteriolar pressure drop is given by:

$$APD = AAR.RBF \tag{3.21}$$

The resulting pressure driving glomerular filtration is given as the sum:

$$PDGF = AP - APD - PCOP - 20.4 \tag{3.22}$$

The glomerular filtration rate is related to this pressure:

$$GFR = FFN_{\times}FKR_{\times}PDGF/128 \qquad (3.23)$$

The feedback signal from the macula densa is a function of the variables controlling glomerular filtration rate:

$$MDAM = \text{median}\ (0.4,\ 15,\ \tfrac{5}{16}{\times}PDGF-4) \qquad (3.24)$$

The rate of tubular reabsorption of fluid is given as the sum of a constant fraction of glomerular filtration rate (glomerular-tubular balance) and a factor dependant on the level of antidiuretic hormone and aldosterone:

$$TRR = 0.8{\times}GFR + 0.025{\times}FFN{\times}FKR - \frac{0.001{\times}FFN{\times}FKR}{ALM{\times}ADHM} \qquad (3.25)$$

Urine flow rate is then given as the difference between glomerular filtration rate and the tubular reabsorption rate, unless this is less than the obligatory urine flow rate:

$$UFR = \max\ (0.0003,\ GFR-TRR) \qquad (3.26)$$

Sodium excretion rate is given as a function of urine flow rate, aldosterone level and extracellular sodium concentration:

$$NER = \frac{1000{\times}UFR}{ALM_{\times}(10.0 - 0.4{\times}(ENC - 142))} \qquad (3.27)$$

These equations, (3.16) - (3.27) form the representation of renal dynamics, one of five subsystems included in the model. Relevant equations constitute the subsystems concerned with the fluid compartmental volumes and protein concentrations in the model. The electrolyte subsystem represents the dynamics of extracellular potassium and sodium, and intracellular potassium. Included in the hormonal subsystem are equations governing the dynamics of aldosterone, angiotensin and antidiuretic hormone. The last subsystem represents the cardiovascular system.

The model was used to simulate the conditions of excitation

of renal nerves, unilateral nephrectomy, aldosterone loading, and acute water loading. The validity of the model was based on the comparison of simulation results of the excitation of renal nerves and aldosterone loading experiments with published data of the same experiments.

Discussion On Models Of Renal Functions.

The paucity of data leads the renal system modeller either to produce a model of some narrow aspects of the renal system, as in the model of Cage and associates (1977), or, with the use of uncertain empirical relationships, to produce a model of overall renal functions, such as the model of Cameron (1977). The approach adopted depends on the purpose for which the model is to be used. Thus, whilst the approach of Cage and associates is appropriate when developing a model with which to investigate the plausibility of physiological hypotheses, the overall model developed by Cameron is clearly more immediately relevant in clinical investigations. In either case, validation of the model is of greater importance in such cases where the structure and parameters are uncertain.

3.2 Renal Dialysis Health Care Models.

In addition to examining models of relevant physiological processes, there is a need to examine, critically, previous models devoted explicitly to renal dialysis. A representative set is considered below.

3.2.1 The Models Of Renal Dialysis.

(1) Ramirez, Lewis And Mickley (1973):

Ramirez and associates have determined an optimal control policy for dialysate flow rate utilizing a three compartmental model for the patient, adapted from a previous model of Gormley and Bell (1970). The optimal strategy is based on the minimization of the time for the removal of waste solutes, with a constraint

on the perturbation of cerebrospinal fluid pressure in the patient in order to avoid the problems associated with such perturbations.

The adapted model represents the dynamics of urea concentrations in the extracellular and intracellular compartments and in the cerebrospinal fluid compartment. The cerebrospinal fluid pressure is related to the difference between the concentrations of urea between the extracellular and cerebrospinal fluid compartments. The equations, using the terminology of Table 3.8, are:

$$V_1 \times \frac{dC_1}{dt} = K_1 \times (C_2 - C_1) + K_2 (C_3 - C_1) - Q_B \times \epsilon \times C_1 + LC_3 \qquad (3.28)$$

$$V_2 \times \frac{dC_2}{dt} = G + K_1 (C_1 - C_2) \qquad (3.29)$$

$$V_3 \times \frac{dC_3}{dt} = K_2 (C_1 - C_3) - LC_3 \qquad (3.30)$$

$$P_G = P_o \times (C_3 - C_1) \qquad (3.31)$$

The effectiveness factor, ϵ, is related to the dialysate flow rate (Ramirez et al, 1972).

Considering perturbations about the steady state, the equations (3,28) - (3.31) are linearized to form the state and measurement equations:

$$\dot{\underline{x}} = A.\underline{x} + b.\underline{u} \qquad (3.32)$$

$$\underline{y} = M.\underline{x} \qquad (3.33)$$

The optimal control problem is to take the system described by the state space equations, of the form of (3.32) and (3.33), from an initial state, $\underline{x} = \underline{x}_o$, to a terminal state, $\underline{x} = \underline{0}$, with practical constraints on the state and control variables, and with the following quadratic performance index to be minimized:

TABLE 3.8. Variables Of The Model By Ramirez, Lewis And Mickley (1973).

V_1	Extracellular fluid volume.
C_1	Concentration of urea in extracellular fluid.
K_1	Intracellular-extracellular mass transfer coefficient.
C_2	Concentration of urea in intracellular fluid.
K_2	Extracellular-cerebrospinal fluid mass transfer coefficient.
C_3	Concentration of urea in cerebrospinal fluid.
L	Coefficient for bulk flow from cerebrospinal fluid to extracellular fluid compartment.
Q_B	Blood flow rate through dialysis machine.
ϵ	Effectiveness factor for dialysis.
V_2	Intracellular fluid volume.
G	Urea generation rate.
V_3	Cerebrospinal fluid volume.
P_G	Cerebrospinal fluid pressure.
P_o	Coefficient for cerebrospinal fluid pressure.

$$I = \frac{1}{2} \int_{t=0}^{t_n} (\underline{x}'.Q.\underline{x} + \underline{u}'.R.\underline{u})dt \qquad (3.34)$$

The solution is the descrete variation in time (half hourly intervals) of the control variable, dialysate flow rate. The optimal solution does not cause the cerebrospinal fluid to rise above the acceptable level of 7.45 mm. H_2O (which corresponds to an uncontrolled, constant dialysate flow rate of 500 mls./min.), yet yields an overall clearance rate corresponding to a flow rate of almost 800 mls./min. (which causes an unacceptable maximum cerebrospinal fluid pressure of 8.01 mm. H_2O). The optimally controlled dialysate flow also affords a 27.1% saving in dialysate fluid when compared with the uncontrolled case with the removal of the same quantity of solute.

(2) Walker, Hall, Sanfelippo And Swenson (1975):

A programme, designed for use on the Hewlett-Packard 65 hand-held programmable calculator, was developed by Walker and associates. The programme calculates predictions of post-dialysis and next pre-dialysis serum urea and creatinine concentrations. The calculations are based on the one-compartmental model of Gotch et al (1974). Using the terminology of Table 3.9, the equations are:

$$C_T = \left(C_{01} - \frac{G}{K_d+K_r}\right) e^{-(K_d+K_r)t_d/V} + \frac{G}{K_d+K_r} \quad \text{(Dialysis)} \quad (3.35)$$

$$C_{02} = \left(C_T - \frac{G}{K_r}\right) e^{-K_r\theta/V} + \frac{G}{K_r} \quad \text{(Interdialysis)} \quad (3.36)$$

TABLE 3.9. Variables Of The Model By Walker, Hall, Sanfelippo And Swenson (1975).

C_T	End-dialysis concentration.
C_{01}	Pre-dialysis concentration.
G	Generation rate.
K_d	Dialyser clearance.
K_r	Residual renal clearance.
t_d	Time on dialysis.
V	Volume of distribution.
C_{02}	Next pre-dialysis concentration.
θ	Time between dialyses.

The input data required for the calculations are pre-dialysis concentrations, residual renal clearance, dialyser clearance, time on dialyis, and time between dialyses. The generation rates and volumes of distribution are calculated using the model with the previous post-dialysis and next pre-dialysis concentrations.

The programme can therefore easily be used in the clinic

to aid in the selection of appropriate values for time on dialysis and time between dialyses to achieve desired post-dialysis and maximum allowable next pre-dialysis serum levels of waste products. It is also suggested (Walker et al, 1975) that deviations from predicted values reflect changes in the clinical state of the patient.

(3) Lott, Moorhouse And Whitt (1977):

Interactive use of the system developed by Lott and associates, aids the clinician in the selection of values for duration of dialysis, blood flow rate through machine and ultrafiltration pressure for optimum dialysis. A one compartmental model, based on the analysis by Renkin (1956), forms the basis of the system. The equations of the model relate the post-dialysis and next pre-dialysis concentration of urea, uric acid and creatinine to the variables of the dialysis therapy. Using the terminology of Table 3.10, these equations are:

$$C^f(n-1) = C^i(n-1) \times e\left(-\frac{(D+R)t}{V}\right) + \frac{G}{(D+R)}\left[1 - e\left(-\frac{(D+R)t}{V}\right)\right] \qquad (3.37)$$

$$C^i(n) = C^f(n-1) \times e\left(-\frac{Ru}{V}\right) + \frac{G}{R}\left[1 - e\left(-\frac{Ru}{V}\right)\right] \qquad (3.38)$$

The volumes of distribution and rates of generation are calculated using the results of previous dialyses.

The change in the body weight of the patient with time is described by consideration of the ultrafiltration pressures, P_1, P_2 ... P_n, during time intervals $(0,t_1)$, (t_1,t_2) ... (t_{n-1},t_n) in dialysis:

$$W^f(n) = W^i(n) + W^g(n) - \sum_{j=1}^{n} \int_{t_{j-1}}^{t_j} P_j \mu A dt \qquad (3.39)$$

Decrease in the permeability of the dialysis membrane through use is represented by having the dialysance and ultrafiltration coefficients as functions of time. By entering

TABLE 3.10. Variables Of The Model By Lott, Moorhouse And Whitt (1977).

$C^f(n)$	Post n^{th} dialysis concentration of waste product.
$C^i(n)$	Pre n^{th} dialysis concentration of waste product.
D	Dialysance.
R	Residual renal function.
V	Volume of distribution.
t	Time on dialysis.
G	Generation rate of waste product.
u	Time between dialyses.
$W^f(n)$	Post n^{th} dialysis weight.
$W^i(n)$	Pre n^{th} dialysis weight.
$W^g(n)$	Weight gained due to food and fluid intake between $(n-1)^{th}$ and n^{th} dialysis.
P	Ultrafiltration pressure.
μ	Ultrafiltration coefficient.
A	Dialysis machine membrane area.

the results of the previous dialysis and the desired final values for serum concentrations of the waste products and body weight, the system aids the clinician in the selection of values for the duration of dialysis, mean ultrafiltration pressure and the blood flow rate through the dialysis machine. The fact that the rate of removal of fluid is higher at the start of dialysis than at the end, is compensated for by the system. The suggested treatment schedule for optimal dialysis, with half hourly increments of ultrafiltration pressure from an initial value below the mean to a final, above, gives a nett removal of fluid from the body equal to that as if the mean pressure had been applied throughout dialysis.

(4) Abbrecht And Prodany (1971):

Abbrecht and Prodany developed a model in which the patient is represented by a two compartmental system with equations describing the dynamics of urea, creatinine and the 'impermeable solutes' in the intracellular and extracellular pools, and the transfer of water between the pools. The impermeable solutes are considered to be all the solutes in the body fluid compartments apart from urea and creatinine. These solutes are assumed to have no nett mass transfer across the cell membrane, and indeed are also assumed to be in balance with the dialysate bath fluid. The dialysate bath is assumed to have an inlet flow rate of fresh dialysate and an overflow rate, leaving a constant bath volume.

The equations of the model described below use the terminology of Table 3.11. The transfer of waste solutes from the extracellular pool to the dialysate bath is governed by the diffusion equation:

$$N_i = D_i \times (C_E - C_B)_i \qquad (3.40)$$

Similarly the movement of urea and creatinine from the intracellular to the extracellular compartment is represented by:

$$M_i = K_i \times (C_I - C_E)_i \qquad (3.41)$$

The rate of change of intracellular fluid volume is given by:

$$\frac{dV_I}{dt} = L_p \times \sum_{j=1}^{3} \sigma_j \times (C_I - C_E)_j / C_w \qquad (3.42)$$

The reflection coefficients, σ_j, $j = 1 - 3$, were taken to be unity for all solute species, and the water concentration, C_w, was assumed to be a constant value of 55.6 mmols./ml..

On the basis of the above assumptions, ten differential equations were derived, describing the dynamics of intracellular and extracellular fluid volume compartments, and the concentrations of urea, creatinine and the impermeable solutes in the intracellular and extracellular fluid compartments, and urea and

TABLE 3.11. Variables Of The Model By Abbrecht And Prodany (1971).

N_i	Rate of flux of solute, i, from the extracellular pool to the dialysate bath.
D_i	Dialysance of solute, i.
C_{Ei}	Extracellular concentration of solute, i.
C_{Bi}	Dialysate bath concentration of solute, i.
M_i	Rate of flux of solute, i, from the intracellular to the extracellular pool.
K_i	Cell membrane mass transfer coefficient for solute, i.
V_I	Intracellular fluid volume.
L_p	Intracellular-Extracellular pressure - filtration coefficient.
σ_i	Staverman reflection coefficient.
C_w	Concentration of water.

creatinine dynamics in the dialysate bath.

The equations were used to simulate actual dialyses on six patients. Cell membrane mass transfer coefficients were adjusted for each patient so that the model gave the best fit to the actual data, and the dialysance parameters were interpolated from the dialysis results for each patient. Other parameters were taken from literature. The authors report that a reasonable match was obtained between actual data and simulation results, and that the model could be used with mean values for the patient dependant parameters to analyse the effects of various therapy strategies in order to minimize the cost of dialysis.

3.2.2. Discussion On Renal Dialysis Models.

The four models described above all share the same general objective - the improvement in the management of renal dialysis patients. The simpler models of Walker et al (1975) and Lott et al (1977) are designed primarily to be used in the clinic to

aid in the selection of parameters of dialysis therapy for individual patients, whereas the models of Ramirez et al (1972) and Abbrecht and Prodany (1971) are designed primarily to be used in the analysis of the effects of different generalized strategies for renal dialysis treatment.

Each model describes the effects of dialysis on the dynamics of the concentrations of the waste products in the body. In addition, certain other factors are incorporated in each model, depending on the precise objectives for the model. For instance, the model of Ramirez et al (1972) incorporates the dynamics of the pressure in the cerebrospinal fluid compartment, and the model of Lott et al (1977) represents the change, with time, in the permeability of the dialysis membrane. Conversely, inherent in each model is a set of assumptions concerning the factors not incorporated in the particular system model.

Each of these models considers the body fluid compartments and the effects of dialysis on them in isolation from any other subsystems of the human organism. However, the well-being of the dialysis patient is dependant of the state of other subsystems, the most obvious being the cardiovascular system. It may be concluded from the omission of any other subsystems, either that these models are not concerned with the overall management problem of the dialysis patient, or that the effects of dialysis on the other subsystems are assumed to be unimportant to patient well-being. However, one of the primary objectives for the work described in this thesis, as discussed in the next section, is the prediction of the overall state of the dialysis patient during and after dialysis.

3.3. Discussion.

The discussion of previous models clearly demonstrates that the form of a model is dictated by the underlying objectives to be met by the analysis. Therefore, examination of the objectives for this work in relation to those of the models previously described indicates the necessary form of the model developed and described in the following chapter.

The objectives for this work, as described in Chapter 1, are to build a mathematical model to be used for the following purposes:

(1) Prediction of the state of the patient during and after dialysis;
(2) Utilization of the model to test various hypotheses concerning the renal - body fluid system;
(3) Examination of the structure of the model and data generated in order to search for the causes of the unexplained phenomena that are occasionally observed during dialysis.

In order to satisfy these objectives, the model representing normal human functions was formulated so that various renal malfunctions could easily be superimposed to represent individual dialysis patients. The overall model consists of the following subsystem models:

(1) Thermoregulatory system model,
(2) Electrolyte (sodium and potassium) and body fluid (intracellular and extracellular) compartments model,
(3) Cardiovascular system model,
(4) Overall renal function (including hormonal control system) model,
(5) Waste products (urea and creatinine) dynamics,
(6) Dialysis machine (switched on or off) model.

The practicalities involved with the clinical use of the model impose a constraint on its overall size in terms of the number of subsystems and the complexity with which they are represented. On the other hand, the hypothesis testing

requirements of the work demands that the model be isomorphic with the system modelled as far as permitted by current knowledge, at least with the subsystems on which these tests are to be performed. From a consideration of these facts, the objectives and previous models, some of which are described in this chapter, the following strategies were adopted for the formulation of the major subsystems of the model.

The thermoregulatory system model plays a role in this work primarily in the analysis of the model structure and data generated in order to determine the causes of phenomena observed during dialysis. The core and surface temperatures of the patients are routinely measured during dialysis. Therefore the passive system was satisfactorily represented simply as core and surface compartments. However, it is clear from the trend in the modelling of this system that the thermoregulatory control of peripheral blood flow greatly influences the dynamics of body temperature. Hence the thermoregulatory controller was considered in more detail during model formulation, as discussed in the following chapter.

During dialysis only a few of the important variables of the cardiovascular system are of interest to the clinician. In addition, short term dynamic effects may be neglected since the clinician is only interested in longer term effects. Therefore a simple model based on that of Guyton (1972) was found to be satisfactory for our purposes.

Although dialysis patients have little or no kidney function, it was considered necessary to examine and represent the renal - body fluid regulating system in some detail for the purpose of utilizing the model as an instrument to test hypotheses. Hence the subsystem model, including the hormonal control systems is based on the physiology described in the preceeding chapter. However, the depth of knowledge of the system is not sufficient to avoid the use of empirical relations for many of the functions in the real system.

Dialysis is then easily represented by superimposing appropriate degrees of renal malfunctions and logically switching the dialysis machine model into the rest of the system model. Appropriate simulation then yields prediction of the dynamics of the clinically important variables. These

results may be used to examine the effects of generalized strategies of dialysis therapy as well as the outcome of a single treatment on a particular patient in the clinic.

The model, as described in the following chapter, was developed on the basis of the considerations discussed above.

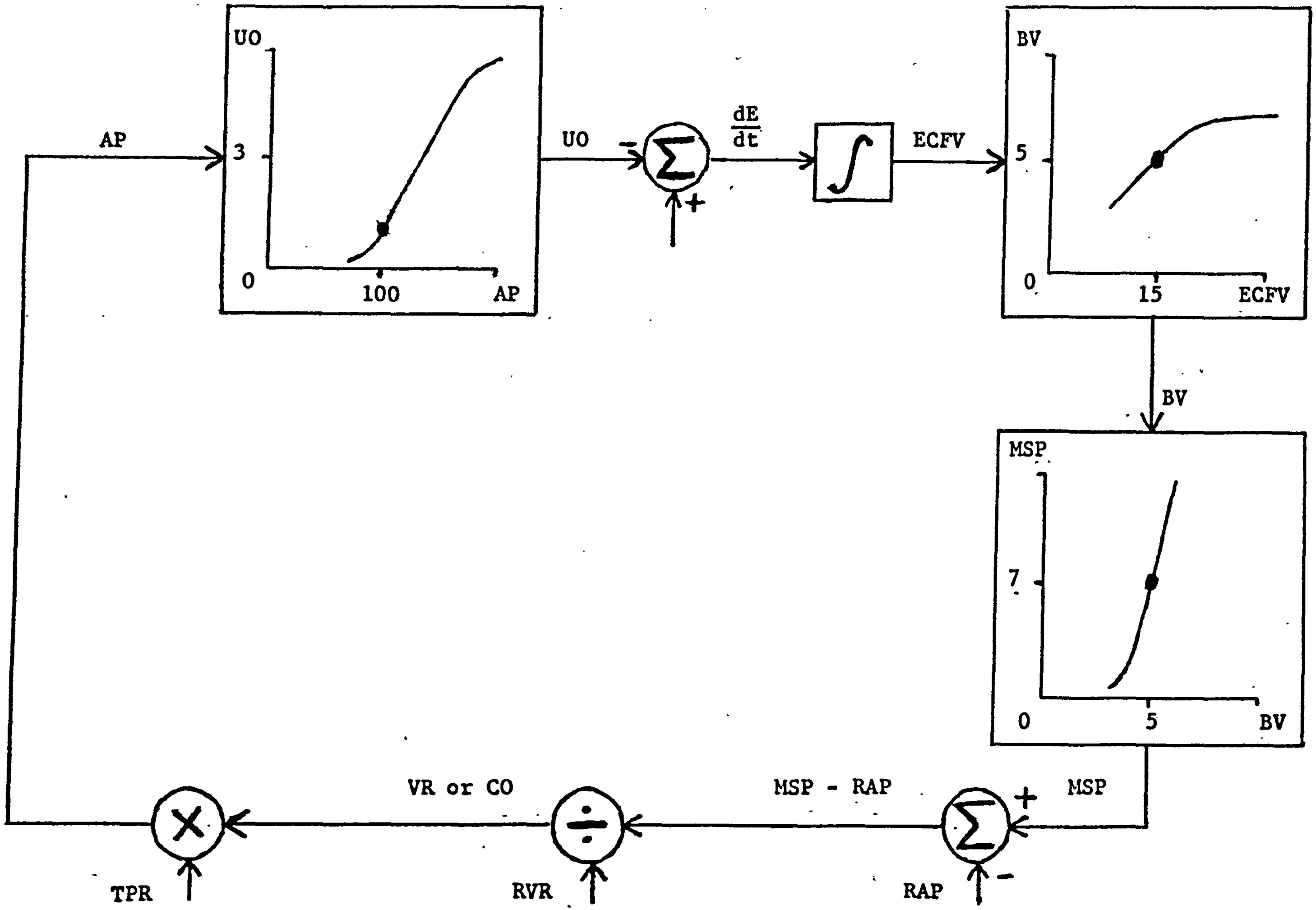

Figure 3.1. Block diagram of basic circulation model (Guyton and Coleman, 1967).

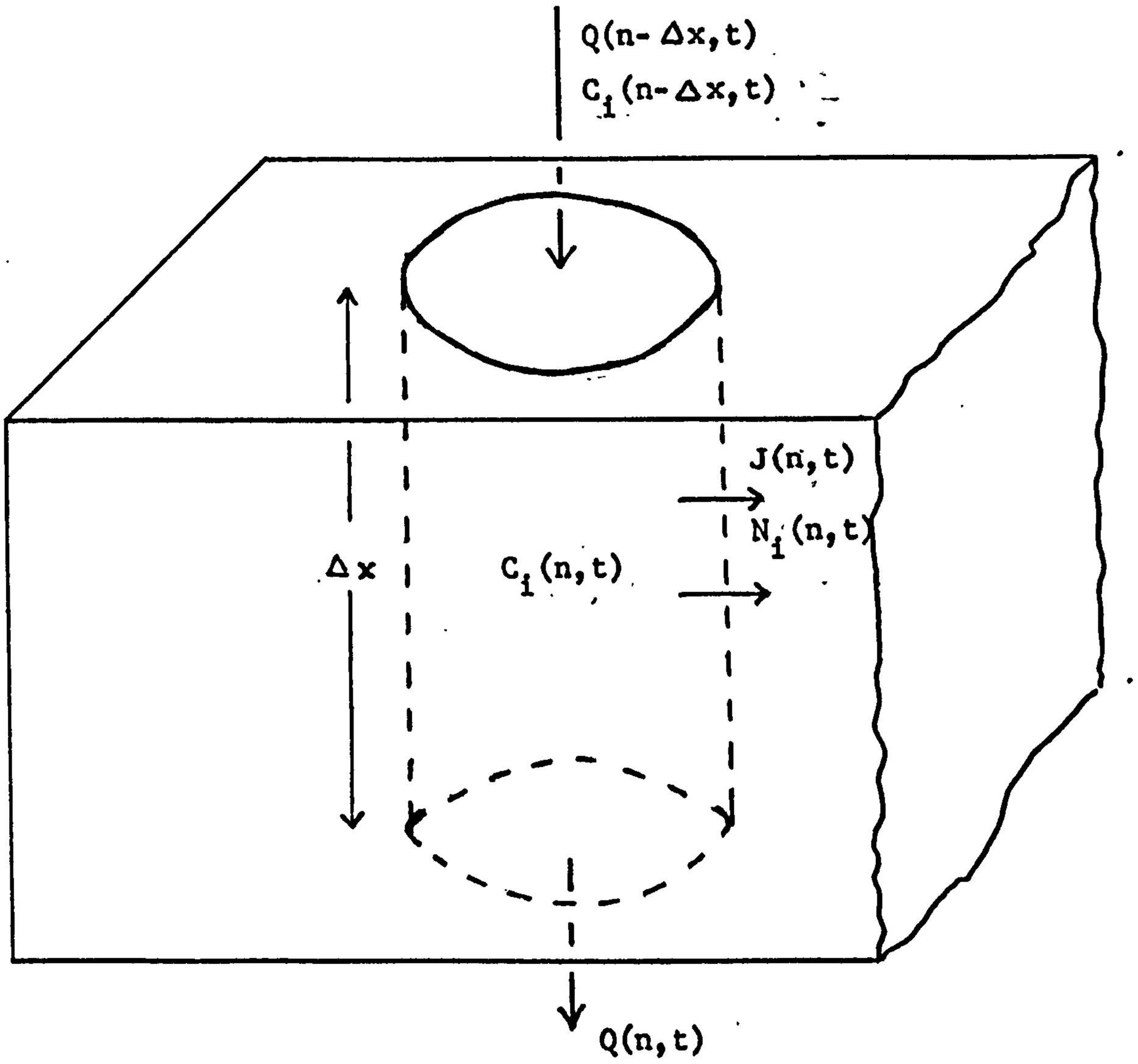

Figure 3.2. Diagram of a segment of a tubule in the medullary interstitium (Cage et al., 1977).

CHAPTER 4

THE MODEL.

In this chapter a detailed account is given of the formulation of the mathematical model built in order to achieve the objectives stated in previous chapters. This model was developed to represent the appropriate functions of the normal human organism so that the effects of varying degrees of renal failure may be superimposed to represent individual patients undergoing dialysis. The structure of the model, consisting of interconnected models of six major systems, is based on current understanding of the appropriate physiology, and as far as possible, the relationships between variables are derived from data presented in the literature.

The major subsystem models and their interconnections are represented in Figure 4.1, and the equations comprising each of the subsystems are derived in the sections below. The nomenclature for the equations is listed in Appendix I, and a full listing of the equations is given in Appendix II.

4.1. Thermoregulatory System Model.

The thermoregulatory system model developed for this work relies on the concepts of the hypothalamic set-point theory for the control of deep body temperature. Control is effected by vasomotor adjustment of the rate of blood flow from the core to the surface of the body.

A conceptual model of the set-point theory of thermoregulation is presented in Figure 4.2. The temperatures in the core and surface of the body are sensed by thermoreceptors, and signals representing these temperatures are transmitted to the hypothalamus. These signals are compared with the hypothalamic 'set-point' temperatures, and signals representing the differences between the actual and set-point temperatures are transmitted to the vasomotor centre of the central nervous system. Appropriate sympathetic or parasympathetic stimulation causes a change in the

rate of blood flow, and therefore heat transfer, from the core to the surface of the body. An increase in the rate of blood flow results in an increase in the temperature of the surface of the body and subsequently, an increase in the rate of heat loss from the surface of the body to the environment. The converse is also true. The actions of the passive and controlling systems of thermoregulation are summarized in Figure 4.3, where the core and surface temperatures in the system model cause an appropriate change in the rate of blood flow to the surface, in order to return the temperatures in the passive system towards their set-point values.

The shivering and sweating heat exchange mechanisms are not incorporated in the system model since it is assumed that patients undergoing dialysis are not subjected to thermal stresses which would require the actions of these temperature control mechanisms.

The passive system is described mathematically by appropriate heat balance equations below, and the controlling system equations are derived in the following subsection.

4.1.1. The Passive System.

Figure 4.4 gives a representation of the mechanisms of heat exchange within the controlled system of the thermoregulatory model. The derivation of the heat balance equations for the core and surface compartments is also dependant on the following assumptions.

(1) For thermoregulation, it is assumed that the human body may be considered as two homogenous concentric cylinders, each with uniformly distributed temperatures, where the surface cylinder represents the outer two centimetre layer of the body, and the core cylinder represents the remainder of the body.
(2) The rate of metabolic heat generation in the patient is assumed to be constant at the basal level.
(3) It is assumed that there is negligible axial heat transfer in the body. Hence, only the radial flux of heat is considered in the system model.

(4) The mechanisms of heat transfer between the portions of the body represented by the two compartments are conduction and convection due to the flow of blood between compartments. The rate of heat transfer by conduction is considered to be proportional to the difference between the temperatures of the two compartments; and the rate of heat transfer by convection, proportional to the product of this temperature difference and the rate of blood flow between the compartments in the system model.

(5) Blood is assumed to be in thermal equilibrium with the portions of the body represented by the core compartment of the model.

(6) It is assumed that the patient undergoing dialysis is not thermally stressed to an extent which causes shivering or sweating. Hence, in the model, the factor representing the rate of heat loss due to evaporation from the surface of the body is constant and equal to the basal level. Similarly, the factor representing the rate of heat loss from the core due to respiration is constant.

(7) It is further assumed that the remaining mechanisms of heat transfer from the surface of the body to the environment, namely convection and radiation, may be represented simply as a factor proportional to the difference in the temperatures of the surface compartment and the environment in the system model.

Hence the heat balance equation for the core compartment is:

$$C_c \times \frac{dT_c}{dt} = BMRC - K_{cs} \times (T_c - T_s) - \rho \times c \times SBF \times (T_c - T_s) - RHL \qquad (4.1)$$

This states that the rate of accumulation of heat in the core compartment is equal to the algebraic sum of the rates of heat gain and heat loss factors in this compartment. The heat gain factor represents the constant metabolic heat generation rate in the core compartment; the heat loss factors represent the rates of conduction and convection of heat to the surface compartment and the constant rate of heat loss to the environment due to respiration.

The heat balance equation for the surface compartment is:

$$C_s \times \frac{dT_s}{dt} = BMRS + K_{cs} \times (T_c - T_s) + \rho \times c \times SBF \times (T_c - T_s) - K_{se} \times (T_s - T_e) - IHL \qquad (4.2)$$

The factors for heat gain by the surface compartment represent the constant basal metabolic heat generation rate assigned to the surface and the rates of conduction and convection of heat from the core to the surface compartment. The heat loss factors represent the radiation, conduction and evaporation heat loss rates from the surface of the body to the environment. The rate of accumulation of heat is given by the algebraic sum of these rates of heat gain and loss.

Numerical values for the parameters of equations (4.1) and (4.2) may be found in Appendix I. These values were derived by appropriately combining the anatomical and thermal parameters used by Stolwijk and Hardy (1966) in their model of human thermoregulation based on seven compartments. The values presented by them are for a standard man of 71 kilogrammes body weight. Hence the calculated values for the thermal capacitances of the core and surface compartments are scaled in the system model according to the weight of the individual patient. In addition, the value for the heat transfer coefficient from the surface of the body to the environment is reduced by a factor, in order to represent a patient lying in bed with bed-clothes.

The passive system model for thermoregulation is therefore described by equations (4.1) and (4.2).

4.1.2. The Controlling System.

The passive system of the thermoregulatory system model, by itself, does not exhibit control characteristics, but does represent a transfer function between a disturbance and the controller (Figure 4.3). It is therefore the controller that regulates the body temperature by adjusting the rate of blood flow from the core to the surface of the body.

When the body needs to dissipate heat (when core temperature rises above the set-point), peripheral blood vessels are caused to vasodilatate, permitting a larger flow of warm arterial blood to the surface of the body. Hence, the temperature at the surface of the body rises, and results in the increase in the rate of transfer of heat to the environment. Thus the temperature at the core of the body is returned towards the set-point. When the body needs to conserve heat, the converse effects are observed, brought about by vasoconstriction of the peripheral blood vessels (Rush and Patton, 1965).

Vasodilatation or vasoconstriction may be considered as the decrease or increase in the resistance to the flow of blood in the surface of the body. Figure 4.5 presents a simple electrical analogy of this concept. The pressure drop, AP, forces blood through the resistances, R_c and R_s, representing the resistances to blood flow through the core and surface blood vessels respectively. Hence, of the total rate of blood flow, CO, the rate at which blood flows through the surface blood vessels, SBF, is dependant on the relative values of the two resistances, R_c and R_s. For the development of the model for the controller in the human thermoregulatory system, the resistance to blood flow through the core of the body is assumed to be constant, whereas the resistance to blood flow through the surface blood vessels is considered to be a function of the passive thermoregulatory system model.

The mechanisms involved in the thermoregulatory controller are well known in a qualitative sense. It is generally accepted that temperature sensitive receptors in the hypothalamus (Hammel et al.,1963), other regions deep in the body (Robinson et al., 1965) and in the skin (Hardy and Stolwijk, 1966) are involved in the transmission of signals that bring about the vasomotor effector actions for thermoregulation. However, little is known quantitatively about the relation between these signals and the resulting vasomotor actions. Therefore, the system model uses the hypothetical relationship of Figure 4.6 as the function between core temperature and the rate of blood flow through the surface of the body. The normal value for the resistances, R_s, for the range of core temperatures, $(36.4 < T_c < 37.0)$, was

derived from consideration of Figure 4.5 and normal values of arterial pressure (100 mm.Hg.), cardiac output (5 litres/min.) and normal surface blood flow (223.0 ml./min.) (Stolwijk and Hardy, 1966).

A lower limit for the rate of blood flow through the surface of the body (hence an upper limit for the resistance, R_s, in the model) exists in order that the supply of necessary nutrients to the tissues of the surface is not stopped. In the system model this lower limit was considered to be one tenth of the normal rate of blood flow, yielding a maximum value for the resistance of 4485 mm.Hg/litre min.$^{-1}$, for a normal arterial pressure of 100 mm.Hg., at core temperatures below 35.0^{o}C.. Similarly, there is a lower limit below which the resistance does not drop, since the surface blood vessels have a finite compliance. This was considered to be a value of 64.0 mm.Hg./litres min.$^{-1}$, yielding a rate of blood flow seven times normal at normal arterial pressure, for values of core temperature greater than 38.5^{o}C.. Figure 4.6 shows that the relationship between the variables in the model representing core temperature and resistance to blood flow through the surface of the body for ranges of core temperature, ($35.0 < T_c \leqslant 36.4$) and ($37.0 \leqslant T_c < 38.5$) are considered to be straight line functions between the limiting values and normal value of resistance, R_s. In addition, for the range of core temperatures which causes no net vasoconstriction or vasodilatation in the model ($36.4 < T_c < 37.0$), the value for skin temperature in the model is considered to control the resistance to blood flow in the surface in accordance with the function described by Figure 4.7. This function is included to represent the local thermoregulatory control of blood flow in the tissues of the surface in order to minimize temperature differences within the body (Ruch and Patton, 1965), and therefore to control the surface temperature of the body.

The rate of blood flow through the surface is then calculated:

$$SBF = AP / R_s \qquad (4.3)$$

where the value for arterial pressure, AP, is obtained from the cardiovascular system model.

The relationships used in the controller system model (Figures 4.6, 4.7) have been derived in a rather arbitrary manner due to the lack of quantitative information regarding the human thermoregulatory controlling system. However, the concepts on which these relationships are based are in agreement with the general theories of thermoregulation. A description of these theories may be found in the recent review by Fox (1974).

4.1.3. Links With Other Subsystem Models.

Figure 4.1 shows that the value for arterial pressure, AP, used in the model above is obtained from the cardiovascular system model, and that the thermoregulatory system model generates a value for total peripheral resistance, TPR, as affected by thermoregulation.

It has been stated that the resistance to blood flow through the core of the body is set to a constant value in the model. The value is calculated on the basis of the system as depicted in Figure 4.5, operating with normal values for the variables. Hence

$$R_c = AP/(CO-SBF) = 100.0/(5.0-0.223)$$
$$= 20.934 \text{ mm.Hg./l.min.}^{-1}$$

The value for total peripheral resistance is then given by considering the two resistances in parallel in Figure 4.5:

$$TPR_{TH} = \frac{R_s \times 20.934}{R_s \times 20.934} \qquad (4.4)$$

4.1.4. Summary Of The Thermoregulatory System Model.

The formulation of the mathematical description of the human thermoregulatory system - indeed, for any system - involved the use of several simplifying assumptions. One major simplification is the consideration of the coefficient for the rate of transfer of heat from the surface of the body to the environment

by convection and radiation, K_{se}, as a constant. A more accurate description of these heat transfer processes would be based on material presented by Hardy and associates (1970). However, the justification for having adopted the simple approach described above stems from the clinical use of the model, since the other approach would not only add to the computer memory requirements, but also add to the complexity in using the system in the clinic for patient management. In addition, it is uncertain whether the need exists for the benefits of using the complex modelling approach for the purposes of this work.

Another simplification is the mathematical treatment of the thermoregulatory controller. This was largely due to the lack of meaningful data regarding this system. However, the functions used were selected on the basis of simulations of the thermoregulatory system model with several candidate functions of the controller. It was found that the model responded satisfactorily without any instability with the controller model described above.

These and other assumptions were deemed to be acceptable from consideration of the results of the validation tests described in subsequent chapters.

4.2. Cardiovascular System Model.

Two basic reasons exist for including a model of the cardiovascular system in the overall system model. Firstly, certain variables of the cardiovascular system interact with other subsystem models as shown in Figure 4.1. Secondly, some of the variables of the cardiovascular system are important in establishing the state of the patient undergoing dialysis. However, for patient management, it is more important to know the trends of these variables rather than their absolute values with accuracy. For instance, the clinician is more interested in whether the arterial pressure of his patient is rising away from or falling back towards a more normal value, rather than to know the precise pressure at a particular instant. Hence, for this reason, and also from consideration of the time spans of simulations necessary for the objectives of this work (30 minutes

to several hours), the primary requirement for the model is prediction of the trends of the key variables in the longer term. Therefore the phenomena which affect the cardiovascular system only in the relative short term were neglected in the modelling process.

The model of Guyton and Coleman (1967), briefly described in the previous chapter, is simple, yet sufficient for the requirements stated above. Hence the model developed below, and shown in block diagram form in Figure 4.8, relies largely on the concepts and data used for the model developed by Guyton and Coleman. The function of each block and the assumptions made in the development of the model are detailed below.

4.2.1. Derivation Of The Model.

Block 1 represents the algebraic summation of the rates of fluid gain by ingestion, FLUMIN, and fluid loss by urine flow, UFL, to give the rate of change of extracellular fluid volume, $\frac{dE}{dt}$.

Block 2 integrates this rate of change, giving the extracellular fluid volume, E, at any instant.

Block 3 represents the non-linear relationship between extracellular fluid volume, E, and blood volume, BV, as established by experiments (Guyton and Coleman, 1967). The relationship is linear up to a value of extracellular fluid volume slightly greater than 20 litres. A further expansion of extracellular fluid volume causes little further increase in blood volume, and marks the onset of the state of oedema, where the excess fluid stays mainly in the interstitium. The quantitative function used to represent this relationship in the model is:

$$\left.\begin{array}{ll} BV = 0.33 \times E & \text{if } E < 21.0 \text{ litres} \\ BV = 0.015 \times E + 6.6 & \text{if } E \geq 21.0 \text{ litres} \end{array}\right\} \qquad (4.5)$$

Mean systemic pressure may be defined as the extent to which The systemic circulation is filled with blood. Theoretically, mean systemic pressure is equal to the sum of the pressures in all the individual segments of the systemic circulation when each

of these pressures is weighted by a factor equal to the compliance of the respective individual segment divided by the compliance of the whole systemic circulation. In practice, it is measured by stopping the circulation and rapidly pumping blood from the arteries to the veins till the pressures are in equilibrium. This equilibrium pressure is then approximately equal to the mean systemic pressure.

Block 4 represents the relationship between blood volume, BV, and mean systemic pressure, MSP, which was experimentally derived by Richardson and associates (1961). This relationship is quantitatively represented in the model by the function:

$$MSP = 3.5 \times BV - 10.5 \qquad (4.6)$$

Sympathetic and parasympathetic stimulation are also determinants of mean systemic pressure. However, since the effects of autonomic nervous activity on the circulation are transient relative to the time spans of interest in this work, the autonomic nervous system is not modelled.

Total peripheral resistance to blood flow is subject to alteration by many factors, including tissue demand for oxygen and nutrients, autonomic nervous activity and levels of circulating pressor substances (Johansson, 1978). For the purpose of this work, the only factors determining the value of total peripheral resistance in the model are the thermoregulatory demand for blood flow, as described previously, and the level of the pressor substance, angiotensin II, in plasma. All other factors are assumed either to have only transient effects on the resistance to blood flow or to remain constant at normal levels in the dialysis patient.

The approximate relation between the level of angiotensin II in plasma and the change in blood pressure due to the pressor effect was derived from the results of experiments of incremental angiotensin II infusion in humans (Oelkers et al.,1974; Deheneffe et al., 1976). The relationship for the change in total peripheral resistance, DTPR, due to the level of angiotensin II in plasma, A, represented by Block 5 in Figure 4.8, was then extrapolated from these data. The resulting function used in the

model is:

$$\left.\begin{aligned} DTPR &= 0.037xA - 1.0 && \text{if } A \leqslant 27.0 \text{ ng./l.} \\ DTPR &= 5.44x\log_{10}(A) - 7.8 && \text{if } A < 27.0 \text{ ng./l.} \end{aligned}\right\} \qquad (4.7)$$

The value for DTPR then modulates the value for total peripheral resistance generated by the thermoregulatory system model, TPR_{TH}, to give the overall value of total peripheral resistance, TPR:

$$TPR = TPR_{TH} + DTPR \qquad (4.8)$$

Block 6 represents the process of equating the cardiac function curve and venous return curve to yield values for right atrial pressure, RAP, and venous return, VR, which, according to the Frank-Starling law of the heart, is equal to cardiac output, CO, (Guyton, 1971). The Frank-Starling law of the heart states that the heart pumps out as much blood as that which flows into it, within physiologic limits. The principle mechanism by which this is achieved is known as the heterometric autoregulation of the heart, whereby the more the muscular walls of the cardiac chambers are stretched by incoming blood, the greater the force of contraction and outflow of blood from the heart (Guyton, 1971). Using this relationship, the function of the heart as a pump is then suitably described by the cardiac function curves, depicted in Figure 4.9, which relate the pressure in the right atrium (that is, the extent to which it is filled) to the rate of blood flowing out of the left ventricle or the cardiac output.

Figure 4.9 shows a set of cardiac function curves, representing the hypoeffective, normal and hypereffective heart. The effectiveness of the heart as a pump varies with certain factors - the short term variation due to sympathetic and parasympathetic stimulation being the most important. Other factors include the deteriorating effects of abnormally high levels of certain cations in the fluids surrounding the heart and the effects of previous damage to heart tissues (Guyton, 1971).

The relatively short term effects of sympathetic and parasympathetic stimulation on the effectiveness of the heart as a

pump are not taken into account in the model. However, the level of hypoeffectiveness of the heart is determined by relationships dependant on a parameter specified by the clinician concerning the state of the heart of the individual patient (see Chapters 6 and 8), and also on the levels of sodium and potassium in the extracellular fluid, PNA and PK respectively.

Although evidence suggests a more complex relationship (Hoff et al., 1939; Friedman et al., 1959), as a first approximation, the relationship between the effectiveness of the heart as a pump, CE, and the excess cations in the extracellular fluid was assumed to be of the form:

$$\left.\begin{array}{ll} CENA = 1.0 & \text{if } PNA < 148.0 \\ CENA = -0.0125 \times PNA + 2.85 & \text{if } PNA \geq 148.0 \end{array}\right\} \quad (4.9)$$

$$\left.\begin{array}{ll} CEK = 1.0 & \text{if } PK < 6.5 \\ CEK = -0.065PK + 1.43 & \text{if } PK \geq 6.5 \end{array}\right\} \quad (4.10)$$

$$CE = (CENA + CEK) \times 0.5 \quad (4.11)$$

In addition, the parameter specified by the clinician for the state of the heart of the patient is also accounted for so that the level of hypoeffectiveness of the heart, and thus the operating pressure - flow relationship of Figure 4.9 is determined.

Block 6 of Figure 4.8 also shows the systemic function curve which relates the rate of blood returning to the heart from the veins to the pressure in the right atrium. This curve is the graphical representation of the relationship between the pressure drop across the systemic veins, (MSP - RAP), the resistance to blood flow in the systemic veins, RVR, and the resulting rate of venous return, VR:

$$VR = (MSP - RAP)/RVR \quad (4.12)$$

The collapse of veins at right atrial pressure of 0 mm.Hg. and below causes a sharp increase in the resistance to blood flow, which is demonstrated by the non-linearity in the systemic function curve. This is seen more clearly in Figure 4.10, which

shows a set of systemic function curves for various values of mean systemic pressure.

In the model, the value for the resistance to venous return, which determines the slope of the linear portions of the systemic function curves, is assumed to be a constant fraction (0.07) of the value for total peripheral resistance (Guyton, 1971).

Hence, the operating cardiac function curve in determined by the level of hypoeffectiveness of the heart as a pump, and the operating curve for systemic function is determined by the values of mean systemic pressure and total peripheral resistance generated previously in the model. Since venous return is equal to cardiac output (Frank-Starling law of the heart) equating the appropriate cardiac function and systemic function curves yields values for venous return or cardiac output, and for right atrial pressure.

Block 7 of Figure 4.8 represents the pressure - flow relationship between total peripheral resistance, TPR, cardiac output, CO and arterial pressure, AP:

$$AP = CO \times TPR$$

In order to accomodate differences in the cardiovascular systems of individual patients, and also to represent very long term effects on the circulation, a steady state bias, calculated from initial condition information, was included in the above relationship:

$$AP = CO \times TPR + DAP_o \qquad (4.13)$$

4.2.2. Summary Of The Cardiovascular System Model.

The model of Guyton and Coleman (1967) utilizes an experimentally derived relationship between arterial pressure and urine flow rate in order to close the loop on their cardiovascular system model. However, for the purposes of this work, the various renal and hormonal factors affecting the rate of urine flow in

the normal human have been modelled in considerably greater detail as described in the following sections of this chapter.

The model of the cardiovascular system, as described above, does not incorporate mathematical representations of many of the controllers which affect the circulation on a relatively short time scale. The anticipated result of these omissions is that the fine detail of the dynamic behaviour of the variables in the real system will not be matched by the simulations. However, as demonstrated in the validation exercises described in subsequent chapters, this limitation is of little consequence, since the more important objective of the prediction of the overall trends of the variables is met.

4.3. The Kidney Function Model.

The functions of the renal system were described in a qualitative manner in Chapter 2 of this thesis. In particular, a discussion was presented in section 2.2.1, with reference to the diagram of Figure 2.4, regarding the currently accepted theories related to the formation of the glomerular filtrate and the subsequent processing of the tubular fluid as it passes through the major segments of the nephrons before entering the bladder as urine.

Considering the kidneys as one large nephron, mathematical expressions are derived below, representing the effects of these kidney functions on the tubular processing and eventual excretion of sodium, potassium and water in the urine. Data reported in the literature were used in the derivation of the relationships between variables wherever possible, but owing to the fact that renal physiology is still not clearly understood, certain assumptions concerning renal function had to be made.

The subsections below state these assumptions and describe the data used to derive the resulting equations, which represent glomerular function, proximal tubular processing, the effects of the loop of Henle and the actions of aldosterone and the anti-diuretic hormone (ADH) on the fluid in the distal portions of the nephron.

4.3.1. Glomerular Function Model.

It was stated in section 2.2.1 that the rate of formation of glomerular filtrate, GFR, is dependant on the nett pressure forcing fluid across the glomerular capillary membranes in the Bowman's capsules of the nephrons. The nett filtration pressure, P_f, is equal to the difference between the hydrostatic pressure in the capillaries, P_g, which is dependant on mean arterial pressure, AP, and the sum of the glomerular colloid osmotic pressure, π_g, and the hydrostatic pressure of the fluid surrounding the capillaries, P_B.

The assumption is made that variations within the physiological ranges of the pressures, π_g and P_B, have negligible effects on glomerular filtration. The data shown in Figure 4.11, resulting from experiments by Shipley and Study (1951), relating GFR and AP, is therefore used to derive the expression below governing GFR:

$$\left.\begin{array}{ll} GFR = 0.0 & \text{if } AP \leqslant 20.0 \text{ mm.Hg.} \\ GFR = 1.92 \times AP - 38.4 & \text{if } 20.0 < AP \leqslant 75.0 \text{ mm.Hg.} \\ GFR = -0.00808 \times AP^2 + 2.195 \times AP - 13.6 & \\ & \text{if } 75.0 < AP \leqslant 120.0 \text{ mm.Hg.} \\ GFR = 0.035 \times AP + 129.2 & \text{if } AP > 120 \text{ mm.Hg.} \end{array}\right\} \quad (4.14)$$

The relative constancy of glomerular filtration rate as renal arterial pressure rises above and beyond the value of 90 mm.Hg. is known as the renal autoregulation of glomerular filtration rate. It has been demonstrated that this phenomenon is due to adaptive changes in the resistance of the afferent arterioles to renal blood flow (Thurau and Krammer, 1959). Hence, this is consistent with the macula densa sodium concentration theory of renin release (Thurau et al., 1967), outlined in Chapter 2 of this thesis, and with the theory of tubulo-glomerular feedback controlling GFR by the renin-angiotensin system (Vander, 1967).

Chemical analysis of the glomerular filtrate fluid, collected from the early portions of the proximal tubule have shown that it is iso-osmotic and isotonic with protein - free

plasma fluid obtained from the glomerulus (Windhager, 1968). Therefore, ignoring the slight error due to the Gibbs-Donnan effect, the rate of filtration of sodium into the proximal tubule, FNA, is given by:

$$FNA = GFR \times PNA / 1000.0 \qquad (4.15)$$

The glomerular filtrate then passes into the proximal and subsequent tubule segments for appropriate processing for homeostatis.

4.3.2. Proximal Tubule Segment.

(i) Sodium.

Approximately three-quarters of the filtered load of sodium is actively reabsorbed in the proximal tubule. The fraction reabsorbed appears to be independant of glomerular filtration rate (Windhager, 1968). This parallel relationship between glomerular filtration rate and the fraction of sodium reabsorbed in the proximal tubule is known as the glomerular-tubular balance.

However, it has been shown that glomerular-tubular balance is upset by changes in the concentration of sodium in the filtrate in the proximal tubule, which is essentially equal to the concentration of sodium in plasma (Johnston et al., 1967). This effect is thought to be mediated by, as yet, an undetermined natriuretic substance acting on the proximal tubule.

Since such a large proportion of the filtered load of sodium is reabsorbed in the proximal tubule, this is the most important mechanism for sodium homeostatis in the body. However, data pertaining to the relationship between intraluminal or plasma concentration of sodium, PNA, and the fraction of filtered load reabsorbed in the proximal tubules of human kidneys, GTB, are not available. Therefore, in the model, the relationship is approximated by the linear function:

$$GTB = -0.0357 \times PNA + 5.815 \qquad (4.16)$$

$$\text{with the constraint} \quad 0.75 \leqslant GTB \leqslant 1.0$$

The rate of reabsorption of sodium in the proximal tubule, SPTR, is then given by:

$$SPTR = GTB \times FNA \tag{4.17}$$

and the rate of flow of sodium into the loop of Henle, SFLH, is:

$$SFLH = FNA - SPTR \tag{4.18}$$

(ii) Water.

In the absence of significant amounts of poorly reabsorbable solutes, the fraction of the water load passively reabsorbed in the proximal tubule is equal to the fraction of the sodium load reabsorbed. This has been shown to occur in the kidney of the rat for a wide range of osmolality of the final urine (Malnic et al., 1966).

Hence, the rate of reabsorption of water in the proximal tubule, EPTR, is represented by the relationship:

$$EPTR = GTB \times GFR \tag{4.19}$$

and the rate of flow of water into the loop of Henle is given by:

$$EFLH = GFR - EPTR \tag{4.20}$$

(iii) Potassium.

Virtually all of the filtered potassium is reabsorbed in the proximal segments of the nephron of the rat (Malnic et al., 1964). Potassium in the urine is therefore due to nett secretion in the distal portions of the tubules. Hence, assuming these results may be extrapolated to human kidneys, only the secretion of potassium in the distal tubule is considered in the model.

4.3.3. The Loop Of Henle.

The morphology and transport characteristics of the loop of Henle, depicted in Figure 2.1, give rise to the primary mechanism

by which the kidneys control the osmolality of the final urine as required by the state of fluid balance in the body. In the course of this process, known as the countercurrent mechanism, the concentrations of the various substances in the tubular fluid undergo drastic changes as the fluid passes along the loop of Henle (Guyton, 1971).

The overall reabsorptive characteristics for sodium and water in the loop of Henle of the animal kidney have been determined experimentally (Landwehr et al., 1968). It has been demonstrated that the fraction of the water load reabsorbed is a function of the transit time, or an inverse function of the rate of flow, whereas the fraction of the sodium load reabsorbed remains fairly constant as the rate of flow of tubular fluid is varied. Hence, extrapolation of the data presented by Landwehr and associates (1968) to the human kidneys yields the following relationship, used in the model, to represent the rates of water, ELHR, and sodium, SLHR, reabsorbed in this nephron segment:

$$\left.\begin{aligned} EBLH &= (-0.01 \times EFLH) + 0.65 \\ ELHR &= EBLH \times EFLH \end{aligned}\right\} \qquad (4.21)$$

$$SLHR = 0.8 \times SFLH \qquad (4.22)$$

The rates of flow of water, EFDT, and sodium, SFDT, into the distal tubule are then given by the following equations:

$$EFDT = EFLH - ELHR \qquad (4.23)$$

$$SFDT = SFLH - SLHR \qquad (4.24)$$

It is assumed that the filtered load of potassium is totally reabsorbed in the proximal segments of the tubule. Hence potassium in the urine is due to active secretion in the distal portions of the nephron.

4.3.4. Distal And Collecting Segments.

The volume and osmolality of urine is controlled finally by the actions of the antidiuretic hormone (ADH) and aldosterone on the distal segments of the tubules. The permeability of these segments to water, and therefore the fraction of the tubular load of water reabsorbed, is controlled by changes in the concentration of ADH in plasma. The rate of reabsorption of sodium and the rate of secretion of potassium across the tubular walls are influenced by the concentration of aldosterone.

These hormonal control systems were described in Chapter 2, and the quantitative relationships which determine the concentrations of the hormones in plasma in the model are derived in section 4.4. The discussion below describes the derivation of the relationships used in the model to represent the actions of ADH and aldosterone on the distal and collecting segments of the nephron in the model.

(i) The Action Of ADH.

The rate of reabsorption of water from the luminal fluid in these nephron segments is controlled by the concentration of ADH in plasma (Guyton, 1971). Although the precise mechanisms involved are unknown, it is clear from experiments by Grantham and associates (1969) on the rabbit tubule, that the rate of reabsorption of water is influenced by some intracellular biochemical reaction initiated by the exposure of the surface of the peritubular membrane to a different concentration of ADH.

Data on the relationship between variations in plasma ADH levels and rates of reabsorption of fluid in the human tubules are not available. However, using data from the literature, Dehaven and Shapiro have derived a quantitative relationship between the plasma level of ADH and the resulting rate of urine flow in man for use in their model (Dehaven and Shapiro, 1970). From their relationship, assuming a normal value for the rate of delivery of tubular fluid to the distal tubule, the relationships below were derived to approximate the effect of variations in the plasma concentration of ADH (ADH) on the rate of reabsorption of fluid from the distal and collecting segments of the human nephron, ERDT:

$$
\begin{cases}
EBDT = 0.0 & \text{if } ADH \leqslant 0.765 \text{ munits/l.} \\
EBDT = 0.383 \times ADH - 0.293 & \text{if } 0.765 < ADH \leqslant 3.0 \\
EBDT = -0.0383 \times ADH^2 + 0.364 \times ADH + 0.109 & \\
\qquad \text{if } 3.0 < ADH \leqslant 5.0 & \\
EBDT = 0.0012 \times ADH + 0.9653 & \text{if } ADH > 5.0 \text{ munits/l.}
\end{cases} \quad (4.25)
$$

$$EDTR = EBDT \times EFDT$$

The rate of flow of urine, UFL, is then given by:

$$UFL = EFDT - EDTR \quad (4.26)$$

The action of ADH on the distally located nephron segments is, thus, represented by equations (4.25) and (4.26).

(ii) The Action Of Aldosterone.

(a) Sodium.

The rate of reabsorption of sodium across the distally located nephron segments in dependant on the plasma concentration of aldosterone (Lowitz et al., 1969). Experiments have shown that the fraction of sodium reabsorbed under the influence of aldosterone is approximately two per cent of the filtered load of sodium (Roemmelt et al., 1949).

Data regarding the effect of variations of the concentration of aldosterone in plasma, ALD, on the resultant rate of reabsorption of sodium across the distal and collecting tubules, SDTR, of the human kidneys are not available. Hence it was necessary to formulate the expression below to represent this function in the model:

$$
\begin{cases}
SDTR = 0.6 \times SFDT & \text{for } ALD \leqslant 0.0 \text{ng./l.} \\
SDTR = (0.003 \times ALD + 0.596) \times SFDT & \text{for } 0.0 < ALD \leqslant 85.0 \\
SDTR = (0.00021 \times ALD + 0.833) \times SFDT & \text{for } 85.0 < ALD \leqslant 800.0 \\
SDTR = SFDT & \text{for } ALD > 800.0 \text{ng./l.}
\end{cases} \quad (4.27)
$$

The expressions, (4.27), are based on the assumptions that when the level of aldosterone in plasma is low, the fraction of the distal tubular load of sodium reabsorbed is 0.6; and when the level of aldosterone in plasma is high (ALD > 800.0 ng./l.), the entire distal tubular load of sodium is reabsorbed. Therefore, the reabsorption of 40% of the distal tubular load of sodium is controlled by aldosterone. Considering steady state values of the filtration rate of sodium (17.75 mEq./min.) and the distal tubular load of sodium (0.8875 mEq./min.), the fraction of the tubular load of sodium under the influence of aldosterone in the model is equal to two per cent of the filtered load of sodium.

The rate of excretion of sodium in the urine, UNA, is then given by:

$$UNA = SFDT - SDTR \tag{4.28}$$

The influence of aldosterone on the reabsorption of sodium from the tubular fluid is, therefore, represented by equations (4.27) and (4.28) in the model.

(b) Potassium.

Malnic and associates have determined that the concentration of potassium in the fluid entering the distal tubule of the rat kidney remains relatively constant at very low levels, even when the kidneys are subjected to a wide variety of forcings. However, different forcings were seen to cause large variations in the rate of excretion of potassium in the urine (Malnic et al., 1966). These findings suggest that virtually all the filtered load of potassium is reabsorbed in the proximally located nephron segments. In addition, the rate of excretion of potassium in the urine is determined by the nett rate of secretion of potassium into the distal tubule, which is dependant on the forcing or conditions imposed on the renal system.

Consideration of the forcings applied led Valtin to propose the probable mechanisms for the secretion of potassium into the distal tubule. These mechanisms are mediated by two major factors, namely the concentration of potassium in the body fluids and the magnitude of the electrical gradient across the walls of the distal tubule (Valtin, 1973). It is proposed that a high

concentration of potassium in the cells of the walls of the distal tubules inhibits reabsorption from, and enhances secretion of potassium into the distal tubular lumen. Also, an increase in the rate of secretion of potassium is observed as the luminal fluid in the distal tubule becomes more negative with respect to the peritubular fluid. Since the electrical gradient increases with increased sodium reabsorption due to an increased concentration of aldosterone in plasma, it is suggested that the reabsorption of sodium and the secretion of potassium are electrically coupled and mediated by the effects of aldosterone.

Owing to the lack of adequate data relating to the excretion of potassium due to homeostatis, UKH, and aldosterone, UKAL, these functions are simply represented in the model by the relationships below:

$$UKH = 0.107 \times PK - 0.505 \tag{4.29}$$

$$\left.\begin{aligned} UKAL &= 0.00028 \times ALD + 0.0062 \quad \text{if ALD} \leqslant 85.0 \text{ ng./l.} \\ UKAL &= 0.00009 \times ALD + 0.0224 \quad \text{if ALD} > 85.0 \text{ ng./l.} \end{aligned}\right\} \tag{4.30}$$

These functions are simply combined to yield the nett rate of excretion of potassium.

$$UK = UKH + UKAL \tag{4.31}$$

Thus, the renal handling of potassium is represented by equations (4.29), (4.30) and (4.31).

4.3.5. Summary On The Kidney Function Model.

The development of the mathematical equations representing the basic kidney functions was presented above. The equations are based on current knowledge and, as far as possible, on meaningful data. However, owing to the obvious difficulties in measuring the variables on humans, these data are generally derived from animal experiments. Therefore, a general assumption in the development of the kidney function model is that data on

the kidneys of relevant animals may be extrapolated to the kidneys of the human.

The most crucial portion of the model, as far as homeostatis of the body fluids is concerned, is the representation of the mechanisms involved in the reabsorption of sodium and fluid from the proximal tubule. The assumption is made that the fraction of the filtered loads of sodium and water reabsorbed is independant of the rate of flow, or in other words, that perfect glomerular tubular balance exists in the proximal tubule. There is some evidence (Imai et al., 1977) that this is not the case in the kidneys of the rabbit. However, the inclusion of relationships to represent the flow - dependant fractional reabsorption of sodium and water from the proximal tubule made little difference to the overall response of the model when used to simulate stresses, of the form described in Chapter 5, on the normal kidneys. In the case of chronic renal failure, though, with greatly diminished glomerular filtration rate, an imperfect glomerular tubular balance is introduced due to hypertrophy of the tubules (Gottschalk, 1971). This effect is discussed further in the development of equations to represent renal failure in section 4.7 of this chapter.

Many other assumptions are inherent in the model. However, the final version of the model presented here was arrived at after adjustments to the structure and parameters were made such that the responses of the model to stresses were satisfactory when compared with physiological data. In this process, it was found that the response was surprisingly insensitive to changes in many of the parameters. The conclusion to be drawn is that because of the inherent feedback loops in the model, the effect of variations of parameters is minimized. Therefore the model can tolerate a degree of inaccuracy in parameter values.

In addition, any detrimental effects of inaccuracies and assumptions introduced by the process of modelling would be greatly reduced when the model is used to simulate the dialysis patient with little or no residual kidney function. The following chapters on validation demonstrate that the kidney function model is adequate to accomplish the aims of this work.

4.4. Hormonal System Models.

Included in the previous section was the derivation of equations representing the effects of the antidiuretic hormone (ADH) and aldosterone on the distal and collecting segments of the nephron. In this section, equations representing the control of the concentrations of these substances in plasma are derived. The relevant physiology was described in section 2.2.2.

4.4.1. Control Of The Concentration Of ADH In Plasma.

The concentration of ADH in plasma is determined by three factors. The first is the rate of release of ADH from the hypothalamus-pituitary system in response to signals from the osmoreceptors of the supraoptic nucleus of the hypothalamus and from volume and pressure receptors in the vascular system (see Chapter 2). The second factor is the rate of clearance of ADH from the body by the liver and kidneys, and the third factor is the volume of distribution of ADH.

It is generally agreed that an increase in the rate of release of ADH follows an increase in the osmolality of the blood compartment, a decrease in the volume of the extracellular compartment or a sudden decrease in arterial pressure due to, for instance, haemorrhage (Toates and Oatley, 1977). However, since arterial pressure is determined by the extracellular fluid volume in the model, and the patient undergoing dialysis is not normally expected to suffer haemorrhage, the baroreceptor influence on the rate of release of ADH is omitted from the model.

Since sodium is the major constituent of plasma, the osmolality of plasma, POS, which is equal to the osmolality of the extracellular fluid, is approximated by the equation:

$$POS = 2.11 \times PNA \tag{4.32}$$

Dehaven and Shapiro (1970) and Bigelow, Dehaven and Shapley (1973) derived a relationship, from physiological data, between the change in the osmolality of plasma and the rate of release of ADH into the blood compartment. This relationship was

adapted to represent the effect of differing osmolalities of plasma on the rate of release of ADH (ADHSP), and used in the model in the form of the equations below:

$$\left.\begin{aligned} \text{ADHSP} &= 0.348\text{xPOS} - 103.43 \quad \text{for POS} \geqslant 299.5 \text{ mosm./l.} \\ \text{ADHSP} &= 0.0285\text{xPOS} - 8.04 \quad \text{for POS} < 299.5 \text{ mosm./l.} \end{aligned}\right\} \tag{4.33}$$

Reeve and Kulhanek (1967) derived a sigmoid shape curve from physiological data for the relationship between the fractional change in the volume of body fluid and the rate of release of ADH. The relationship was adapted so that the variable causing the release of ADH was the deviation of the volume of extracellular compartment, DWV, from the normal volume, E_N:

$$\text{DWV} = E - E_N \tag{4.34}$$

The resulting relation between the deviation of extracellular fluid volume from normal, DWV, and the rate of release of ADH (ADHSV) is approximated by the equations:

$$\left.\begin{aligned} \text{ADHSV} &= 0.0 \quad \text{for DWV} \geqslant 1.8 \\ \text{ADHSV} &= 0.15 - 0.083\text{xDWV} \quad \text{for } 1.8 > \text{DWV} \geqslant 1.0 \\ \text{ADHSV} &= 0.813 - 0.75\text{xDWV} \quad \text{for } 1.0 > \text{DWV} \geqslant -1.2 \\ \text{ADHSV} &= 1.71 \quad \text{for } -1.2 > \text{DWV} \end{aligned}\right\} \tag{4.35}$$

The results of experiments by Johnson and associates (1970) on sheep suggest that the signals for the release of ADH are additive. Simulation of stresses involving water and hypertonic saline loading with different methods of combining the variables, ADHSP and ADHSV, suggest that the signals for the release of ADH are, indeed, simply additive. However, for the condition when both the osmolality and the volume of the extracellular fluid compartment are above normal, the optimal combined signal was found, by comparison of simulation results with reported experimental data, to be the sum of the weighted signals in favour of the signal from the volume receptors. This is in agreement with the concepts presented by Arndt (1965). Therefore, the resulting

signal for the release of ADH in the model, ADHS, is given by:

$$\left.\begin{aligned} &\text{ADHS} = ((17.0 \times \text{DWV} \times \text{ADHSV}) + \text{ADHSP})/((17.0 \times \text{DWV}) + 1.0) \\ &\qquad \text{for POS} > 299.6 \text{ mosm./l.} \quad \text{and} \quad \text{DWV} > 2.01. \\ &\text{ADHS} = (((33.0 \times \text{DWV} - 32.0) \times \text{ADHSV}) + \text{ADHSP}) \\ &\qquad / ((33.0 \times \text{DWV} - 32.0) + 1.0) \\ &\qquad \text{for POS} > 299.6 \quad \text{and} \quad 1.0 \leqslant \text{DWV} \leqslant 2.0 \\ &\text{ADHS} = (\text{ADHSV} + \text{ADHSP})/2.0 \quad \text{for all other conditions.} \end{aligned}\right\} \quad (4.36)$$

The valid mathematical representation of the clearance of ADH from the body is as important as is the representation of the release of ADH. However, data concerning the clearance of ADH are scanty and unreliable. Fabian and associates (1969) report a value for the clearance of ADH of 1.0 l./min., whereas Lauson (1960) reports a value of 0.125 l./min; but consideration of the steady state for equations (4.33), (4.35) and (4.36) yield a rate of release of ADH of 0.825 munits/min.. The normal value reported for the concentration of ADH in plasma is 4.0 munits/l. (Bigelow et al., 1973). This yields a value for the clearance rate of ADH from plasma of 0.206 l/min. in the steady state. There is evidence, however, that the rate of clearance of ADH varies with the level of ADH in plasma (Czaczkes et al., 1964). Hence, the relationship between the concentration of ADH in plasma (ADH) and the rate of clearance in the model, DADH, is of the same general form as that used by Bigelow and associates (1973) in their model of the renal system:

$$\left.\begin{aligned} &\text{DADH} = 0.206 \qquad \text{for ADH} > 4.0 \text{ munits/l.} \\ &\text{DADH} = 0.374 - 0.042 \times \text{ADH} \qquad \text{for ADH} \leqslant 4.0 \text{ munits/l.} \end{aligned}\right\} \quad (4.37)$$

The work of Reeve and Kulhanek (1967) suggests that ADH is mainly confined in the plasma compartment. The volume of the plasma compartment, PV, in the model is considered to be a constant fraction of the blood volume, BV:

$$\text{PV} = 0.6 \times \text{BV} \quad (4.38)$$

Therefore, the balance equation for ADH is:

$$\frac{d(ADH)}{dt} = (ADHS - ADH * DADH)/PV \qquad (4.39)$$

The equations in the model representing the dynamics of ADH are, therefore equations (4.32) to (4.39).

4.4.2. The Control Of Aldosterone Concentration.

Aldosterone is the final component of the renin-angiotensin-aldosterone (R-A-A) system, the function of which is to effect feedback control on the rates of excretion of sodium and potassium, and thereby influence the volumes of the intracellular and extracellular fluid compartments. The underlying physiological theories concerning the R-A-A system were described in Chapter 2, and the mathematical representation of the effects of aldosterone on the rates of reabsorption of sodium from and secretion of potassium into the distal and collecting tubules of the nephron were presented in the preceding section. The derivation of mathematical equations representing the control of the levels of each of the components of the R-A-A system in plasma is presented below.

(i) Renin.

Renin is an enzyme stored and released from the granular cells of the juxtaglomerular apparatus which lies between, and in contact with, the afferent arteriole and the beginning of the distal tubule of each nephron. Due to the location of the juxtaglomerular apparatus, many theories concerning the control of the release of renin have arisen. These theories suggest a role for renin in feedback systems for the control of body sodium and fluid volume. The three main theories, described in Chapter 2, are outlined below for the purpose of modelling the control of the release of renin.

The intrarenal vascular receptor theory for renin release (Tobian et al., 1959) suggests that the granular cells are sensitive to the stretch of the walls of the afferent arteriole such

that a decrease in stretch due to a reduction in perfusion pressure produces an increase in the rate of release of renin from the granular cells. This leads to an increase in the level of aldosterone in plasma, which causes the increased reabsorption of sodium from the distally located nephron segments. Concurrent with the resulting reduced renal excretion of sodium is the osmotically induced expansion of extracellular fluid volume, which serves to raise the mean arterial pressure and hence the renal perfusion pressure. Thus the signal for the increase in the rate of release of renin is removed.

The macula densa sodium load theory for the release of renin (Vander and Miller, 1964) states that the rate of release of the enzyme is increased due to a decrease in the sodium load at the beginning of the distal tubule, sensed by the macula densa cells of the juxtaglomerular apparatus. If the assumption is made that the sodium load at the distal tubule is directly related to the plasma concentration of sodium or to the extracellular fluid volume, then the macula densa sodium load theory is the basis of a possible feedback system for the control of the plasma concentration of sodium or the volume of the extracellular fluid compartment, and hence of blood pressure. The mechanics of the system are identical to those of the system based on the intrarenal vascular receptor theory for renin release.

The macula densa intraluminal sodium concentration theory (Thurau et al., 1967) states that an increase in the concentration of sodium in the tubular fluid at the macula densa cells causes an increase in the rate of release of renin into the blood of the afferent arteriole. It is proposed that the increased local concentration of renin causes an increase in the concentration of the pressor substance, angiotensin II, which in turn causes the constriction of the afferent arteriole, thereby reducing the glomerular filtration rate and, thus, the signal for the increase in the rate of release of renin.

The local effects of the release of renin due to the intraluminal sodium concentration theory of renin release form the basis of the probable mechanism by which the glomerular filtration rate is autoregulated (Thurau, 1971). Since the relationship in the model between arterial pressure and glomerular filtration rate, equation (4.14), incorporates the characteristics of renal

autoregulation, there is no need to consider the effects of the intraluminal sodium concentration theory for renin release for the modelling process.

If the assumption is made that the sodium load entering the distal tubule is directly related to the sodium content of the body, which determines the extracellular fluid volume and, thus, the mean arterial pressure, then the intrarenal vascular receptor theory and the macula densa sodium load theory both relate an increase in the rate of release of renin to a decrease in extracellular fluid volume. Thus a single mathematical relationship between the sodium load entering the distal tubule and the rate of release of renin would represent both these theories.

Owing to the lack of adequate data, the linear relationship of equation (4.40) was postulated as a representation of the control of the release of renin, RS, due to the load of sodium entering the distal tubule, SFDT:

$$RS = 0.0163 - 0.0093 \times SFDT \qquad (4.40)$$

The effects of other factors, such as posture (Gorden et al., 1967) sympathetic stimulation (Taquini et al., 1964), ADH and angiotensin II levels (Shade et al., 1973), on the rate of release of renin are assumed to be negligible.

The rate of release of renin into plasma is therefore represented by equation (4.40). The steady state value of the rate of release of renin given by this equation, 0.008GU./min., is in agreement with the value quoted by Blaine and associates (1972). The value for the normal concentration of renin is quoted as 0.06GU/l. (Blaine et al., 1972). Renin is removed from the circulation on passage through the liver (Heacox et al., 1967). Therefore the rate of clearance of renin from plasma can be assumed to be constant if the hepatic blood flow is assumed to be constant. The resultant rate of clearance is calculated from steady state considerations.

$$\text{Secretion rate} = \text{removal rate}$$
$$= \text{clearance rate} \times \text{steady state concentration} \qquad (4.41)$$

This yields a clearance rate for renin of 0.135 l./min..

Thus the balance equation for the concentration of renin, R, in plasma is:

$$\frac{dR}{dt} = (RS - 0.135 \times R)/PV \qquad (4.42)$$

The dynamics of renin in plasma are, thus, represented in the model by equations (4.40) and (4.42).

(ii) Angiotensin.

The enzyme, renin, acts on its substrate to release angiotensin I. This physiologically inactive substance is rapidly converted to angiotensin II by enzymes chiefly located in the lungs. Angiotensin II, the active component of the renin-angiotensin system, controls the rate of release of aldosterone, and also has a pressor effect on the circulation.

The rate of release of renin substrate from the liver is controlled by the level of angiotensin II in plasma. This is due to a positive feedback mechanism by which the concentration of the substrate in plasma remains relatively constant in the face of varying rates of utilization for the formation of angiotensin II (Reid et al., 1978). Other known factors that effect the concentration of renin substrate in plasma are the variations in glucocorticoids and estrogens in the body (Reid et al., 1978).

Renin cleaves angiotensin I from its substrate in plasma, The rate of formation of angiotensin I by the enzyme - substrate reaction appears to follow a Michaelis-Menten equation, where the rate of formation of angiotensin I is dependant on the concentrations of both renin and its substrate (Haas and Goldblatt, 1967).

Angiotensin I is then converted to angiotensin II by enzymes located chiefly in the lungs. The rate of conversion appears to be extremely rapid, such that the conversion is complete on a single passage of blood through the lungs (Ng and Vane, 1968).

The parameters for the Michaelis-Menten equation, to describe the rate of formation of angiotensin II given the concentrations of renin and its substrate, were experimentally determined by Haas and Goldblatt (1967). In using this equation

in the model it is assumed that the concentration of renin substrate remains constant. In other words, it is assumed that the positive feedback mechanism for the control of the concentration of renin substrate is totally effective; in addition, it is assumed that glucocorticoid activity is maintained at a normal level in the patient; also, it is assumed that estrogen is not being administered to the patient.

The general form of the Michaelis-Menten equation is:

$$\frac{dx}{dt} = \frac{k_3 \times E \times S}{K_m + S} \qquad (4.43)$$

where x represents the quantity of the product formed (units/ml.serum)

k_3 is the velocity constant of the reaction (units of product/unit of enzyme/min.)

E is the concentration of the enzyme (units/ml.serum)

S is the concentration of the substrate (units/ml.serum)

K_m is the Michaelis-Menten constant (unit product/ml.serum)

The values for the parameters of the Michaelis-Menten equation to represent the human renin - renin substrate reaction in the formation of angiotensin II as determined by Haas and Goldblatt are:

Michaelis-Menten, constant, K_m = 0.56 units of angiotensin II /ml.serum

Velocity constant, k_3 = 1.7 units of angiotensin II /unit of renin/minute

Average substrate concentration, S = 2.5 units/ml.serum

Incorporating these values into the Michaelis-Menten equation, (4.43), and converting units from Goldblatt units to nanogrammes by a multiplicative factor of 420.0 (Laragh and Sealey, 1973), the rate of formation of angiotensin II, AS, is represented in the model by the equation:

$$AS = \frac{1.7 \times 2.5 \times R}{0.56 + 2.5} \times PV \times 420.0 \text{ ng./min.} \qquad (4.44)$$

Angiotensin II is rapidly removed from the circulation either by the action of binding to receptor sites or by the degradation to inactive products due to the action of angiotensinases. Assuming a normal concentration of angiotensin II in plasma of 26.0 ng./l. (Blaine et al., 1972), and that the rate of clearance of this substance remains constant for all conditions, the application of equation (4.41) yields a value for the rate of clearance of angiotensin II from plasma of 4.04 litres/minute. Therefore, the balance equation regulating the concentration of angiotensin II in plasma, A, in the model is:

$$\frac{dA}{dt} = (AS - 4.04 \times A)/PV \qquad (4.45)$$

Angiotensin II has two major functions in the mechanisms for the homeostatis of the fluid compartments of the human body. Firstly, it acts as a pressor substance on the circulation as described mathematically is section 4.2. Secondly, the concentration of angiotensin II in plasma is the most potent regulator of aldosterone release from the adrenal cortex in man.

(iii) Aldosterone.

The factors known to increase the rate of release of aldosterone from the adrenal cortex are (Guyton, 1971):

(1) An increase in the concentration of angiotensin II in plasma,

(2) A decrease in sodium balance or concentration of sodium in plasma,

(3) An increase in potassium balance or concentration of potassium in plasma,

(4) An increase in circulating adrenocorticotropic hormone (ACTH).

Since a decrease in the concentration of sodium in plasma causes an increase in the rate of release of renin (equations (4.15), (4.16), (4.17), (4.18), (4.22), (4.24) and (4.40)), which results in the increase in the circulating angiotensin II in the model, the effects of sodium balance is assumed to be mediated by the effect of the renin-angiotensin system on the release of aldosterone in the model. In addition, the role of ACTH in this

control system is known to be relatively minor (Guyton, 1971), and is assumed to be negligible for present purposes. Therefore, only the effects of angiotensin II and the concentration of potassium in plasma are considered in the process of modelling the control of the rate of release of aldosterone.

The relationship between the concentration of angiotensin II in plasma and the rate of secretion of aldosterone in sheep was found experimentally to be of the form of the typical sigmoid shaped dose - response curve (Blair-West et al., 1962). These results were extrapolated by Blaine and associates (1972) to represent approximately the relationship between the concentration of angiotensin II in plasma, A, and the rate of secretion of aldosterone, ALSA, is numerically represented below for use in the model:

$$\begin{aligned} ALSA &= A && \text{for } A < 18.0 \text{ ng./l.} \\ ALSA &= 4.43xA - 61.7 && \text{for } 18.0 \leqslant A < 34.0 \\ ALSA &= 0.78xA + 62.5 && \text{for } A \geqslant 34.0 \text{ ng./l.} \end{aligned} \tag{4.46}$$

The effect of the concentration of potassium on the rate of release of aldosterone has been investigated by Seif (1974). The relationship given below has been extrapolated from their findings to represent the rate of secretion of aldosterone, ALSK, due to the concentration of potassium in plasma, PK, in the model:

$$ALSK = 21.64 \times PK - 55.5 \tag{4.47}$$

Since the manner in which the signals for the release of aldosterone are combined in the human organism is unknown, it was postulated that the nett signal, ALS, is the sum of the signals, ALSA and ALSK, weighted by appropriate factors. By simulation of the model using various weighting factors, it was determined that a satisfactory response is obtained when the signals are weighted as shown:

$$ALS = (ALSA \times 3.0 + ALSK)/4.0 \tag{4.48}$$

This is also satisfactory from a physiological point of view, since it is thought that the renin-angiotensin system is the most potent stimulant for the release of aldosterone (Blaine et al., 1972).

The normal concentration of aldosterone in the body fluids is reported to be 85.0 ng./l.. The assumptions are made that the volume of distribution of aldosterone is equal to the plasma volume, and that the rate of removal of aldosterone is proportional to the concentration of aldosterone in the plasma compartment. Thus, application of the expression (4.41) yields a value for the rate of clearance of aldosterone of 0.62 l./min.. Hence the equation representing the dynamics of the level of aldosterone, ALD, is:

$$\frac{d(ALD)}{dt} = (ALS - 0.62 \times ALD)/PV \qquad (4.49)$$

The control of the secretion and of the level of aldosterone in the body is thus represented by equations (4.46) to (4.49), and the actions of aldosterone were mathematically derived in equations (4.27) to (4.31).

4.4.3. Summary Of The Hormonal Systems Model.

The mathematical representation of the control of the levels of the antidiuretic hormone (ADH) and aldosterone was derived in the section above. Several difficulties had to be overcome in the development of this subsystem model.

The major difficulties arose because of uncertainties or total lack of knowledge regarding the mechanisms of parts of the control system. An example of this is the uncertainty surrounding the manner in which the signals for the release of ADH due to a deviation of the osmolality of plasma and the expansion of fluid volume are combined. This problem was tackled by postulating several possible mechanisms for the combination of the signals and inserting the corresponding mathematical representations for each of the mechanisms in turn in the basic model. Simulations of physiological experiments of the type reported in Chapter 5

were then generated using the various versions of the model, and the version which generated the most satisfactory response was chosen as that containing the appropriate representation of the uncertain mechanism for the eventual model.

This process, however, is complicated by there being more than one area of uncertainty in the control system, all of which have to be resolved simultaneously in the manner described. An example of this is the combination of uncertainties of the ADH system regarding the combining of signals, described above, and the clearance factor for ADH from plasma. It is clear that in such instances, the solutions are not necessarily unique.

Numerous postulated variations on the basic structure of the renin-angiotensin-aldosterone (R-A-A) system may be found in the literature. Among the many variations are the three hypotheses regarding the control of the release of renin, which were outlined above. Other hypotheses for which there is supporting evidence are as follows. It is postulated (Shade et al., 1973) that the concentration of angiotensin II exerts an influence via negative feedback on the rate of release of renin in order to prevent an excessive rise in the concentration of angiotensin II. There is evidence also for the hypothesis that the potency of angiotensin II to release aldosterone from the adrenal cortex is modulated by the state of sodium balance in the body (Oelkers et al., 1974).

As progress in the research of the renal system is made, these and other hypotheses will either be accepted or rejected by physiologists on the grounds of further experimental evidence. Therefore, the model of the R-A-A system derived above consists of the representation of the most widely accepted concepts regarding this system. The model thus forms a basis on which various hypotheses may be tested, and hence may make contributions to the advancement of knowledge regarding the physiology of the renal system.

Apart from the uncertainties regarding the structures of the control systems, the values of the parameters used in the model are also uncertain. For instance, the rate of release of aldosterone from the adrenal cortex for a normal man under normal steady state conditions is quoted as a range from 20 g,/day to 200 g./day (Ledingham et al., 1967). There are two main reasons for the uncertainty. Firstly, parameter variations are

seen to exist between individuals. Secondly, measurement noise is introduced due to the difficulties in measuring these variables. Therefore, parameter values used in the subsystem model above were, in the main, derived from previous models (Dehaven and Shapiro, 1970; Bigelow et al., 1973; Reeve and Kulhanek, 1967; Blaine et al., 1972).

These difficulties tended to cast doubts on the accuracy of the representations of the hormonal control systems, and therefore, the potential of the overall model for accomplishing its objectives. However, owing to the inherent negative feedback nature of the control systems, a degree of uncertainty appears not to have detrimental effects on the performance of the model, as demonstrated in subsequent chapters. In addition, since the patients undergoing dialysis have little or no remaining kidney function, the extent to which the inaccuracies in the model affect the results of simulations of these patients is appropriately reduced.

4.5. Artificial Kidney Machine Model.

The mathematical expressions representing the artificial kidney machine are so arranged that they may be logically switched into and out of the overall model of the patient - artificial kidney machine system, as specified by the candidate therapy proposed by the clinician. The details of how the overall model may be used for the prediction of the outcomes of candidate therapies are given in Chapter 8. Section 2.3 presented the outline of the mechanisms of haemodialysis by which the lost functions of the kidneys are compensated for. This section presents the mathematical expressions which represent the effects of dialysis on the renal failure patient in the model.

Dialysis is performed in order to remove excess body fluid by ultrafiltration, waste products and excess electrolytes by diffusion. Of the many waste and possibly toxic materials that accumulate in the body following renal failure, the dynamics of the two most closely monitored in the patient, urea and creatinine, are modelled. Similarly, the manner in which dialysis affects the plasma concentrations of sodium and potassium is modelled,

as these variables have to be carefully controlled because of their influence on fluid balance and on the cardiovascular system.

4.5.1. Ultrafiltration Of Water.

Fluid is forced out of the blood compartment into the dialysate compartment by the controllable pressure difference across the semi-permeable membrane of the dialysis machine. The rate at which fluid traverses the membrane, ULTRF, is dependant on the value at which the pressure difference across the membrane, PCP, is set, according to the function (Thompson, 1977):

$$\left.\begin{aligned} \text{ULTRF} &= 0.0139 \times \text{PCP} + 0.7 \quad \text{if PCP} < 100.0 \text{ mm.Hg.} \\ \text{ULTRF} &= 0.042 \times \text{PCP} - 2.1 \quad \text{if PCP} \geq 100.0 \text{ mm.Hg.} \end{aligned}\right\} \qquad (4.50)$$

4.5.2. Diffusion Of Electrolytes And Waste Products.

The analysis of mass transfer across the dialyzing membrane, based on the "film theory" approach, and the subsequent integration of the resulting equation representing Fick's law of diffusion (Cooney, 1976; Renkin, 1956) yields the following expression for the extraction ratio, E^*, which characterizes the performance of the dialysis machine in terms of the permeability of the membrane for a solute, K, the surface area of the membrane, A_r, and the rate of flow of blood through the machine, Q_B:

$$E^* = 1 - \exp\left(-\frac{KA_r}{Q_B}\right)$$

The extraction ratio, E^*, is defined in terms of the concentrations of the solute in the blood as it enters and leaves the dialysis machine, C_{Bi} and C_{Bo} respectively, and the concentration of the solute in the dialysate as it enters the machine, C_{Di}:

$$E^* = \frac{C_{Bi} - C_{Bo}}{C_{Bi} - C_{Di}} \qquad (4.51)$$

Combining the above two equations and rearranging, gives:

$$C_{Bo} = C_{Bi} - (C_{Bi} - C_{Di})\times\left(1 - \exp\left(-\frac{KAr}{Q_B}\right)\right) \qquad (4.52)$$

The equation for the rate of change of the quantity of the solute in the extracellular fluid compartment is:

$$\frac{d(C_{Bi} \times E)}{dt} = Q_B \times (C_{Bo} - C_{Bi}) \qquad (4.53)$$

Substituting for C_{Bo} from equation (4.52), this becomes:

$$\frac{d(C_{Bi} \times E)}{dt} = Q_B \times (C_{Bi} - C_{Di}) \times \left(\exp\left(-\frac{KAr}{Q_B}\right) - 1\right) \qquad (4.54)$$

Equation (4.54) represents the rate of transfer of a substance across the dialyzing membrane due to diffusion, given the membrane parameters, K and A the rate of flow of blood through the machine, Q_B, and the difference between the concentrations of the substances in the blood and the dialysate compartments. It is assumed that the flow arrangement for the dialysate is such that the concentrations of the various substances in the dialysate entering the dialysis machine remain constant.

It is further assumed that the nett electrical force on the transfer of electrolytes across the membrane is negligible. Equation (4.54), with appropriate values for membrane permeability, may then be applied to represent the effects of dialysis on the transfer of sodium and potassium across the dialyzing membrane. The parameter values used for equation (4.54) are given in Table 4.1.

4.5.3. Summary Of The Artificial Kidney Machine Model.

The effects of the dialysis machine on the extraction of fluid by ultrafiltration is represented in the model by equation (4.49), and the diffusion of the waste products, urea and creatinine, and the electrolytes, sodium and potassium, is represented by equation (4.54) with the appropriate values for the parameters.

TABLE 4.1. Parameter Values For The Dialysis Machine Model.

Parameter	Value
Q_B	User specified
C_{Di}	User specified
K_{urea}	0.07 m./min.
$K_{creatinine}$	0.06 m./min.
K_{sodium}	0.10 m./min.
$K_{potassium}$	0.05 m./min.
Ar	1.5 m^2.

However, in accordance with the philosophy underlying this work - that the model forms a basis on which it is possible to build - the removal of other waste products and electrolytes, such as uric acid, calcium, and bicarbonate and chloride anions, by the artificial kidney machine from the body fluids may easily be represented, if need be, by the appropriate use of the general equation (4.54).

A possible source of errors in the simulation of dialyses arises due to the gradual deterioration of the permeability characteristics of the dialyzing membrane through use (Thompson, 1977; see also discussion on model of Lott and associates (1977) in section 3.2.1 of this thesis). This effect is not represented in the model. However, as demonstrated by the validity tests described in Chapter 6, which presents the results of the simulations of actual dialyses, the representation of the effects of dialysis by equations (4.49) and (4.54) is adequate for the prediction of patient state following dialysis.

4.6. The Balance Equations For Fluid, Electrolytes And Waste Materials.

The body fluids and their constituents are considered to reside in two compartments in the model, where the compartments

represent the intracellular and the extracellular fluid pools in the body. The balance equations for the volume of these compartments and for the sodium, potassium, creatinine and urea in these compartments are derived in this section. These equations depend on such factors as the rate of accumulation of a substance in a compartment due to ingestion, generation or transfer from the other compartment, and the rate of removal of a substance due to kidney or artificial kidney machine function or transfer to the other compartment.

Since the concentrations of the electrolytes in the fluid compartments influence the osmotic shift of fluid across the cellular membranes, the balance equations for sodium and potassium in the intracellular and extracellular compartments are derived below. The subsection following presents the equations representing the balance for the volumes of the fluid compartments and the dynamics of urea and creatinine respectively.

4.6.1. Sodium And Potassium Balance.

Sodium and potassium enter the extracellular fluid pool through the gut as a result of ingestion, and leave the extracellular pool by way of the kidneys or the artificial kidney machine. In the model, the rate at which these substances enter the extracellular fluid compartment is considered to be the time average of the daily ingestion rates of these electrolytes by the human, SODMIN and POTMIN. The rate at which the electrolytes leave the body via the kidneys, UNA and UK, have been derived elsewhere (equations 4.28 and 4.31). Hence the rates of change of the quantities of sodium and potassium in the extracellular compartment, when the model is used to simulate a human with normal kidney functions, are:

$$\frac{d(TENA)}{dt} = SODMIN - UNA \tag{4.55}$$

$$\frac{d(TEK)}{dt} = POTMIN - UK \tag{4.56}$$

Equation (4.54) is combined with equations (4.55) and (4.56) to represent a patient with diminished kidney functions to excrete sodium and potassium, UNA′ and UK′, who is undergoing dialysis:

$$\frac{d(TENA)}{dt} = Q_B \times (PNA - SODDIA) \times \left(\exp \left(- \frac{K_{sodium} \times A_r}{Q_B} \right) - 1 \right) + SODMIN - UNA' \quad (4.57)$$

$$\frac{d(TEK)}{dt} = Q_B \times (PK - POTDIA) \times \left(\exp \left(- \frac{K_{potassium} \times A_r}{Q_B} \right) - 1 \right) + POTMIN - UK' \quad (4.58)$$

After integration of equations (4.55) and (4.56), or equations (4.57) and (4.58), the concentrations of sodium and potassium in the extracellular compartment, PNA and PK respectively, are given by the quotients:

$$PNA = TENA / E \quad (4.59)$$

$$PK = TEK / E \quad (4.60)$$

The concentration of sodium in the extracellular pool is much higher than in the intracellular pool, and the concentration of potassium is much higher in the intracellular pool than in the extracellular pool. As a result there is nett diffusion of sodium from the extracellular to the intracellular pool, and nett diffusion of potassium from the intracellular pool to the extracellular pool. These fluxes are compensated for by an active transport process which shifts sodium and potassium against their respective concentration gradients.

The assumption is made that the active transport process balances the transcellular transfer of electrolytes by diffusion, so that there is negligible nett transfer of electrolytes across the cellular barrier. This is represented mathematically below:

$$\frac{d(TINA)}{dt} = 0 \quad (4.61)$$

$$\frac{d(TIK)}{dt} = 0 \tag{4.62}$$

Again, after integration of equations (4.61) and (4.62), the concentration of sodium and potassium in the intracellular compartment, INA and IK respectively, are given by:

$$INA = TINA / I \tag{4.63}$$

$$IK = TIK / I \tag{4.64}$$

Thus equations (4.55), (4.56) and (4.59) to (4.64) represent the dynamics of sodium and potassium in the intracellular and extracellular fluid compartments of a patient not undergoing dialysis; and equations (4.57) to (4.64) are used to simulate the dynamics of the electrolytes in the fluid compartments of a patient while being dialyzed.

4.6.2. Fluid Balance.

Ingested water is considered to pass into the extracellular compartment from the gut at a constant rate, FLUMIN, and is removed in the form of urine by the kidneys, UFL, or by ultrafiltration, ULTRF, by the artificial kidney machine at rates determined by equations (4.26) and (4.49). Thus, the balance equation for the volume of the extracellular fluid compartment in a person with normal kidney function is:

$$\frac{dE}{dt} = FLUMIN - UFL \tag{4.65}$$

The balance equation for a patient with diminished kidney function to excrete urine, UFL , undergoing dialysis is:

$$\frac{dE}{dt} = FLUMIN - UFL - ULTRF \tag{4.66}$$

Water is transferred from the extracellular pool to the intracellular pool almost instantaneously so that osmotic

equilibrium is constantly maintained (Guyton, 1971). However, the analysis of subsection 4.6.1 yields values for the intracellular and extracellular concentrations of sodium and potassium before osmotic equilibration of the compartments is considered to take place. Since sodium and potassium are the major constituents, the values of their concentrations, PNA, PK, INA, IK, are used to approximate the osmolalities, POS and IOS, of the two fluid compartments before equilibration:

$$POS = PNA + PK + PC \tag{4.67}$$

$$IOS = INA + IK + IC \tag{4.68}$$

PC and IC are constant terms to represent the osmotic effects of the remaining constituents in the body fluid compartments.

The overall osmolality of the body fluids, AVOS, is then:

$$AVOS = \frac{POS \times E + IOS \times I}{E + I} \tag{4.69}$$

Fluid shifts across the cell membrane barrier such that both intracellular and extracellular osmolalities are equal to AVOS. Hence, the fluid volumes after equilibration (E' and I') are given by:

$$E' = \frac{POS \times E}{AVOS} \tag{4.70}$$

$$I' = \frac{IOS \times I}{AVOS} \tag{4.71}$$

Since sodium and potassium do not cross the cell membrane barrier in the model, the values for extracellular and intracellular concentrations of sodium and potassium after osmotic equilibration (PNA', PK', INA', and IK') are given by the expressions:

$$PNA' = \frac{PNA \times AVOS}{POS} \tag{4.72}$$

$$PK' = \frac{PK \times AVOS}{POS} \tag{4.73}$$

$$INA' = \frac{INA \times AVOS}{IOS} \tag{4.74}$$

$$IK' = \frac{IK \times AVOS}{IOS} \tag{4.75}$$

4.6.3. Urea And Creatinine Dynamics.

There exists some debate regarding the site of generation of the metabolic end-products, urea and creatinine (Frost and Kerr, 1977). However, in the development of the model, it is assumed that these products are effectively generated entirely in the intracellular compartment. These substances then diffuse across the cell membrane barrier at rates dependant on the concentration gradients ($C_I - C_E$) and the cell permeability constants, $k_{I,E}$. In normal health and considering steady state conditions, the rate of clearance of a substance, K_r, must be such that the rate of removal by the kidneys is equal to the rate of generation, G, of the substance. Therefore, the generalized form of the mass balance equations for the waste products in the intracellular and extracellular fluid compartments in normal health are written as:

$$\frac{d(C_I \times I)}{dt} = G - k_{I,E} \times (C_I - C_E) \tag{4.76}$$

$$\frac{d(C_E \times E)}{dt} = k_{I,E} \times (C_I - C_E) - K_r \times C_E \tag{4.77}$$

The diet of a patient with renal insufficiency to excrete urea and creatinine, K_r', is controlled such that the rates of generation of these waste products, G', are reduced. Therefore, the balance equations representing the dynamics of urea and creatinine in the intracellular and extracellular fluid compartments of the patient undergoing dialysis become:

$$\frac{d(C_I \times I)}{dt} = G' - k_{I,E} \times (C_I - C_E) \tag{4.78}$$

$$\frac{d(C_E \times E)}{dt} = k_{I,E} \times (C_I - C_E) - K_r' \times C_E$$

$$- Q_B (C_E - C_{Di}) \times \left(\exp \left(- \frac{KAr}{Q_B} \right) - 1 \right) \qquad (4.79)$$

TABLE 4.2. Parameter Values For Urea And Creatinine Model.

Parameter	Urea*	Creatinine	Reference
G (g./min.)	0.021	0.00042	Cooney, 1976
G (g./min.)	0.0084	0.00014	Cooney, 1976
$k_{I,E}$ (1./min.)	0.7	0.4	Frost and Kerr, 1977
$C_I - C_E$ (g./l.)**	0.15	0.03	Cooney, 1976
Predialysis C_E (g./l.)	0.9	0.15	Cooney, 1976
K_r (1./min.)	0.14	0.014	— ***
K_r' (1./min.)	User specified	User specified	—

* Blood urea nitrogen values.

** Steady state values for normal kidney function.

*** Calculated using expression (4.41) with the values for C_E and G.

The values for the parameters for equations (4.76) to (4.79) are given in Table 4.2.

4.6.4. Summary Of The Balance Equations.

The differential equations presented in this section, equations (4.55) to (4.58), (4.61), (4.62), (4.65), (4.66), (4.76) to (4.79), together with the differential equations representing the dynamics of the hormones in plasma, equations (4.39), (4.42), (4.45) and (4.49), and the differential equations of the thermoregulatory

model, equations (4.1) and (4.2), are placed together in the computer program in the subroutine, MODEL. These equations are integrated by the fourth order variable step Runge-Kutta integrator, subroutine INTEGR, to generate values for the state variables at intervals of one minute of simulated time. The organization of the complete computer program, listed in Appendix III, is described in Chapter 8.

In the development of the mass balance equations for the electrolytes, it was assumed that there is negligible nett transfer of electrolytes across the cell membrane barrier. This assumption is based on the comparison of two sets of simulation of the types reported in Chapters 5 and 6. The first set of simulations was the response of the model with the appropriate equations altered to incorporate factors representing the active and passive transport of sodium and potassium across the cell membrane barrier, based on data presented by Tosteson (1955). The second set was the simulation of the identical stresses using the model of sodium and potassium balance as presented above. Comparison of these simulations indicates that the inclusion of the representation of the diffusion and active transport processes has negligible effect on the response of the key variables.

Due to the controlled diet and reduced clearance of waste products in patients suffering from renal failure, the values of the parameters for the mass balance equations for urea and creatinine are altered as shown in Table 4.2. There is evidence (Bergstrom and Furst, 1976) that the human body adapts to these unusual conditions, the result of which is the further alteration of these parameters. The simulations of Chapter 6 indicate that there is variation between patients of their parameters for the mass balance of urea, in particular. Therefore, the parameter representing the rate of generation of urea, together with other parameters of the model, were subject to optimal estimation using data of dialysis on a particular patient, as described in Chapter 7. The model thus represents a particular patient, and as such, is capable of the prediction of the state of that patient with greater accuracy.

The mass balance equations representing a patient with renal insufficiency and undergoing dialysis included factors representing diminished kidney functions. In many of the simulations described

in Chapter 6 these factors are set to zero because the patient being simulated is anuric. However, the mechanism by which the model estimates the effects of the reduced renal functions is described in the following section.

4.7. Representation Of Renal Failure.

The common underlying mechanism for all forms of renal failure is the decrease in the number of functioning nephrons. A brief description of the various causes of renal failure was presented in section 2.3, which stated that in chronic renal failure, the number of functioning nephrons gradually decreases until the patient is anuric, whereas the onset of acute renal failure is marked by the sudden cessation of urine flow. However, acute renal failure is a potentially reversible condition, and if the patient is fortunate, the number of functioning nephrons in his kidneys gradually increases till the patient is returned to a state of near normal health. When renal insufficiency is not severe, conservative management of diet is generally adequate therapy to combat the effects of renal failure. However, dialysis therapy is required when renal insufficiency is severe.

Renal failure, or the large reduction of the number of functioning nephrons, as far as the variables in the model are concerned, has the effect of reducing the functions of the kidneys to excrete water, sodium, potassium and the waste products, and to secrete renin. However, it is often found that each of these functions is reduced by various extents in the patient with near - complete renal shut-down, since the disorder causing renal failure may only affect part of the nephron. It is sometimes the case that the ability of the kidneys to secrete renin remains relatively intact, whereas the rate of formation of urine is reduced to almost zero. Similarly, since potassium, the waste products, sodium and water undergo differing processes of reabsorption and secretion on passage through the tubules, renal failure may result in the reduction of the rates of excretion of each of these species by varying extents.

Appropriate alterations, therefore, need to be made to the model of normal kidney functions, presented in previous sections

of this chapter, in order that the model may be used to simulate patients with varying degrees of renal insufficiency and in need of dialysis therapy. A simple though not entirely accurate method of accomplishing this is to multiply the appropriate equations in the model by factors, values for which are specified by the clinician, which represent the extent to which the kidney functions are reduced in the patient being simulated. These factors thus take a value in the range from zero to unity, where zero represents the anuric state and unity represents the healthy state.

The multiplicative factors, then, are defined as follows:

FACT1 : Fraction representing remaining kidney function to excrete sodium and water.

FACT2 : Fraction representing remaining kidney function to secrete renin.

FACT3 : Fraction representing remaining kidney function to excrete potassium.

FACT4 : Fraction representing remaining kidney function to excrete urea and creatinine.

To represent renal insufficiency, the following equations are modified, as shown:

$$\left.\begin{aligned} GFR &= 0.0 && \text{if } AP \leqslant 20.0 \text{ mm.Hg.} \\ GFR &= (1.92 \times AP - 38.4) \times FACT1 \\ & && \text{if } 20.0 < AP \leqslant 75.0 \\ GFR &= (-0.00808 \times AP^2 + 2.195 \times AP - 13.6) \times FACT1 \\ & && \text{if } 75.0 < AP \leqslant 120.0 \\ GFR &= (0.035 \times AP + 129.2) \times FACT1 \\ & && \text{if } AP > 120.0 \text{ mm.Hg.} \end{aligned}\right\} \quad (4.14a)$$

If FACT1 > 0.0

$$EBLH = (-0.01 \times EFLH/FACT1) + 0.65 \quad (4.21a)$$

$$UK = (UKH + UKAL) \times FACT3 \quad (4.31a)$$

If FACT1 > 0.0

$$RS = (0.0163 - 0.0093 \times SFDT/FACT1) \times FACT2 \qquad (4.40a)$$

The general balance equations for waste products, urea and creatinine in the extracellular compartment are modified as below:

For the interdialysis period:

$$\frac{d(C_E \times E)}{dt} = k_{I,E}(C_I - C_E) - K_r \times C_E \times FACT4 \qquad (4.77a)$$

For the dialysis period:

$$\frac{d(C_E \times E)}{dt} = k_{I,E}(C_I - C_E) - K_r \times C_E \times FACT4 - Q_B(C_E - C_{Di}) \times \left(\exp\left(-\frac{KAr}{Q_B} \right) - 1 \right) \qquad (4.79a)$$

The values for these factors are introduced into the model by way of the sections of the computer program which interact with the user for the communication of information. This aspect is described in greater detail in Chapter 8.

When the number of functioning nephrons in the kidneys is reduced, the remaining nephrons undergo hypertrophy so that the lost effects of nephrons no longer functioning are compensated for to a certain extent (Gottschalk, 1971). In addition, as demonstrated by the polyuric stage during the onset of chronic renal failure, other changes occur, regarding the capabilities of the nephrons to concentrate tubular fluid. Therefore, it appears that the method of representing a reduced number of functioning nephrons, as described above, is inaccurate. However, since the model is used to simulate patients undergoing dialysis who have very few or no healthy nephrons, taking no account of these adaptive changes in the remaining nephrons would not result in significant errors in the prediction of patient state.

4.8. Summary.

The derivation of the mathematical model of the patient - artificial kidney machine system was presented in the previous

sections of this chapter. The model consists of submodels of several of the systems of the human organism, appropriately interconnected. The systems modelled contain the variables (and those that are the major determinants of the variables) which need to be closely monitored by the clinical staff to assess the clinical state of the patient with renal failure and undergoing dialysis therapy. Thus, the model, incorporated in a suitable system, may be used in the clinical environment to give predictions of the future state of the patient undergoing dialysis therapy, given parameters representing the present state of the patient and the proposed therapy.

The equations of the model were derived, as far as possible, from relevant quantitative data presented in the literature. However, considering the complexity of the system being modelled, there exists uncertainty, and, undoubtedly, total lack of knowledge in some instances, concerning certain areas of the physiology. In particular, as suggested by the results of the simulations of dialyses presented in Chapter 6, the interaction between the thermoregulatory system and other systems is not adequately represented. Very recent data from experiments performed on humans (Graveney, 1979) indicate that correlation exists between the variables of the thermoregulatory system model and other variables represented in the model. However, the mechanisms which give rise to the correlation between some of these variables are not clearly understood at this time. Therefore, this apparent inadequacy in the model is due to the shortcomings of physiological knowledge. Uncertainty also exists regarding the representation of the cardiovascular system. In addition to the lack of quantitative information regarding the relationships between the variables of this highly complex system, the objectives of this work dictate that the mathematical representation of the shorter term control mechanisms of the human circulatory system be omitted. However, from the results of the simulations presented in the subsequent chapters, it is clear that these, and other possible omissions have little effect on the potential of the model to satisfy the main objectives of this work.

Since the equations of the model are based on the widely accepted current theories regarding the relevant physiology, the

validated model may be used as an instrument for the testing of hypotheses regarding the complex control mechanisms of the renal - body fluid system. Examples of the use of the hypothesis testing facility of the model are presented in the following chapter.

In addition, the model, having been designed on the basis of interconnected submodels, lends itself to the possibility of expansion by the augmentation of additional submodels representing further systems of the human organism. Thus, the model, suitably adapted, may be used to serve other related clinical functions. A discussion on the other possible uses for the model is presented in the final chapter of this thesis.

Having presented the derivation of the mathematical model in this chapter, it now remains to present the results of the investigation of the validity of the model, or in other words, of the capabilities of the model to satisfy the objectives of this work. This investigation was conducted in three distinct stages. The first stage was designed to establish the validity of the model of the renal - body fluid system of a normal human, and therefore, the capability of the model to be used as a hypothesis testing instrument. The second stage examined the potential of the model to serve as a health care aid in predicting the outcome of a single dialysis on a patient. In the final stage, the capability of the model to predict patient state in the longer term was examined. The results of the three stages of validation of the mathematical model are presented in the following three chapters.

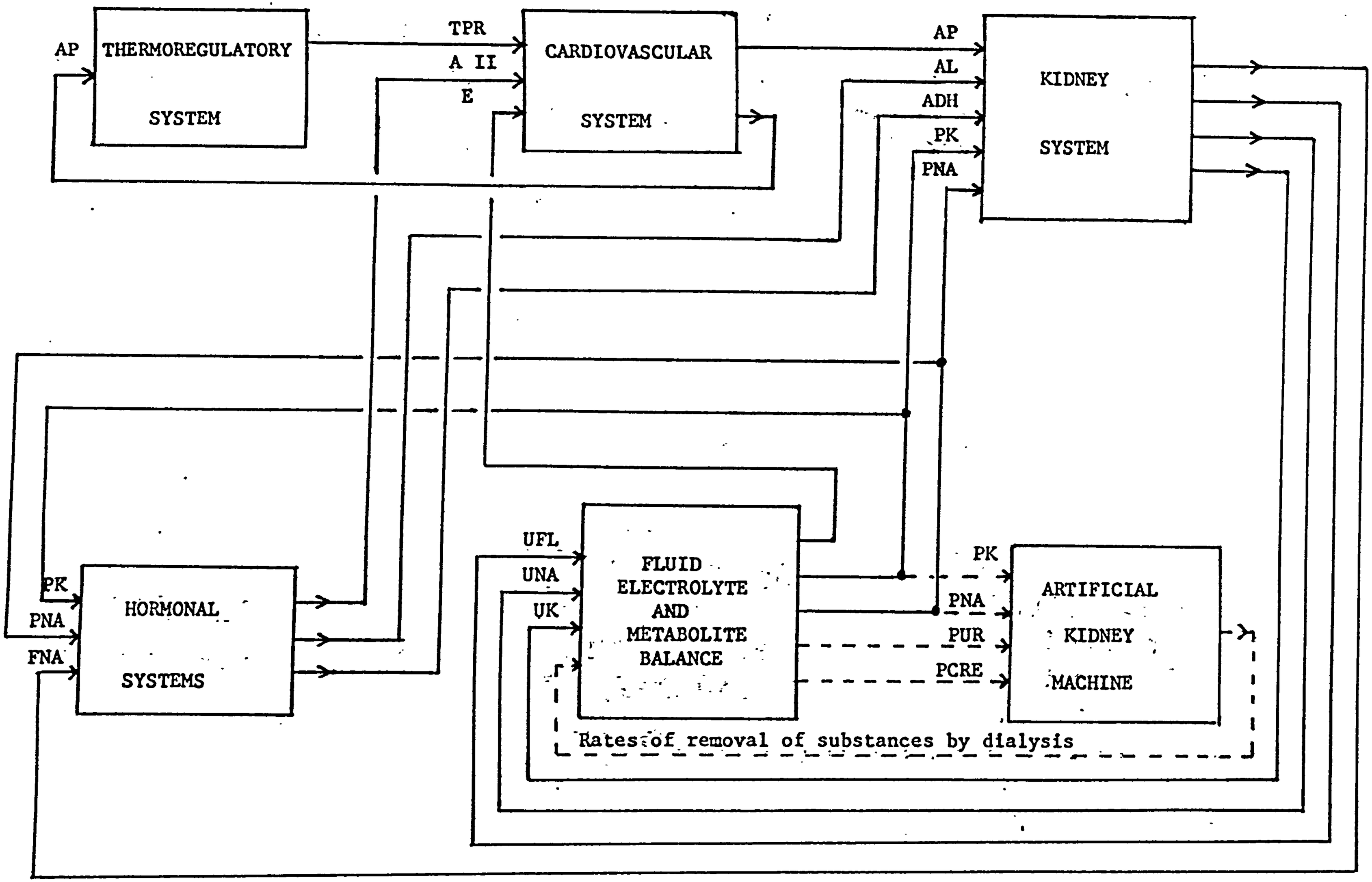

Figure 4.1. Subsystems and their interacting variables in the model.

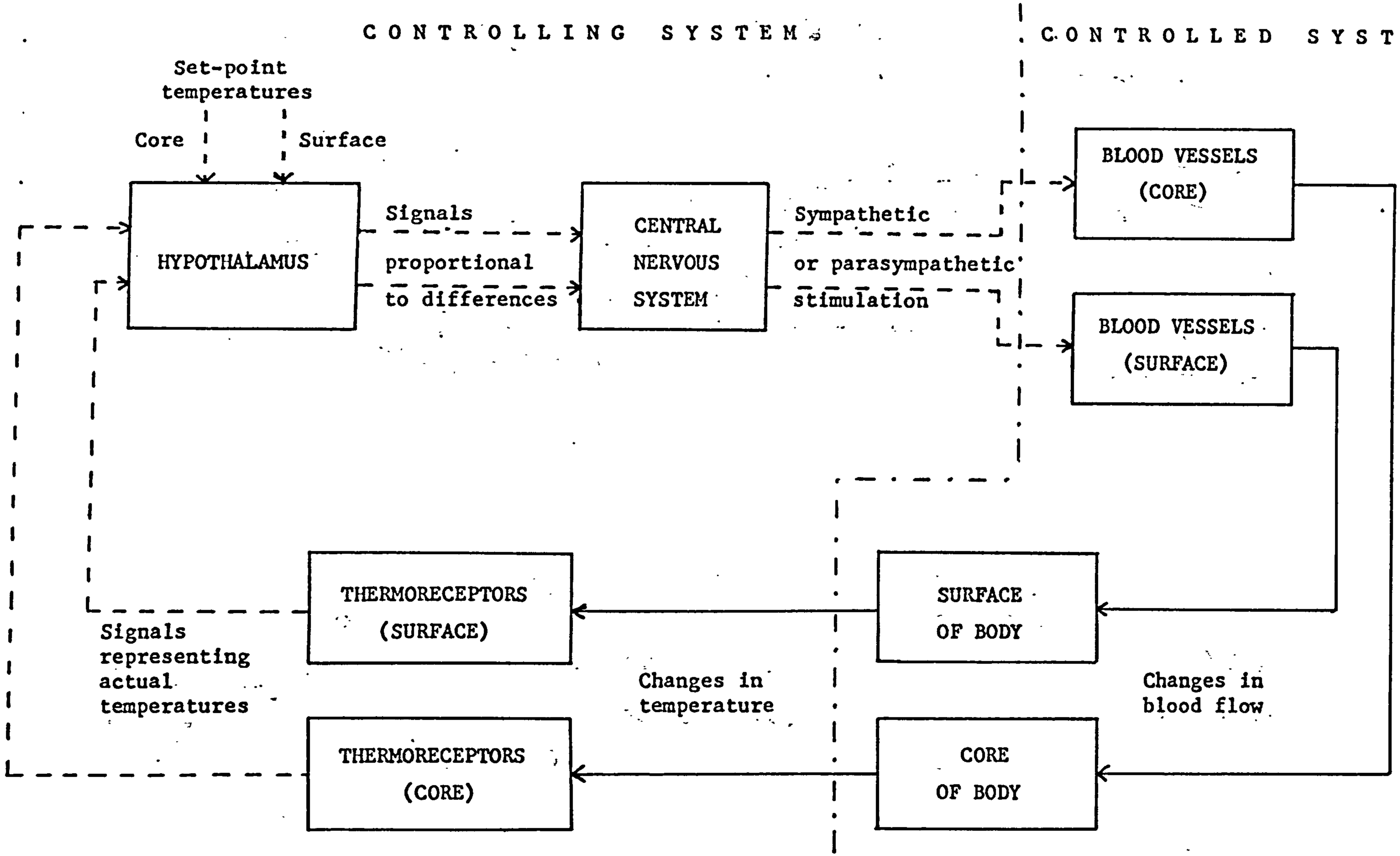

Figure 4.2. Diagram representing the 'set-point' theory of the human thermoregulatory system.

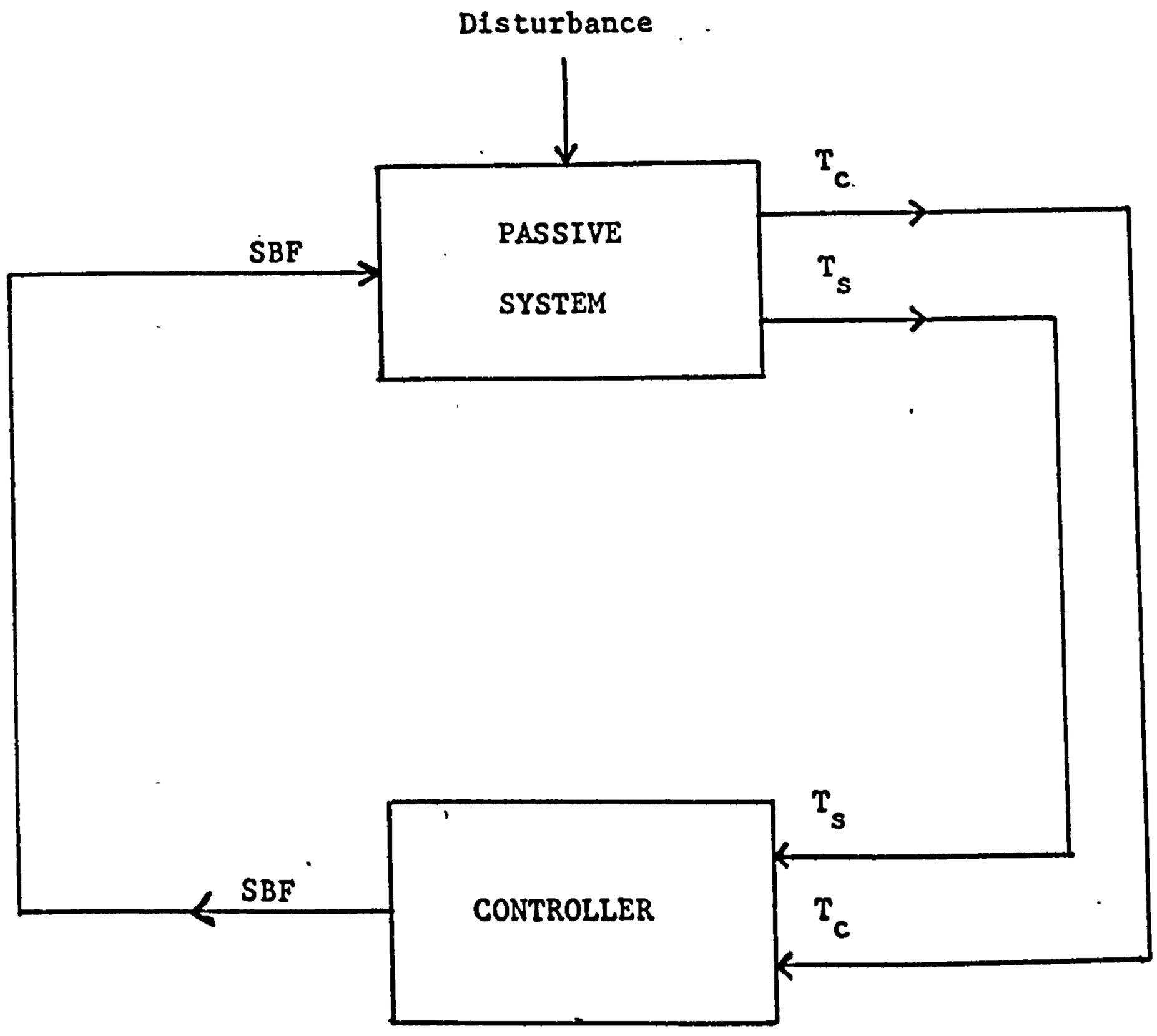

Figure 4.3. Configuration of the passive system and controller in the thermoregulatory model.

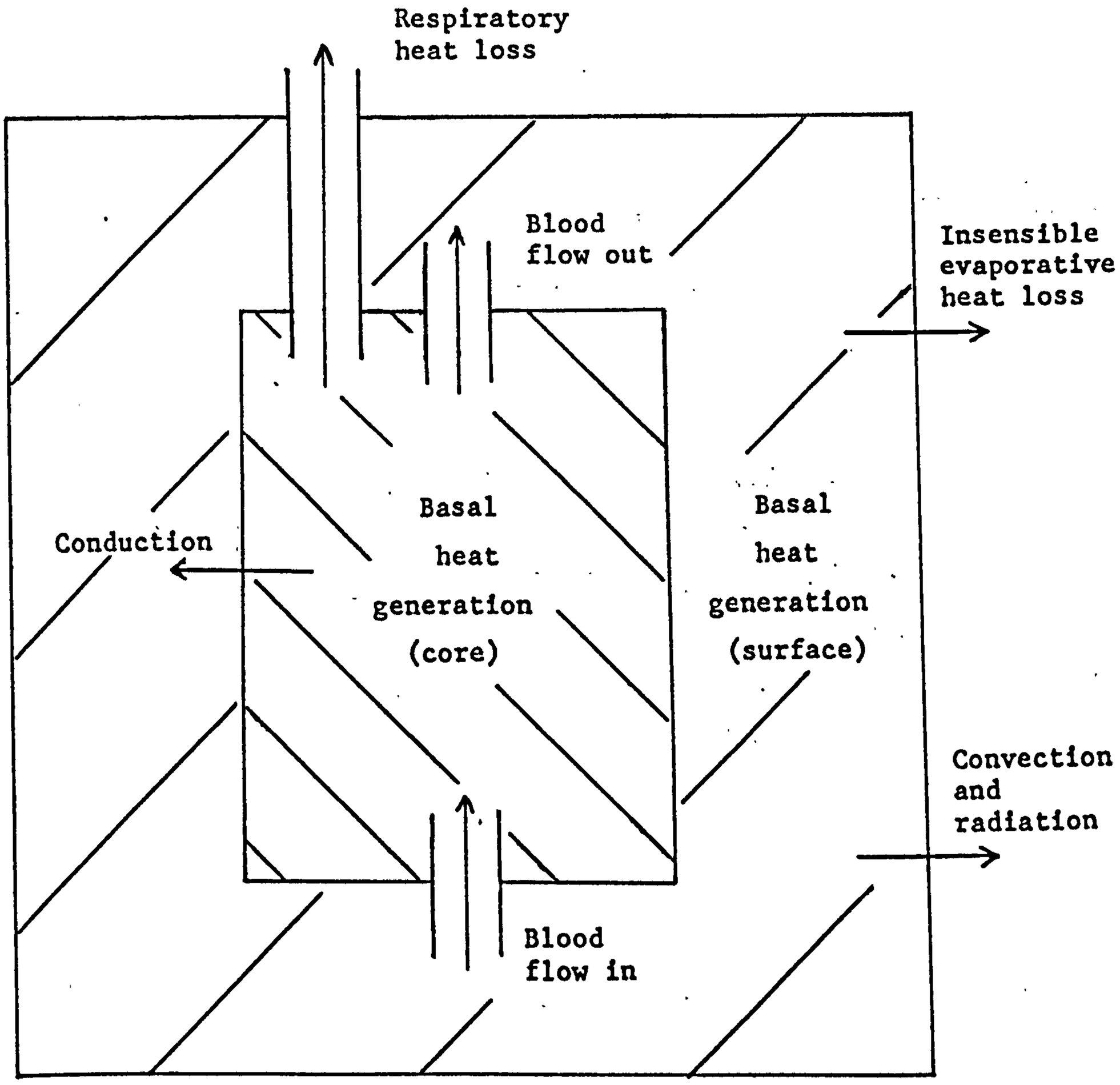

Figure 4.4. Mechanisms of heat transfer between core, surface and environment in the thermoregulatory system model.

PAGE NUMBERING AS ORIGINAL

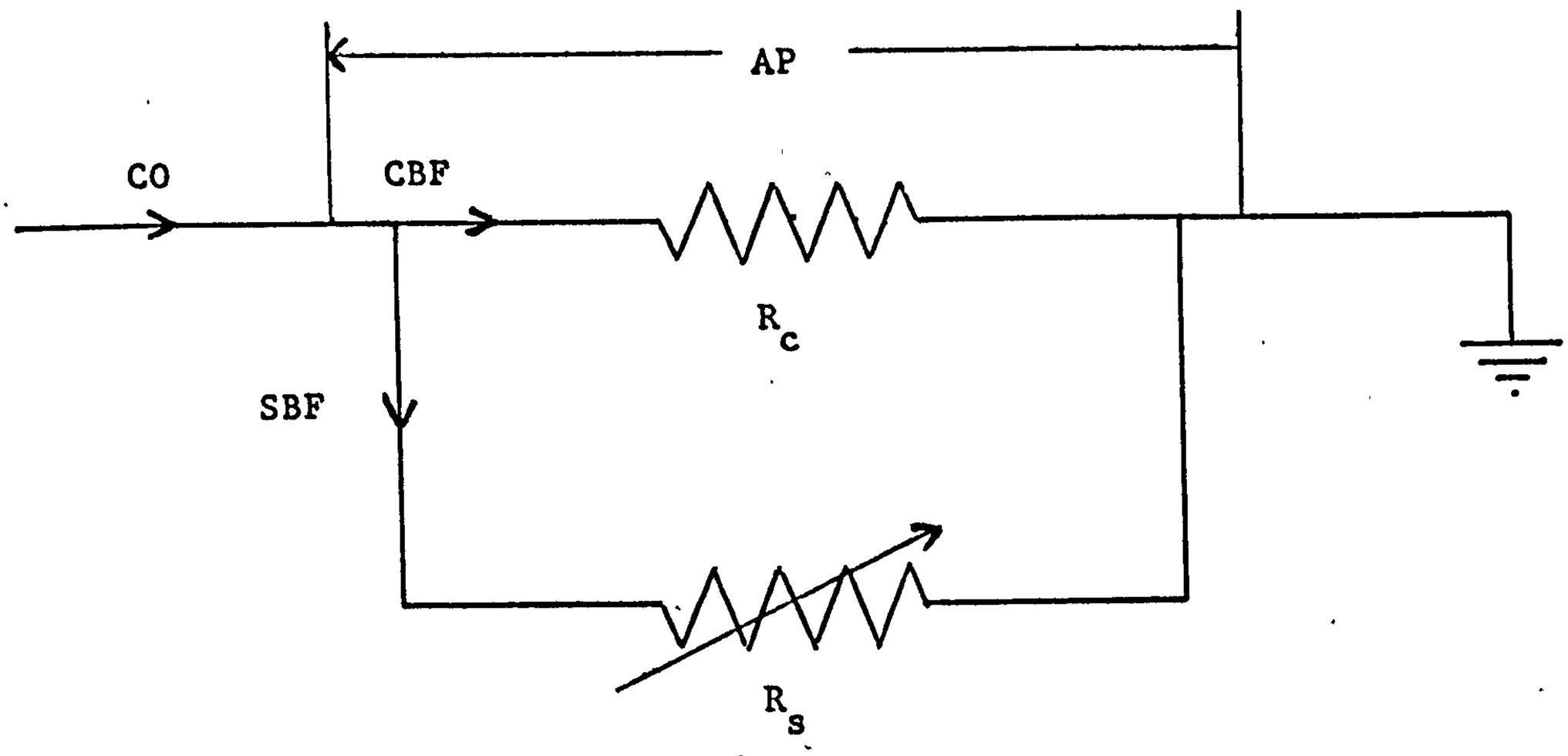

Figure 4.5. Electrical analogy for blood flow through core and surface of the body in thermoregulation.

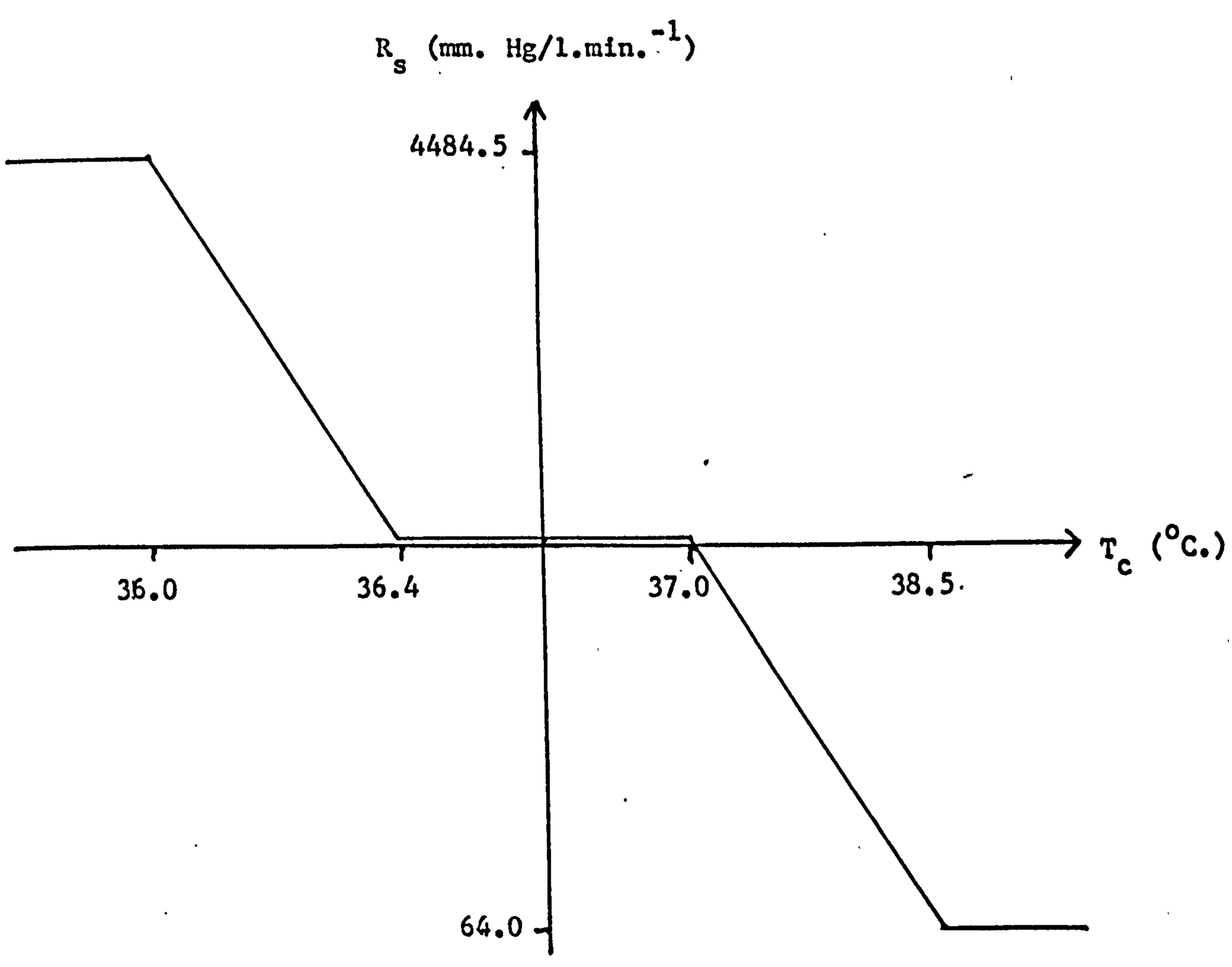

Figure 4.6. Postulated function between core temperature and resistance to blood flow (not to scale).

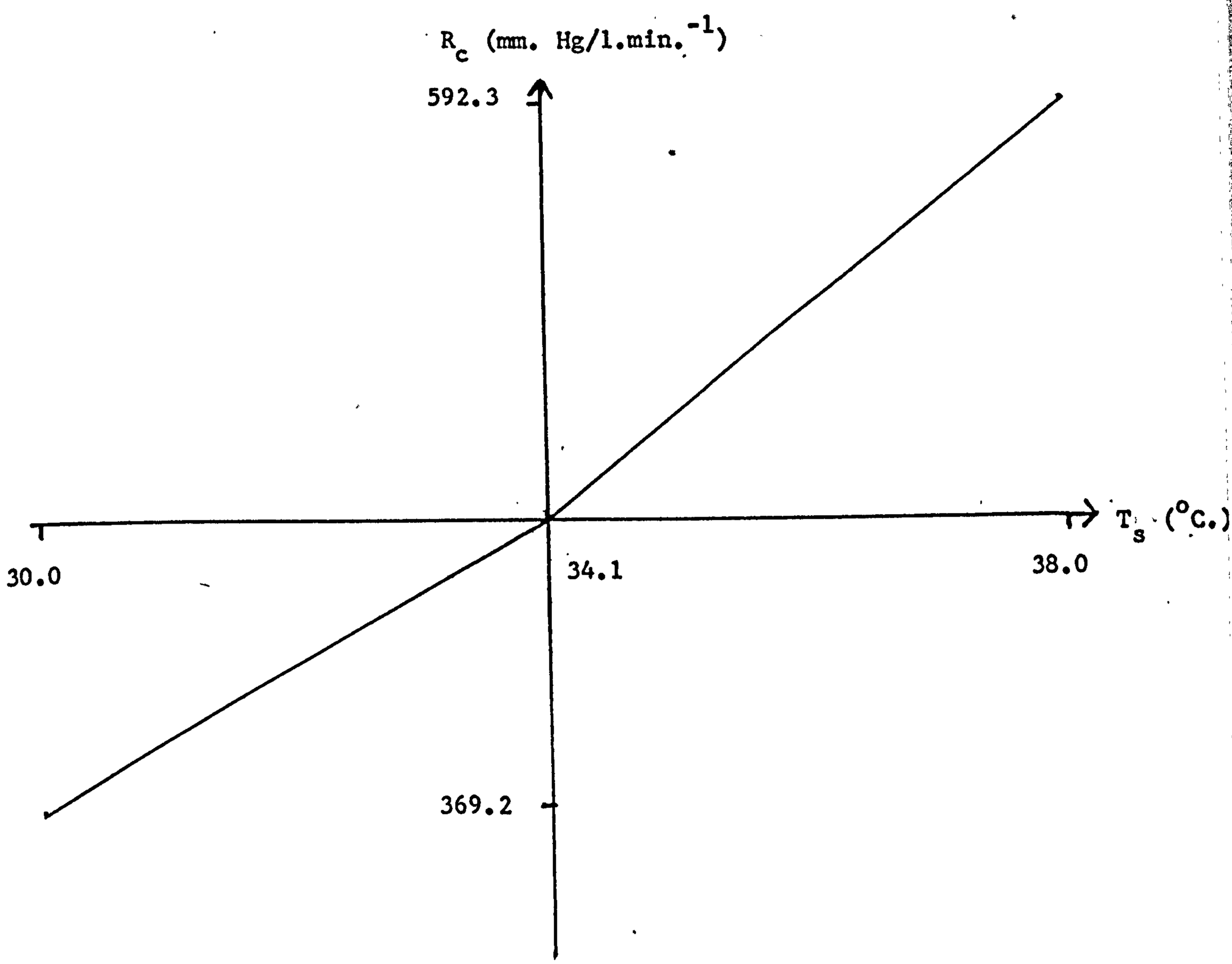

Figure 4.7. Effect of surface temperature on resistance to blood flow through the surface of the body.

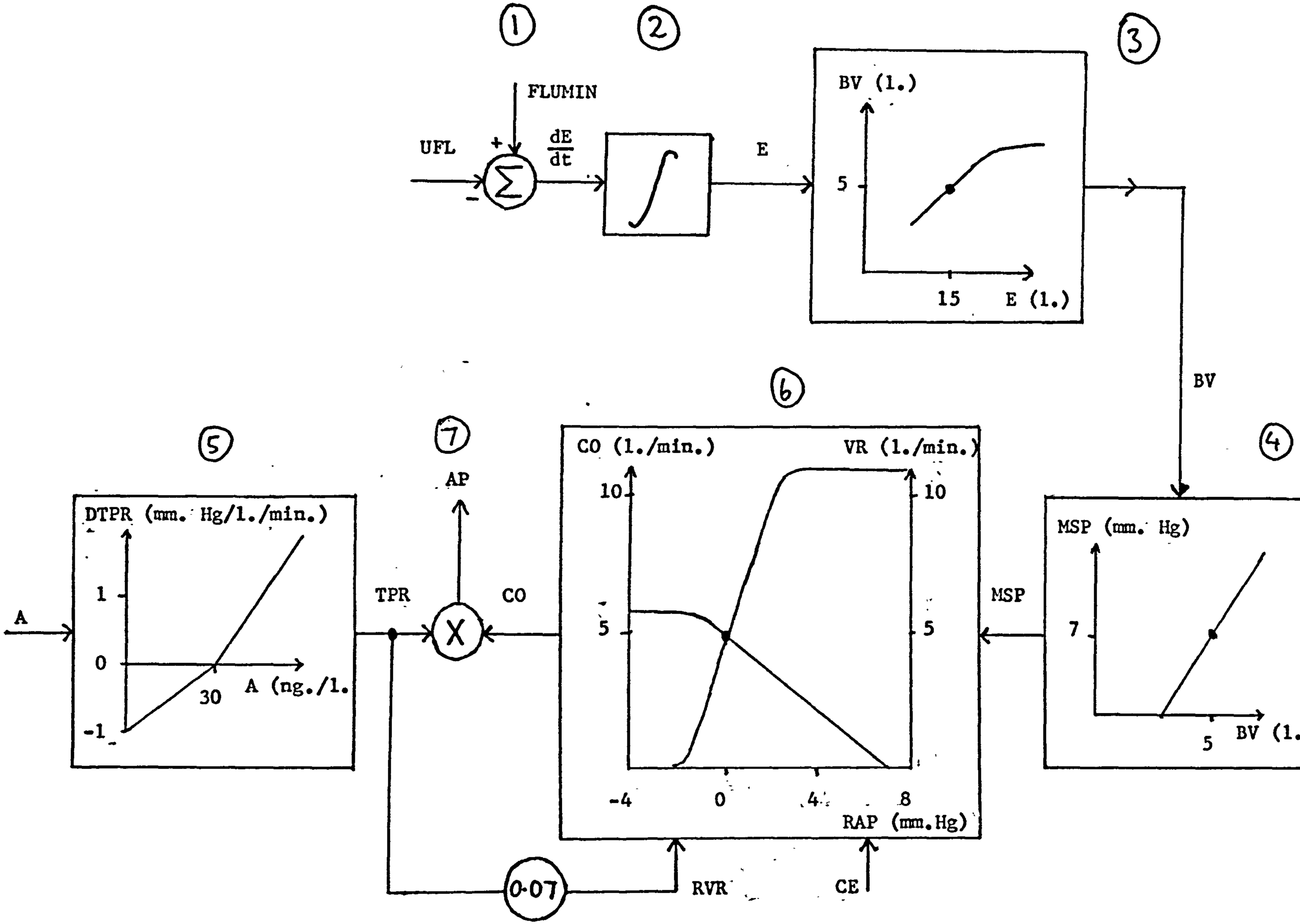

Figure 4.8. Block diagram of cardiovascular system.

PAGE NUMBERING AS ORIGINAL

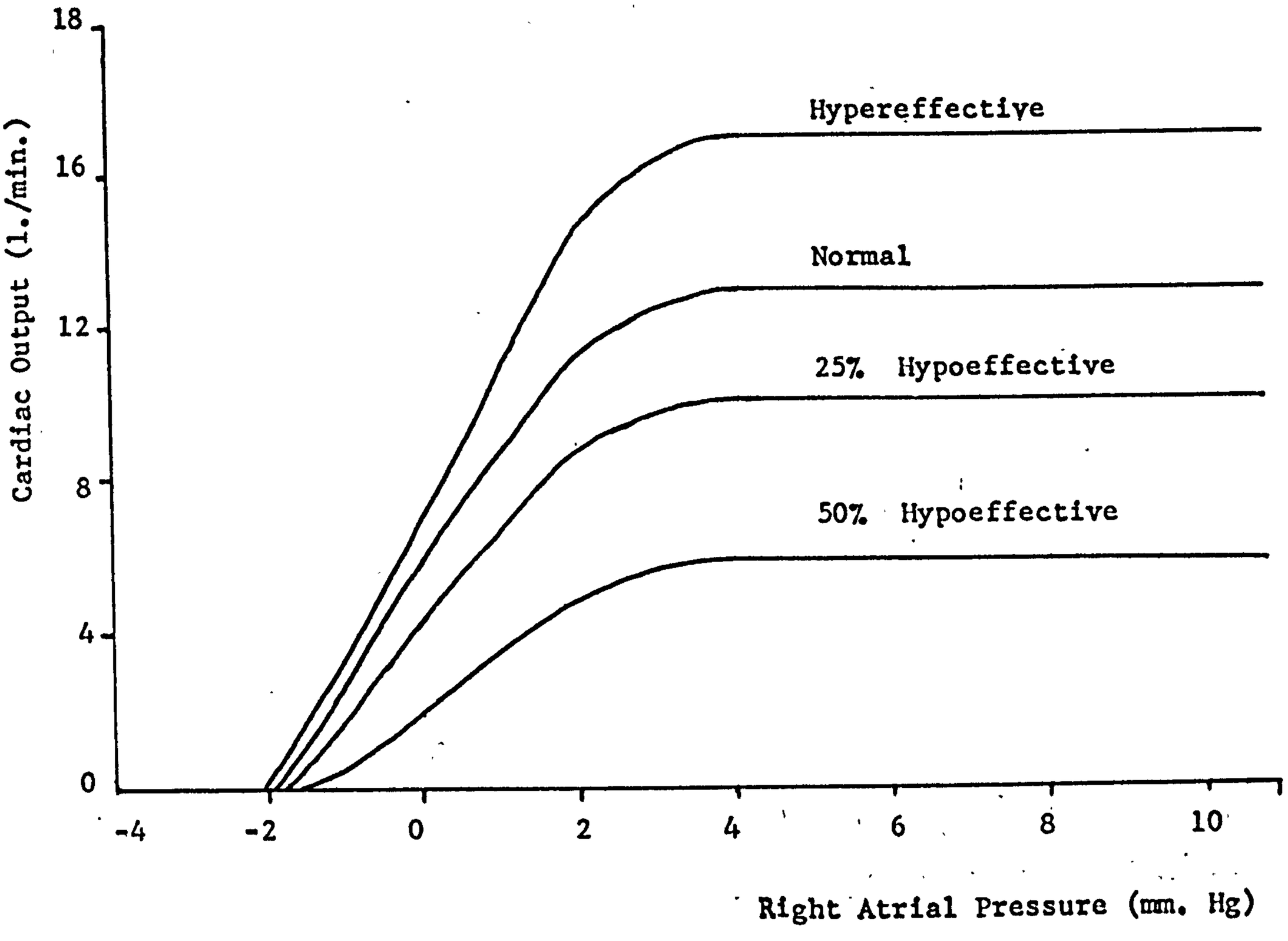

Figure 4.9. A set of cardiac function curves.

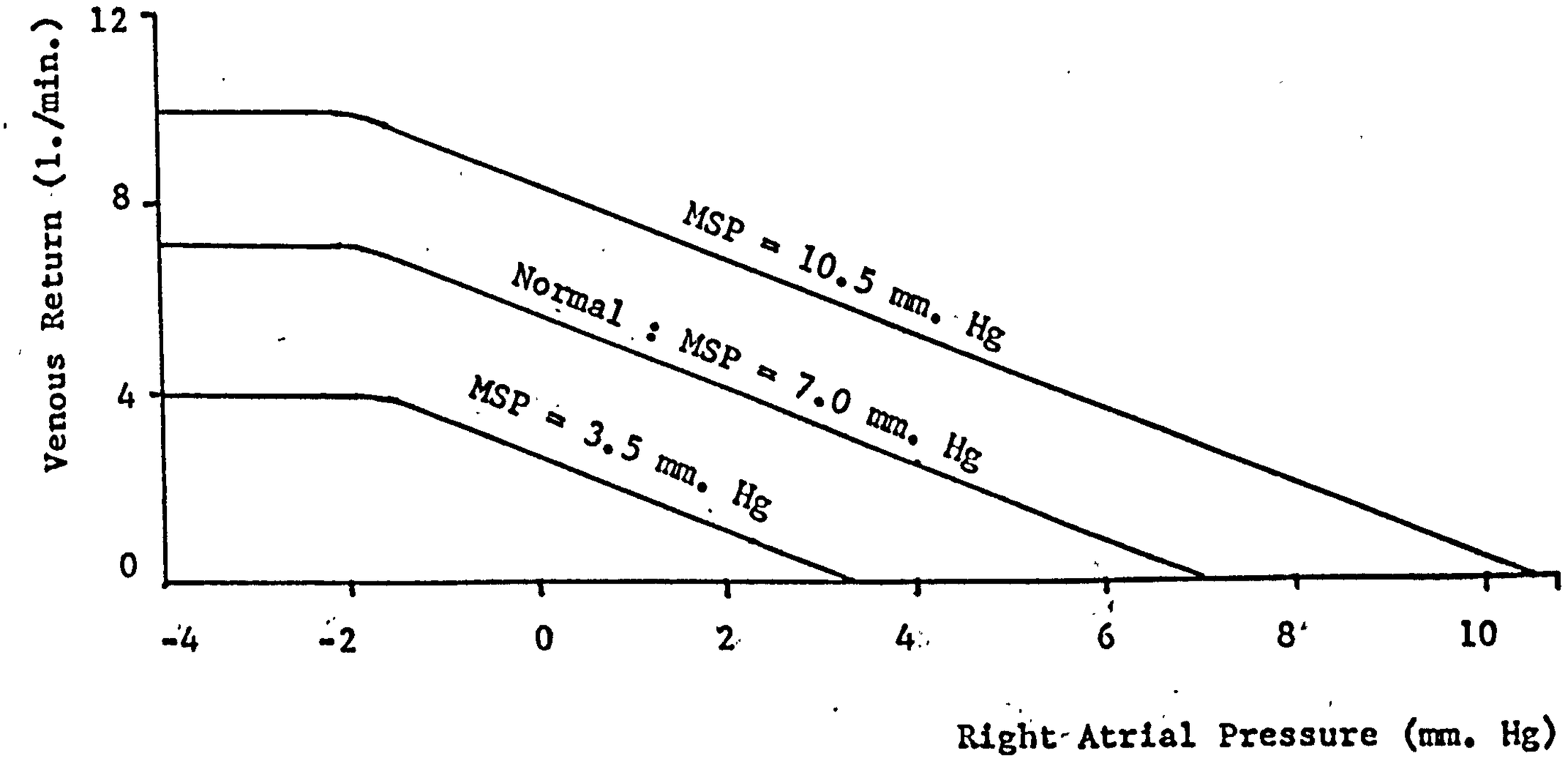

Figure 4.10. A set of systemic function curves.

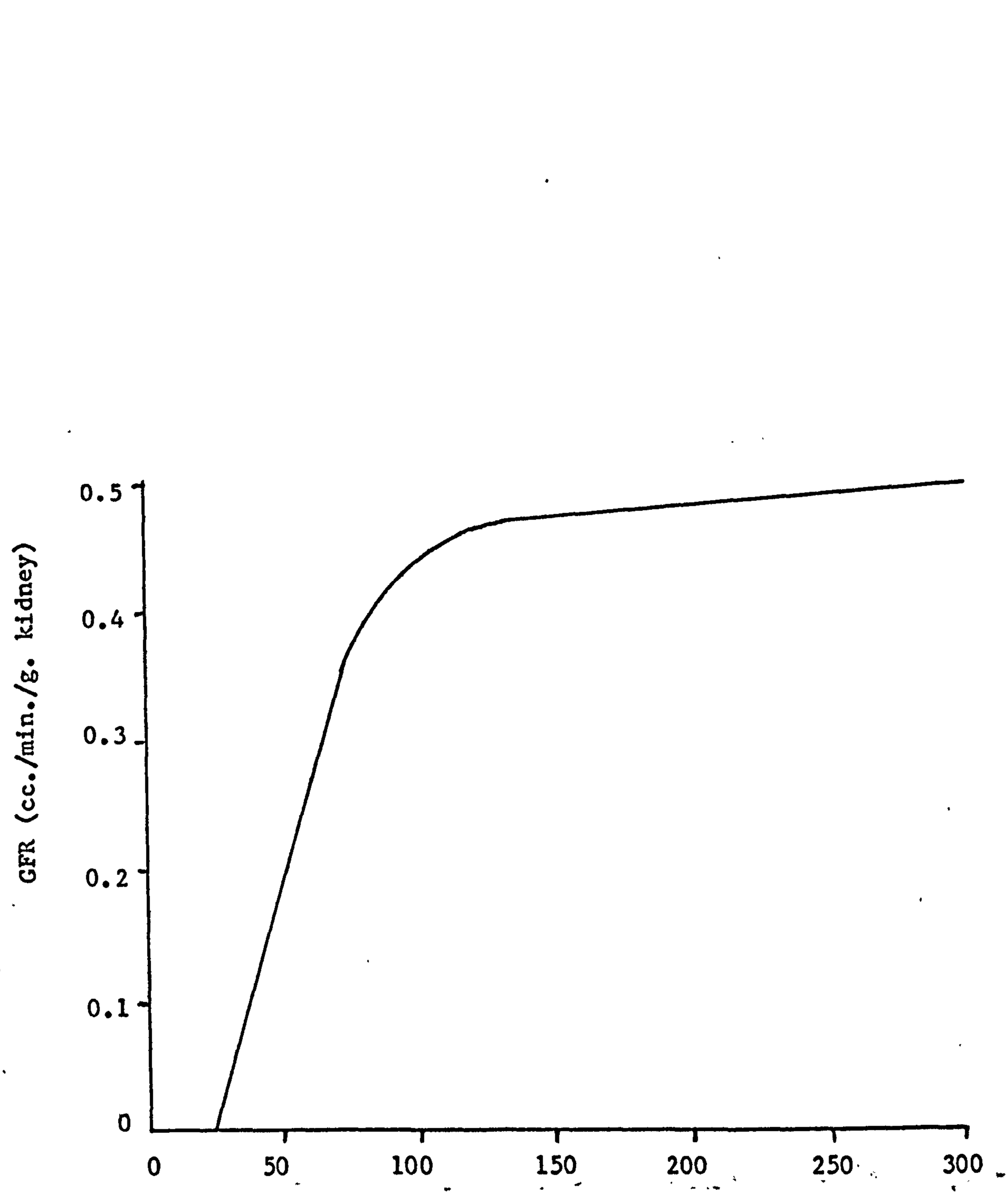

Figure 4.11. Relation between GFR and mean arterial blood pressure derived by Shipley and Study (1951).

CHAPTER 5

SIMULATIONS USING THE MODEL AS A REPRESENTATION OF A NORMAL HUMAN.

The mathematical equations comprising the model of the patient - artificial kidney machine system were presented in the previous chapter. The modelling process, however, is not complete until the model is shown to satisfy tests to establish its validity; that is, it has to be demonstrated that the model is a sufficiently accurate representation of the real system to be capable of meeting its objectives.

In practice, the validation exercise forms part of the feedback path of an iterative optimization process, where the uncertain model structures and parameters are adjusted until the model is a sufficiently accurate representation of the real system to satisfy the validation tests. Therefore, it is important that the strategy adopted to test the validity of a mathematical model be relevant to the tasks to which the model is eventually to be applied.

The overall model, presented in the previous chapter, was formulated for the main purpose of prediction of the future state of the patient undergoing dialysis, and thus to serve as an aid in patient management. A further objective of this work, however, is to examine various controller structures that may exist in the human body by using the model as an instrument to test hypotheses. Therefore, the tests chosen to examine the validity of the model are such that the results indicate the capabilities of the model to achieve these objectives.

The model presented in the previous chapter is the final product of the manual optimization procedure, outlined above, based on the simulation tests and optimal results described in this and the following chapter. The simulation tests in this chapter are related to the use of the model to represent the renal - body fluid system of an average, healthy human, and the tests in the subsequent chapter examine the capabilities of the model to represent the process of dialysis on a patient with renal failure.

This chapter presents the results of simulations of certain relevant experiments on healthy humans as reported in the literature. Comparison of the reported experimental results and the simulation results serves as an indication of the validity of the model of the renal - body fluid system of the healthy human. The experiments were chosen on the basis that the validity of all the subsystem models of the renal - body fluid system would be tested, but that the validity of the subsystem models with greatest uncertainty - the hormonal control systems - would be under greatest scrutiny. Therefore, the experiments chosen from the literature are the effects of:

(1) Water loading,
(2) Hypertonic saline loading,
(3) Saline loading after the reduction of renal mass,
(4) Aldosterone loading.

In addition, simulations which confirm the validity of certain assumptions made in the process of the development of the model are presented. This serves to demonstrate the manner in which the model of the renal - body fluid system of a healthy human may be used to test further hypotheses.

5.1. The Effect Of A Water Load.

The experiment, reported by Baldes and Smirk (1934), consisted of monitoring the urine flow rate in a human subject following the rapid ingestion of one litre of water. The results of this experiment are shown in Figure 5.1. Similar experiments were conducted by Forsling (1979) at the Department of Physiology of the Middlesex Hospital in London. The time course of the mean of these results, together with their standard deviation are shown in Figure 5.2. The major difference between these two sets of results, considering gross features, is the absence of the oscillations and plateau at the peak of the curve in the results of Forsling. Consideration of the results of the individual experiments conducted by Forsling, an example of which is shown in Figure 5.3, suggests that this difference is not due to the

effects of averaging the results of eight subjects. Rather, it appears that these features in the much publicised data reported by Baldes and Smirk are due to the peculiarities of the single subject on whom the experiment was conducted. However, apart from this difference, the features of the two sets of data are generally in agreement.

The experiment was simulated with the use of a model described by the equations presented in sections 4.2, 4.3, 4.4 and 4.6 of the previous chapter. The ingestion of water was simulated by increasing the water content of the extracellular fluid compartment by one litre at an instant in simulated time; and the effect of the transfer of fluid across the walls of the stomach into the fluid compartment on the response in the actual experiments was approximated by introducing a pure delay of fifteen minutes in the simulated response immediately after the expansion of the extracellular compartment.

The simulation results are plotted on Figure 5.1 for comparison. It is seen that the general features of the simulated urine flow rate response match those of the data presented by Baldes and Smirk. The simulated response curve exhibits the same characteristics of a sharp rise, followed by a relatively flat portion and a sharp fall. However, the features of the simulated response are seen to match those of the data reported by Forsling to a much greater extent.

Examination of the responses of the other variables of the model to the simulated water load stress indicates that the urine flow rate response is mediated by changes in the concentration of ADH in plasma. However, in the development of the model of the ADH system, there was uncertainty regarding the representation of the clearance of ADH from plasma. Therefore, the following subsection examines the effects of various clearance control structures on the response of the model to the water load.

5.1.1. Clearance Of ADH.

Owing to the difficulties in measuring low concentrations of ADH, uncertainty exists regarding the rates of clearance of ADH at levels below the normal concentration of ADH in plasma.

Czaczkes and assosiates (1964) suggested that the rate of clearance of ADH increases as the concentration of ADH decreases. Lauson (1960), however, suggested that under physiological conditions, the rate of clearance of ADH is essentially constant. In the development of the model, it was assumed that the rate of clearance of ADH is a decreasing function of its concentration up to its normal concentration in plasma. This is in agreement with the concepts presented by Czaczkes and associates, and the function used is similar to that of a previous model of the human ADH system (Bigelow et al., 1973). However, the control action for the removal of ADH used in the model, equation (4.37), presented in Chapter 4, was adopted following simulations of the water load and other experiments using the model with several candidate control actions. Two of the simulation results are presented below.

(i) Constant Rate Of Clearance Of ADH.

The model was adjusted so that the rate of clearance of ADH was considered to be independent of the concentration of ADH in plasma. The constant rate of clearance of ADH was set to a value equal to that calculated from steady state considerations (equation (4.41)). This was achieved by replacing equations (4.37) and (4.39) by equation (5.1):

$$PV_x \frac{d(ADH)}{dt} = ADHS - 0.206 x ADH \qquad (5.1)$$

The model in this form was used to simulate the water load experiment. The simulation results are shown in Figure 5.4. The features of the results of this simulation are not matched to the features of the actual experiment (Figures5.1 and 5.2) as well as the simulation results presented above. Thus, as evident from the simulations above, the rate of clearance of ADH increases as the concentration of ADH in plasma decreases.

(ii) Third Control Strategy For The Clearance Of ADH.

A high rate of clearance at low levels of ADH in plasma is perhaps unphysiological since the system would then be relatively unresponsive when returning from a state of hydration (low ADH

level) to normal hydration. Therefore, the third candidate function, equations (5.2), was proposed for the relationship between the rate of clearance of ADH and the concentration of ADH in plasma:

$$\begin{cases} DADH = 0.145 \times ADH & \text{if } ADH < 2.0 \text{ mu./ l.} \\ DADH = -0.042 \times ADH + 0.374 & \text{if } 2.0 \leqslant ADH \leqslant 4.0 \\ DADH = 0.206 & \text{if } ADH > 4.0 \text{ mu./ l.} \end{cases} \qquad (5.2)$$

The results of the simulation of the water load experiment using the model with the function (5.2) representing the relationship for the rate of clearance of ADH are shown in Figure 5.5. Comparison of the responses shown in Figures 5.1 and 5.5 indicates that the representation of the clearance of ADH from plasma as in the model of Chapter 4 results in the more accurate simulation of the water load experiment.

5.1.2. Conclusions On The Water Load Test.

Comparison of the simulation results and the experimental results reported by Baldes and Smirk (1934) and Forsling (1979) (Figures 5.1 and 5.2) indicates that the model is sufficiently valid to reproduce the features of response of the rate of flow of urine when a normal human is subjected to a water load stress. In particular, this test confirms the validity of the representation of the ADH control system in the model, since the variation in the rate of flow of urine is affected by the changes in fluid volume and the osmolality of plasma and subsequent changes in the concentration of ADH in plasma.

Furthermore, candidate hypothetical functions to represent the clearance of ADH from plasma were proposed. Two of the functions were described above. The results of simulations of the water load experiment and of other conditions, using the model with each of the proposed functions in turn indicated that the features of the experimental results were best matched to the simulation responses of the model incorporating the

function of equation (4.37) to represent the clearance of ADH from plasma. It is to be concluded, then, that the clearance of ADH from plasma in the real system may be approximated by the function of equation (4.37).

The other area of uncertainty regarding the ADH system is the manner in which the signals for the release of ADH due to changes in the osmolality of plasma and fluid volume, respectively, are combined. For modelling purposes, the following control action for the combining of these signals was proposed in section 4.4.1. For the condition when the osmolality of plasma and fluid volume are both above normal, the nett signal is considered to be equal to the sum of the signals weighted such that the weighting factor for the signal due to the fluid volume is an increasing function of the excess fluid (equation (4.36)); and for all other conditions, the nett signal is considered to be the simple average of the two signals. Simulation of the water load experiment confirms the validity of the control action for the condition of increased fluid volume and decreased osmolality of plasma, when the nett signal is considered to be the average of the two signals. The following test of the validity of the model, however, investigates the validity of the control action for the release of ADH when the increased osmolality of plasma tends to increase, and the simultaneous increase in fluid volume tends to decrease the rate of release of ADH.

5.2. Effect Of A Hypertonic Saline Load.

Experiments involving the infusion of hypertonic saline loads into adults and infants, and the subsequent monitoring of the rates of flow of urine, were reported by Dean and McCance in 1949. Each subject was deprived of fluid for sixteen hours before being infused with a solution of ten per cent sodium chloride. Dean and McCance (1949) reported the urine flow rate response for one adult, who was infused with a dose of 0.91 grammes of sodium chloride per kilogramme of body weight over a period of sixty-five minutes, and the average of the responses of all the adults, who were infused with various dosages over varying periods of time, as well as the responses of the infants.

The features of the response of the single adult, plotted in Figure 5.6, where the start of the experiment is considered to be the mid-point of the period of administration of the solution, are similar to those of the averaged response of the adults.

The experiment of loading the adult with a hypertonic saline load was simulated using the model of the renal - body fluid system of a normal human of 70.0 kilogrammes. This was achieved by appropriately programming values for the variables representing the rates of ingestion of sodium and water as follows:

<u>For 0.0 hours $<$ time $<$ 16.0 hours</u>

Rate of ingestion of sodium = Normal

Rate of ingestion of water = 0.0 ml./min.

<u>For 16.0 hours $\leqslant$ time $\leqslant$ 17.08 hours</u>

Rate of ingestion of sodium = 16.7 mEq./min.

Rate of ingestion of water = 9.8 ml./min.

<u>For time $>$ 17.08 hours</u>

Rate of ingestion of sodium = Normal

Rate of ingestion of water = Normal

Since representations of the stomach and intestines do not exist in the model, ingestion of the saline solution is equivalent to infusion in the real system.

The results of the simulation are plotted on Figure 5.6 for comparison with the response data of the actual system. It is seen that there is close agreement between the response of the real system and that of the simulation, to the stress of the infusion of hypertonic saline.

During the course of simulations of this experiment, it was determined that the response is sensitive to variations in two areas of uncertainty in the model. The first is the parameter representing the fraction of the glomerular filtrate reabsorbed in the proximal tubule, and the second is the manner in which the signals for the release of ADH due to the hyperosmolality of plasma and expanded fluid volume are combined. Simulation results presented in the following subsections demonstrate the sensitivity of the simulation response to perturbations in these areas of uncertainty.

5.2.1. Glomerular-Tubular Balance.

Approximately three-quarters of the filtered load of sodium is actively reabsorbed in the proximal tubule. A similar fraction of the water load is iso-osmotically reabsorbed. The phenomena that this fraction is independant of the rate of glomerular filtration is known as glomerular-tubular balance (Windhager, 1968). However, there is some evidence (Johnson et al., 1967) that this balance is upset by changes in the plasma concentration of sodium, and it has been postulated that the balance is then controlled by an as yet undetermined natriuretic hormone (Tobian et al., 1967).

In the model, the fraction of the tubular load of sodium and water reabsorbed, GTB, is given as a function of the plasma concentration of sodium, PNA:

$$\left.\begin{aligned} &GTB = -0.0357.PNA + 5.815 \\ &GTB = 1.0 \quad \text{if} \quad GTB > 1.0 \\ &GTB = GTB \quad \text{if} \quad 0.75 \leqslant GTB \leqslant 1.0 \\ &GTB = 0.75 \quad \text{if} \quad GTB < 0.75 \end{aligned}\right\} \qquad (4.16)$$

Comparison of the experimental data of Figure 5.6 and the results of simulations of this experiment using the model with differing lower constraints on the value of GTB, indicated that the optimum lower limit for the value of GTB is 0.75. The sensitivity of the simulation response to variations in this parameter is demonstrated by the comparison, in Figure 5.7, of responses of the model with values for this parameter of 0.6 and 0.75, and the response of the real system. Thus, from these simulations, it may be concluded that the normal glomerular-tubular balance is unaffected by the increase above normal, of the concentrations of sodium in plasma, associated with the infusion of hypertonic saline.

5.2.2. Combination Of The Signals To Release ADH.

The similarity of the features of the experimental and simulation results of the water load test described in the previous section confirms the validity of the assumptions regarding the control action for combining the signals for the release of ADH for the condition when the increase in fluid volume and the decrease in the osmolality of plasma both tend to inhibit the release of ADH. In the case of a hypertonic saline load, however, the increase in fluid volume tends to inhibit, and the increase in the osmolality of plasma tends to stimulate the release of ADH, respectively. Comparison of the experimental results and simulation response, presented in Figure 5.6, confirms the validity of the assumptions made in the development of the model regarding the combining of these signals for this condition (section 4.4.1). However, the function for the combining of these signals (equation (4.36)) was arrived at by consideration of the simulation responses of the model incorporating several candidate functions and the results of the saline infusion experiment. In order to demonstrate the sensitivity of the simulation response to variations in the control action for the combining of the signals for the release of ADH due to excess fluid volume, ADHSV, and hyperosmolar plasma, ADHSP, respectively, to give the nett signal for the release of ADH, ADHS, the simulation responses of the model incorporating three candidate functions are presented with the experimental results in Figure 5.8. The candidate functions, replacing equation (4.36) in the model are:

(a)

$$ADHS = (ADHSV + ADHSP) / 2.0 \quad \text{for all conditions.} \qquad (5.3)$$

(b)

$$\left.\begin{aligned} ADHS &= ((15.0 \times DWV \times ADHSV) + ADHSP)/((DWV \times 15.0) + 1.0) \\ &\text{for } POS > 299.6 \text{ mosm./l.} \quad \text{and} \quad DWV > 2.0 \text{ l.} \\ ADHS &= (((29.0 \times DWV - 28.0) \times ADHSV) + ADHSP) \\ &\quad / ((29.0 \times DWV - 28.0) + 1.0) \\ &\text{for } POS > 299.6 \text{ mosm./l.} \quad \text{and} \quad 1.0 \leqslant DWV \leqslant 2.0 \\ ADHS &= (ADHSV + ADHSP)/2.0 \quad \text{for all other conditions.} \end{aligned}\right\} \qquad (5.4)$$

(c)

$$\left.\begin{aligned}
&ADHS = ((20.0 \times DWV \times ADHSV) + ADHSP)/((DWV \times 20.0) + 1.0) \\
&\qquad \text{for } POS > 299.6 \text{mosm./l.} \quad \text{and} \quad DWV > 2.0 \text{ l.} \\
&ADHS = (((39.0 \times DWV - 38.0) \times ADHSV) + ADHSP) \\
&\qquad / ((39.0 \times DWV - 38.0) + 1.0) \\
&\qquad \text{for } POS > 299.6 \text{ mosm./l.} \quad \text{and} \quad 1.0 \leqslant DWV \leqslant 2.0 \\
&ADHS = (ADHSV + ADHSP)/2.0 \quad \text{for all other conditions.}
\end{aligned}\right\} \quad (5.5)$$

The rate of release of ADH due to the hyperosmolar plasma in the model incorporating candidate function (a) is such that the concentration of ADH in plasma is maintained at a high level throughout the simulation time; and the effects of the signal to inhibit the release of ADH due to the excess fluid volume is masked. The result is that urine is caused to flow at very low rates in the simulation. Thus, the functions of the form of candidate hypotheses (b) and (c), with variable weighting factors were proposed in order to overcome this drawback, and the optimal function was found to be the one eventually used in the model, equation (4.39).

5.2.3. Conclusions On The Hypertonic Saline Infusion Test.

Comparison of the urine flow rate response to hypertonic saline infusion, as reported by Dean and McCance (1949), with the simulation response of the model of the renal - body fluid system of the average human, in Figure 5.6, indicates that the model is sufficiently valid to reproduce the real response to within acceptable limits. In particular, this test for the model confirms the validity of the kidney function model and the ADH control system model.

Furthermore, this test is of special interest, since the infusion of a hypertonic saline solution gives rise to conflicting signals for the release of ADH. Since the concentration of ADH in plasma is a major determinant of the rate of urine flow, the successful simulation of this experiment indicates that the control

action for combining the signals for the release of ADH in the real system is adequately represented in the model.

The optimum function to represent the control action for combining the signals for the release of ADH was determined by the iterative technique of minimizing the error between the experimental result and the simulation response of the saline infusion test. The minimum fraction of sodium and water reabsorbed in the proximal tubule was similarly determined from simulations. These latter simulations provide evidence that the normal glomerular-tubular balance ratio of 0.75 is not affected by the elevated plasma concentration of sodium, and hence, evidence against the theory of the existence of a natruiretic substance, as proposed by Tobian and associates (1967).

However, these optimal functions were determined independently, although variations in each affects the simulation in a similar manner. Thus, these optimal functions may only represent a local optimum. Several simulations with various values for the minimum glomerular-tubular balance ratio and various functions representing possible control actions for combining the signals for the release of ADH were performed in order to demonstrate that the functions used in the model are the globally optimal functions. Figure 5.9 presents the simulation responses of the model incorporating two pairs of functions:

(a) $GTB_{MIN} = 0.7$

$$ADHS = ((14.0 \times DWV \times ADHSV) + ADHSP)/((DWV \times 14.0) + 1.0)$$

for POS > 299.6 mosm./l. and DWV > 2.0 l.

$$ADHS = (((27.0 \times DWV - 26.0) \times ADHSV) + ADHSP) / ((27.0 \times DWV - 26.0) + 1.0)$$

for POS > 299.6 mosm./l. and $1.0 \leqslant DWV \leqslant 2.0$

ADHS = (ADHSV + ADHSP) /2.0 for all other conditions.

(b) $GTB_{MIN} = 0.6$

$$ADHS = ((10.0 \times DWV \times ADHSV) + ADHP)/((DWV \times 10.0) + 1.0$$

for POS $>$ 299.6 mosm./l. and DWV $>$ 2.0 l.

$$ADHS = (((19.0 \times DWV - 18.0) \times ADHSV) + ADHSP) / ((19.0 \times DWV - 18.0) + 1.0)$$

for POS $>$ 299.6 mosm./l. and $1.0 \leq DWV \leq 2.0$

$$ADHS = (ADHSV + ADHSP)/2.0$$ for all other conditions.

The model incorporating each of the pairs of functions, (a) and (b), generated locally optimal simulations. However, comparison of Figures 5.6 and 5.9 indicates that the simulation generated by the model incorporating the functions of equations (4.16) and (4.36) is the optimally matched simulation.

The results of the water load and hypertonic saline infusion experiments were reported as the resultant dynamic response of the urine flow rate. Therefore, using these experimental results, the validity of the model was estimated by comparing these urine flow rate dynamic responses with those of the simulations of these experiments. The factors which directly influence the rate of flow of urine are those incorporated in the models of the kidney functions, presented in section 4.3, and the ADH system, presented in subsection 4.4.1. Hence, the validity of these system models to reproduce features of response is demonstrated by the results of these tests.

In addition, since the other system models, the cardiovascular system model, the renin-angiotensin-aldosterone model, the fluid and electrolyte balance model, all indirectly affect the rate of flow of urine, the results of these tests place a fair degree of confidence in these other system models. Nonetheless, the following two tests of the validity of the model compare more of the key variables, so that the validity of these other system models may be estimated.

5.3. Reduced Renal Mass With Increased Sodium Intake.

A simulation was performed, using a detailed, extensive model of the circulation and renal - body fluid system, to represent the events during the development of hypertension (Guyton et al., 1972). This model was discussed in section 3.1.2. Due to the level of detail incorporated in this model, it was decided that comparison of these simulations results and those generated by simulating the same conditions using the model presented in this work would be a suitable challenge.

The condition simulated by Guyton and associates is the following. Renal mass is reduced to one-third normal; simultaneously, the rates of intake of sodium and water are increased to fivefold and double normal, respectively. The results of this simulation are presented in Figure 5.10, where the dynamic responses of the variables representing the extracellular fluid volume, blood volume, cardiac output, total peripheral resistance, arterial pressure and urinary output are plotted against time.

This condition was simulated, using the model presented in Chapter 4, by the following manoeuvres. The reduction in renal mass was represented by setting the multiplicative factors, used to represent renal insufficiency, as discussed in section 4.7, to 0.33. However, compensatory, adaptive changes are known to occur in the remaining nephrons when the number of functioning nephrons is reduced. These changes are most marked in the glomeruli and proximal tubule segments of the remaining nephrons (Gottschalk, 1971). Extrapolation from experiments, where the relation between the percentage of glomeruli remaining after subtotal nephrectomy of dogs and glomerular filtration rate is determined (Hayman et al., 1939), yields the result that glomerular filtration rate is reduced to sixty per cent of its value when renal mass is reduced to one-third normal. Therefore, this was appropriately incorporated in the model. In addition, the rates of intake of sodium and water were programmed:

Rate of intake of sodium = 0.66 mEq./min.
Rate of intake of water = 2.0 ml./min.

The computer programme was run such that the above changes were

made in the model after one day of simulated time had elapsed.

The results of this simulation are shown in Figure 5.10 for comparison with the results of the simulation performed by Guyton and associates. It is seen that the urinary output response curve of this simulation corresponds with that of the simulation carried out by Guyton and associates. This is to be expected, since the previous two tests of validity demonstrated that the model is capable of reproducing features of urine flow rate responses. The initial features of the total peripheral resistance (TPR) response curves are in agreement. However, the curve of the simulation, carried out by Guyton and associates, then rises. This, according to the authors, is mainly due to the long term control of local blood flow, when excess blood flow through tissues causes progressive constriction of the blood vessels; and this is the underlying mechanism for the development of hypertension. Since longer term control mechanisms are omitted from the model of this work, this feature of the TPR response is not present in the simulation response generated using the model of this work. Similarly, the curve representing the response of cardiac output in the simulation, carried out by Guyton and associates, rises and then gradually falls back to a normal value. The fall is said to be due to the effect of adaption of the baroreceptors on the heart. Since there is no representation of nervous control of the heart, the simulation of the model of this work does not exhibit this feature. The arterial pressure curve of the simulation, carried out by Guyton and associates, is seen to rise at a slightly faster rate than the response of this simulation. This appears to be caused by the gradual rise in TPR in the simulation, carried out by Guyton and associates, since arterial pressure is given by the product of cardiac output and TPR (equation (4.13)). The blood volume curves are seen to match.

Finally, there appears to be no match between the respective responses of the extracellular fluid volume. Examination of the other variables of this simulation indicates that the value for the concentration of sodium in the extracellular compartment rises to an unphysiological level. It is this that causes the serious overload of the extracellular compartment. In reality, it is debatable whether a human, subject to these conditions of

severely reduced renal mass and increased sodium and water intake, would achieve the steady state value of extracellular fluid volume suggested by these authors.

However, taking into account the recent findings that oral sodium loading produces a greater natriuresis than intravenous sodium administration in man, without there being any differences in the aldosterone response (Carey, 1978), an interesting explanation may be offered for this discrepancy between the simulation results, if those of the simulation, carried out by Guyton and associates, are considered to be physiologically correct. It is suggested (Carey, 1978) that natriuresis following oral administration of sodium is due to a natriuretic agent released in response to receptors in the gastrointestinal tract which monitor the quantity of sodium presented to them. It is then postulated that this natriuretic agent acts on the proximal tubule segments in the nephrons so that the normal glomerular-tubular balance ratio is reduced, thus causing the large, rapid natriuresis. There is, as yet, no evidence either to support of disprove this postulation. However, if the postulation is correct, the fraction of the proximal tubular load reabsorbed is related, not to the concentration of sodium in plasma, as suggested by equation (4.16), but to the rate of intake of sodium. (Incidentally, this quantity remains essentially constant in the patient undergoing dialysis). The explanation as to why, in the experiment of the infusion of a hypertonic saline solution, the glomerular-tubular balance ratio remains normal in the presence of an elevated concentration of sodium in plasma, is then, that the sodium receptors in the gastrointestinal tract were not stimulated to cause the release of the postulated natriuretic agent.

In the conditions being considered in this section, according to the above postulations, the glomerular-tubular balance ratio is reduced. Since there is no relevant data, however, the extent to which it is reduced is unknown. But the same conditions were simulated using the model with the minimum value of glomerular-tubular balance ratio reduced 0.3, and the results are shown in Figure 5.11. It is seen that in this case, there is agreement between the simulations regarding the extent to which the human, subject to these conditions, would be overloaded. In addition, the simulated concentration of sodium in plasma remains

within physiological levels.

In summary, the condition of reduced renal mass with increased sodium and water intake were simulated, and the results were compared with the simulation results reported by Guyton and associates (1972). The features of the results of the simulations are in agreement except for the following aspects. Firstly, there are deviations in the simulated responses of total peripheral resistance and cardiac output. These variables in the simulation, carried out by Guyton and associates, behave in a manner in accordance with the effects of long term control mechanisms not incorporated in the model of this work. In the development of the model of this work, it was considered that the inclusion of these longer term control mechanisms was unnecessary for the model to achieve its objectives. Secondly, disagreement exists regarding the extent to which the extracellular fluid compartment is overloaded as a result of the simulated condition. However, an example, of how the use of mathematical models serves to highlight areas of weak knowledge and indicates the direction for further experimentation, is created by this discrepancy.

5.4. Aldosterone Loading.

Relman and Schwartz (1952) conducted a fluid and electrolyte balance study during the course of daily intramuscular administration of 20 milligrammes of deoxycorticosterone acetate (DOCA)* to three groups of healthy adult humans. Each group was on a high, normal or low salt intake regimen. Davis and Howell (1953) conducted a similar experiment on four dogs on a controlled, normal salt diet.

The results of the experiments, averaged for the humans on the normal diet, and for the four dogs, are shown in Figure 5.12 as the time course of the following variables: extracellular fluid volume (extrapolated from weight gain data), arterial

* DOCA is a mineralocorticoid whose effects, apart from potency, are very similar to those of aldosterone.

pressure, hormone level and sodium excretion rate. The most significant aspect of these results is the demonstration of the phenomenon of 'escape', where, after an initial fall due to the high level of sodium retaining hormone, the rate of excretion of sodium rises to match the rate of intake.

The experiments were simulated, using the model of the healthy human, by multiplying the rate of secretion of aldosterone by a factor of four, throughout the period of simulation. This approximately represents the administration of DOCA as described above (Cameron, 1977).

The simulation results are shown in Figure 5.12 for comparison with the experimental results. It is seen that the features of response of the variables of the simulation representing extracellular fluid volume, arterial pressure, hormone level and the rate of excretion of sodium are in agreement with those of the experimental data. In particular, the 'escape' phenomenon is clearly apparent in the simulation response. Examination of the other variables of the simulation indicate that the contributing factors to 'escape' are the elevation of glomerular filtration rate, due to the expanded extracellular fluid compartment and elevated arterial pressure, and the increase in the concentration of sodium in plasma, resulting in the increased rate of filtration, and hence excretion, of sodium. It is of interest to note that 'escape' occurs without the adjustment of the glomerular-tubular balance ratio by the supposed natriuretic hormone in the simulation.

The simulation results, presented in Figure 5.12, thus contribute to the evidence of previous simulation tests, suggesting that the model is a sufficiently valid representation of the renal - body fluid system of a normal, healthy human, to reproduce features of responses due to a variety of stresses. This test, in particular, serves to demonstrate the validity of the representation of the aldosterone system, the cardiovascular system, fluid balance and the renal handling of sodium.

5.5. Conclusions.

The results of the tests of the validity of the model of the renal - body fluid system of the normal human, indicate its capabilities and limitations. The water load and hypertonic saline infusion simulations suggest that the model is capable of reproducing features of response, in the relative short term, of the output variable - urine flow rate. However, comparison of the simulations of the condition of reduced renal mass and increased sodium intake, made apparent the limitation that the model is not capable of predicting the long term effects of stresses. This was to be expected, since consideration of the objectives of this work dictated that representations of the relevant long term controllers be excluded from the model. The simulation of sustained sodium - retaining hormone administration displays the characteristics of renal 'escape', as expected; and analysis of the simulation variables indicate the mechanisms involved in this phenomenon.

The model offers the facility for the testing of hypotheses. Using the model as a basis, the probable function between the rate of clearance of ADH and its concentration in plasma was determined for the range of low concentrations which are difficult to measure. In addition, the means by which opposing signals for the release of ADH are effectively combined was suggested by the minimization of errors between the features of the simulation response and actual results of the hypertonic saline infusion experiment.

The model was also used in an attempt to resolve questions regarding the existence of an undetermined natriuretic substance which, it is postulated, acts on the proximal tubule in order to control the level of sodium in the body fluids. The results of simulations indicate that the natriuretic agent is released by signals from receptors monitoring the ingestion of sodium, so that corrective action is taken before the level of sodium in the body is perturbed to any large extent. However, the need for experimentation is made apparent, and the direction in which this should proceed may be determined by the use of the model.

Hence, the overall model of the patient - artificial kidney machine system, adapted to represent the renal - body fluid

system of the normal human, satisfies the tests set to determine its validity to reproduce features of response to stresses. It may thus be used to test further hypotheses regarding the relevant control systems of the human organism. The results of the test of the validity of the overall model, and therefore, of its capabilities of predicting the future state of the patient undergoing dialysis, is presented in the following chapter.

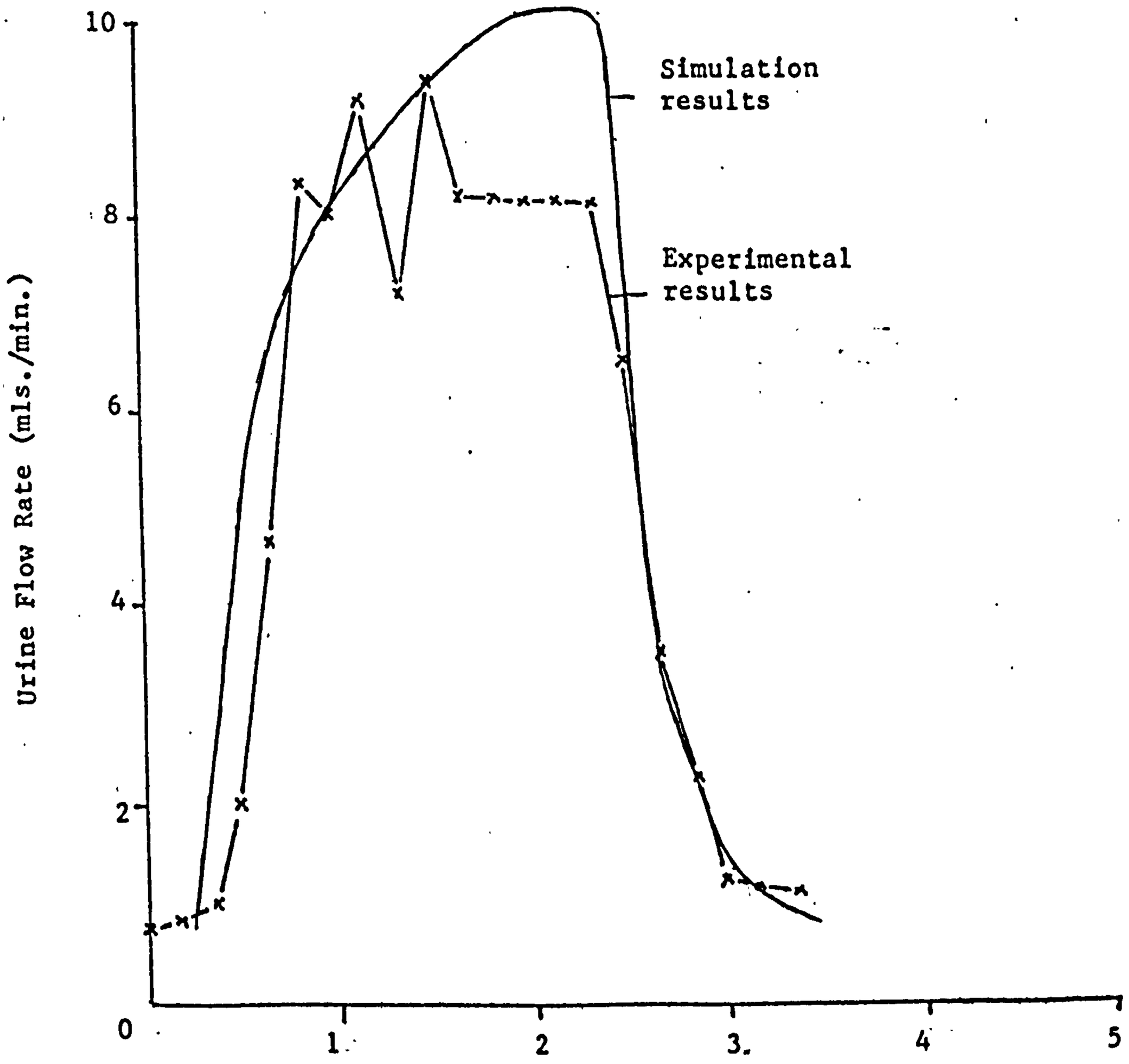

Figure 5.1. Urine flow following ingestion of one litre of water.

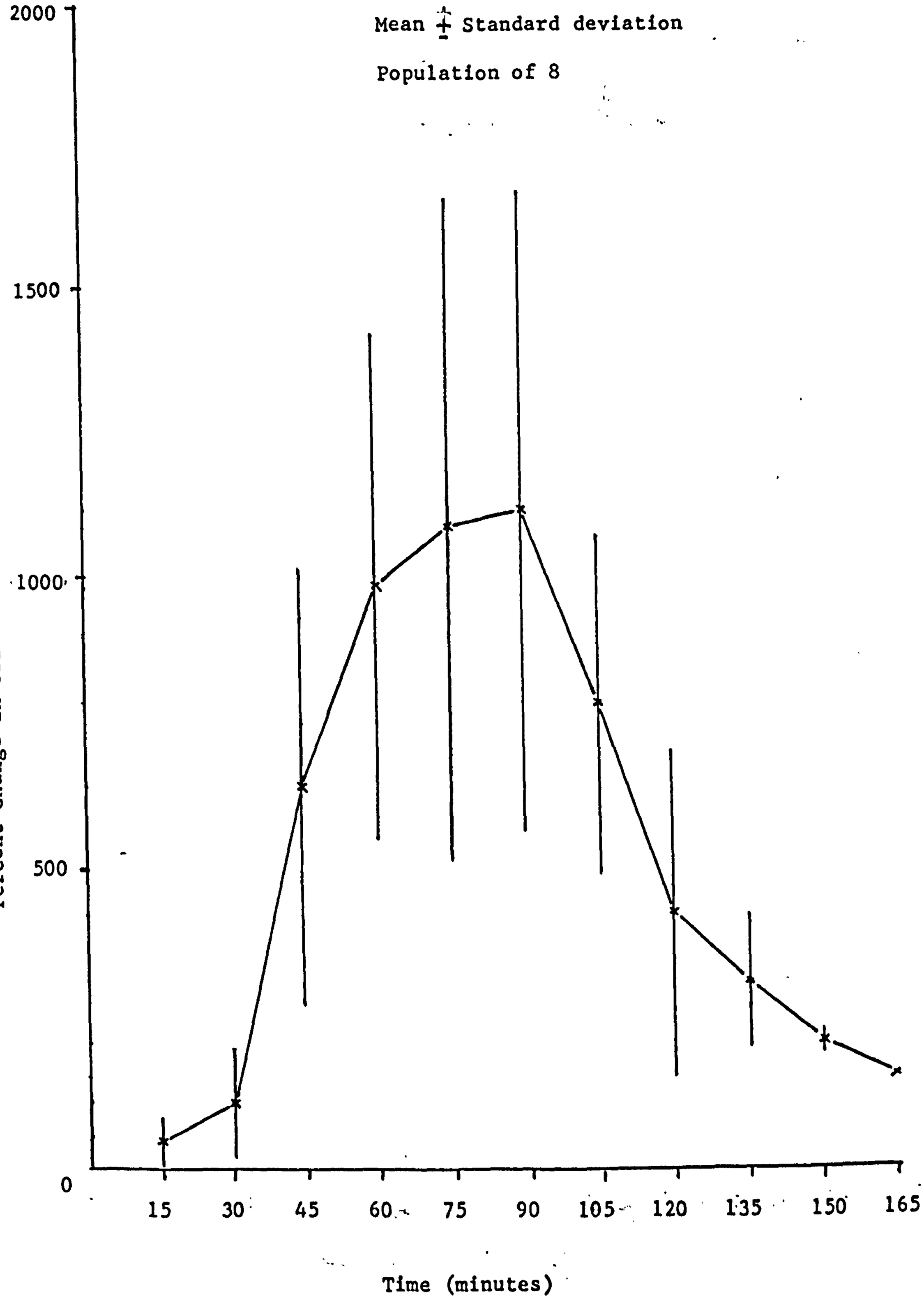

Figure 5.2. Average response of eight subjects to a water load stress. (Data from Forsling (1979)).

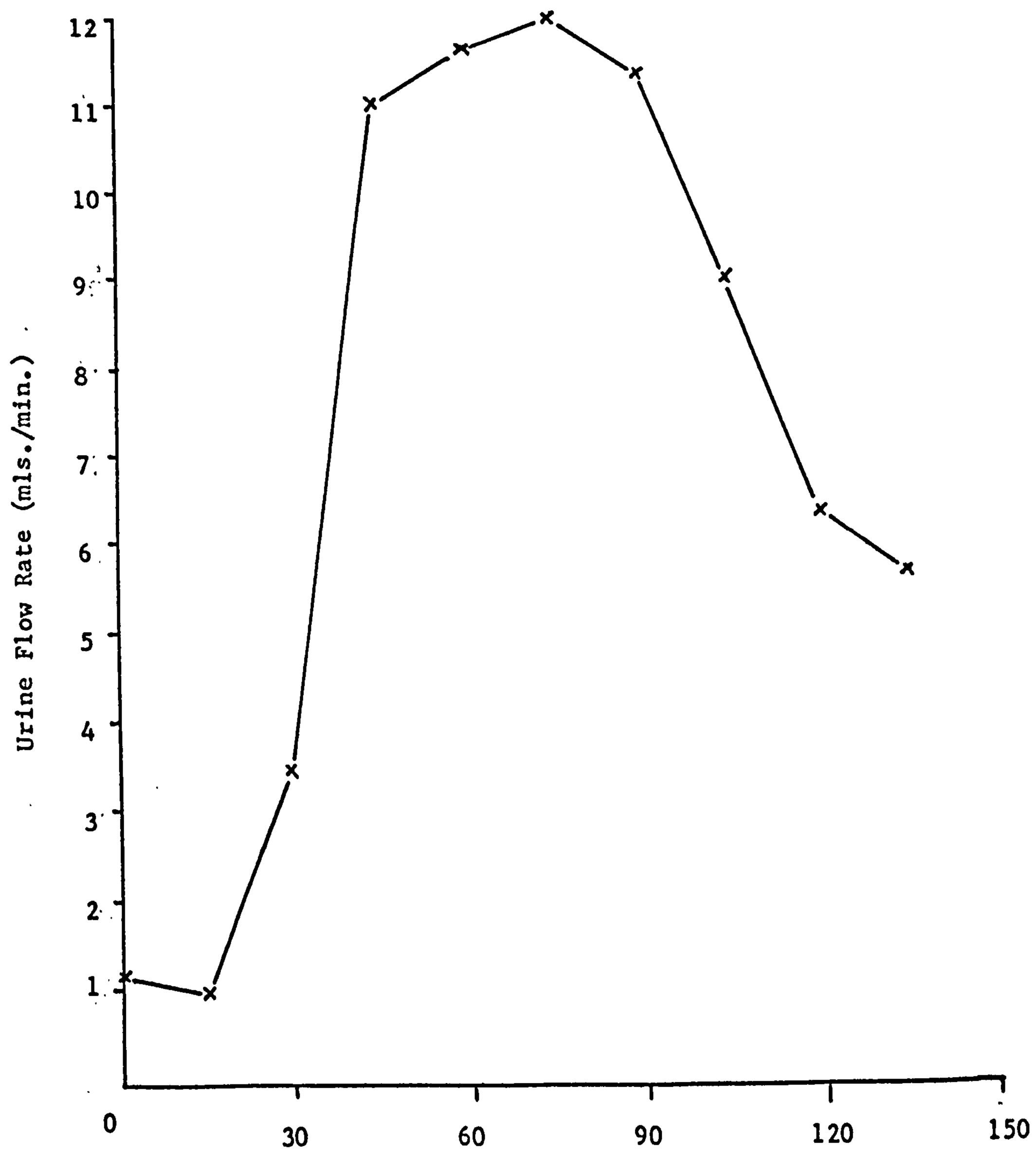

Figure 5.3. Result of a single water load test conducted by Forsling (1979).

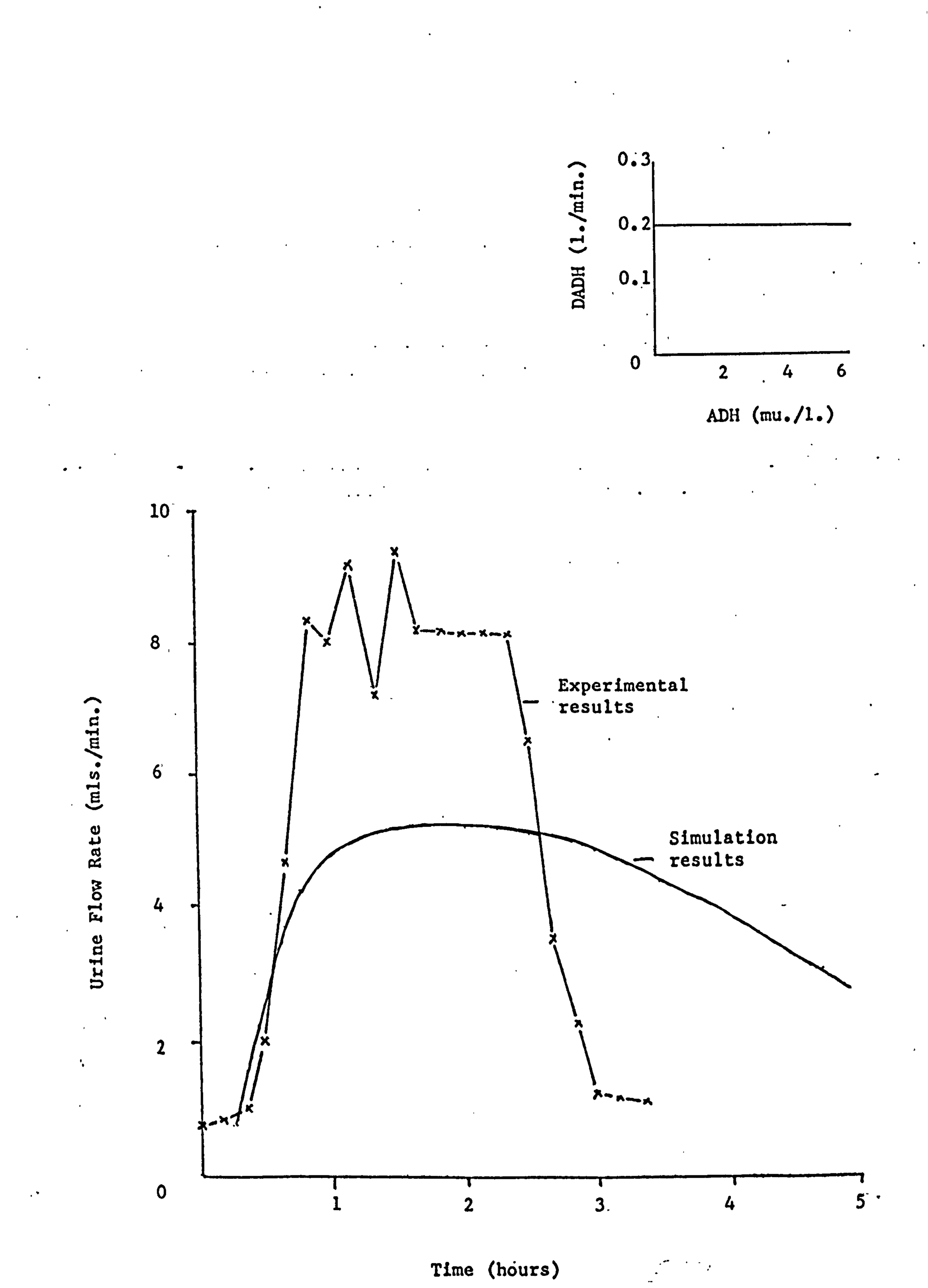

Figure 5.4. Urine flow following ingestion of one litre of water with constant rate of clearance of ADH.

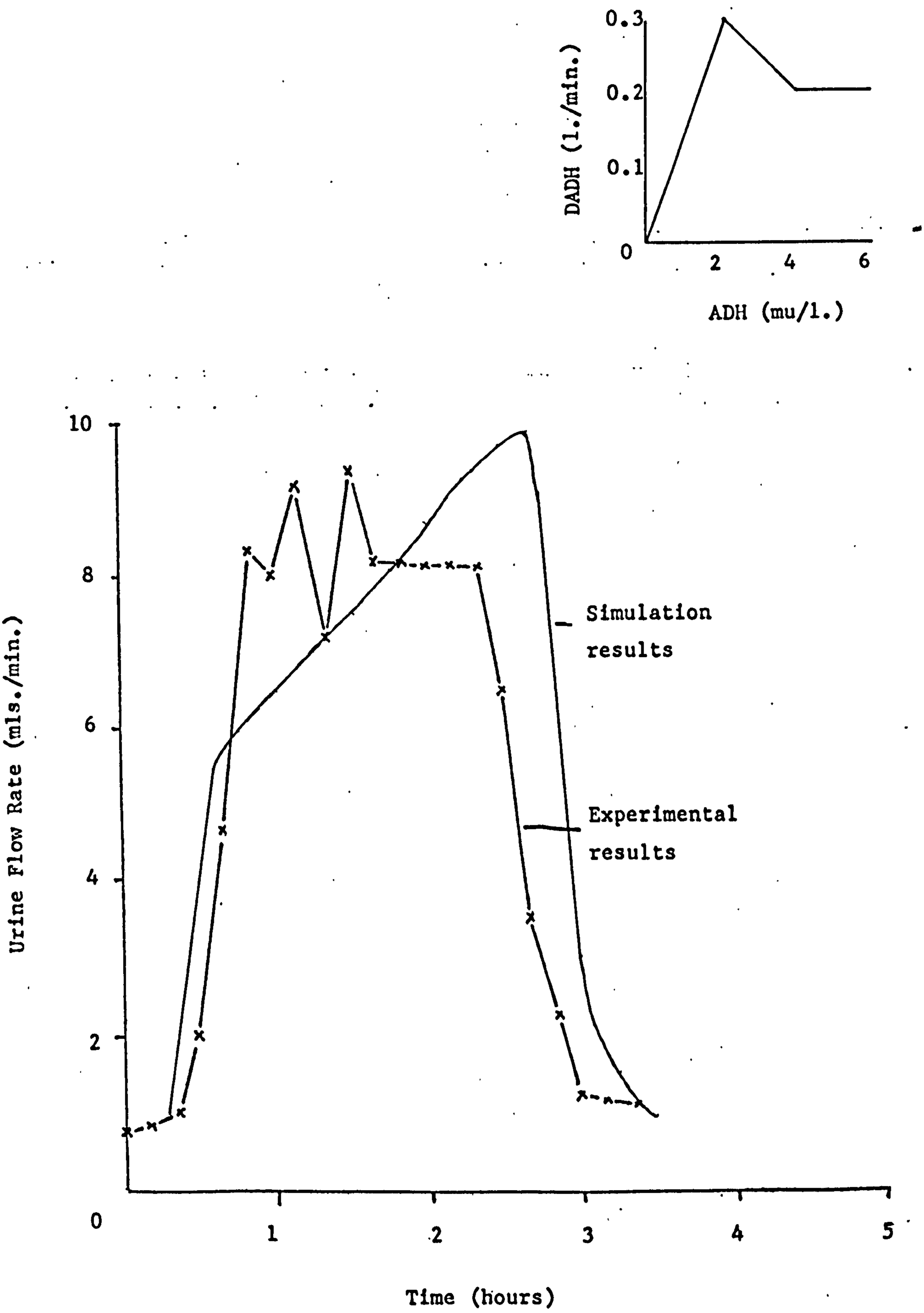

Figure 5.5. Urine flow following ingestion of one litre of water with third control strategy for the clearance of ADH.

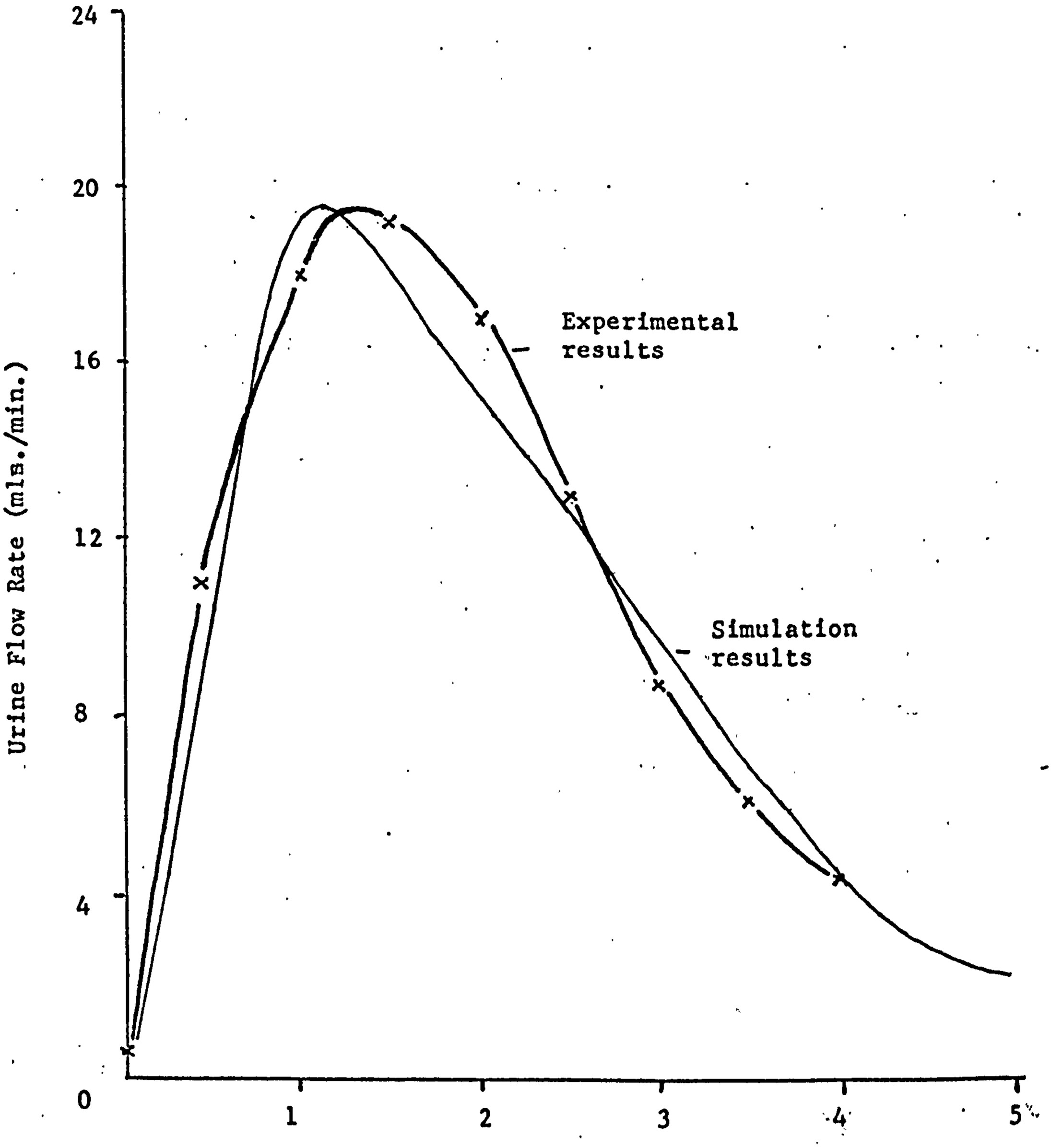

Figure 5.6. Urine flow following ingestion of hypertonic saline.

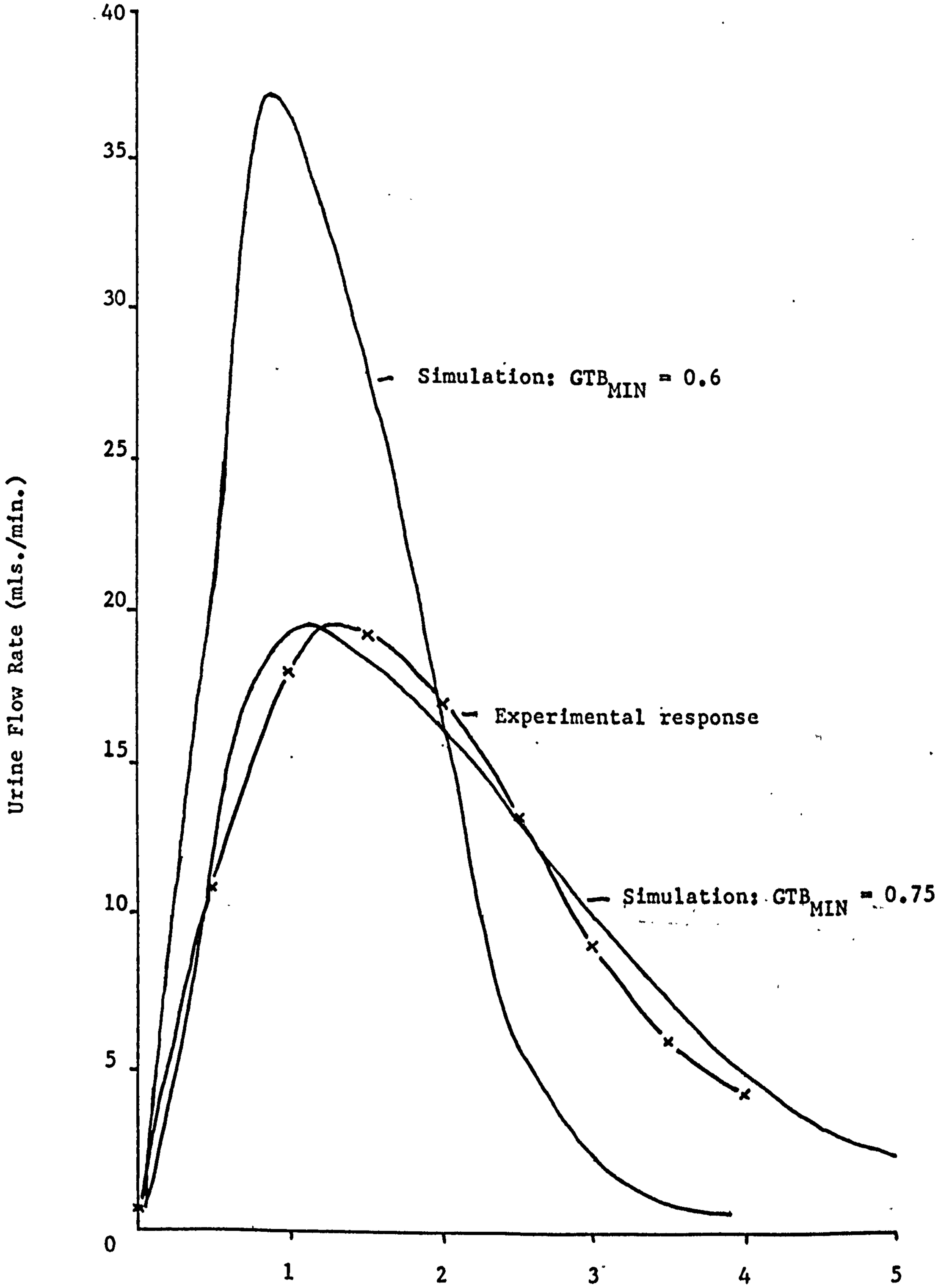

Figure 5.7. Sensitivity of simulation response of hypertonic saline infusion experiment to variation in glomerular tubular balance.

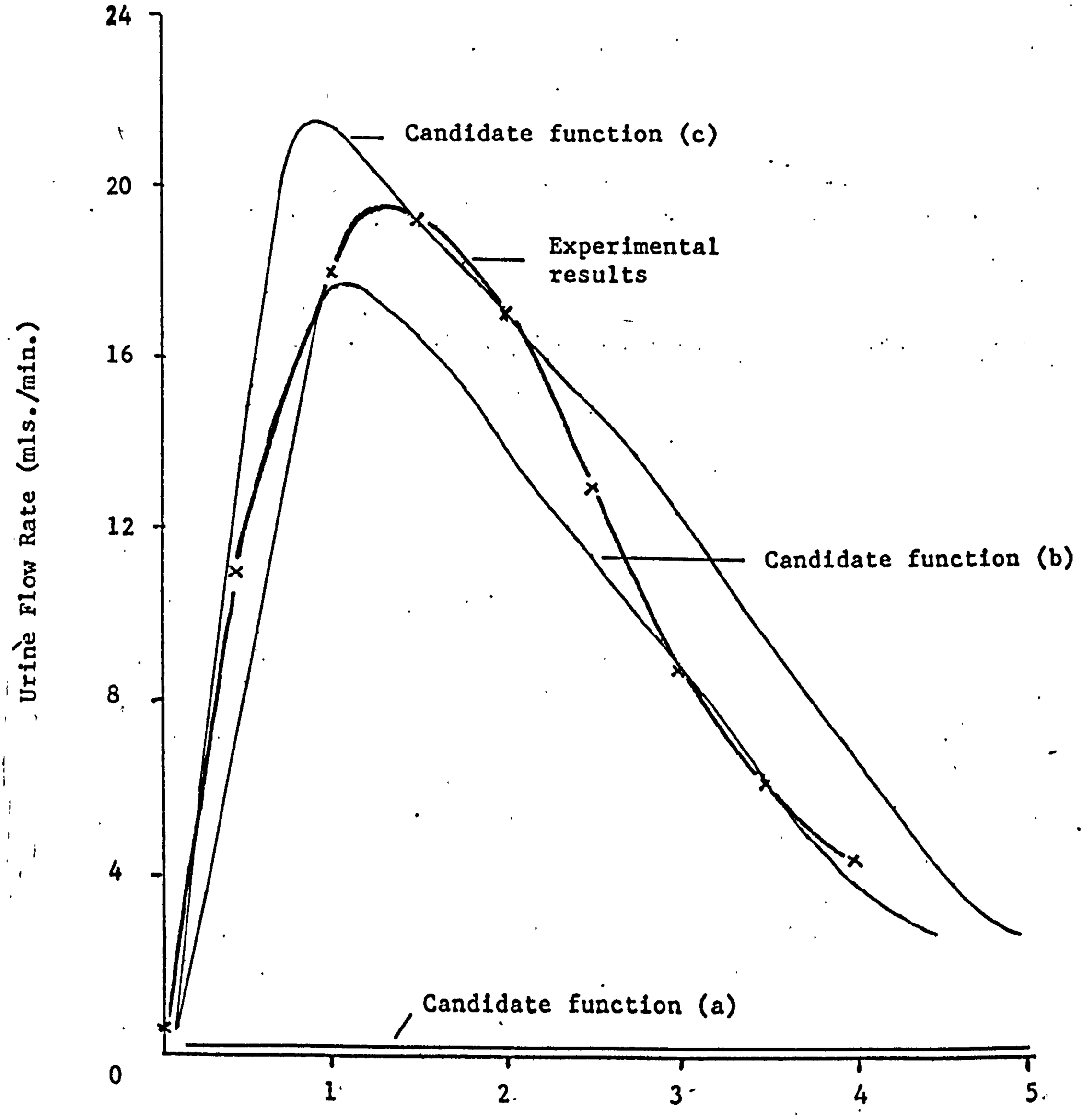

Figure 5.8. Urine flow following ingestion of hypertonic saline using various controller strategies for the release of ADH.

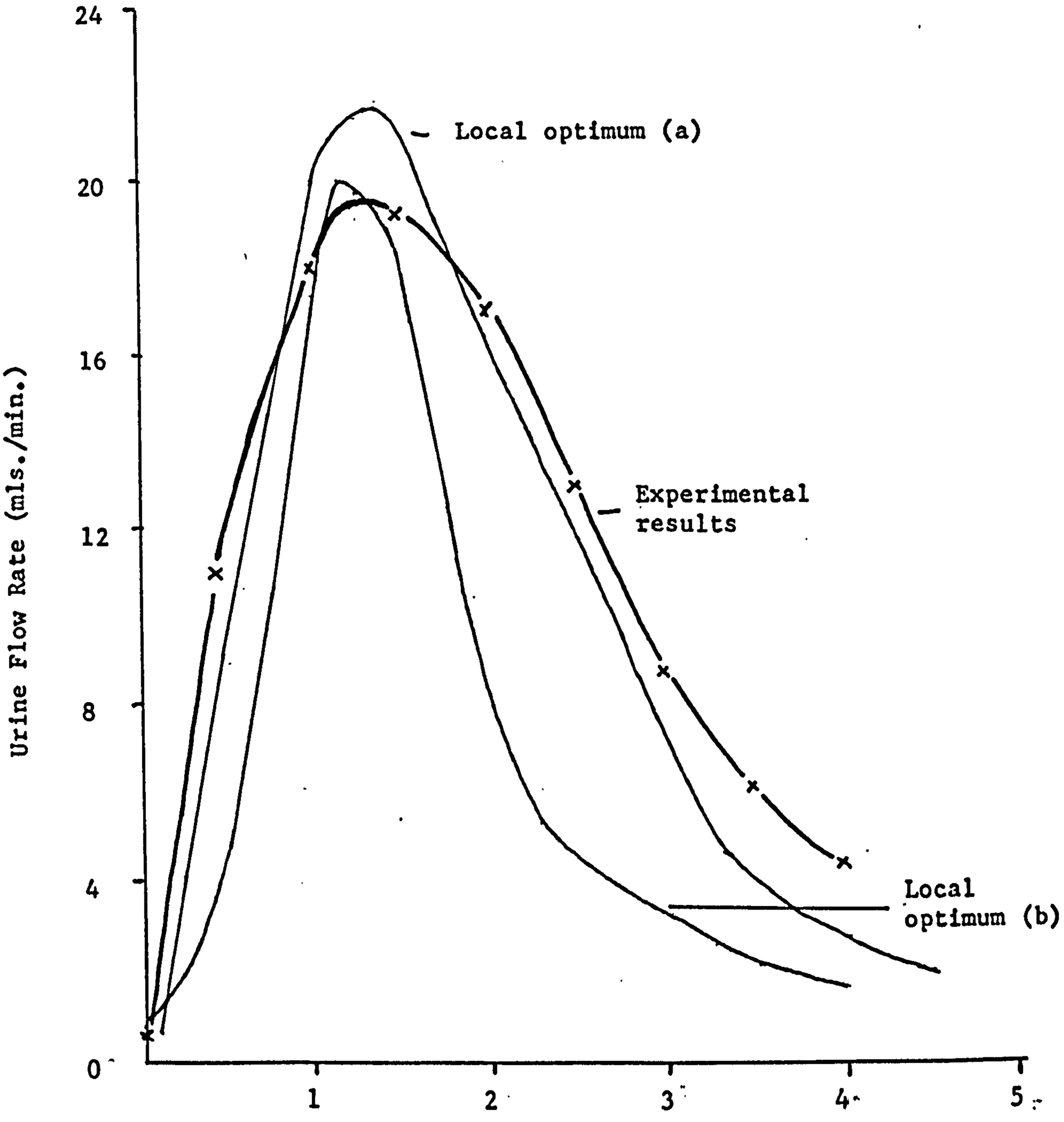

Figure 5.9. Urine flow following ingestion of hypertonic saline showing locally optimal simulations.

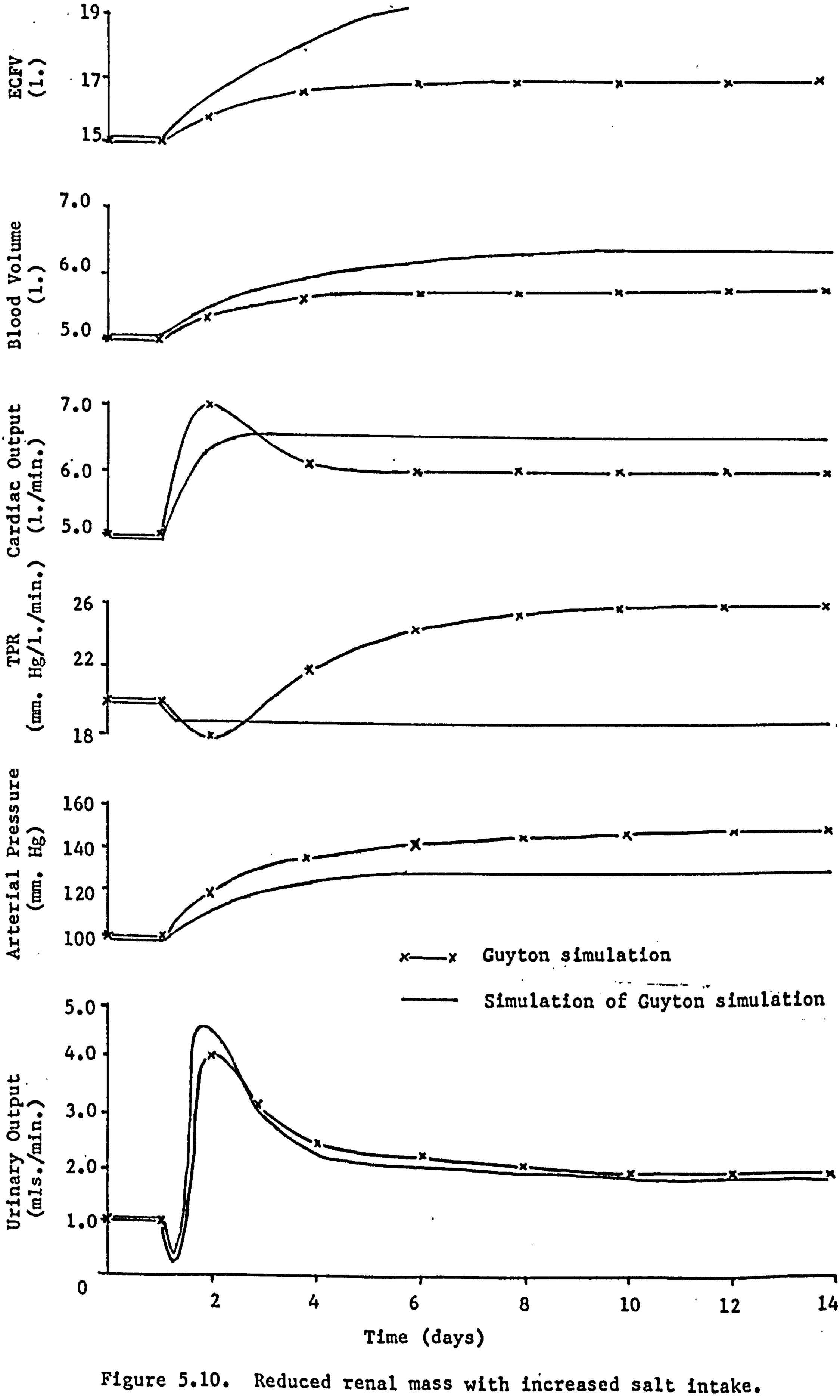

Figure 5.10. Reduced renal mass with increased salt intake.

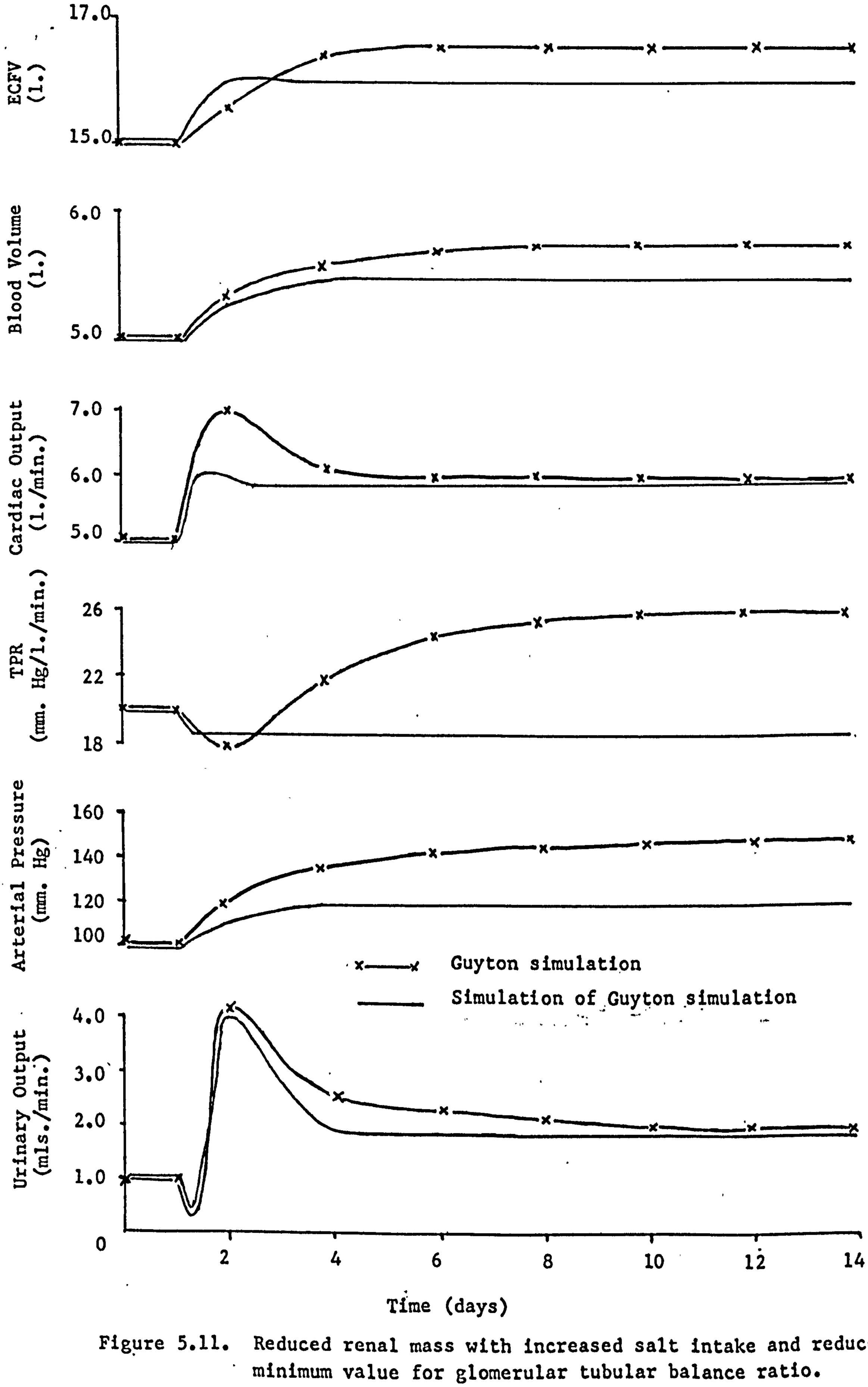

Figure 5.11. Reduced renal mass with increased salt intake and reduced minimum value for glomerular tubular balance ratio.

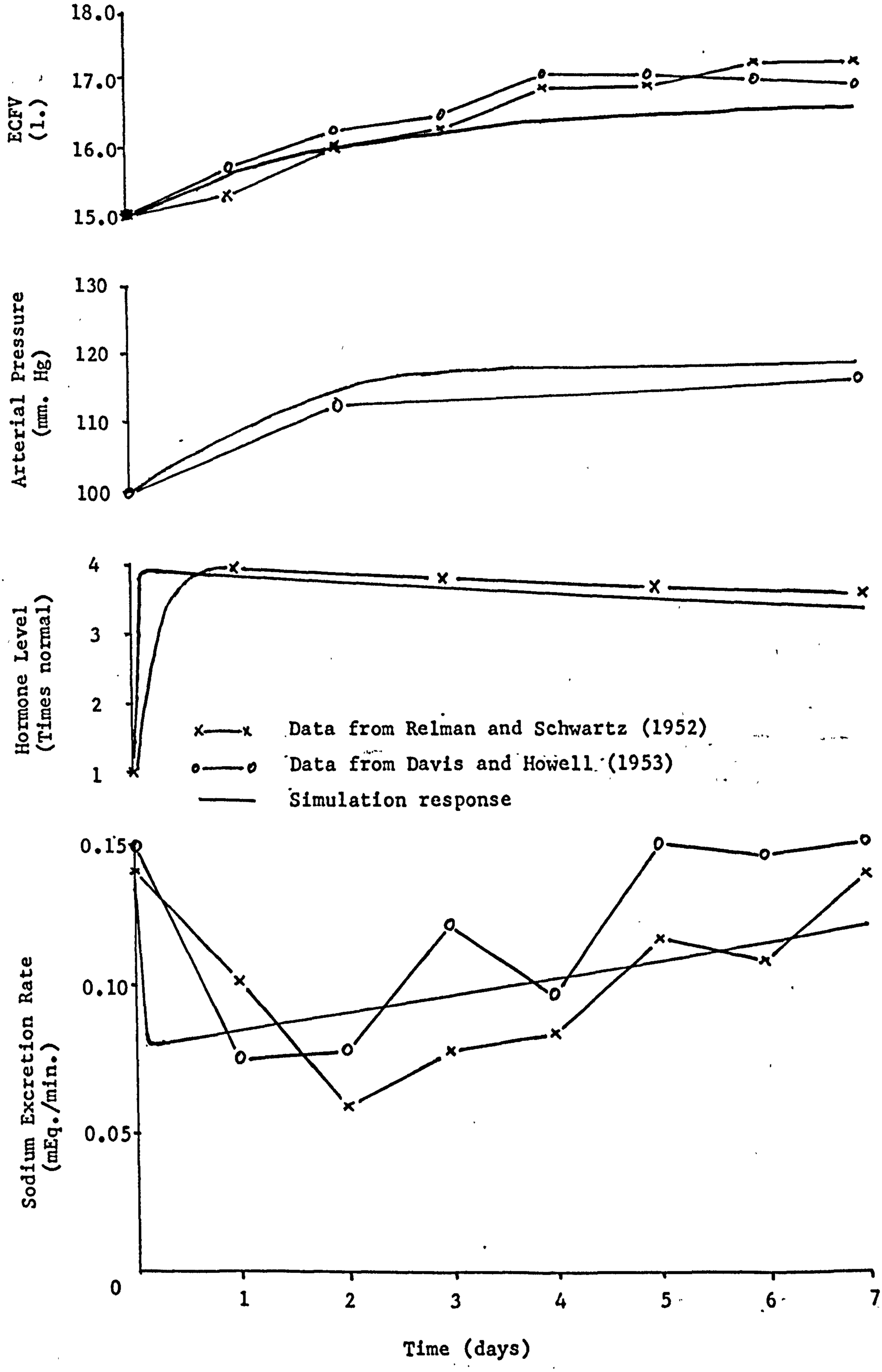

Figure 5.12. Aldosterone loading.

CHAPTER 6

VALIDATION OF THE MODEL FOR PREDICTION OF THE OUTCOME OF DIALYSIS THERAPY.

The simulation results presented in the previous chapter demonstrate the validity of the model of the renal - body fluid system of the normal, healthy human in terms of the capabilities of the model to reproduce features of response to stresses. In this chapter, the capabilities of the model of the patient - artificial kidney machine system (the model of the renal - body fluid system combined with relationships derived in sections 4.1, 4.5 and 4.7) to predict the outcome of dialysis are examined. This is achieved by the simulation of actual dialyses, and the comparison of clinically important features of the responses of the simulations with the data of the actual dialyses.

Several factors tend to cause errors in the model response. The first concerns the errors in the clinician specified parameters needed to generate the simulation of dialysis for the individual patient. The sensitivity of the simulation responses is investigated in the second section of this chapter. The second factor is concerned with the individual differences between patients. Due to the nature of these differences, it is not possible to characterise the patient in these aspects by parameters specified by the clinician. Rather, it appears that it is necessary to adjust the internal parameters of the model for this purpose. Therefore, the parameter estimation exercise, presented in the following chapter, serves to indicate the manner in which this is to be performed for more accurate prediction of the future state of the patient. Finally, certain discrepancies between real test data and simulation response highlight areas of model inadequacy due to lack of knowledge of the relevant physiology. However, the simulations presented in section 6.1 indicate that improved patient management may be obtained in the renal unit through use of a system incorporating the model to predict the outcome of candidate therapies for the individual patient. The description of such a system is presented in Chapter 8.

6.1. Simulation Of Dialyses.

The simulation results of eight dialyses on six patients are reported. The overall model of the patient - artificial kidney machine system requires the input of certain data in order to simulate a dialysis. The data required are specified in Table 6.1, and required data, as specified by the clinician for the eight dialyses, are listed in Table 6.2. The software designed to receive these input data is included in the programme listing of Appendix III.

The inadequacies of the thermoregulatory system model, owing to lack of physiological knowledge, and the omission of representations of the longer term and very short term control mechanisms from the cardiovascular system model were discussed in Chapter 4. The expected deviations of the simulation responses from the actual data are seen to arise as a result of these inadequacies in, and omissions from, the model. Therefore, in accordance with the objectives of this work, only gross features of response of the variables of these subsystems in the actual dialysis data are compared with those of the simulation responses. In the main, these features are the slopes of the response curves. Taking this into account, in the final subsection, features of the data of the actual dialyses are compared with those of the simulations in a quantitative manner.

6.1.1. Simulation Of Dialysis On S.C.

The data representing the state of the chronic renal failure patient, S.C., indicate that there exists little residual kidney function, which results in the patient being overloaded with fluid and, therefore, hypertensive. The concentration of sodium in plasma is maintained at a level slightly below normal by the effects of a controlled diet, but the levels of waste products are elevated.

The effects of dialysis on this patient are shown in Figure 6.1 and Table 6.3. It is seen that the hypertension is controlled by the removal of fluid during dialysis.

TABLE 6.1. Data Required To Simulate Dialysis.

A. State Of Patient.

FACT1 : Fraction of kidney function to excrete sodium and water remaining.

FACT2 : Fraction of kidney function to secrete renin remaining.

FACT3 : Fraction of kidney function to excrete potassium remaining.

FACT4 : Fraction of kidney function to excrete urea and creatinine remaining.

IHF : Extent to which heart pumping ability is diminished.

W : Pre-dialysis weight of patient (kgs).

B. Average Daily Ingestion Rates.

FLUDAY : Average daily fluid intake (l.).

SODDAY : Average daily sodium intake (mEq.).

POTDAY : Average daily potassium intake (mEq.).

C. Initial Conditions At The Start Of Dialysis.

T_{co} : Core temperature (^{o}C.).

T_{so} : Skin temperature (^{o}C.).

E_o : Extracellular fluid volume (l.).

PNA_o : Sodium concentration in plasma (mEq./l.).

PK_o : Potassium concentration in plasma (mEq./l.).

I_o : Intracellular fluid volume (l.).

INA_o : Sodium concentration in intracellular fluid (mEq./l.).

IK_o : Potassium concentration in intracellular fluid (mEq./l.).

R_o : Plasma renin concentration (GU/l.).

A_o : Plasma angiotensin II concentration (ng./l.).

ALD_o : Plasma aldosterone concentration (ng./l.).

AP_o : Arterial pressure (mm. Hg).

ADH_o : Plasma A.D.H. concentration (munits/l.).

TABLE 6.1. (continued)

EUR_o : Urea concentration in extracellular fluid (g./l.). *

$ECRE_o$: Creatinine concentration in extracellular fluid (g./l.). *

D. Parameters Defining Proposed Dialysis Therapy.

SODDIA : Sodium concentration in dialysate (mEq./l.).

POTDIA : Potassium concentration in dialysate (mEq./l.).

T : Length of time on dialysis (hours).

PCP : Ultrafiltration pressure (mm. Hg.).

Q_B : Average blood flow rate through machine (mls./min.).

* Initial concentration of waste products in intracellular compartment are assumed to be equal to the initial concentrations in the extracellular compartment.

The levels of waste products in plasma are significantlly reduced, and the concentration of sodium is raised across dialysis.

The results of the simulation of this dialysis, using the appropriate input data listed in Table 6.2, are shown in Figure 6.1 and Table 6.3 for comparison with the actual data. It is seen that the reduction in arterial pressure across dialysis in the simulation response is present, though not to the extent observed in the data of the actual dialysis. In addition, the values for weight loss across dialysis (calculated from the volume of fluid lost in the simulated dialysis), and post-dialysis levels of electrolytes and waste products in plasma in the simulated dialysis are approximately in agreement with the actual dialysis data.

TABLE 6.2: Input Data For The Simulation Of Dialyses.

	S.C.	G.W.	M.G.	K.F.	R.R.	D.G.1	D.G.2	D.G.3
FACT1	0.12	0.13	0.00	0.12	0.00	0.00	0.00	0.37
FACT2	0.17	0.50	0.00	0.17	0.00	0.87	0.87	0.87
FACT3	0.17	0.17	0.00	0.17	0.00	0.00	0.00	0.62
FACT4	0.12	0.37	0.00	0.12	0.00	0.00	0.00	0.12
IHF	0.0	0.5	0.5	0.0	0.25	0.0	0.0	0.0
W	64.8	74.8	68.0	73.2	77.0	66.0	66.3	66.0
FLUDAY	1.00	1.20	1.20	1.20	0.80	0.60	0.75	2.70
SODDAY	100.0	120.0	110.0	100.0	80.0	190.0	50.0	120.0
POTDAY	60.0	80.0	70.0	80.0	50.0	40.0	50.0	60.0
T_{co}	37.0	36.3	37.0	36.8	37.0	36.2	36.0	35.6
T_{so}	34.0	28.0	34.0	33.4	34.0	34.0	34.0	34.0
E_o	19.0	22.0	15.0	16.0	21.5	19.0	17.0	15.0
PNA_o	137.0	144.0	142.0	141.0	138.0	129.0	128.0	135.0
PK_o	4.8	4.6	5.6	7.4	5.1	6.2	6.0	4.1
I_o	26.0	28.0	25.0	25.0	27.5	25.0	25.0	25.0
INA_o	9.0	10.0	10.0	10.0	9.0	9.0	9.0	10.0
IK_o	139.0	141.0	141.0	141.0	144.0	143.0	143.0	141.0
R_o	0.08	0.06	0.0	0.06	0.0	0.07	0.07	0.06
A_o	30.0	27.0	0.0	26.0	0.0	28.0	28.0	26.0
ALD_o	85.0	80.0	20.0	85.0	80.0	100.0	90.0	85.0
AP_o	150.0	85.0	50.0	138.0	122.0	110.0	97.0	101.0
ADH_o	0.5	0.5	5.0	2.0	0.5	0.5	0.5	2.0
EUR_o	2.91	1.74	2.16	2.58	1.80	3.17	2.75	2.99
$ECRE_o$	0.153	0.159	0.129	0.204	0.156	0.078	0.075	0.051
SODDIA	135.0	130.0	138.0	140.0	134.0	135.0	135.0	139.0
POTDIA	2.0	2.0	1.0	2.0	2.0	2.3	2.3	2.3
T	7.0	7.0	6.0	7.0	7.0	4.0	4.0	4.0
PCP	160.0	100.0	140.0	180.0	180.0	30.0	90.0	100.0
Q_B	250.0	300.0	250.0	300.0	350.0	150.0	200.0	150.0

TABLE 6.3. Comparison Of Effects Of Dialysis On Weight Loss And Plasma Biochemistry Of Patient S.C.

	Pre-Dialysis	Post-Dialysis Real Data	Post-Dialysis Simulation
Weigh loss (kgs.)	-	2.2	2.2
Plasma Sodium (mEq./l.)	137	139	140.9
Plasma Potassium (mEq./l.)	4.8	3.6	3.4
Plasma Urea (g./l.)	2.91	1.50	1.28
Plasma Creatinine (g./l.)	0.153	0.082	0.078

6.1.2. Simulation Of Dialysis On G.W.

From the data concerning the pre-dialysis state of the patient, G.W., it is seen that small fractions of the kidney functions are remaining, and the patient appears to be normotensive. However, the patient is seriously overloaded with fluid and sodium, and this results in the decrease in heart performance. The level of urea in the body fluids is high, and the level of creatinine is very high. The core and surface temperatures of the patient during dialysis have been recorded.

Figure 6.2 and Table 6.4 show the effects of dialysis on this patient. It is seen that the core temperature progressively rises, whereas there is a less smooth rise in surface temperature across dialysis. The arterial pressure curve is seen to fall slightly at the onset of dialysis, and then progressively rise till the fourth hour on dialysis, after which it falls again before reaching steady state. Dialysis removes a significant quantity of sodium, urea and creatinine, and a moderate quantity of potassium from the fluid compartments of this patient.

The results of the simulation of this dialysis are presented in Figure 6.2 and Table 6.4 for comparison. It is seen that there are gradual rises in the core and surface temperature variables of the simulation response. The arterial pressure

TABLE 6.4. Effect Of Dialysis On G.W.

	Pre-Dialysis	Post-Dialysis Real Data	Post-Dialysis Simulation
Weight loss (kgs.)	-	2.2	1.3
Plasma Sodium (mEq./l.)	144	139	137.8
Plasma Potassium (mEq./l.)	4.6	3.4	3.6
Plasma Urea (g./l.)	1.74	0.84	0.64
Plasma Creatinine (g./l.)	0.159	0.072	0.080

response of the simulation exhibits similar features when compared with the actual dialysis data, apart from the initial drop in the arterial pressure in the patient, which may be due to a psychological factor. There is a gradual rise in the arterial pressure variable of the simulation response after the first hour till the fifth hour, after which there is a relatively significant drop. Finally, the post-dialysis values of sodium, potassium and creatinine concentrations in plasma, generated by the simulation, compare well with those of the actual data, whereas the values for weight loss across dialysis and post-dialysis urea concentration generated by the simulation do not compare as favourably with the actual data. These latter two factors, and the comparatively sluggish arterial pressure simulation response, are discussed in a subsequent section of this chapter, with regard to errors in the values for the parameters specified by the clinician and the 'tuning' of the model to represent individual patients.

6.1.3. Simulation Of Dialysis On M.G.

Consideration of the relevant data in Table 6.2 regarding the pre-dialysis state of the patient, M.G., suggests that chronic renal failure has progressed to result in the patient being anuric, that is, having totally lost the ability to form and

TABLE 6.5. Effect Of Dialysis On M.G.

	Pre-Dialysis	Post-Dialysis Real Data	Post-Dialysis Simulation
Weight loss (kgs)	-	1.8	1.1
Plasma Sodium (mEq./l.)	142	142	143.2
Plasma Potassium (mEq./l.)	5.6	2.8	2.8
Plasma Urea (g./l.)	2.16	0.80	1.13
Plasma Creatinine (g./l.)	0.129	0.058	0.065

therefore to excrete urine. In addition, the patient, with an elevated level of potassium in plasma, suffers from hypotension and decreased heart function. The levels of waste products in the body fluids are also high. However, the patient is not overloaded with sodium or fluid.

Dialysis for a duration of six hours results in the time response of arterial pressure as shown in Figure 6.3, where a rise in arterial pressure for the first hour is followed by a gradual fall for the remainder of the period of dialysis. Table 6.5 presents the effects of dialysis on the other variables. There is seen to be considerable weight loss, and significant decreases in the levels of potassium, urea and creatinine in plasma; but there is no change in the level of sodium in plasma.

The results of the simulation of this dialysis are presented in Figure 6.3 and Table 6.5 for comparison. The arterial pressure response curve of the simulation is seen to differ from the actual response in that the initial rise is not present in the simulation response. However, the slopes of the two curves after this initial period are approximately the same. This suggests that the initial rise in the actual arterial pressure response is due to some factor not represented in the simulation — such as the effect of some therapeutic manoeuvre, administered to elevate the blood pressure in the patient, and which has not been recorded in the medical data made available for this work, or the compensatory effects of nervous control of the circulation due to the tendency for arterial pressure to drop. There are also discrepancies

between the values, in the actual dialysis data and the simulation results of Table 6.5, for weight loss and the change in the concentration of urea in plasma. These are discussed in a following section of this chapter. However, values generated by the simulation for post-dialysis concentrations of sodium, potassium and creatinine are in approximate agreement with the corresponding values in the actual data.

6.1.4. Simulation Of Dialysis On K.F.

The pre-dialysis state of the patient, K.F., as defined by the relevant input data listed in Table 6.2 suggests that this patient has some residual kidney function, and is not overloaded. However, the patient is slightly hypertensive and hyperkalemic, and has elevated levels of waste products in the body fluids. The core and surface temperatures of this patient were recorded during dialysis.

TABLE 6.6. Effect Of Dialysis On K.F.

	Pre-Dialysis	Post-Dialysis Real Data	Post-Dialysis Simulation
Weight loss (kgs)	-	2.4	2.15
Plasma Sodium (mEq./l.)	141	142	145.6
Plasma Potassium (mEq./.)	7.4	3.8	3.9
Plasma Urea (g./l.)	2.58	0.90	1.02
Plasma Creatinine (g./l.)	0.204	0.088	0.092

The effects of dialysis on the relevant variables of the patient are presented in Figure 6.4 and Table 6.6. In Figure 6.4, it is seen that there is a very slight rise in core temperature

for the entire period of dialysis, after an initial oscillatory period. Surface temperature rises till the third hour on dialysis, then abruptly falls in the next hour, and finally decreases gradually for the remainder of the treatment session. It is possible that the response of surface temperature in the third hour of dialysis is due to, for instance, bedclothes being removed from the patient after the patient, with skin temperature of 34.6^{o}C, complains of feeling warm. The arterial pressure response indicates that hypertension is controlled by dialysis, since arterial pressure is seen to fall progressively to a normal level. It is suspected (Thompson, 1978) that the reading at the end of the fifth hour of dialysis is a misrecorded value, since no other explanation can be offered for the sudden drop, followed by a sudden rise back to the previous value of arterial pressure. The effects of dialysis on the other relevant variables are listed in Table 6.6, which shows significant decreases in potassium, urea and creatinine concentrations, and a slight increase in the concentration of sodium, in plasma.

The results of the simulation of this dialysis are presented in Figure 6.4 and Table 6.6 for comparison. Core temperature, in simulation response, is seen to remain essentially constant throughout dialysis; and surface temperature falls gradually, after an initial increase, as it does in the initial and latter portions of the actual surface temperature response. The simulated arterial pressure response is similar to the actual response in that arterial pressure falls, essentially, throughout the period of dialysis. The values generated by the simulation for the other variables of interest, listed in Table 6.6, compare well with the corresponding values in the actual dialysis data, apart from the slight discrepancy in the values for the post-dialysis concentration of sodium in plasma. This discrepancy, together with the simulation response for core temperature and arterial pressure, are discussed in a following section of this chapter, concerning errors in the data specified by the clinician.

6.1.5. Simulation Of Dialysis On R.R.

The pre-dialysis state of this chronic renal failure patient is defined by the relevant parameters specified by the clinician in Table 6.2. It is seen that this patient is anuric and slightly hypertensive at the start of dialysis. The patient is overloaded with fluid, and has a correspondingly low concentration of sodium in plasma. The levels of urea and creatinine, however, are elevated.

The effects of dialysis on the relevant variables of this patient are presented in Figure 6.5 and Table 6.7. Hypertension is seen to be controlled by dialysis, and the levels of waste products and potassium in the body fluids are significantly reduced, whereas the level of sodium in plasma is slightly reduced. The patient is reported to have vomited during dialysis.

TABLE 6.7. Effects Of Dialysis On R.R.

	Pre-Dialysis	Post-Dialysis Real Data	Post-Dialysis Simulation
Weight loss (kgs.)	-	2.5	2.0
Plasma Sodium (mEq./l.)	138	137	139.5
Plasma Potassium (mEq./l.)	5.1	3.1	3.4
Plasma Urea (g./l.)	1.80	0.63	0.95
Plasma Creatinine (g./l.)	0.156	0.057	0.080

The results of the simulation of this dialysis are presented in Figure 6.5 and Table 6.7 for comparison. The simulation of the arterial pressure response is seen to correspond closely with the general shape of the actual response. The levels of potassium, urea and creatinine in the body fluids are all reduced significantly in the simulation response, but there is a slight increase in the level of sodium in plasma. It is suspected that the slightly inaccurate simulation results for weight loss, and the concentrations

of sodium and waste products in the body fluids are due to the unaccountable disturbance to the fluid compartments of the patient due to vomiting.

6.1.6. Simulation Of Dialysis: D.G. 1

This, and the two subsequent dialyses being considered for simulation, the data for which are listed in Table 6.2, were performed on the same patient at different times during his episode of acute renal failure. This first dialysis being simulated is, in fact, the first dialysis the patient underwent following the onset of acute renal failure. The patient is, therefore, anuric, though the function to secrete renin is relatively unimpaired. The patient is overloaded and hyperkalemic, though the concentration of sodium in plasma is seen to be very low. In addition, the patient is catabolic, which results in the extremely high level of urea in the body fluids, and the need for dialysis to be performed daily. As a consequence, the level of creatinine in the body fluids is only slightly elevated.

Data describing the effects of this dialysis are presented in Figure 6.6 and Table 6.8. Across dialysis, arterial pressure remains essentially constant, and the temperature of the core of the patient rises steadily. The concentration of sodium in plasma is elevated, whereas the concentrations of creatinine and potassium are reduced slightly, and the concentration of urea in the body fluids is reduced significantly. The change in the weight of the patient across dialysis was not recorded.

The results of the simulation of this dialysis are also presented in Figure 6.6 and Table 6.8. It is seen that the simulated arterial pressure response remains constant throughout the period of dialysis; and the simulated core temperature rises, but at a slightly lower rate than that indicated by the clinical data. This discrepancy may be due to the fact that no account was taken of the patient being in a catabolic state, with a high basal rate of metabolism. The concentration of sodium in plasma is increased in the simulation, but to a value somewhat higher than

TABLE 6.8. Effect Of Dialysis: D.G. 1.

	Pre-Dialysis	Post-Dialysis Real Data	Post-Dialysis Simulation
Weight loss (kgs.)	No Data		-
Plasma Sodium (mEq./l.)	129	131	133.3
Plasma Potassium (mEq./l.)	6.2	5.3	4.4
Plasma Urea (g./l.)	3.17	2.33	2.12
Plasma Creatinine (g./l.)	0.078	0.066	0.055

indicated by the clinical data; the concentrations of potassium, urea and creatinine are all reduced in the simulation of the dialysis, but, in each case, the values for the post-dialysis concentrations generated by the simulation are slightly lower than the corresponding values in the clinical data. In the case of urea, this slight difference is, again, probably due to the fact that no account was taken, in the simulation, that the patient was catabolic, and therefore, had a rate of generation of urea which was somewhat higher than normal. The concentration of creatinine in the body fluids is lowered very slightly by dialysis. Thus, although there is a large relative error between the actual, and the simulated, changes in creatinine concentrations, the absolute error is not significant.

6.1.7. Simulation Of Dialysis: D.G. 2.

The patient was dialysed daily, throughout the anuric stage of acute renal failure. The simulation presented here is of the fifth dialysis performed on the patient — approximately in the middle of the anuric stage of acute renal failure. The relevant data in Table 6.2 indicate that the extent to which the patient is overloaded with fluid is gradually being reduced, though the concentration of sodium in plasma is still low, and the concentrations of potassium and urea are still high.

TABLE 6.10. Effects Of Dialysis: D.G. 3.

	Pre-Dialysis	Post-Dialysis Real Data	Post-Dialysis Simulation
Weight loss (kgs)	No Data		-
Plasma Sodium (mEq./l.)	135	137	138.4
Plasma Potassium (mEq./.l)	4.1	3.5	3.5
Plasma Urea (g./l.)	3.00	2.27	1.75
Plasma Creatinine (g./l.)	0.050	0.040	0.036

potassium in plasma are at more normal levels than the pre-dialysis values reported for the previous two simulations. However, the high level of urea in the body fluids indicates that the patient is still catabolic, and in need of frequent dialysis therapy to prevent uraemia.

For this dialysis, the dialyser was primed with blood instead of saline or dextrose, as is the usual case. The effects of the dialysis are presented in Figure 6.8 and Table 6.10. It is seen that the core temperature of the patient and the arterial pressure rise across dialysis. In addition, there is a slight increase in the concentration of sodium, and reductions in the concentrations of potassium, urea and creatinine across dialysis. No data were recorded for the loss in weight of the patient across dialysis.

The priming of the dialysis machine with blood was simulated simply by increasing the volume of the blood compartment by the priming volume, 0.4 litres, one minute after the start of dialysis. The simulation results are presented in Figure 6.8 and Table 6.10. It is seen that the core temperature response of the simulation corresponds with that of the actual dialysis, in that there is an increase in core temperature throughout dialysis. The increase in arterial pressure in the simulation response is rather more abrupt than in the actual response. This may be due to the lack of representations of the compensatory control mechanisms of the cardiovascular system in the model. However, the overall increase in arterial pressure in the simulation response is approximately the same as in the actual response.

Finally, the post-dialysis values generated by the simulations for the concentrations of sodium, potassium and creatinine are in close agreement with the corresponding values in the clinical data. The lower value generated by the simulation for the post-dialysis concentration of urea in the body fluids is probably due to the fact that no account was taken of the patient being catabolic in simulation. This discrepancy is discussed further in a later section of this chapter.

6.1.9. Summary.

The results of the simulations of dialyses, performed on several patients in differing clinical states, were presented above. The comparison of clinical data with the relevant simulation results was also discussed, but in a qualitative manner. In order to assess the capabilities and limitations of the model to predict the outcome of a dialysis, a quantitative, concise method of presentation of the errors between the clinical data and the above simulation responses is required. The feature map, Table 6.11, is a suitable method for this purpose.

Certain key features and variables in the clinical data were selected by the clinician as important in assessing the effectiveness of the dialysis. These are listed across the top of the feature map of Table 6.11.. Listed vertically, on the left hand side, are the simulations of dialyses discussed above, so that a matrix is formed. A particular feature, such as a positive or negative overall slope of response of a variable, in the simulation response was compared with that of the clinical data. If the features matched, the appropriate space in the feature map was marked with a positive sign; and if the features did not match, the space was marked with a negative sign. If there were no clinical data relevant to that feature, a zero was placed in the space. Variables, such as the change in the concentration of a substance in plasma across dialysis, were treated in a similar manner. A positive sign was recorded when the value for

the variable generated by the simulation agreed with the corresponding value in the clinical data with a certain specified relative accuracy, or with an absolute accuracy calculated as twice the measurement accuracy. The measurement accuracy for a variable was derived from Table 6.12, which presents the accuracies with which the parameters, used as input for the model to generate a simulation of dialysis, are specified.

The resulting feature map for the above simulations is presented in Table 6.11. Consideration of the distribution of the mismatched features leads to certain inferences concerning the simulations.

It is seen, from Table 6.11, that the results of the simulation of the dialysis performed on patient, R.R., deviate from the real data in respect of several variables; these are the weight loss and the change in the concentrations of certain substances in plasma across dialysis. The patient, R.R., is reported to have vomited on more than one occasion during the dialysis. This, obviously, would explain the erroneous result for the weight loss in the simulation response. In addition, vomiting constitutes a disturbance to the fluid compartments of the body, and, therefore, the ommission of the representation of this disturbance in the simulation is the probable cause for the errors in the variables representing the concentrations of substances in the fluid compartment in the simulation response.

Apart from vomiting, noise, which affects primarily the weight loss variable, is introduced into the system by the pass- of faeces and the ingestion of food and liquids by the patient during the course of dialysis. Since the length of time on dialysis extends to seven hours in some cases, it is likely that these bodily functions may occur during this period. Unfortunately, no record was kept of these, and, therefore, less confidence is placed on the values for weight loss across dialysis generated by the simulation.

The other variable which is seen to have suffered more than the occasional mismatch is the change in the level of urea across dialysis. Apart from the usual uncertainties associated with models representing subsystems of the human organism, as discussed in Chapter 4, the model representing the dynamics of urea in a patient suffering from renal failure is even more prone

TABLE 6.12. Accuracies With Which Input Data Is Specified.

FACT1	:	± 0.12	T_{co}	:	± 0.1°C
FACT2	:	± 0.17	T_{so}	:	± 0.1°C
FACT3	:	± 0.17	E_o	:	± 3.0 litres
FACT4	:	± 0.12	PNA_o	:	± 1.0 mEq./l.
IHF	:	± 0.12	PK_o	:	± 0.2 mEq./l.
W	:	± 0.01 kgs	I_o	:	± 5.0 litres
			INA_o	:	± 2.0 mEq./l.
FLUDAY	:	± 0.1 litres	IK_o	:	± 10.0 mEq./l.
SODDAY	:	± 10 mEq.	R_o	:	± 0.02 GU/l.
POTDAY	:	± 10 mEq.	A_o	:	± 5.0 ng./l.
			ALD_o	:	± 15.0 ng./l.
SODDIA	:	± 1.0 mEq./l.	AP_o	:	± 5.0 mm Hg
POTDIA	:	± 0.2 mEq./l.	ADH_o	:	± 1.0 munits/l.
T	:	± 5 min.	EUR_o	:	± 0.05 g./l.
PCP	:	± 25 mm Hg	$ECRE_o$	:	± 0.005 g./l.
Q_B	:	± 25 mls./min.			

to uncertainty with regard to the parameter representing the rate of generation of urea in equation (4.78). This is so since, associated with renal failure, it is often the case that the rate of metabolism, and, therefore, the rate of generation of urea, is altered from a normal value in either direction (Thompson, 1978). Since the clinician is unable to quantify the rate of generation of urea in a patient, this and other parameters, discussed in the following section, need to be estimated by some means in order that the model may yield more accurate predictions of the outcome of dialysis when used as a predictive aid in patient management. The method by which the estimation of these parameters may be achieved is described in the following chapter.

In summary, the feature map of Table 6.11 offers a measure of how accurately the model is capable of simulating the dialysis process. It is seen that the simulation response matches important features in the clinical data with sufficient accuracy

for the model to be of use as a predictive instrument in the renal unit. However, the performance of such a system would be improved with the availability of more extensive data regarding factors which affect the weight of the patient during dialysis. In addition, certain parameters, such as the rate of generation of urea, are found to be 'patient - dependent', and greater accuracy of simulation may be obtained if these parameters are 'tuned' so that the model represents the individual patient.

Finally, the simulation responses are prone to errors due to inaccuracies in the values specified by the clinician for the input data needed for the simulation of dialysis. The sensitivity of the simulation responses to these possible errors is examined in the following section.

6.2. Effects Of Errors In Clinician-Specified Data On The Simulation Response.

The simulation of dialysis, using the model of the patient-artificial kidney machine system presented in Chapter 4, is dependent on values being specified for the variables listed in Table 6.1. The simulations described above were performed using the values for these variables, listed in Table 6.2, which were specified by the clinician. However, owing to measurement difficulties, it was necessary for the clinician to estimate the values for some of the variables; and the other variables had associated measurement noise. The estimated margins of errors associated with each of these variables is given in Table 6.12. For the clinical applicability of this work, it is necessary to determine how sensitive the performance of the model is to potential inaccuracies in the values for these variables. A discussion on the sensitivity of the simulations to inaccuracies in the values of Table 6.2 is presented in the following subsection.

6.2.1. Sensitivity Of The Simulations To Errors In The Clinician - Specified Data.

The values listed in Table 6.2 are approximate values, as discussed above. The true value for each variable for each simulation may be considered to lie in a probable range specified by the value in Table 6.2 and the appropriate range, given in Table 6.12. The simulations were repeated, but with each variable, in turn, taking on the extreme values in the range. In this manner, an indication of the sensitivity of the simulation responses to potential inaccuracies in these variables was obtained.

Since an alteration in the value of a variable had similar effects on all simulations, only the results of the simulations of the dialysis performed on patient, S.C., are presented below, though the results of the other simulations are also discussed briefly in general terms. The results of the previous simulation of dialysis performed on patient, S.C., presented in Figure 6.1 and Table 6.3, are presented again in Table 6.13 for convenience.

TABLE 6.13. Simulation Of Dialysis On S.C. With Input Data Of Table 6.2.

	Pre-Dialysis	Post-Dialysis Real Data	Post-Dialysis Simulation
Mean Arterial Pressure (mm. Hg)	150	115	124.8
Weight loss (kgs)	-	2.2	2.2
Plasma Sodium (mEq./l.)	137	139	140.9
Plasma Potassium (mEq./l.)	4.8	3.6	3.4
Plasma Urea (g./l.)	2.91	1.50	1.28
Plasma Creatinine (g./l.)	0.153	0.082	0.078

(i) State Of Patient.

Parameters representing the fractions of the functions of the normal kidneys remaining in the patients needed to be estimated from medical records by the clinician. These parameters are therefore subject to relatively large margins of error. The simulations for patients with residual kidney functions were repeated with the values for the parameters, FACT1, FACT2, FACT3, FACT4, perturbed in turn. The patients who were reported to have no residual kidnay functions were anuric. Therefore, the values for these parameters were assumed to be accurate, and further simulations of the dialyses performed on these patients were not generated.

The results of the simulations of the dialyses performed on patient, S.C., are presented in Table 6.14. The effects of the variations in the values of the parameters on the simulation results are representative of all the dialyses simulated. It is seen that the simulation response, with regard to arterial pressure, weight loss and the change in the concentration of sodium in plasma across dialysis, is sensitive to changes in the value of the parameter, FACT1, which represents the remaining fraction of the normal kidney function to excrete sodium and water. The variations in the above variables are seen to exceed twice the measurement errors for these variables. The simulation responses were relatively insensitive to variations in the values assigned to parameters, FACT2 and FACT3, which represent the remaining fractions of the functions of the kidneys to secrete renin and to excrete potassium, respectively. However, variations in the values for FACT4, the parameter representing the remaining fraction of the function of the kidneys to excrete urea and creatinine, influenced the change in the concentration of urea in the body fluids in the simulation response. Again, the variations in the concentration of urea exceeds twice the measurement error for this variable.

Finally, the parameter, IHF, representing the extent to which the pumping ability of the heart is decreased, was altered for each of the patients. The appropriate results, given in Table 6.14, of the simulation of the dialysis performed on patient, S.C., with this parameter altered indicate that the simulation

TABLE 6.14. Post-Dialysis Simulation Results With Variation Of Parameters Representing State Of Patient.

	FACT1=0.0	FACT1=0.24	FACT2=0.0	FACT2=0.33	FACT3=0.0	FACT3=0.33	FACT4=0.0	FACT4=0.24	IHF=0.25
MAP	129.6	117.5	124.5	125.0	124.8	124.8	124.8	124.8	125.5
Wt. Loss	1.6	3.0	2.2	2.2	2.2	2.2	2.2	2.2	2.2
PNA	139.7	142.7	140.8	140.9	140.9	140.9	140.9	140.9	140.9
PK	3.4	3.5	3.4	3.4	3.4	3.4	3.4	3.4	3.4
EUR	1.26	1.28	1.28	1.28	1.28	1.28	1.47	1.10	1.28
ECRE	0.077	0.079	0.078	0.078	0.078	0.078	0.079	0.077	0.078

TABLE 6.15. Post-Dialysis Simulation Results With Variation Of Parameters Representing Daily Rates Of Ingestion Of Substances.

	FLUDAY=0.9	FLUDAY=1.1	SODDAY=90.0	SODDAY=110.0	POTDAY=50.0	POTDAY=70.0
MAP	124.5	125.1	124.7	124.8	124.6	124.9
Wt. Loss	2.2	2.2	2.2	2.2	2.2	2.2
PNA	140.9	140.8	140.8	140.7	140.9	140.8
PK	3.4	3.4	3.4	3.4	3.3	3.5
EUR	1.28	1.28	1.28	1.28	1.28	1.28
ECRE	0.078	0.078	0.078	0.078	0.078	0.078

response is relatively insensitive to potential inaccuracies in the evaluation of this parameter. This was found to be the case for all the simulations of dialyses.

In summary, for greater accuracy of prediction of the outcomes of dialysis, the parameters, FACT1 and FACT4, need to be specified with smaller margins of uncertainty. However, the simulation responses are relatively insensitive to variations of the other parameters, relevant to defining the clinical state of the patient, within the stated ranges of uncertainties.

(ii) Average Daily Ingestion Rates.

Patients undergoing dialysis therapy are generally maintained on strictly controlled diets. In addition, the input and output of fluid and electrolytes are recorded on a daily basis. Therefore, by refering to medical records, the clinician is able to specify values for the average daily rates of ingestion of fluid, sodium and potassium, FLUDAY, SODDAY and POTDAY, respectively, with small degrees of uncertainty, as suggested by the appropriate expected margins of errors, quoted in Table 6.12.

In order to determine the sensitivity of the simulation responses to variations in these parameters within these margins of errors, the simulations were repeated with different values for these variables. The results of these simulations of the dialysis performed on the patient, S.C., are presented in Table 6.15. These results indicate that the simulation response is relatively insensitive to variations within the ranges of uncertainties for these parameters, since the variation in any variable did not exceed the measurement error for the variables. This was found to be the case for all the simulations of dialyses performed.

(iii) Initial Conditions.

The values representing initial condition information were perturbed in a similar manner. The results of these tests on the simulation of the dialysis on patient S.C., are presented in

TABLE 6.11. Feature Map For Assessing Adequacy Of Patient - Artificial Kidney Machine Model.

	Core Temp. Slope (+ve or -ve)	Surface Temp. Slope (+ve or -ve)	Arterial Pressure Slope (± 30%)	Change In Plasma Sodium (± 15%)	Change In Plasma Potassium (± 15%)	Change In Plasma Urea (± 15%)	Change In Plasma Creatinine (± 15%)	Weight Loss (± 10% or ± 0.1 kg)
S.C.	O	O	+	+	+	+	+	+
G.W.	+	+	−	+	+	−	+	−
M.G.	O	O	+*	+	+	−	+	−
K.F.	−	+	−	−	+	+	+	+
R.R.**	O	O	+	−	+	−	−	−
D.G.1	+	O	+	−	−	−	+	O
D.G.2	+	O	+	+	−	+	+	−
D.G.3	+	O	+	+	+	−	+	O

Legend:- + : Match between features of response in clinical data and simulation.

− : No match between features of response in clinical data and simulation.

O : No clinical data.

* Slopes calculated by considering final five hours of arterial pressure response curves.

** Inaccuracies introduced due to patient vomiting during dialysis.

TABLE 6.16. Post-Dialysis Simulation Results With Variation Of Initial Values Of Patient Variables.

	E_o=22.0	E_o=16.0	PNA_o=138.0	PNA_o=136.0	PK_o=4.5	PK_o=4.1	I_o=31.0	I_o=21.0	INA_o=11.0	INA_o=7.0
MAP	130.8	122.5	122.6	128.0	124.5	125.1	125.8	123.7	124.8	124.8
Wt. Loss	2.2	2.1	2.3	2.1	2.2	2.2	2.2	2.2	2.2	2.2
PNA	141.0	140.4	141.3	140.3	140.9	140.8	140.7	141.0	140.9	140.9
PK	3.5	3.3	3.4	3.4	3.4	3.3	3.4	3.4	3.4	3.4
EUR	1.28	1.29	1.28	1.28	1.28	1.28	1.33	1.24	1.28	1.28
ECRE	0.078	0.078	0.078	0.078	0.078	0.078	0.083	0.074	0.078	0.078

	IK_o=149.0	IK_o=129.0	R_o=0.1	R_o=0.06	A_o=35.0	A_o=25.0	ALD_o=100.0	ALD_o=70.0
MAP	124.5	125.1	124.8	124.8	124.3	125.3	124.8	124.8
Wt. Loss	2.2	2.2	2.2	2.2	2.2	2.2	2.2	2.2
PNA	141.0	140.8	140.9	140.9	140.9	140.9	140.9	140.9
PK	3.4	3.4	3.4	3.4	3.4	3.4	3.4	3.4
EUR	1.28	1.28	1.28	1.28	1.28	1.28	1.28	1.28
ECRE	0.078	0.078	0.078	0.078	0.078	0.078	0.078	0.078

TABLE 6.16. (continued)

	AP_o=155.0	AP_o=145.0	ADH_o=1.5	ADH_o=0.0	EUR_o=2.96	EUR_o=2.86	$ECRE_o$=0.158	$ECRE_o$=0.148
MAP	129.8	119.8	124.8	124.8	124.8	124.8	124.8	124.8
Wt. Loss	2.2	2.2	2.2	2.2	2.2	2.2	2.2	2.2
PNA	140.9	140.9	140.9	140.9	140.9	140.9	140.9	140.9
PK	3.4	3.4	3.4	3.4	3.4	3.4	3.4	3.4
EUR	1.28	1.28	1.28	1.28	1.31	1.26	1.28	1.28
ECRE	0.078	0.078	0.078	0.078	0.078	0.078	0.081	0.075

TABLE 6.17. Post-Dialysis Simulation Results With Variation In Parameters Representing Dialysis Therapy.

	SODDIA=136	SODDIA=134	POTDIA=2.2	POTDIA=1.8	T=425.0	T=415.0	PCP=185	PCP=135	Q_B=275	Q_B=225
MAP	125.5	124.1	125.1	124.5	124.3	125.3	120.2	129.2	124.9	124.6
Wt. Loss	2.3	2.2	2.2	2.2	2.2	2.2	2.7	1.7	2.2	2.2
PNA	141.6	140.0	140.8	141.0	140.9	140.9	142.0	139.7	140.8	141.0
PK	3.4	3.4	3.6	3.2	3.4	3.4	3.4	3.4	3.4	3.4
EUR	1.29	1.28	1.28	1.28	1.27	1.30	1.29	1.27	1.27	1.30
ECRE	0.078	0.078	0.078	0.078	0.078	0.079	0.079	0.077	0.077	0.079

Table 6.16.

In general, it was found that model simulations were particularly insensitive to variations in the values for initial conditions. There were some notable exceptions. Firstly, variation of the values for initial extracellular fluid volume, E_o, resulted in moderate variations in final values for mean arterial pressure, MAP. Secondly, the final values for the concentration of urea in plasma, EUR, was seen to be more than slightly sensitive to variations in the values for initial intracellular fluid volume. However, the magnitudes of the variations in the final values of these two variables were less than twice the quoted margins of measurement errors for these variables in all the tests performed. Thirdly, the final values for arterial pressure, AP, were apparently sensitive to variations in the initial values for arterial pressure, AP.; but consideration of equation 4.13 suggests that this was to be expected. The offset in the final value of arterial pressure is expected to be equal to the offset in the initial value. Thus the slope of the simulated arterial pressure response, which is used as a variable in the feature map of Table 6.11, is unaltered by variations in the initial value of arterial pressure.

Therefore, these tests demonstrated that the response of the model of the patient - artificial kidney machine system is not significantly sensitive to errors in the values representing the initial conditions of the state variables of the model.

(iv) Parameters Defining Proposed Dialysis Therapy.

The values representing the proposed dialysis therapy were perturbed in the same manner as described above for each of the simulations. The results of these sensitivity tests on the simulation of dialysis on patient S.C., are presented in Table 6.17.

It was found that the final values for the concentrations of sodium and potassium in the extracellular fluid were sensitive to values for the concentrations of sodium and potassium respectively, in the dialysate. In general, however, the variations in the final values did not exceed twice the margin of measurement error for that variable as defined in Table 6.12.

The model responses, in terms of the final values for mean arterial pressure, weight loss and the concentration of sodium in the extracellular fluid, were found to be sensitive to possible errors in the values for post coil pressure, which is the pressure set across the dialyzer membrane to remove fluid from the patient by ultrafiltration. This finding suggests that the deviation between the simulations of dialyses presented in section 6.1 from the real data may have been partly due to inaccuracies in the values used for post coil pressure in the simulations.

When the model is used as a predictive aid in patient management, an optimal value for post coil pressure would be determined by the method described in Chapter 8. Theoretically, if the model is a valid representation of the patient, this value would be applied in the actual dialysis, and would not be changed. Therefore, the margin of error associated with this variable would be considerably smaller, and correspondingly, there would be less uncertainty in the response of the model.

The sensitivity of the model response to possible errors in the values for time on dialysis and rate of flow of blood through the dialysis machine was found to be insignificant for the purposes of this work.

6.2.2. Conclusions On The Sensitivity Tests.

The results of sensitivity tests indicate that the response of the model of the patient - artificial kidney machine system is sensitive to possible errors in the values of some of the input parameters. In particular, it was determined that possible errors in the values specified for FACT1, FACT4 and post coil pressure could have caused variations in the response of the model such that the deviations of the final values of the clinically important variables would have exceeded the margins of measurement errors for these variables. Therefore, the values for these input parameters need to be specified with lesser uncertainty in order that more confidence may be placed on the long term predictive capabilities of the model when it is used in the

clinical environment as an aid in patient management.

6.3. Optimal Feature Map.

The simulations of the eight dialyses were repeated, with changes to some of the values for the input parameters within the ranges of measurement error listed in Table 6.12, in order to optimize the feature map of Table 6.11. The resultant feature map is shown in Table 6.18, where a change in sign from negative to positive is indicated by the positive sign being encircled.

It was observed that improved simulation responses were obtained primarily by changes in the values for FACT1, FACT4 and post coil pressure. Changes in the values for some of the initial condition input variables also caused some improvement in some instances. However, the conclusion that emerged was that for greater accuracy of model prediction, the values for FACT1, FACT4 and post coil pressure would need to be specified with smaller margins of error.

Consideration of the feature map of Table 6.18 indicates that the dynamics of urea are still not satisfactorily simulated for all patients. As outlined in the discussion in section 4.6.4, a long term adaptive mechanism is responsible for alterations in the rate of generation of urea in the patient suffering from renal failure (Bergstrom and Furst, 1976; Thompson, 1978). This suggests that the value for the rate of generation of urea varies between patients and also with time. Therefore, the deviations in the final values for plasma urea levels between the real data and the simulation responses, using the model with a constant value for the rate of generation of urea, are to be expected. Thus, for more accurate prediction of plasma urea dynamics, the value for the rate of generation of urea in the patient being considered should be determined and substituted into the model.

The adjustment of the values of the input parameters was not seen to affect the accuracy with which weight loss across dialysis was simulated. This supports the suggestion presented in section 6.1.9, that the actual weight loss in the patients

TABLE 6.18. Feature Map Optimized By Adjusting Values For Input Parameters.

	Core Temp. Slope (+ve or -ve)	Surface Temp. Slope (+ve or -ve)	Arterial Pressure Slope (± 30%)	Change In Plasma Sodium (± 15%)	Change In Plasma Potassium (± 15%)	Change In Plasma Urea (± 15%)	Change In Plasma Creatinine (± 15%)	Weight Loss (± 10% or ± 0.1 kg.)
S.C.	0	0	+	+	+	+	+	+
G.W.	+	+	⊕	+	+	⊕	+	-
M.G.	0	0	+*	+	+	-	+	-
K.F.	-	+	⊕	⊕	+	+	+	+
R.R.	0	0	+	⊕	+	-	⊕	-
D.G.1	+	0	+	⊕	-	-	+	0
D.G.2	+	0	+	+	⊕	+	+	-
D.G.3	+	0	+	+	+	-	+	0

* Slopes calculated by considering final five hours of arterial response curves.

across dialysis affected by disturbances due to the ingestion of food and liquids, excretion of faeces and vomiting by the patients during dialysis. These events were not recorded in the patient data.

6.4. Summary.

Validation tests were performed on the model of the patient - artificial kidney machine system model, using available real data representing actual dialyses. The results of these tests were presented quantitatively in the form of a feature map. It was found that the results were generally acceptable, but that certain important clinical variables were not simulated accurately, and that the simulation results of the dialysis on one patient were not in close agreement with the real data. However, this patient had vomited quite severely during dialysis, and this constitutes a disturbance to the system which could account for the discrepancy between the simulation results and the real data for this dialysis.

Discrepancies may have also arisen due to errors in the values specified for the input parameters needed for the execution of the model. Therefore, the sensitivity of the response of the model to errors in each of these parameters was investigated. It was determined that the sensitivity of the model response was particularly sensitive to variations within the margins of errors in values for FACT1, FACT4 and post coil pressure.

By manipulating values for the input parameters within the regions of uncertainties in repeated simulations, it was determined that most of the discrepancies between real dialysis data and the simulation responses could be accountable to inaccuracies in the values of the input parameters. However, discrepancies still existed in two of the important features. These were the weight loss in the patient across dialysis and the final concentration of urea in the extracellular fluid compartment. Vomiting, ingestion and periodic excretion of wastes during dialysis constitute disturbances to the system which could not

be taken into account in the simulations since the relevant data were not recorded. Therefore, discrepancies in the weight loss feature were not unexpected. Also, as discussed above, the rate of formation of urea in patients suffering from renal failure is expected to vary. Thus, the model with the rate of generation of urea set as a constant was found to be inappropriate.

Post coil pressure is subject to variation during the course of dialysis. The values used for the simulations represent approximate time average values, and therefore, these values have a large range of uncertainty. When the model is used for predictive purposes, and optimal value for post coil pressure would be determined by the method described in Chapter 8. This value would have a negligible range of uncertainty, and therefore the simulation response would be relatively insensitive to possible errors in its value.

Thus, for more accurate long term prediction of patient state, it is necessary to obtain more accurate estimates for the values for FACT1, FACT4 and the rate of generation of urea for the patient being considered. A method for obtaining these values, using past patient data and a parameter estimation routine is discussed in the following chapter.

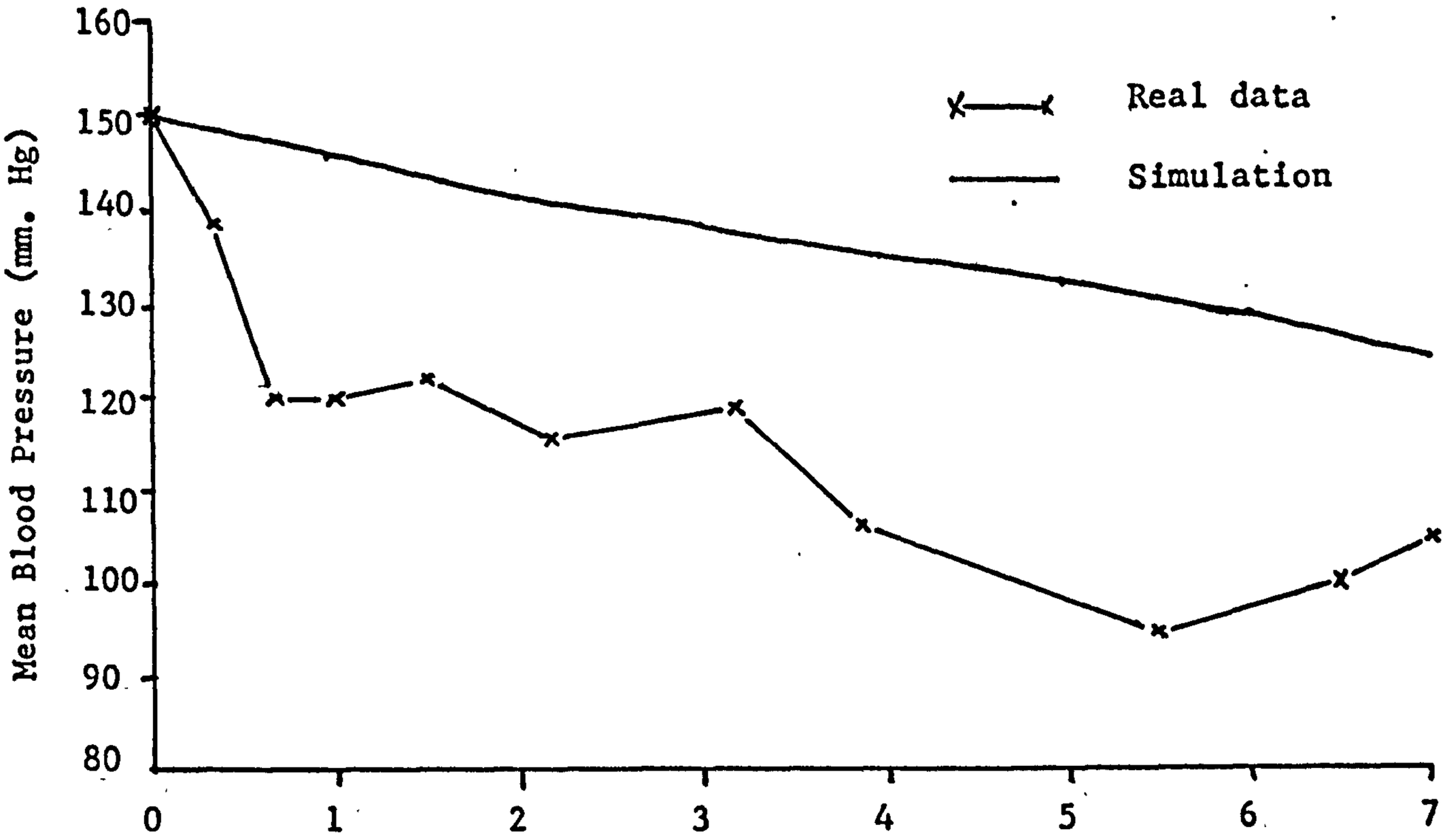

Figure 6.1. Effect of dialysis on S.C..

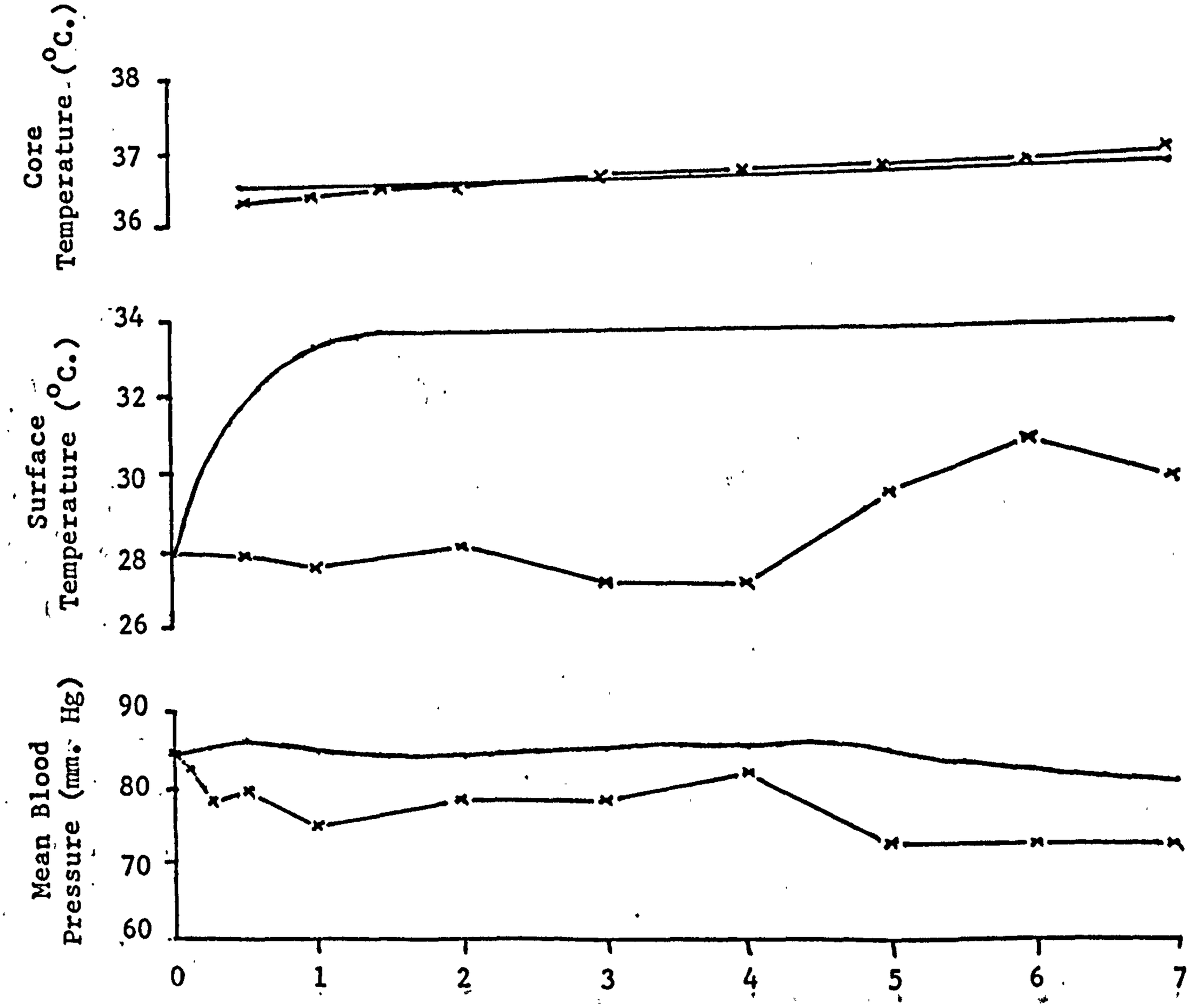

Figure 6.2. Effect of dialysis on G.W..

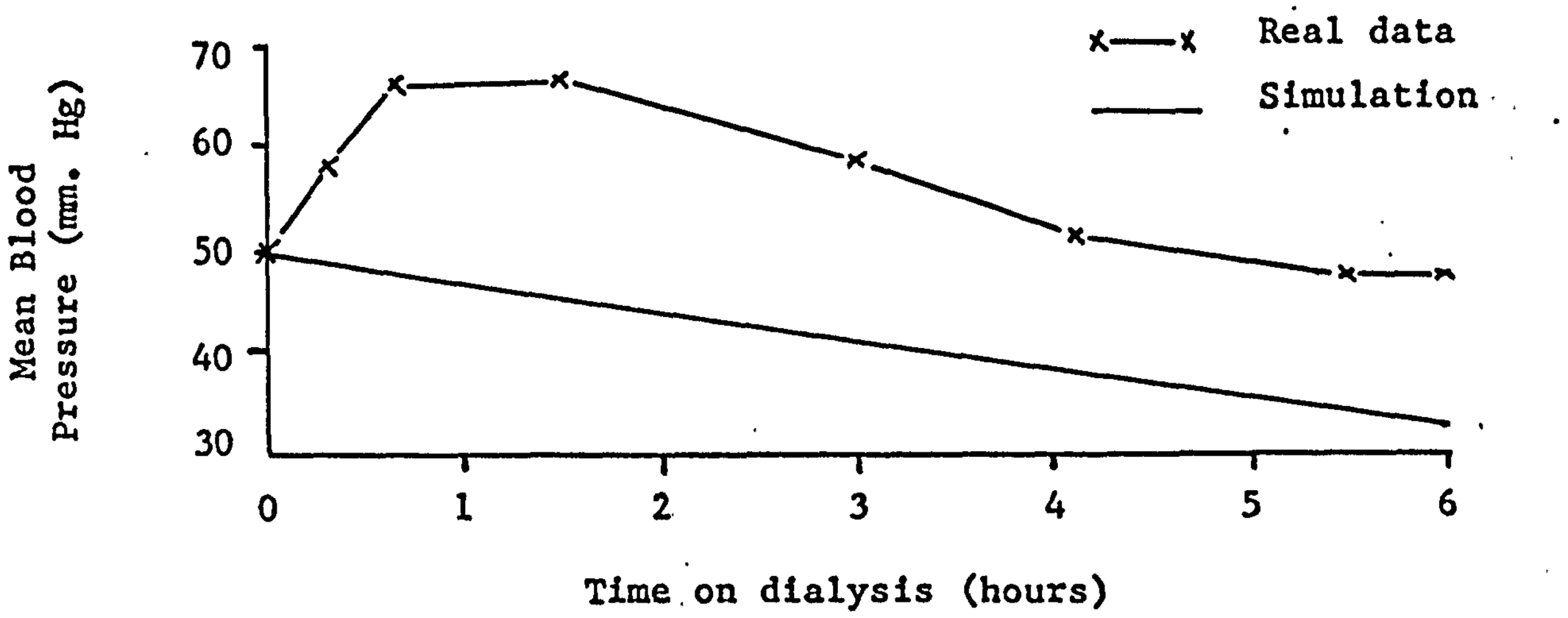

Figure 6.3. Effect of dialysis on M.G..

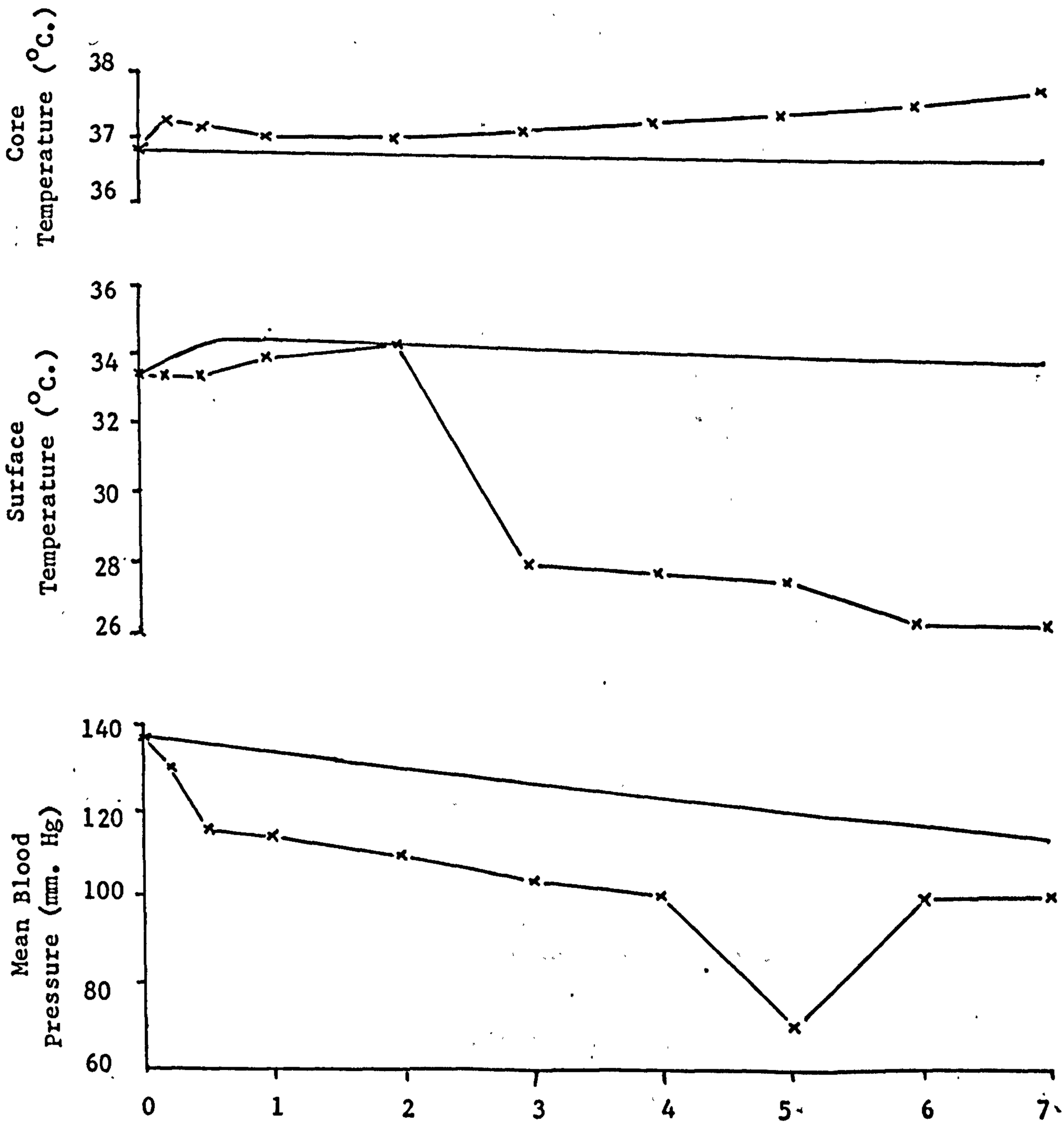

Figure 6.4. Effect of dialysis on K.F..

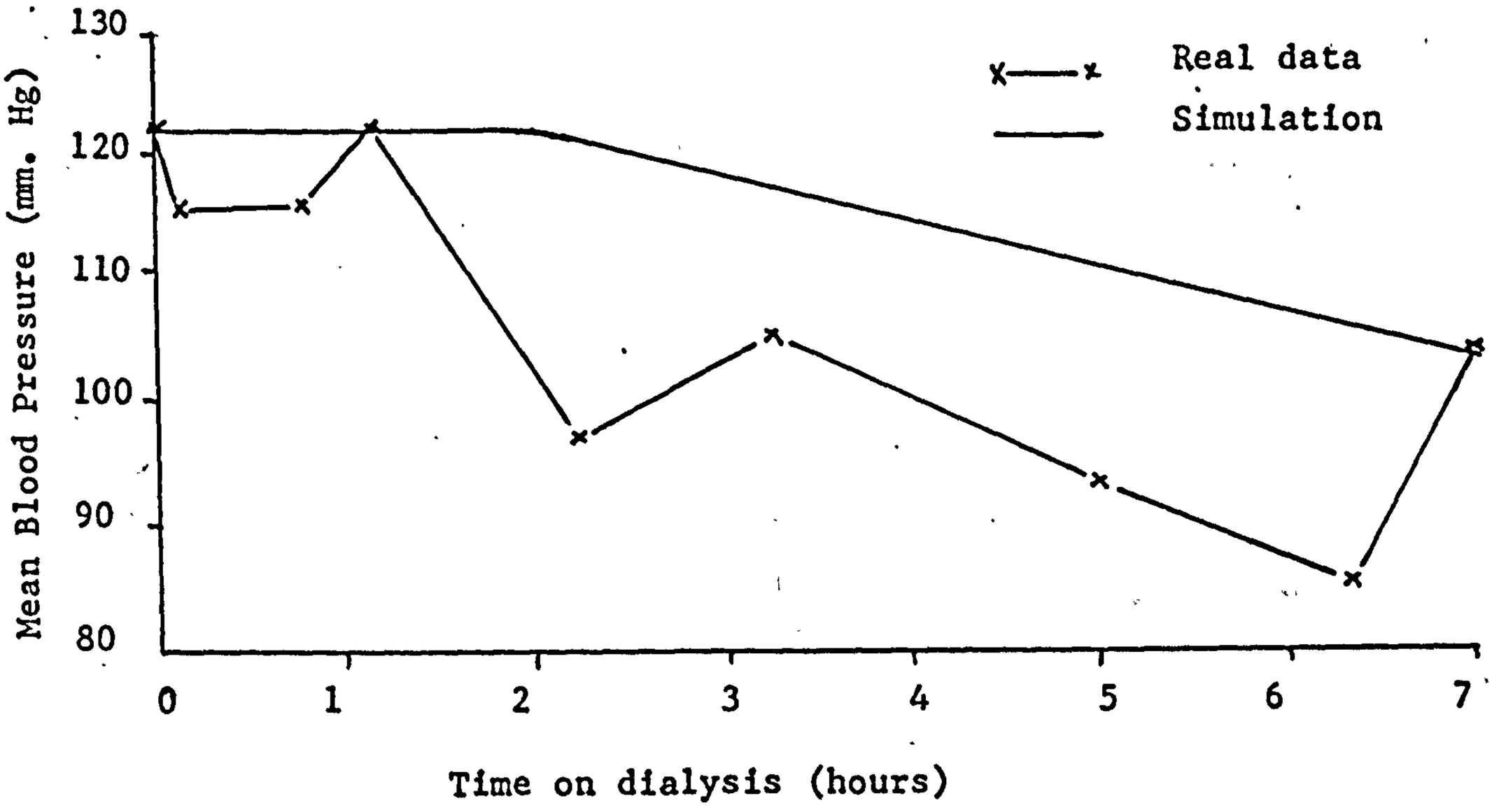

Figure 6.5. Effect of dialysis on R.R..

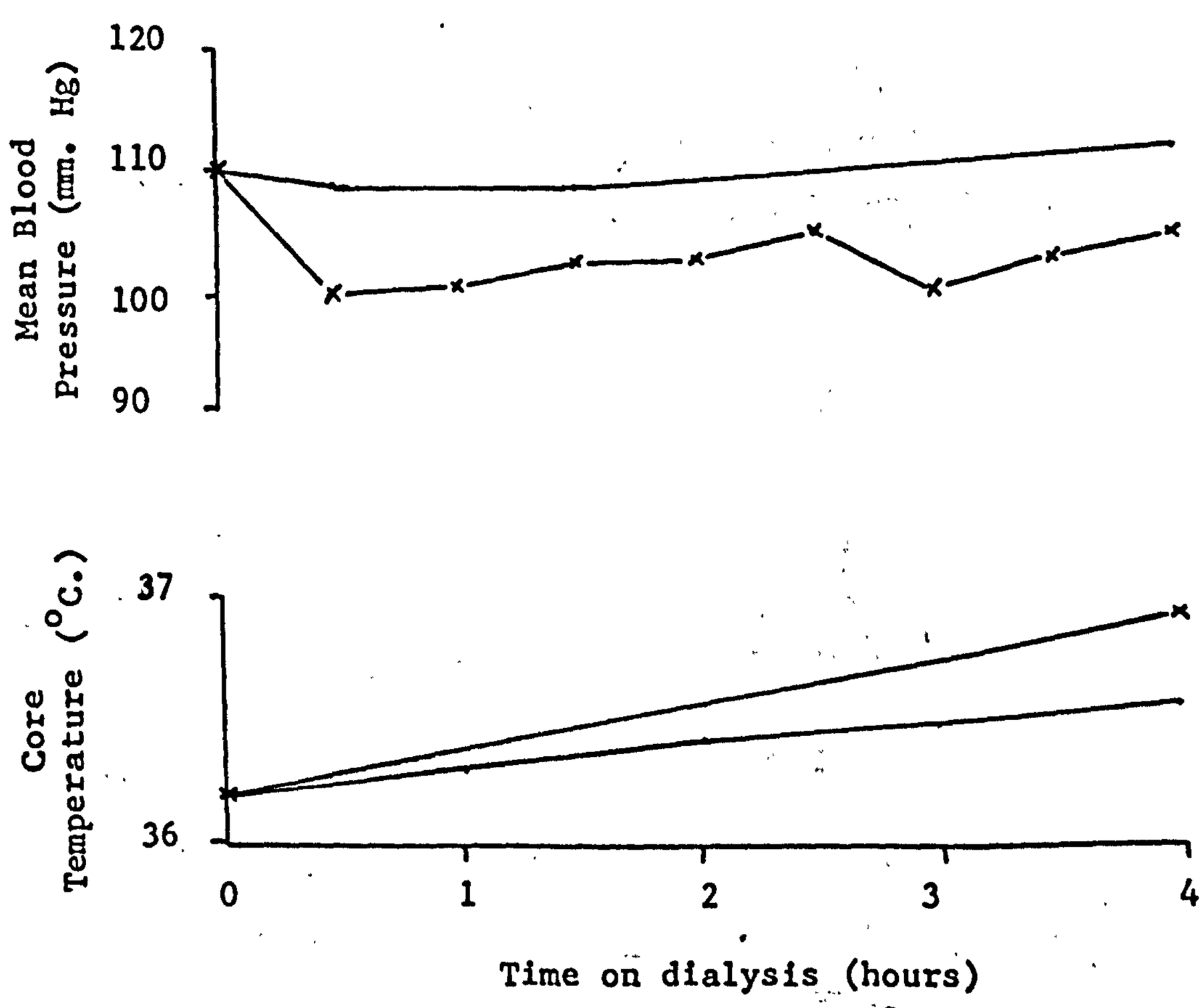

Figure 6.6. Effect of dialysis: D.G. 1.

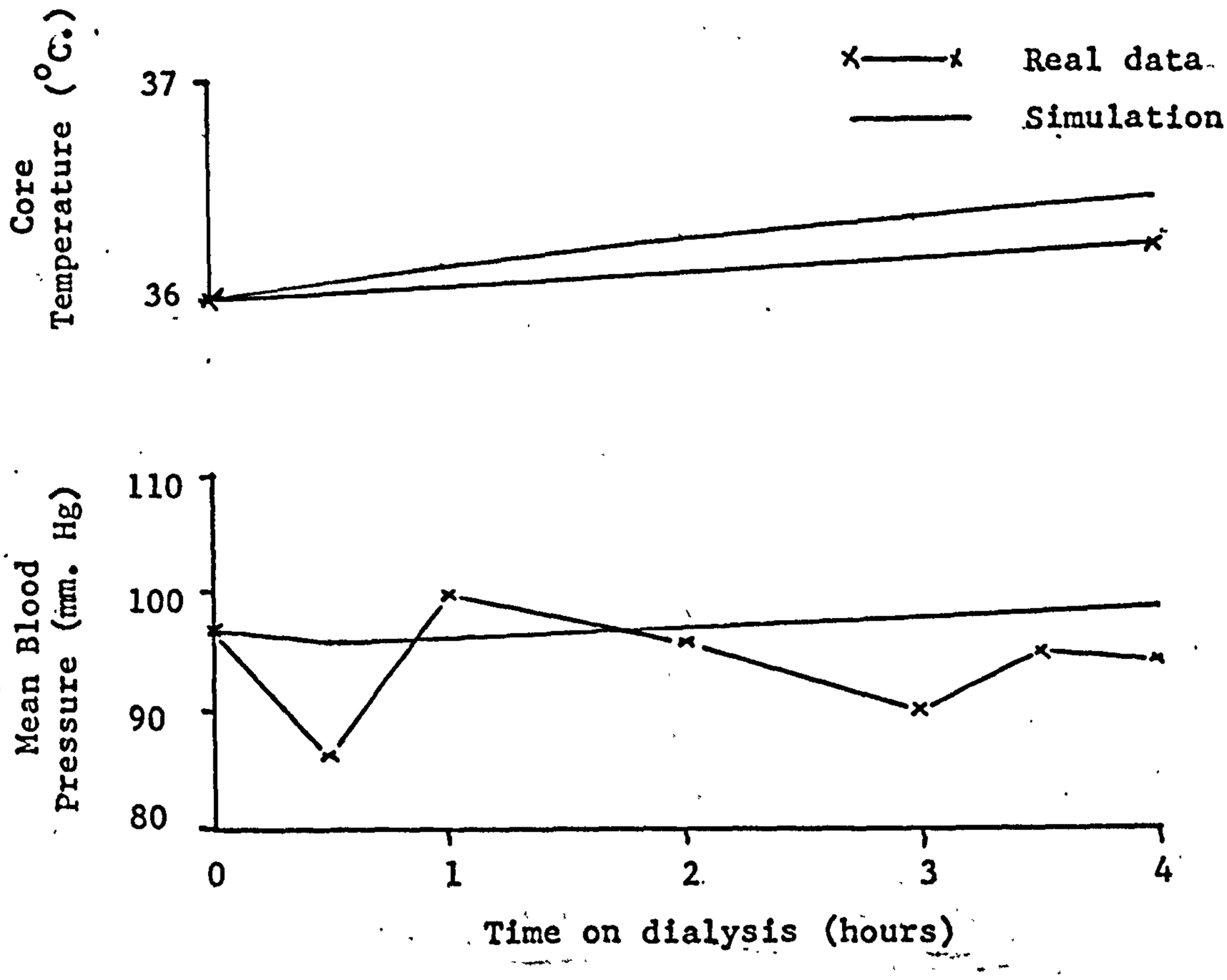

Figure 6.7. Effect of dialysis: D.G. 2.

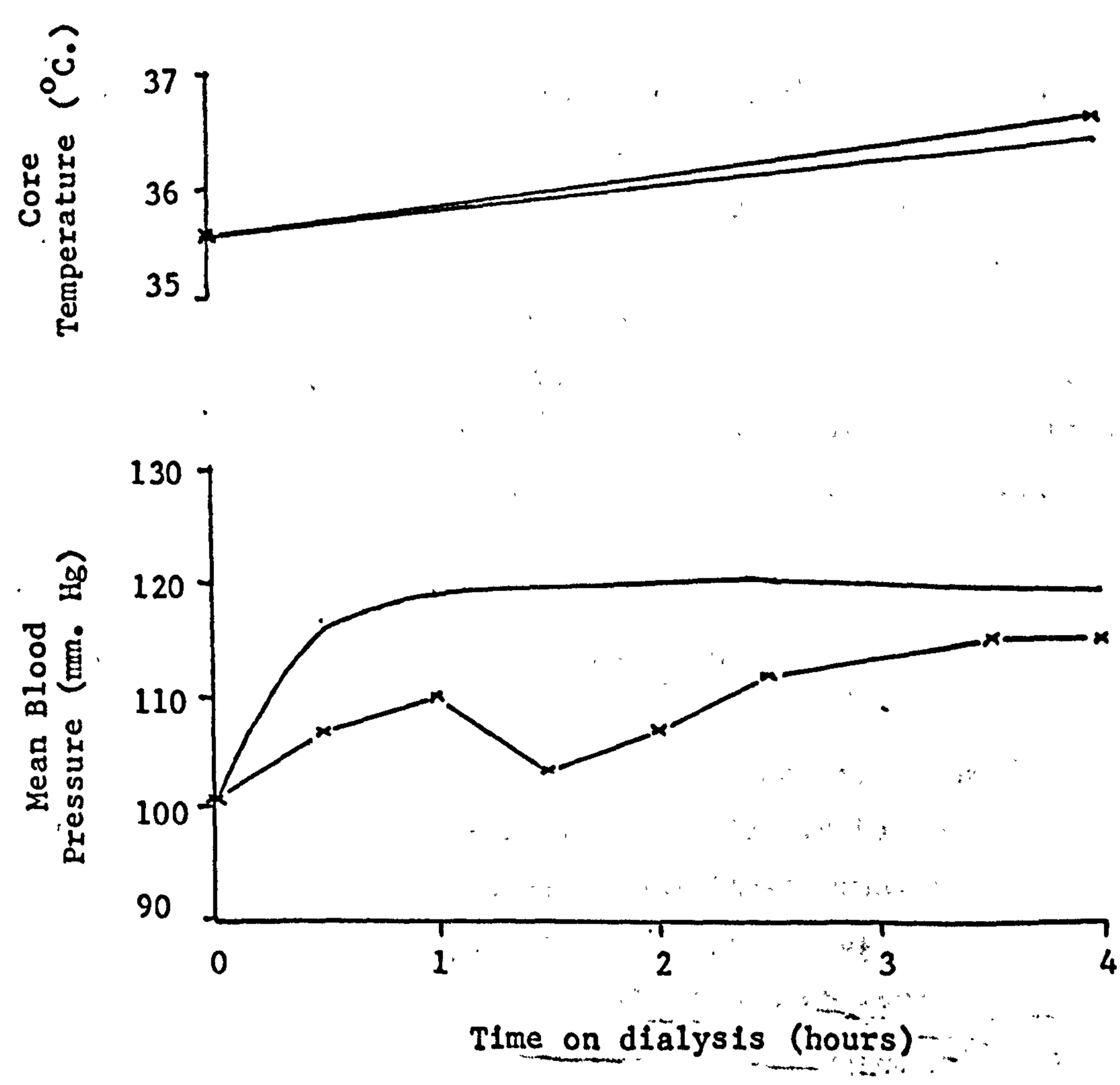

Figure 6.8. Effect of dialysis: D.G. 3.

CHAPTER 7

PARAMETER ESTIMATION FOR IMPROVED MODEL ACCURACY.

The major objective of this work is the development of the mathematical model of the patient - artificial kidney machine system which would be used as a predictive tool in aiding in the selection of an optimal dialysis therapy for the patient. To this end, the model described in Chapter 4 was formulated, and its performance as a predictive tool was tested. The results of these tests were presented in the previous chapter.

These results demonstrate that the model is adequate for the prediction of the outcomes of dialysis therapies for optimal therapy selection. However, greater accuracy of prediction, especially for longer term prediction, might be forthcoming, given better estimates for the values for the parameters which represent the extent to which the functions of the kidneys to excrete water and sodium, FACT1, and urea and creatinine, FACT4, and the rate of formation of urea, GUREA, in the patient.

In the clinical environment, these better estimates may be obtained by using a parameter estimation routine on the data of the previous dialysis of the patient concerned. In order to demonstrate the manner in which parameter estimation may be performed, and the resulting improved accuracy of the model response, parameter estimation was performed using the data for the three dialyses, D.G. 1, D.G. 2 and D.G. 3, presented in the previous chapter. The procedure for parameter estimation is described in section 7.1, and the results are presented in section 7.2.

7.1. Method For Parameter Estimation.

Parameter estimation was performed using the Fortran IV software package, GIDENT (Roberts, 1977), which is based on the Simplex method for optimization of a non-linear dynamic model with multiple outputs. The model of the patient - artificial kidney machine system was inserted into GIDENT as a user routine such that GIDENT called and evaluated the model at each parameter estimation

TABLE 7.1. Output And Parameter Requirements For Parameter Estimation.

		Definition	Typical Values	Time Dependant Weighting Factors								
				w_{i1}	w_{i2}	w_{i3}	w_{i4}	w_{i5}	w_{i6}	w_{i7}	w_{i8}	w_{i9}
Outputs	Y_1	AP	100	0.2	0.1	0.1	0.1	0.1	0.1	0.1	0.1	0.2
	Y_2	50xPUR	150	1.0	0.5	0.5	0.5	0.5	0.5	0.5	0.5	1.0
	Y_3	1000xPCRE	70	1.0	0.5	0.5	0.5	0.5	0.5	0.5	0.5	1.0
Parameters				Initial Values								
	P_1	1-FACT1	0.9	0.0								
	P_2	1-FACT4	0.9	0.0								
	P_3	10x(1-GUREA)	0.85	0.85								

iteration using various values for the parameters to be estimated.

The requirements for the optimization routine are presented in Table 7.1. The variables of the model used as outputs were chosen such that the estimation problem was identifiable. However, the output variables were redefined in order that their values were normalized as shown in Table 7.1. Arterial pressure data at thirty minute intervals were available, and data at thirty minute intervals for plasma concentrations of urea and creatinine were generated by linear interpolation between the pre-dialysis and post-dialysis data values for these variables. Time dependant weighting factors were set as shown in Table 7.1 to reflect the reliability of the data. The parameters to be estimated were also redefined as shown in Table 7.1, since the optimization is performed best when the values of the parameters to be estimated are approximately unity. Initial estimates were always set to nominal values for the average healthy human.

Parameter estimation was based on the minimization of the sum of the squares of the errors between model response and data values. The error term for each variable was evaluated at each thirty minute interval, and the squares of each of these values were multiplied by the appropriate weighting factors, w_{ij}. These values were then added together to give a value for the sum of the weighted squares of errors, and this value was minimized by subsequent iterations of the optimization routine using various

values for the parameters as set by the Simplex method. Full details of the optimization procedure may be found in Roberts (1977).

7.2. Results Of Parameter Estimation.

The optimal values for the parameters, FACT1, FACT4 and GUREA were determined for the three dialyses D.G. 1, D.G. 2 and D.G. 3 by the method outlined above. These values were then substituted into the model and the three dialyses were simulated. These results are presented in section 7.2.1.

For each of the simulations of dialysis, the model was allowed to run on till the time corresponding to the start of the next dialysis on the patient, with the submodel of the artificial kidney machine switched off. The simulation results representing the patient at the start of the next dialysis were then compared with the corresponding real data, where available. These results are discussed in section 7.2.2.

7.2.1. Estimated Parameters And Resulting Simulation Of Dialyses.

The values for the parameters obtained by optimal estimation for the three dialyses are listed in Table 7.2. The corresponding parameter values used in the simulations presented in the previous chapter are also listed in Table 7.2 for comparison.

It is known that the patient was suffering from acute renal failure. The values for the clinician specified parameters for patient state, FACT1 and FACT4, suggest that it was the opinion of the clinician that the patient was in an anuric stage during the first and second dialyses, D.G. 1 and D.G. 2, but that he had regained the excretory functions of the kidneys to some extent by the time of the third dialysis, D.G. 3. The values obtained by optimal estimation for FACT1 and FACT4 for dialyses D.G. 1 and D.G. 2 correspond exactly with the values specified by the clinician. However, the optimally estimated values for FACT1 and FACT4 during the third dialysis suggest

that the patient had not regained the excretory functions of the kidneys at this time.

The third parameter, GUREA, was specified as a constant for the simulation of the dialyses presented in the previous chapter. However, the results of the validation tests of the previous chapter indicated that this was not appropriate, and this conclusion is supported by the fact that the values for GUREA determined by optimal estimation for the first two dialyses are approximately four times the constant value, whereas the value for the third dialysis is equal to that of the constant.

The results of the simulations D.G. 1, D.G. 2, D.G. 3, using the appropriate optimally estimated values for FACT1, FACT4 and GUREA are presented in Tables 7.3, 7.4 and 7.5. The corresponding values for real data and the results of the simulations using the clinician specified values for these parameters are also presented in these tables for comparison.

The optimal values reached by GIDENT for the parameters for dailyses D.G. 1 and D.G. 2 differed from the clinician specified values only in respect of GUREA. The results of the simulations of D.G. 1 and D.G. 2, using the optimally estimated parameters, differed from the results of the simulations using clinician specified parameters only in the final concentration of urea in plasma, PUR, as shown in Tables 7.3 and 7.4. It is seen that optimal estimation of parameters has resulted in a significant improvement in the prediction of the final value of PUR in D.G. 1. However, the error in the final value of PUR in D.G. 2 is larger in the results of the simulation using the optimally estimated parameter values compared with the error seen between the real data and the results of the simulation of D.G. 2 using the clinician specified parameter values.

The values for FACT1 and FACT4 for dialysis D.G. 3 obtained by optimal estimation are seen to differ significantly from the corresponding values as specified by the clinician, whereas the values for GUREA are in agreement. These values are shown in Table 7.2. The results of the simulation of dialysis D.G. 3 using the optimally estimated parameter values are presented in Table 7.5. It is seen that the simulation response for PNA and PUR are significantly better than the corresponding results using the parameter values as specified by the clinician. The final

TABLE 7.2. Optimally Estimated Parameter Values.

		FACT1	FACT4	GUREA
D.G. 1	Specified	0.0	0.0	0.015
	Estimated	0.0	0.0	0.055
D.G. 2	Specified	0.0	0.0	0.015
	Estimated	0.0	0.0	0.056
D.G. 3	Specified	0.37	0.12	0.015
	Estimated	0.0	0.0	0.015

values for the other variables are essentially the same.

The discussion above demonstrates that optimal estimation of the values for parameters, FACT1, FACT4 and GUREA in the model of the patient - artificial kidney machine may lead to more accurate results in the simulation of dialysis than those obtained by using the values for these parameters as specified by the clinician.

7.2.2. Simulation Of The Inter-Dialysis Period.

The capabilities of the model of the patient - artificial kidney machine system to predict patient state in the inter-dialysis period were then examined. Certain clinical data concerning the state of the patient at the start of the dialyses following dialyses D.G. 1 and D.G. 3 were used for this purpose. The data for the dialysis following D.G. 2 were not available.

The model was allowed to run on following the end of the simulated dialysis periods for the number of hours of simulated time corresponding to the start of the next dialyses. The sub-model of the artificial kidney machine was switched off in this period of simulated time. Two simulations were performed for each of the inter-dialysis periods. The first used values for FACT1, FACT4 and GUREA as specified by the clinician, and the

TABLE 7.3. Results Of Simulation Of D.G. 1 Using Optimal Parameter Values.

	AP	PNA	PK	PUR	PCRE
Pre-dialysis*	110.0	129.0	6.2	3.17	0.078
Clinical Data*	103.3	131.0	5.3	2.33	0.066
Non-Optimal	110.8	133.3	4.4	2.12	0.055
Optimal	110.8	133.3	4.4	2.28	0.055

TABLE 7.4. Results Of Simulation Of D.G. 2 Using Optimal Parameter Values.

	AP	PNA	PK	PUR	PCRE
Pre-dialysis*	97.0	128.0	6.0	2.75	0.075
Clinical Data*	93.0	131.0	4.9	1.67	0.052
Non-Optimal	97.4	133.1	4.2	1.76	0.051
Optimal	97.4	133.1	4.2	1.93	0.051

TABLE 7.5. Results Of Simulation Of D.G. 3 Using Optimal Parameter Values.

	AP	PNA	PK	PUR	PCRE
Pre-dialysis*	101.0	135.0	4.1	3.0	0.050
Clinical Data*	115.0	137.0	3.5	3.27	0.040
Non-Optimal	119.2	138.4	3.5	1.75	0.036
Optimal	118.9	137.7	3.4	1.92	0.036

* Pre-dialysis and Clinical Data values taken from clinical records.

second simulations were performed using the optimally estimated values for these parameters. The simulation results are presented in Tables 7.6 and 7.7.

The results of the simulation of the seventeen hour period following dialysis D.G. 1, using parameter values specified by the clinician are shown in Table 7.6. Considering that these results represent the end of a seventeen hour period of simulated time, the simulation results compare favourably with the corresponding clinical data apart from the final values for the concentrations of sodium and urea in plasma. However, the concentration of sodium in plasma, PNA, is seen to have fallen in the patient, whereas the simulation results indicate a slight rise. Also the level of urea in the patient, PUR, is seen to rise by 0.8 g./l. in the inter-dialysis period, whereas the corresponding rise in the first simulation is 0.4 g./l.

The results of the simulation using the optimally estimated parameter values, also shown in Table 7.6, are the same as those of the first simulation with regard to all the variables except the final level of urea in plasma. This is due to the fact that the only difference between the parameter values specified by the clinician and those obtained by optimal estimation is in the value for GUREA as shown in Table 7.2. Considering the dynamics of urea in these simulations, it is seen that the rise in the level of urea is only 50% of the actual rise, whereas the rise in the second simulation is 140% of the actual rise. This suggests that although the high value for GUREA established by the optimization routine for the dialysis period, D.G. 1, is appropriate, the value for the inter-dialysis period should be lower than that for the dialysis period.

The results of the simulation of the twenty-four hour period following the dialysis, D.G. 3, using parameter values specified by the clinician are shown in Table 7.7. It is seen that the final values for mean arterial pressure, MAP, and plasma sodium concentration, PNA, generated by this simulation compare well with the clinical data. However, the values for the concentrations of potassium, PK, and creatinine, PCRE, are seen to have risen, and the level of urea has fallen. These are not in accordance with the clinical data.

The results of the simulation of this post-dialysis period

TABLE 7.6. Simulation Of Post-Dialysis D.G. 1.

Hours	MAP (mm. Hg)			PNA (mEq./l.)			PK (mEq./l.)			PUR (g./l.)			PCRE (g./l.)		
	1	2	3	1	2	3	1	2	3	1	2	3	1	2	3
0	110.0	-	-	129	-	-	6.2	-	-	3.17	-	-	0.078	-	-
4	103.3	110.8	110.8	131	133.3	133.3	5.3	4.4	4.4	2.33	2.12	2.28	0.066	0.055	0.055
21	106.7	121.3	121.3	128	134.7	134.7	5.9	5.7	5.7	3.12	2.52	3.61	0.070	0.076	0.076

TABLE 7.7. Simulation Of Post-Dialysis D.G. 3.

Hours	MAP (mm. Hg)			PNA (mEq./l.)			PK (mEq./l.)			PUR (g./l.)			PCRE (g./l.)		
	1	2	3	1	2	3	1	2	3	1	2	3	1	2	3
0	101.0	-	-	135	-	-	4.1	-	-	3.00	-	-	0.051	-	-
4	115.0	119.2	118.9	137	138.4	137.7	3.5	3.5	3.4	2.27	1.75	1.92	0.040	0.036	0.036
28	111.6	120.1	143.7	142	142.0	129.6	3.6	5.0	6.6	2.52	1.42	2.38	0.038	0.065	0.063

Legend:- 1 : Clinical data.

2 : Simulation results using parameter values specified by the clinician.

3 : Simulation results using parameter values estimated by optimization routine.

using the optimally estimated parameter values are also presented in Table 7.7. The values for the final mean arterial pressure, plasma sodium and potassium concentrations deviate from the clinical data more than the corresponding values generated by the first simulation. However, the value for the final level of urea in the patient is in close agreement with the clinical data.

These results appear to indicate that the value for FACT1 as specified by the clinician, 0.37, is more appropriate for the post-dialysis period than the value, 0.0, obtained by optimal estimation using the clinical data representing the state of the patient during dialysis, D.G. 3. This is also seen to be the case by intuitively considering the effects of having a lower value for FACT1 in the post-dialysis period. The lower value for FACT1 leads to greater fluid retention over the post-dialysis period, and hence a higher value for mean arterial pressure and a lower concentration of sodium in the body fluid. In order to maintain osmotic equilibrium and compensate for the drop in sodium concentration in the extracellular compartment, potassium is drawn from the intracellular to the extracellular compartment, thus raising its concentration in the extracellular compartment. Examination of other clinical records relevant to this patient revealed that in a four day period encompassing the twenty-eight hour period from the start of dialysis, D.G. 3, the daily rate of flow of urine increased from 150 mls. to 1,800 mls. It is evident, therefore that the value for FACT1 increases with time in this four day period. Thus, although the optimally estimated value for FACT1, 0.0, appears to be more appropriate during the period of dialysis, D.G. 3, the value specified by the clinician generates the better simulation results for the post-dialysis period. However, it is seen from the final values for the level of urea in the patient, that the value for FACT4, 0.0, obtained by optimal estimation appears to be more appropriate than the value specified by the clinician, 0.12, even for the post-dialysis period.

The results of the simulations of the two post-dialysis periods of patient D.G. may now be summarized. It appears that in this patient, the actual rate of generation of urea in the period following dialysis D.G. 1 and the ability of the kidneys to excrete sodium and water in the period following D.G. 3 are

changing rapidly. Thus, the results of the simulations of the patient for the periods following dialyses D.G. 1 and D.G. 3, using the optimally estimated values for FACT1, FACT4 and GUREA which were obtained using the clinical data of dialyses D.G. 1 and D.G. 3 respectively, show little or no improvement over the results of the simulations using the values for these parameters as specified by the clinician.

7.3. Summary.

A method for 'tuning' the model of the patient - artificial kidney machine system to fit the individual patient has been demonstrated in this chapter. Data representing three dialyses on a patient suffering from acute renal failure were used to obtain three sets of optimal values for the patient - dependant parameters. The three dialyses were then simulated using the optimal values for these parameters and the results of these simulations were compared with those of the simulations using parameter values specified by the clinician. It was found that in two out of three cases, the results of the simulations using the optimally estimated parameter values matched the clinical data more closely than the results of the simulations using parameter values specified by the clinician. This finding indicated that improved accuracy of prediction of the future state of the dialysis patient may be achieved by the use of an optimal estimation routine on past patient data.

The long term predictive capabilities of the model were then tested. These tests, however, were inconclusive. The patient, whose clinical data were used for these tests, was suffering from acute renal failure, and was gradually regaining the functions of his kidneys. Therefore, the actual values of some of the parameters which were optimally estimated for the model were not constant in the patient. This factor, therefore, gave rise to the somewhat inappropriate simulations of the patient in the inter-dialysis periods.

Although the tests of the validity of the model for long term prediction of patient state were inconclusive due to inappropriate test data, the overall indication from the work

presented in this chapter is that the optimal estimation of certain patient - dependant parameters would lead to improved accuracy of simulation response. Further, it appears that the long term prediction of patient state would be more successful for the chronic renal failure patient, whose values for the patient - dependant parameters would remain essentially constant, than for the acute renal failure patient. The following chapter, therefore, describes the overall system, incorporating the mathematical model, to be used in the renal unit to aid in the selection of optimal dialysis therapies for renal failure patients.

CHAPTER 8

CLINICAL APPLICATION OF THE MODEL.

The derivation of the model of the patient - artificial kidney machine system was presented in Chapter 4. The results of tests to demonstrate the validity of the model have been presented in the preceding three chapters. To be of use as a clinical aid in the renal unit, however, the model needs to be incorporated within an appropriate software system.

The necessary associated software has been developed as part of this research programme. The major function of this software is to enable the clinical user, assumed to have little or no experience with computer systems, to enter into the system, via an interactive terminal of the computer, parameters representing the state of the patient and the candidate dialysis therapy. These parameters are listed in Table 6.1.

The other function of the associated software system is to enable the clinical user to run the model several times for one patient using parameters representing different candidate therapies so that an optimal therapy may be selected for actual use on the patient.

The overall software system is presented in this chapter, and a listing of the source code is given in Appendix III. Hardware system requirements are also addressed below.

8.1. Description Of The Overall Software System.

The overall software system is written in Fortran IV computer language. The routines representing the mathematical model comprise the core of the software system; the remainder of the system consists of an integration routine, used to solve the differential equations of the model, and the routines which cause the clinical user to interact with the system in order to feed in the appropriate parameter values for the model. The function of each routine is described below:-

MAIN ROUTINE: The purpose of the main routine is to direct the execution of the subroutines in a particular sequence. This sequence may be influenced by the responses of the user. Detailed discussion of this aspect is presented in the following section of this chapter. The main routine also causes the model predictions to be printed on the computer output device.

SUBROUTINE READFA: This routine prompts the user to enter into the system, via an interactive computer terminal, parameter values specified by the clinician which represent the state of health of the patient.

SUBROUTINE READIN: This routine prompts the user to enter values representing the daily rates of ingestion of substances. The daily rates are then transformed to rates of ingestion per minute.

SUBROUTINE READIC: This routine prompts the user to enter initial condition information. These data are then transformed to represent initial values for the state variables of the model.

SUBROUTINE READTH: This routine prompts the user to enter values representing the candidate dialysis therapy.

SUBROUTINE CONTRL: This routine solves the algebraic equations of the model.

SUBROUTINE MODEL: This routine contains the differential equations of the model which are solved by the integration routine.

SUBROUTINE INTEGR: This routine is a Runge - Kutta fourth order variable step integration routine which is used to solve the differential equations of the model. The iteration step length is one minute.

SUBROUTINE OSMOS: This subroutine establishes osmotic equilibrium between the intracellular and extracellular compartments of the model at the end of each iteration.

The equations comprising the subroutines CONTRL, MODEL and OSMOS were presented in Chapter 4, and are listed in Appendix II in algebraic form. The calling sequence of the routines is presented in the diagram of Figure 8.1, and the organisation of the prompts for the user to enter parameter values into the system is shown in Figure 8.2.

8.2. Facilities Offered By The Software System.

Incorporated in the software system, described here, are certain logical switches to be set by the user. These switches enable the user to run the model with several candidate dialysis therapies so that an optimal therapy may be selected for actual use on the patient. The manner in which the system is to be used is described below and a flowchart of the functions of the programme is presented in Figure 8.3.

On initiation of the programme, the user is prompted to enter into the system the required data, as shown in Figure 8.2. The model is then run using these data values so that prediction of the outcome of dialysis is obtained. The prediction is listed on the output device in tabular form such that the values of the clinically important variables are printed every thirty minutes of simulated time for the duration of the proposed dialysis. Analysis of the prediction would give the user or the clinician an indication of any abnormal patient states that may arise during the actual dialysis on the patient.

The user is then asked whether another candidate dialysis therapy is to be proposed. If the response of the user is affirmative, the system then returns the user to the part of the programme where the parameter representing the proposed dialysis therapy are to be entered by the user. The model is then run again using the original parameters representing the patient, but with the revised parameters for the dialysis therapy, and a new prediction of the outcome of dialysis is obtained.

By entering this loop repeatedly, several candidate dialysis therapies may be tried on the model with the same set of parameters representing the patient. The optimal therapy for that patient may then be selected by considering the different model predictions.

When the user is satisfied that an optimal therapy has been selected, an exit from this loop is gained simply by entering the negative response in reply to the question. A second switch is then set by the user which either halts the system or prepares it for the purpose of prediction of the state of the patient for some time after the completion of the proposed dialysis therapy.

If prediction of the post-dialysis state of the patient is requested, then the system causes the user to update, if necessary,

the parameter values representing the state of the patient and the rates of ingestion of substances. The model is then run for a specified length of simulated time with the model of the artificial kidney machine switched off and the initial values for the state variables set equal to the final values generated in the last simulation of dialysis. The user would then be able to estimate, from the resulting model predictions, when the next dialysis would need to be performed. In addition, these model predictions would give indications of any undesirable patient states that may arise in the inter-dialysis period.

Finally, the system gives the user the option to try another candidate dialysis therapy in case the predicted post-dialysis state of the patient is found to be unsatisfactory. Used in this manner, the software system described above offers the user the facility to select an optimal dialysis therapy, for the patient, in terms of the state of the patient during dialysis.

8.3. Computer Hardware Requirements.

The computer hardware necessary for the implementation of the software system for a renal unit should be relatively easy to set up. Most hospitals either have their own, or have access to computer facilities.

The minimum hardware requirement is for an interactive teletype terminal, in or near the renal unit, which is linked to a medium sized or a mainframe computer system with a Fortran compiler. The software programme would be stored in the bulk memory of the computer system, to be loaded into core whenever there was a need for it. With this arrangement, it is important that the computer system is not overloaded with other uses such that the response time of the system for interactive users is so great that it becomes impractical to use the software system as a predictive clinical aid to patient management.

If speed of use of the software system is a crucial factor, then an arrangement consisting of a visual display unit and a high-speed line printer, linked to the computer, could be adopted. With this arrangement, only some of the model predictions would be directed to the line printer for "hard copy", whereas user

interaction and general testing of model responses would be carried out on the visual display unit. The software system would require slight modifications to permit its use in this manner.

The software system was run on a mainframe computer, the ULCC CDC 7600 computer system, in batch mode, and interactively on a medium sized computer, the PDP 12 with OS/8 operating system. The size of core needed for the programme was 13 K words of 16 bits each. The mainframe computer used twenty-one seconds of processor time to generate model predictions of two hundred hours. Using the system in the interactive mode, an experienced user of the system required approximately six minutes to enter the data needed for the model to run, and the model prediction for a six hour dialysis was generated in approximately four minutes.

8.4. Summary.

The system described above offers a method for the input of parameter values for the model. The system is designed such that the software system may be used relatively easily by clinical staff who may not have experience with computer systems.

The system used in the manner described above results in predictions of the outcome of several candidate therapies so that an optimal therapy may be selected for use on the patient. In addition, these predictions would indicate any problems that may occur during dialysis. Further, using the post-dialysis prediction results, the clinician would be able to estimate when the next dialysis would need to be performed and also ensure that no complications arise in the condition of the patient in the period between dialyses. Thus, the model incorporated in the software system described above may be used to maintain the renal dialysis patient in an optimal state.

Timing considerations demonstrate that the system may be used interactively in a renal unit in an economical manner.

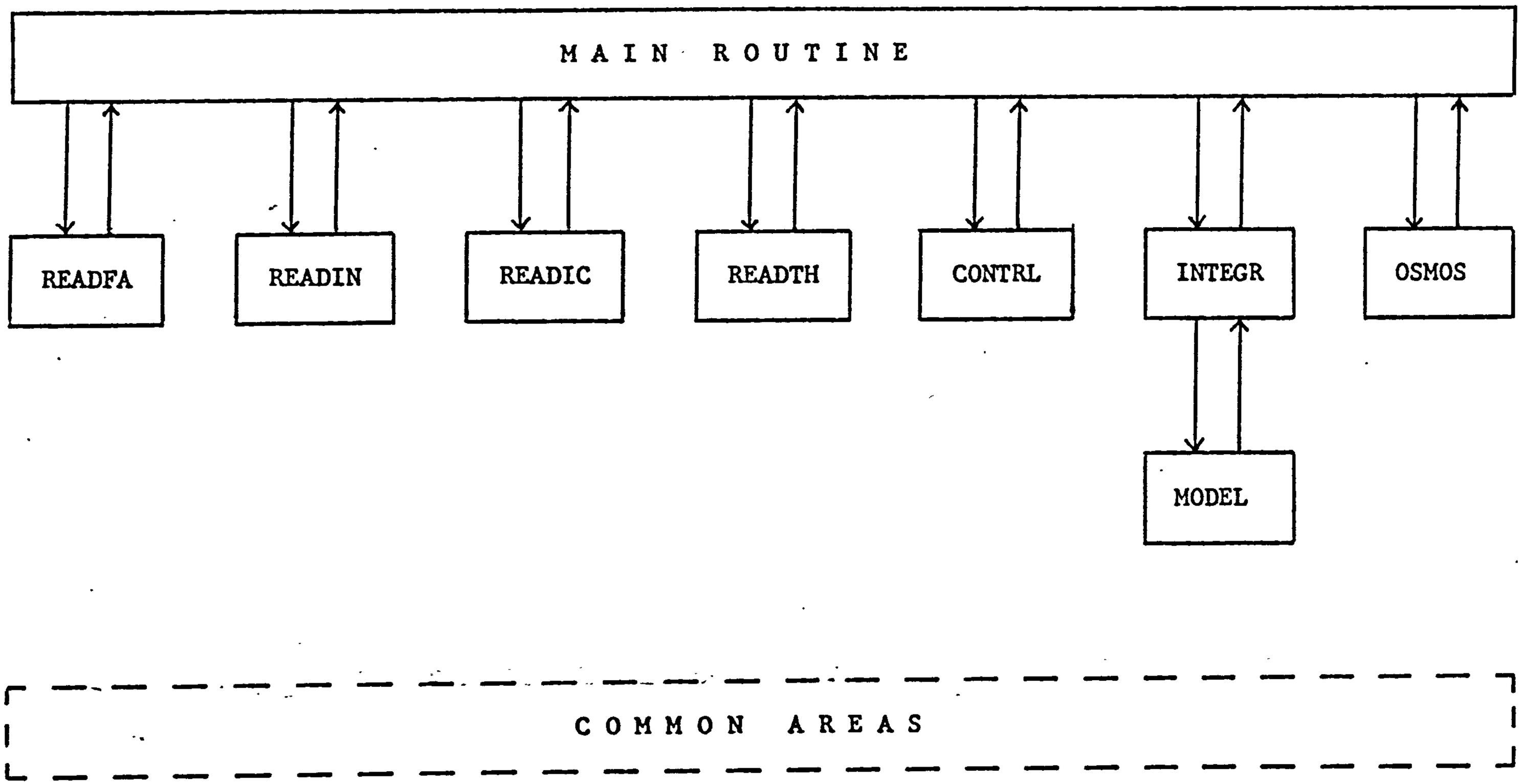

Figure 8.1. Organisation of the routines of the software system.

```
  THIS PROGRAM RUNS A MATHEMATICAL MODEL OF THE PATIENT-ARTIFICIAL KIDNEY MACHINE SYSTEM
TO GIVE PREDICTIONS FOR THE OUTCOMES OF DIALYSISTHERAPIES. THE USER WILL BE PROMPTED TO INPUT
DATA NEEDED FOR THE MODEL TO RUN.



     THE PATIENT IS SUFFERRING FROM RENAL FAILURE. THE SYSTEM REQUIRES
 INFORMATION ON THE EXTENT TO WHICH THE NORMAL KIDNEY FUNCTIONS HAVE BEEN
 IMPAIRED.

   HOW MUCH OF THE KIDNEY FUNCTION TO EXCRETE SODIUM AND WATER REMAINS INTACT?
0.12

    HOW MUCH OF THE KIDNEY FUNCTION TO SECRETE RENIN REMAINS INTACT?
0.17

    HOW MUCH OF THE KIDNEY FUNCTION TO EXCRETE POTASSIUM REMAINS INTACT?
0.17

    HOW MUCH OF THE KIDNEY FUNCTION TO EXCRETE UREA AND CREATININE REMAINS INTACT?
0.12

     IS HEART PUMPING ABILITY DECREASED?
1.NO. 2.BY 25%. 3.BY 50%. :
2.0

     WEIGHT OF PATIENT IN KGS.:
64.6
```

Figure 8.2. Interaction between system and user for input of parameter values.

```
     THE SYSTEM WILL NOW ASK FOR THE DAILY INGESTION RATES OF
SUBSTANCES IN THE DIET OF THE PATIENT.

   HOW MUCH FLUID HAS THE PATIENT BEEN TAKING IN MILLILITRES PER DAY?
1000.0

    HOW MUCH SODIUM IN MILLIEQUIVALENTS PER DAY?
100.0

    HOW MUCH POTASSIUM IN MILLIEQUIVALENTS PER DAY?
60.0



     THE MODEL REQUIRES INITIAL VALUES TO START IT OFF.

TYPE CORE TEMPERATURE  :
37.0
TYPE SKIN TEMPERATURE  :
34.0
TYPE EXTRACELLULAR FLUID VOLUME  :
19.0
TYPE PLASMA SODIUM CONCENTRATION  :
137.0
TYPE PLASMA POTASSIUM CONCENTRATION  :
4.8
TYPE INTRACELLULAR FLUID VOLUME  :
26.0
TYPE INTRACELLULAR SODIUM CONCENTRATION  :
9.0
TYPE INTRACELLULAR POTASSIUM CONCENTRATION  :
139.0
```

Figure 8.2. Continued.

```
TYPE RENIN CONCENTRATION  :
0.08
TYPE ANGIOTENSIN 11 CONCENTRATION  :
30.0
TYPE ALDOSTERONE CONCENTRATION  :
85.0
TYPE ARTERIAL PRESSURE  :
150.0
TYPE A.D.H. CONCENTRATION  :
0.5
TYPE UREA CONCENTRATION  :
2.91
TYPE CREATININE CONCENTRATION  :
0.153
CONSTANT FACTOR FOR INTRACELLULAR-EXTRACELLULAR EQUILIBRIUM IS  : -11.20

      SYSTEM REQUIRES
INFORMATION CONCERNING THE PROPOSED THERAPY.

TYPE CONCENTRATION OF SODIUM IN THE DIALYSATE  :
135.0
TYPE CONCENTRATION OF POTASSIUM IN THE DIALYSATE  :
2.0
TYPE PROPOSED TIME IN MINUTES FOR DIALYSIS  :
420.0
TYPE POST COIL PRESSURE  :
160.0
 TYPE BLOOD FLOW RATE THROUGH MACHINE IN ML5/MIN  :
250.0
```

Figure 8.2. Continued.

THE PREDICTION OF THE VARIABLES DURING DIALYSIS IS AS FOLLOWS:-

R E S U L T S

END OF DIALYSIS

DO YOU WISH TO CHANGE ANY OF THE VARIABLES OF THE DIALYSIS THERAPY?

1.YES. 2.NO. :
2.0

DO YOU WISH TO KNOW THE PREDICTION OF THE PATIENTS STATE AFTER DIALYSIS?

1.YES. 2.NO. :
2.0

Figure 8.2. Continued.

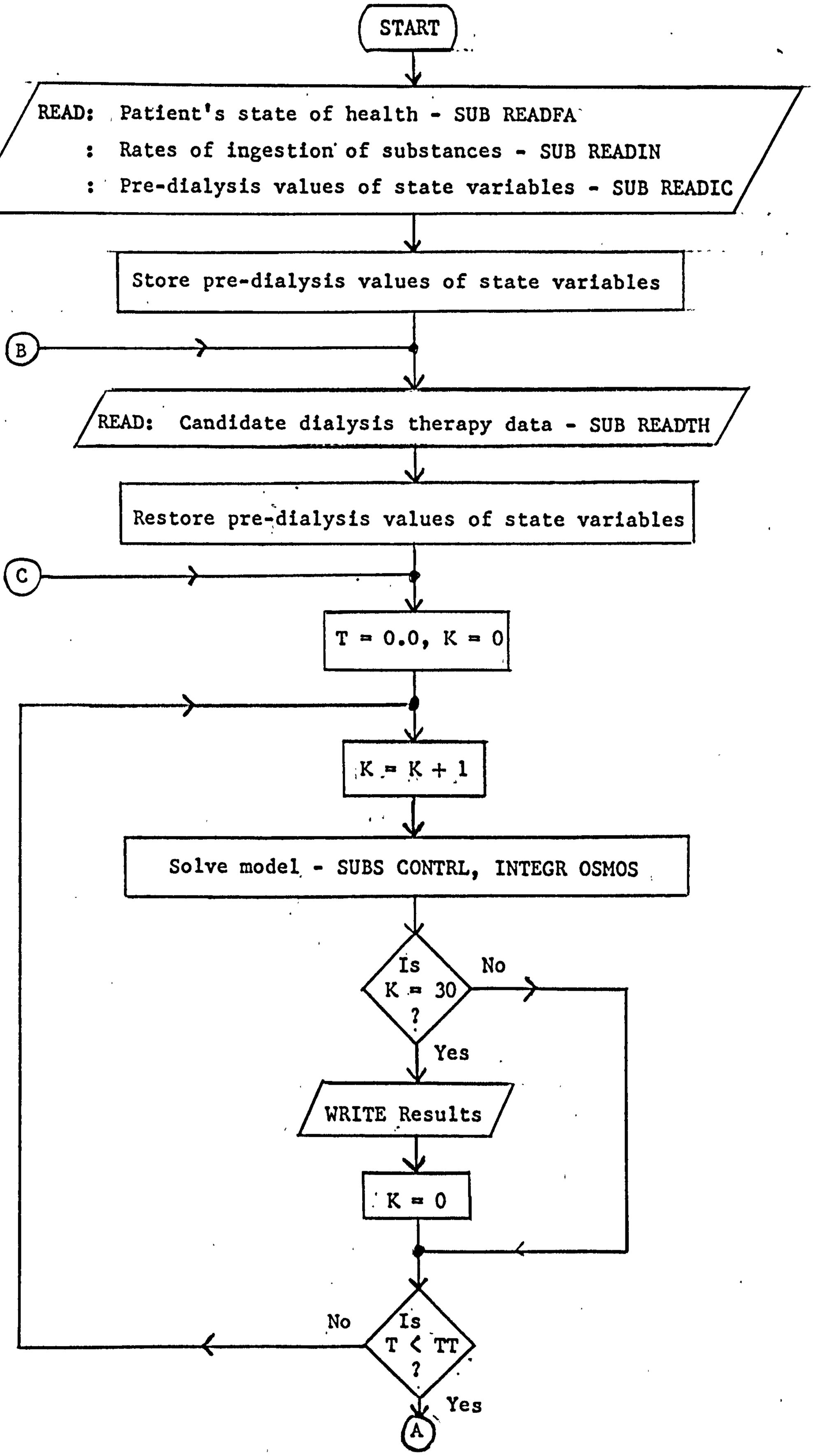

Figure 8.3. Flowchart of overall software system.

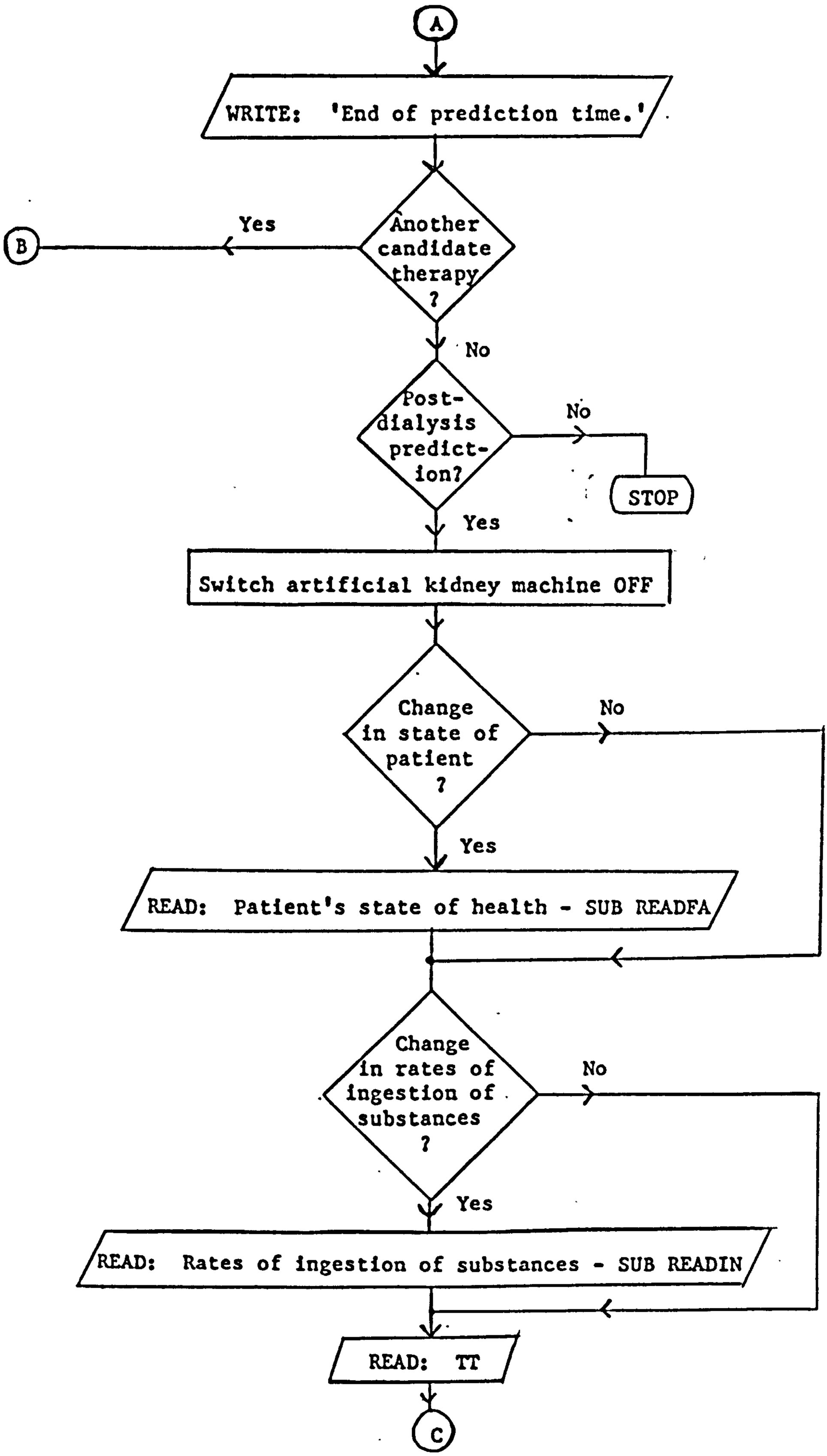

Figure 8.3. (continued)

NAMELIST FOR FLOWCHART.

T : Simulated time in minutes.

K : Counter used for printing prediction results once every thirty minutes of simulated time.

TT : Length of time for which dialysis or post-dialysis predictions are required.

Figure 8.3. (continued)

CHAPTER 9

CONCLUSIONS.

The primary aim for this research programme is to investigate the feasibility of the application of a mathematical model as an aid in patient management in renal dialysis. To this end, the mathematical model of the patient - artificial kidney machine was developed for use in an interactive mode to generate predictions of the outcome of candidate dialysis therapies on the patient. This model consists of interconnected models of subsystems of the human organism, and is based on the current knowledge of the relevant physiology.

During the modelling process, it was necessary to make several simplifying assumptions with regard to some complex and poorly understood control mechanisms in these human subsystems. However, the validation tests, which were designed to examine the capability of the model to satisfy its objectives, revealed that the performance of the model was adequate. Firstly, it was determined that the model of the renal - body fluid system, a submodel of the model of the patient - artificial kidney machine system, was capable of simulating the effects of certain stresses to the human renal - body fluid system, and thus this submodel could be used as a vehicle with which to test hypotheses related to the renal - body fluid system.

Secondly, using the available clinical data, it was established that the model is capable of predicting the outcomes of dialysis therapies on patients with sufficient accuracy to be of use to the renal dialysis clinician as a predictive tool. However, sensitivity tests revealed that greater accuracy of simulation response may be obtained given better estimates for values of certain parameters representing the state of health of the patient than those suggested by the clinician. Using available patient data, the parameter estimation exercises were conducted. The resulting improvement in simulation responses of two out of three dialyses indicated that the model may be useful for the prediction of patient state in the longer term in the inter-dialysis period. However, due to the lack of useful clinical data, no

definite conclusions can be drawn with regard to the third objective of this work - that of being able to use the model to predict the state of the patient in the inter-dialysis period. Thus, as far as the limited available clinical data permitted, the validity of the model for clinical application was established. However, it is recognized that further extensive validation of the model, both for simulation of the dialysis and the inter-dialysis periods, is necessary before this work may safely be applied in a clinical environment. It is unfortunate that clinical data of sufficient quality and quantity for this purpose were not available during the course of this research programme.

Two major areas of weak knowledge, where assumptions needed to be made for the modelling process, were discovered. The first is concerned with the interrelationships between the thermoregulatory system model and the other subsystem models. Recent data (Graveney, 1979) resulting from experiments on humans have shown that there is an unexpectedly high degree of correlation between the temperature of the human body and many of the clinically important variables of the model. The second area is related to the effects of changes in the concentrations of electrolytes in the body fluids on the pumping ability of the heart and on the cardiovascular system as a whole. The use of the model as a hypothesis testing tool on appropriate experimental data, in a manner similar to that reported in Chapter 5, may lead to a better understanding of these areas of weak knowledge, and help to explain some of the phenomena that are sometimes observed in patients undergoing dialysis.

Apart from its use as an aid in dialysis therapy selection for the individual patient, and as a tool to expand knowledge about the functioning of the human body, the model has another potential application to benefit dialysis patients. It may be used as a test - bed on which to examine the effects of various generalized long term strategies for the treatment of dialysis patients in order to minimize the 'cost' of dialysis. Cost would be a measure of some combination of factors including patient well-being, financial cost and, not least of all, overall time on dialysis for the patient. Less time on dialysis would mean that each expensive artificial kidney machine, of

which there is an insufficient number, may serve more renal failure patients in need of dialysis treatment. Thus the toll, in terms of human life, taken by renal failure may be reduced.

In addition to the potential benefits for medical science outlined above, this research programme has also contributed to the field of systems science. It has been demonstrated that valid complex, structural biological models, which are as isomorphic with the system being modelled as permitted by current knowledge, may be formulated. Further, it has been shown that such models can be useful for clinical applications. Finally, validation of such models is found to be an important and integral part of the model formulation process. Validation exercises should therefore be formulated specifically to test the capabilities of the model to accomplish the functions that the model is designed to perform.

REFERENCES AND BIBLIOGRAPHY.

ABBRECHT, P.H., and PRODANY, N.W. (1971).
A model of the patient-artificial kidney system.
IEEE Trans. Vol. BME-18 4: 257 - 264.

ARNDT, J.O. (1965).
Diuresis induced by water infusion into the carotid loop and its inhibition by small haemorrage.
Pflugers Arch. f. gesam. Physiol. 282: 313 - 322.

BALDES, E.J., and SMIRK, F.H. (1934).
The effect of water drinking, mineral starvation and salt administration on the total osmotic pressure of the blood in man, chiefly in relation to the problems of water absorption and water diuresis.
J. Physiol. Lond. 82: 62 - 74.

BENEKEN, J.E.W., and DEWIT, B. (1967).
A physical approach to hemodynamic aspects of the human cardiovascular system. In: Physical Bases Of Circulatory Transport: Regulation And Exchange. Eds. E.B. Reeve and A.C. Guyton. (Philadelphia: W.B. Saunders & Co.).

BERGSTROM, J., and FURST, P. (1976).
Uremic middle molecules.
Clin. Nephrol. 5: 143 - 152.

BIGELOW, J.H., DEHAVEN, J.C., and SHIPLEY, M.L. (1973).
Systems analysis of the renal function.
J. Theor. Biol. 41: 287 - 322.

BIRON, P., MEYER, P., and PANISSET, J.C. (1968).
Removal of angiotensins from systemic circulation.
Can. J. Physiol. Pharmacol. 46: 175 - 178.

BLAINE, E.H., DAVIS, J.O., and PREWITT, R.L. (1971).
Evidence for a renal vascular receptor in control of renin secretion.
Am. J. Physiol. 226: 1593 - 1597.

BLAINE, E.H., DAVIS, J.O., and HARRIS, P.D. (1972).
A steady state control analysis of the renin-angiotensin-aldosterone system.
Circ. Res. 30: 713 - 730.

BLAIR-WEST, J.R., COGHLAN, J.P., DENTON, D.A., GODING, J.R., MUNRO, J.A., PETERSON, R.E., and WINTOUR, M. (1962).
Humoral stimulation of adrenal cortical secretion.
J. Clin. Invest. 41: 1606 - 1627.

BLESSER, W.B. (1969).
A Systems Approach To Bioengineering. (New York: McGraw - Hill Book Company).

BURTON, A.C., and TAYLOR, R.M. (1940).
A study of the adjustment of peripheral vascular tone to the requirements of the regulation of body temperature.
Am. J. Physiol. 129: 563 - 577.

CAGE, P.E., CARSON, E.R., and BRITTON, K.E. (1977).
A model of the human renal medulla.
Comp. & Biomed. Res. 10: 561 - 584.

CAMERON, W.H. (1977).
A model framework for computer simulation of overall renal function.
J. Theor. Biol. 66: 551 - 572.

CAREY, R.M. (1978).
Evidence for a splanchnic sodium input monitor regulating renal sodium excretion in man: Lack of dependence upon aldosterone.
Circ. Res. 43: 19 - 23.

COOKE, C.R., BROWN, T.C., ZACHERLE, B.J., and WALKER, W.G. (1970).
Effect of altered sodium concentration in the distal nephron segments on renin release.
J. Clin. Invest. 49: 1630 - 1638.

COONEY, D.O. (1976).
Biomedical Engineering And Instrumentation. Vol.2: Biomedical Engineering Principles. (New York: Dekker).

CZACZKES, J.W., KLEEMAN, C.R., and KOENIG, M. (1964).
Physiologic studies of antidiuretic hormone by its direct measurement in human plasma.
J. Clin. Invest. 43: 1625.

DEAN, R.F.A., and McCANCE, R.A. (1949).
The renal responses of infants and adults to the administration of hypertonic solutions of sodium chloride and urea.
J. Physiol. 109: 89 - 97.

DEHAVEN, J.C., and SHAPIRO, N.Z. (1970).
Simulation of the renal effects of antidiuretic hormone in man.
J. Theor. Biol. 28: 261 - 286.

DEHENEFFE, J., CUESTA, V., BRIGGS, J.D., BROWN, J.J., FRASER, R., LEVER, A.F., MORTON, J.J., ROBERTSON, J.I.S., and TREE, M. (1976).
Response of aldosterone and blood pressure to angiotensin II infusion in anephric man.
Circ. Res. 39: 183 - 190.

DE WARDENER, H.E. (1973).
The control of sodium excretion. In: Handbook Of Physiology. Sec.8, Renal Physiology, 677 - 720. Eds. J. Orloff and R.W. Berliner. (Washington D.C.: American Physiological Society).

FABIAN, M., FORSLING, M.L., JONES, J.J., and PRYOR, J.S. (1969).
The clearance and antidiuretic potency of neurohypophysical hormones in man, and their plasma binding and stability.
J. Physiol. 204: 653 - 668.

FORSLING, M.L. (1979).
Personal communication.

FOX, R.H. (1974).
Temperature regulation with special reference to man. In: Recent Advances In Physiology: 9. Ed. R.J. Linden. (Edinburgh: Churchill Livingstone).

FRIEDMAN, S.M., JAMIESON, J.D., and FRIEDMAN, C.L. (1959).
Sodium gradient, smooth muscle tone, and blood pressure regulation.
Circ. Res. 7: 44 - 53.

FROST, T.H., and KERR, D.N.S. (1977).
Kinetics of hemodialysis: A theoretical study of the removal of solutes in chronic renal failure compared to normal health.
Kidney International 12: 41 - 50.

GAUER, O.H., HENRY, J.P., and BEHN, C. (1970).
The regulation of extracellular fluid volume.
Ann. Rev. Physiol. 32: 547 - 595.

GOCKE, D.J., GERTER, J., SHERWOOD, L.M., and LARAGH, J.H. (1969).
Physiological and pathological variations of plasma angiotensin II in man. Correlation with renin activity and sodium balance.
Circ. Res. 24 (Suppl.1): 131 - 146.

GOORMAGHTIGH, N. (1945).
Facts in favour of an endocrine function of renal arterioles.
J. Pathol. Bacteriol. 57: 392 - 393.

GORDON, R.D., KUCHEL, O., LIDDLE, G.W., and ISLAND, D.P. (1967).
Role of the sympathetic nervous system in regulating renin and aldosterone production in man.
J. Clin. Invest. 46: 599 - 605.

GORMLEY, W., and BELL, R. (1970).
The dynamics of urea transfer and cerebral pressure during rapidly changing urea levels in the blood.
Chem. Eng. Prog. Symp. Ser. 66(99): 1.

GOTCH, F.A., SARGENT, J.A., KEEN, M.L., and LEE, M. (1974).
Individualized quantified dialysis therapy of uremia.
Proc. Clin. Dialysis Transplant Forum 4: 27.

GOTTSCHALK, C.W. (1971).
Function of the chronically diseased kidney: The adaptive nephron.
Circ. Res. 28 (Suppl. 2): 1 - 13.

GRANTHAM, J.J., GANOTE, C.F., BURG, M.B., and ORLOFF, J. (1969).
Paths of transtubular water flow in isolated renal collecting tubules.
J. Cell. Biol. 41: 562 - 576.

GRAVENEY, T. (1979).
Personal communication.

GUYTON, A.C., and COLEMAN, T.G. (1967).
Long term regulation of the circulation: interrelationships with body fluid volumes. In: Physical Bases Of Circulatory Transport: Regulation And Exchange. Eds. E.B. Reeve and A.C. Guyton. (Philadelphia: W.B. Saunders & Co.).

GUYTON, A.C. (1971).
Textbook Of Medical Physiology. (Philadelphia: W.B. Saunders & Co.).

GUYTON, A.C., COLEMAN, T.G., and GRANGER, P. (1972).
Circulation: Overall regulation.
Ann. Rev. Physiol. 34: 13 - 46.

HAAS, E., and GOLDBLATT, H. (1967).
Kinetic constants of the human renin and human angiotensin reaction.
Circ. Res. 20: 45 - 55.

HAMMEL, H.T., JACKSON, D.C., STOLWIJK, J.A.J., HARDY, J.D., and STROMME, S.B. (1963).
Temperature regulation by hypothalamic proportional control with adjustable set point.
J. Applied Physiol. 18: 1146 - 1154.

HANDLER, J.S., and ORLOFF, J. (1973).
The mechanism of action of antidiuretic hormone. In: Handbook Of Physiology. Sec. 8, Renal Physiology, 791 - 814. Eds. J. Orloff and R.W. Berliner. (Washington D.C.: American Physiological Society).

HARDY, J.D., and STOLWIJK, J.A.J., (1966).
Partitional calorimetric studies of man during exposures to thermal transients.
J. Applied Physiol. 21: 1799 - 1806.

HARDY, J.D., GAGGE, A.P., STOLWIJK, J.A.J. (Eds.) (1970).
Heat transfer in the environment. In: Physiological And Behavioral Temperature Regulation. Part II: 25 - 202.

HAYMAN, J.M. Jr., SHUMWAY, N.P., DUMKE, P., and MILLER, M. (1939).
Experimental hyposthenuria.
J. Clin. Invest. 18: 195.

HEACOX, R., HARVEY, A.M., and VANDER, A.J. (1967).
Hepatic inactivation of renin.
Circ. Res. 21: 149 - 152.

HOFF, H.E., SMITH, P.K., and WINKLER, A.W. (1939).
The relation of blood pressure and concentration in serum of potassium, calcium and magnesium.
Am. J. Physiol. 127: 722 - 730.

IMAI, M., SELDIN, D.W., and KOKKO, J.P. (1977).
Effect of perfusion rate on the fluxes of water, sodium, chloride and urea across the proximal convoluted tubule.
Kidney International.. 11: 18 - 27.

JOHANSSON, B. (1978).
Processes involved in vascular smooth muscle contraction and relaxation.
Circ. Res. 43 (Suppl.1): 14 - 20.

JOHNSON, J.A., MOORE, W.W., and SEGAR, W.E. (1969).
Small changes in left atrial pressure and plasma antidiuretic hormone titers in dogs.
Am. J. Physiol. 217: 210 - 214.

JOHNSON, J.A., ZEHR, J.E., and MOORE, W.W. (1970).
Effects of seperate and concurrent osmotic and volume stimuli on plasma ADH in sheep.
Am. J. Physiol. 218: 1273 - 1280.

JOHNSTON, C.I., DAVIS, J.O., HOWARDS, S.S., and WRIGHT, F.S. (1967).
Cross circulation experiments on the mechanism of the natriuresis during saline loading in the dog.
Circ. Res. 20: 1 - 10.

KITNEY, R.I. (1974).
The analysis and simulation of the human thermoregulatory control system.
Med. & Biol. Eng. 12: 57 - 65

LANDWEHR, D.M., SCHNERMANN, J., KLOSE, R.M., and GIEBISCH, G. (1968).
Effect of reduction in filtration rate on renal tubular sodium and water reabsorption.
Am. J. Physiol. 215: 687 - 695.

LARAGH, J.H., and SEALEY, J.E. (1973).
The renin-angiotensin-aldosterone hormonal system and regulation of sodium, potassium, and blood pressure homeostatis. In: Handbook Of Physiology. Sec. 8, Renal Physiology, 831 - 908. Eds. J. Orloff and R.W. Berliner. (Washington D.C.: American Physiological Society).

LAUSON, H.D. (1960).
Vasopressin and oxytocin in the plasma of man and other mammals.
In: Hormones In Human Plasma. Ed. H.N. Antoniade. (Boston: Little, Brown & Co.).

LEDINGHAM, J.G.G., BULL, M.B., and LARAGH, J.H. (1967).
The meaning of aldosteronism in hypertensive disease.
Circ. Res. 21: 177 - 186.

LEE, M.R. (1969).
Renin And Hypertension: A Modern Synthesis.
(London: Lloyd - Luke Ltd.).

LOTT, R.S., MOORHOUSE, K.E.S., and WHITT, C.N. (1977).
The application of mathematical models on an interactive computer graphics display for renal patient management.
In: Technical Aspects Of Renal Dialysis. Ed. T.H. Frost.
(Pitman).

LOWITZ, H.D., STUMPE, K.D., and OCHWADT, B. (1969).
Micropuncture study of the action of angiotensin II on tubular sodium and water reabsorption in the rat.
Nephron 6: 173 - 187.

MALNIC, G., KLOSE, R.M., and GIEBISCH, G. (1964).
Micropuncture study of renal potassium excretion in the rat.
Am. J. Physiol. 206: 674 - 686.

MALNIC, G., KLOSE, R.M., and GIEBISCH, G. (1966).
Micropuncture study of distal tubular potassium and sodium transport in the rat nephron.
Am. J. Physiol. 211: 529 - 547.

MAUDE, D.L. (1977).
Kidney Physiology And Kidney Disease. (Philadelphia: J.B. Lippincott Company).

MEYER, P., MENARD, J., PAPANICOLAOU, N., ALEXANDRE, J.M., DEVAUX, C., and MILLIEZ, P. (1968).
Mechanism of renin release following furosemide diuresis in rabbit.
Am. J. Physiol. 215: 908 - 915.

MINORSKY, N. (1962).
Nonlinear Oscillations. (London: Van Nostrand).

MOSES, A.M., and MILLER, M. (1974).
Osmotic influences on the release of vasopressin. In: Handbook Of Physiology. Sec. 7, Endocrinology, 225 - 242. Eds. R.O. Greep and E.B. Astwood. (Washington D.C.: American Physiological Society).

MULLER, J. (1971).
Regulation Of Aldosterone Biosynthesis. (New York: Springer - Verlag).

NG, K.K.F., and VANE, J.R. (1968).
Fate of angiotensin I in the circulation.
Nature 218: 144 - 150.

NASH, F.D., ROSTORFER, H.H., BAILIE, M.D., WATHEN, R.L., and SCHNEIDER, E.G. (1968).
Renin release: relation to renal sodium load and dissociation from hemodynamic changes.
Circ. Res. 22: 473 - 487.

OELKERS, W., BROWN, J.J., FRASER, R., LEVER, A.F., MORTON, J.J., and ROBERTSON, J.I.S. (1974).
Sensitization of the adrenal cortex to angiotensin II in sodium-depleted man.
Circ. Res. 34: 69 - 77.

PULLEN, H.E. (1976).
"Studies in the modelling and simulation of the human cardiovascular system with application to the effects of drugs."
Ph.D. Thesis, The City University, London.

RAMIREZ, W.F., MICKLEY, M.C., and LEWIS, D.W. (1972).
Mathematical modelling of a Kill hemodialyzer.
Med. & Biol. Eng. 10: 267.

RAMIREZ, W.F., LEWIS, D.W., and MICKLEY, M.C. (1973).
Optimal control of the artificial-kidney-patient system.
Med. & Biol. Eng. 11: 743 - 746.

REEVE, E.B., and KULHANEK, C. (1967).
Regulation of body water content: A preliminary analysis.
In: Physical Bases Of Circulatory Transport. Eds. E.B. Reeve and A.C. Guyton. (Philadelphia: W.B. Saunders & Co.).
REID

REID, I.A., MORRIS, B.J., and GANONG, W.F. (1978).
The renin angiotensin system.
Ann. Rev. Physiol. 40: 377 - 410.

RELMAN, A.S., and SCHWARTZ, W.B. (1952).
The effect of DOCA on electrolyte balance in normal man and its relation to sodium chloride intake.
Yale J. Biol. Med. 24: 540 - 558.

RENKIN, E.M. (1956).
The relation between dialysance, membrane area, permeability and blood flow in the artificial kidney.
Trans. Am. Soc. Artif. Intern. Organs. 2: 102 - 105.

RICHARDSON, T.Q., STALLINGS, J.O., and GUYTON, A.C. (1961).
Pressure-volume curves in live intact dogs.
Am. J. Physiol. 201: 471.

ROBERTS, P.D. (1977).
Parameter estimation in non-linear dynamic mathematical models - user manual for subroutines IDENT and PERAS.
Research Memorandum: DSS/PDR/127. The City University, London.

ROBINSON, S., MEYER, F.R., NEWTON, J.L., TS'AO, C.H., and HOLGERSEN, L.O. (1965).
Relation between sweating, cutaneous blood flow and body temperature in work.
J. Applied Physiol. 20: 575.

ROEMMELT, J.C., SARTORIUS, O.W., and PITTS, R.F. (1949).
Excretion and reabsorption of sodium and water in the adrenalectomized dogs.
Am. J. Physiol. 159: 124 - 136.

RUCH, T.C., and PATTON, H.D. (1965).
Physiology And Biophysics. (Philadelphia: W.B. Saunders & Co.).

SEALEY, J.E., GERTEN-BANES, J., and LARAGH, J.H. (1972).
The renin system: Variations in man measured by radioimmunouassay or bioassay.
Kidney International 1: 240 - 253.

SEIF, F.J. (1974).
Systemanalyse der Aldosteronesekretion. (Stuttgart: Georg Thieme Verlag).

SHADE, R.E., DAVIS, J.O., JOHNSON, J.A., GOTSHALL, R.W., and SPIELMAN, W.S. (1973).
Mechanisms of action of angiotensin II and antidiuretic hormone on renin secretion.
Am. J. Physiol. 224: 926 - 929.

SHARE, L. (1974).
Blood pressure, blood volume, and the release of vasopressin.
In: Handbook Of Physiology. Sec. 7, Endocrinology, 243 - 256. Eds. R.O. Greep and E.B. Astwood. (Washington D.C.: American Physiological Society).

SHIPLEY, R.E., and STUDY, R.S. (1951).
Changes in renal blood flow, extraction of insulin, glomerular filtration rate, tissue pressure and urine flow with acute alterations of renal artery blood pressure.
Am. J. Physiol. 167: 676 - 688.

SKEGGS, L.T., LENTZ, K.E., HOCHSTRASSER, H., and KAHN, J.R. (1964).
The chemistry of renin substrate.
Can. Med. Assoc. J. 90: 185 - 189.

STOLWIJK, J.A.J., and HARDY, J.D. (1966).
Temperature regulation in man - A theoretic study.
Pflugers Archiv. 291: 129 - 162.

TAQUINI, A.C., BLAQUIER, P., and TAQUINI, A.C., Jr. (1964).
On the production and role of renin.
Can. Med. Assoc. J. 90: 210 - 213.

THOMPSON, F.D. (1976).
Personal communication.

THOMPSON, F.D. (1977).
Personal communication.

THOMPSON, F.D. (1978).
Personal communication.

THURAU, K., and KRAMMER, K. (1959).
Weitere untersuchungen zur myogen Natur der Autoregulation des Nierenkrieslaufes.
Arch. Ges. Physiol. 269: 77 - 93.

THURAU, K., SCHNERMANN, J., NAGEL, W., HORSTER, M., and WOHL, M. (1967).
Composition of tubular fluid in the macula densa segment as a factor regulating the function of the juxtaglomerular apparatus.
Circ. Res. 21 (Suppl.2): 79 - 89.

THURAU, K. (1971).
Micropuncture evaluation of local control of arteriolar resistance of kidney and brain.
Circ. Res. 28 (Suppl.1): 106 - 114.

THURAU, K., DAHLHEIM, H., GRUNER, A., MASON, J., and GRANGER, P. (1972).
Activation of renin in the single juxtaglomerular apparatus by sodium chloride in the tubular fluid at the macula densa.
Circ. Res. 31 (Suppl.2): 182 - 186.

TOATES, F.M., and OATLEY, K. (1977).
Control of water excretion by antidiuretic hormone: Some aspects of modelling the system.
Med. & Biol. Eng. & Comput. 15: 579 - 588.

TOBIAN, L., TOMBOULLAN, A., and JANECEK, J. (1959).
Effect of high perfusion pressures on the granulations of juxtaglomerular cells in an isolated kidney.
J. Clin. Invest. 38: 605 - 610.

TOBIAN, L., COFFEE, K., and McCREA, P. (1967).
Evidence for a humoral factor of non-renal and non-adrenal origin which influences renal sodium excretion.
Trans. Assoc. Am. Physicians. 80: 200 - 206.

TOSTESON, D.C. (1955).
Electrolytes In Biological Systems. (Washington D.C.: American Physiological Society).

VALTIN, H. (1973).
Renal Function: Mechanisms Preserving Fluid And Solute Balance In Health. (Boston: Little, Brown & Co.).

VANDER, A.J., and MILLER, R. (1964).
Control of renin secretion in the anesthetized dog.
Am. J. Physiol. 207: 537 - 546.

VANDER, A.J. (1967).
Control of renin release.
Physiol. Rev. 473: 59 - 82.

VANDER, A.J., and LUCIANO, J.R. (1967).
Effects of mercurial diuresis and acute sodium depletion on renin release in dog.
Am. J. Physiol. 212: 651 - 656.

VANDER, A.J., and CARLSON, J. (1969).

VANDER, A.J., and CARLSON, J. (1969).
Mechanism of the effects of furosemide on renin secretion in anesthetized dogs.
Circ. Res. 25: 145 - 152.

VANDER, A.J. (1970).
Direct effects of potassium on renin secretion and renal function.
Am. J. Physiol. 219: 455 - 459.

VERNEY, E.B. (1947).
The antidiuretic hormone and the factors which determine its release.
Proc. Roy. Soc., London, Ser. B. 135: 25 - 106.

WALKER, W.E., HALL, D.A., SANFELIPPO, M.L., and SWENSON, R.S. (1975).
Application of a programmable pocket calculator to a single compartment mathematical model of solute kinetics.
Comput. Programmes in Biomed. 75: 99 - 104.

WINDHAGER, E.E. (1968).
Micropuncture Techniques And Nephron Function. (New York: Appleton-Century- Crofts).

WISSLER, E.H. (1963).
In: Temperature - Its Measurement And Control In Science And Industry, 603 - 612. Ed. J.D. Hardy, Vol.3, pt.3. (New York: Reinhold).

WYNDHAM, C.H., and ATKINS, A.R. (1960).
An approach to the solution of the human biothermal problem with the aid of an analog computer.
Proc. 3rd Internat. Conf. Med. Electronic. (London).

APPENDIX I

VARIABLES OF THE MODEL.

Symbol	Definition	Nominal Value
A	Concentration of angiotensin II in plasma (ng./l.)	27.0
ADH	Concentration of ADH in plasma (munits/l.)	4.0
ADHS	Nett release rate of ADH (munits/min.)	0.825
ADHSP	Release rate of ADH due to plasma osmolality (munits/min.)	0.84
ADHSV	Release rate of ADH due to diminished fluid volume (munits/min.)	0.81
ALD	Concentration of aldosterone in plasma (ng./l.)	85.0
ALS	Nett rate of secretion of aldosterone (ng./min.)	52.7
ALSA	Release rate of aldosterone due to a angiotensin II (ng./min.)	52.7
ALSK	Release rate of aldosterone due to plasma potassium concentration (ng./min.)	52.7
AP	Arterial pressure (mm. Hg)	100.0
Ar	Surface area of dialysis membrane ($m.^2$)	1.5
AS	Rate of formation of angiotensin II (ng./min.)	105.0
AVOS	Equilibrium osmolality of body fluids (mosm./l.)	299.6
BMRC	Basal metabolic rate in core compartment (cals./min.)	1165.3
BMRS	Basal metabolic rate in surface compartment (cals./min.)	21.5
BV	Blood volume (l.)	5.0
C_c	Thermal capacitance of core of body ($cals./^oC.$)	55860.0 *
C_s	Thermal capacitance of surface of body ($cals./^oC.$)	3030.0 *
c	Specific heat of blood ($cals./^oC./kg.$)	920.0
C_{Bi}	Concentration of solute in blood entering dialysis machine (mEq./l.) or (g./l.)	-

* Value for a normal 71 kg. man.

** Patient dependant value.

Symbol	Definition	Nominal Value
C_{Di}	Concentration of solute in dialysate (mEq./l.) or (g./l.)	-
C_{Ei}	Extracellular concentration of waste substance (g./l.)	-
C_{Ii}	Intracellular concentration of waste substance (g./l.)	-
CE	Cardiac effectiveness	1.0
CEK	Cardiac effectiveness due to abnormal potassium level	1.0
CENA	Cardiac effectiveness due to abnormal sodium level	1.0
CO	Cardiac output (l./min.)	5.0
DADH	Clearance rate of ADH (l./min.)	0.206
DAP_o	Steady state bias on arterial pressure (mm. Hg)	P.D. **
DTPR	Pressor effect of angiotensin II on circulation (mm. Hg/l./min.)	0.0
DWV	Excess fluid in extracellular compartment (l.)	0.0
E	Extracellular fluid volume (l.)	15.0
E_N	Normal extracellular fluid volume (l.)	15.0
EBDT	Fraction of water load reabsorbed in the distal nephron segments	0.952
EBLH	Fraction of water load reabsorbed in the loop of Henle	0.33
ECRE	Extracellular concentration of creatinine (g./l.)	0.030
EDTR	Rate of reabsorption of water in the distal nephron segments (mls./min.)	19.7
EFDT	Rate of flow of water into the loop of Henle (mls./min.)	31.25
ELHR	Rate of reabsorption of water in the loop of Henle (mls./min.)	10.55
EPTR	Rate of reabsorption of water in proximal tubule (mls./min.)	93.75
EUR	Extracellular concentration of urea (g./l.)	0.15
FACT1	Fraction of remaining kidney function to excrete sodium and water	1.0
FACT2	Fraction of remaining kidney function to secrete renin	1.0
FACT3	Fraction of remaining kidney function to excrete potassium	1.0
FACT4	Fraction of remaining kidney function to excrete urea and creatinine	1.0
FLUMIN	Rate of ingestion of water (mls./min.)	P.D. **
FNA	Filtered load of sodium (mEq./min.)	17.75

Symbol	Definition	Nominal Value	
G_i	Generation rate of waste substance (g./min.)	-	
GFR	Glomerular filtration rate (mls./min.)	125.0	
GTB	Fraction of filtered load of sodium reabsorbed in proximal tubule	0.75	
I	Intracellular fluid volume (l.)	25.0	
IC	Osmolality of constituents apart from sodium and potassium in intracellular pool (mosm./l.)	161.2	
ICRE	Intracellular concentration of creatinine (g./l.)	0.030	
IHL	Insensible evaporative heat loss rate from surface of body (^{o}C./min.)	149.3	
IK	Intracellular concentration of potassium (mEq./l.)	141.0	
INA	Intracellular concentration of sodium (mEq./l.)	10.0	
IOS	Osmolality of intracellular fluid compartment (mosm./l.)	299.6	
IUR	Intracellular concentration of urea (g./l.)	0.15	
K_{cs}	Heat transfer coefficient due to conduction between core and surface of body (^{o}C.)	405.6	
K_{ri}	Renal clearance of waste substance (l./min.)	-	
K_{se}	Heat transfer coefficient due to convection and radiation between surface of body and environment (cals./min./^{o}C.)	100.0	
$k_{I,Ei}$	Cell permeability coefficient for waste substance (l./min.)	-	
MSP	Mean systemic pressure (mm. Hg)	7.0	
PC	Osmolality of constituents apart from sodium and potassium in the extracellular pool (mosm./l.)	156.2	
PCP	Controllable pressure difference across dialysis machine membrane (mm. Hg)	-	
PK	Extracellular concentration of potassium (mEq./l.)	5.0	
PNA	Extracellular concentration of sodium (mEq./l.)	142.0	
POS	Osmolality of plasma (mosm./l.)	299.6	
POTDIA	Concentration of potassium in dialysate (mEq./l.)	P.D.	**
POTMIN	Rate of ingestion of potassium (mEq./min.)	P.D.	**
PV	Plasma volume (l.)	3.0	

Symbol	Definition	Nominal Value
Q_B	Blood flow rate through dialysis machine (l./min.)	P.D. **
R	Concentration of renin in plasma (GU./l.)	0.06
R_c	Resistance to blood flow through core of body (mm. Hg/l./min.)	20.93
R_s	Resistance to blood flow through surface of body (mm. Hg/l./min.)	448.4
RAP	Right atrial pressure (mm. Hg)	0.0
RHL	Respiratory heat loss rate (cals./min.)	150.0
RS	Rate of release of renin (GU./min.)	0.008
RVR	Resistance to venous return (mm. Hg/l./min.)	1.4
SBF	Rate of blood flow to surface of body (l./min.)	0.223
SDTR	Rate of reabsorption of sodium from the distal nephron segments (mEq./min.)	0.757
SFDT	Rate of flow of sodium into distal tubule (mEq./min.)	0.89
SFLH	Rate of flow of sodium into loop of Henle (mEq./min.)	4.44
SLHR	Rate of reabsorption of sodium from the loop of Henle (mEq./min.)	3.55
SODDIA	Concentration of sodium in dialysate (mEq./l.)	P.D. **
SODMIN	Rate of ingestion of sodium (mEq./min.)	P.D. **
SPTR	Rate of reabsorption of sodium in proximal tubule (mEq./min.)	13.3
T_c	Temperature of core of body (^{o}C.)	36.7
T_e	Ambient temperature (^{o}C.)	-
T_s	Temperature of surface of body (^{o}C.)	34.1
TEK	Total extracellular potassium (mEq.)	75.0
TENA	Total extracellular sodium (mEq.)	2130.0
TIK	Total intracellular potassium (mEq.)	3525.0
TINA	Total intracellular sodium (mEq.)	250.0
TPR	Total peripheral resistance (mm. Hg/l./min.)	20.0
TPR_{TH}	Value of TPR generated by thermoregulatory system model (mm. Hg/l./min.)	20.0
UFL	Urine flow rate (mls./min.)	1.0
UK	Nett rate of excretion of potassium (mEq./l.)	0.06
UKAL	Rate of excretion of potassium due to aldosterone (mEq./min.)	0.03
UKH	Rate of excretion of potassium due to homeostatis (mEq./min.)	0.03

Symbol	Definition	Nominal Value
ULTRF	Ultrafiltration rate of fluid across dialysis machine membrane (mls./min.)	P.D. **
UNA	Rate of excretion of sodium (mEq./min.)	0.128
VR	Venous return (l./min.)	5.0
W	Weight of patient (kgs.)	P.D. **
ρ	Density of blood (kgs./l.)	1.0

APPENDIX II

EQUATIONS OF THE MODEL.

A2.1. Thermoregulatory System Model.

$$C_c \times \frac{dT_c}{dt} = BMRC - K_{cs} \times (T_c - T_s) - \rho \times c \times SBF \times (T_c - T_s) - RHL \qquad (4.1)$$

$$C_s \times \frac{dT_s}{dt} = BMRS + K_{cs} \times (T_c - T_s) + \rho \times c \times SBF \times (T_c - T_s) - K_{se} \times (T_s - T_e) - IHL \qquad (4.2)$$

$$R_s = f(T_c, T_s)$$

$$SBF = AP \; / \; R_s \qquad (4.3)$$

$$TPR_{TH} = \frac{R_s \times 20.934}{R_s + 20.934} \qquad (4.4)$$

A2.2. Cardiovascular System Model.

$$\frac{dE}{dt} = FLUMIN - UFL$$

$$E = \int \frac{dE}{dt} \times dt$$

$$\left.\begin{array}{ll} BV = 0.33 \times E & \text{if } E < 21.0 \text{ l.} \\ BV = 0.015 \times E + 6.6 & \text{if } E \geqslant 21.0 \text{ l.} \end{array}\right\} \qquad (4.5)$$

$$MSP = 3.5 \times BV - 10.5 \qquad (4.6)$$

$$\left.\begin{array}{ll} DTPR = 0.037 \times A - 1.0 & \text{if } A \leqslant 27.0 \text{ ng./l.} \\ DTPR = 5.44 \times \log_{10}(A) - 7.8 & \text{if } A > 27.0 \text{ ng./l.} \end{array}\right\} \qquad (4.7)$$

$$TPR = TPR_{TH} + DTPR \tag{4.8}$$

$$\left.\begin{aligned} CENA &= 1.0 && \text{if } PNA < 148.0 \\ CENA &= -0.0125 \times PNA + 2.85 && \text{if } PNA \geq 148.0 \end{aligned}\right\} \tag{4.9}$$

$$\left.\begin{aligned} CEK &= 1.0 && \text{if } PK < 6.5 \\ CEK &= -0.065 \times PK + 1.43 && \text{if } PK \geq 6.5 \end{aligned}\right\} \tag{4.10}$$

$$CE = (CENA + CEK) \times 0.5 \tag{4.11}$$

$$CO = f(CE, MSP, TPR)$$

$$AP = CO \times TPR + DAP_o \tag{4.13}$$

A2.3. Kidney Function Model.

$$\left.\begin{aligned} GFR &= 0.0 && \text{if } AP \leq 20.0 \text{ mm. Hg} \\ GFR &= 1.92 \times AP - 38.4 && \text{if } 20.0 < AP \leq 75.0 \text{ mm. Hg} \\ GFR &= -0.00808 \times AP^2 + 2.195 \times AP - 13.6 && \text{if } 75.0 < AP \leq 120.0 \text{ mm. Hg} \\ GFR &= 0.035 \times AP + 129.2 && \text{if } AP > 120.0 \text{ mm. Hg} \end{aligned}\right\} \tag{4.14}$$

$$FNA = GFR \times PNA / 1000.0 \tag{4.15}$$

$$GTB = -0.0357 \times PNA + 5.815$$
$$\text{with the constraint} \quad 0.75 \leq GTB \leq 1.0 \tag{4.16}$$

$$SPTR = GTB \times FNA \tag{4.17}$$

$$SFLH = FNA - SPTR \tag{4.18}$$

$$EPTR = GTB \times GFR \tag{4.19}$$

$$EFLH = GFR - EPTR \tag{4.20}$$

$$\left.\begin{aligned} &\text{If } FACT1 > 0.0 \\ &\quad EBLH = (0.01 \times EFLH/FACT1) + 0.65 \\ &\quad ELHR = EBLH \times EFLH \end{aligned}\right\} \tag{4.21a}$$

$$SLHR = 0.8 \times SFLH \tag{4.22}$$

$$EFDT = EFLH - ELHR \tag{4.23}$$

$$SFDT = SFLH - SLHR \tag{4.24}$$

$$\left.\begin{aligned}
&EBDT = 0.0 && \text{if } ADH \leqslant 0.765 \text{ munits/l.}\\
&EBDT = 0.0383 \times ADH - 0.293 && \text{if } 0.765 < ADH \leqslant 3.0\\
&EBDT = -0.0383 \times ADH^2 + 0.364 \times ADH + 0.109 && \\
& && \text{if } 3.0 < ADH \leqslant 5.0\\
&EBDT = 0.0012 \times ADH + 0.9653 && \text{if } ADH > 5.0 \text{ munits/l.}\\
&EDTR = EBDT \times EFDT &&
\end{aligned}\right\} \tag{4.25}$$

$$UFL = EFDT - EDTR \tag{4.26}$$

$$\left.\begin{aligned}
&SDTR = 0.6 \times SFDT && \text{if } ALD \leqslant 0.0 \text{ ng./l.}\\
&SDTR = (0.003 \times ALD + 0.596) \times SFDT && \\
& && \text{if } 0.0 < ALD \leqslant 85.0\\
&SDTR = (0.00021 \times ALD + 0.833) \times SFDT && \\
& && \text{if } 85.0 < ALD \leqslant 800.0\\
&SDTR = SFDT && \text{if } ALD > 800.0 \text{ ng./l.}
\end{aligned}\right\} \tag{4.27}$$

$$UNA = SFDT - SDTR \tag{4.28}$$

$$UKH = 0.107 \times PK - 0.505 \tag{4.29}$$

$$\left.\begin{aligned}
&UKAL = 0.00028 \times ALD + 0.0062 && \text{if } ALD \leqslant 85.0 \text{ ng./l.}\\
&UKAL = 0.00009 \times ALD + 0.0224 && \text{if } ALD > 85.0 \text{ ng./l.}
\end{aligned}\right\} \tag{4.30}$$

$$UK = (UKH + UKAL) \times FACT3 \tag{4.31a}$$

A2.4. Hormonal System Models.

$$POS = 2.11 \times PNA \tag{4.32}$$

$$\left.\begin{aligned}
&ADHSP = 0.348 \times POS - 103.4 && \text{if } POS \geqslant 299.5 \text{ mosm./l.}\\
&ADHSP = 0.0285 \times POS - 8.04 && \text{if } POS < 299.5 \text{ mosm./l.}
\end{aligned}\right\} \tag{4.33}$$

$$DWV = E - E_N \tag{4.34}$$

$$\left.\begin{aligned} ADHSV &= 0.0 && \text{if } DWV \geq 1.8\ 1. \\ ADHSV &= 0.15 - 0.083 \times DWV && \text{if } 1.8 > DWV \geq 1.0 \\ ADHSV &= 0.813 - 0.75 \times DWV && \text{if } 1.0 > DWV \geq -1.2 \\ ADHSV &= 1.71 && \text{if } -1.2 > DWV \end{aligned}\right\} \tag{4.35}$$

$$\left.\begin{aligned} ADHS &= ((17.0 \times DWV \times ADHSV) + ADHSP)/((17.0/DWV) + 1.0) \\ &\quad \text{if } POS > 299.6 \text{ mosm./l. and } DWV > 2.0\ 1. \\ ADHS &= (((33.0 \times DWV - 32.0) \times ADHSV) + ADHSP) \\ &\qquad / ((33.0 \times DWV - 32.0) + 1.0) \\ &\quad \text{if } POS > 299.6 \text{ and } 1.0 \leq DWV \leq 2.0 \\ ADHS &= (ADHSV + ADHSP)/2.0 \quad \text{for all other conditions.} \end{aligned}\right\} \tag{4.36}$$

$$\left.\begin{aligned} DADH &= 0.206 && \text{if } ADH > 4.0 \text{ munits/l.} \\ DADH &= 0.374 - 0.042 \times ADH && \text{if } ADH \leq 4.0 \text{ munits/l.} \end{aligned}\right\} \tag{4.37}$$

$$PV = 0.6 \times BV \tag{4.38}$$

$$\frac{d(ADH)}{dt} = (ADHS - ADH \times DADH) / PV \tag{4.39}$$

$$RS = (0.0163 - 0.0093 \times SFDT/FACT1) \times FACT2 \tag{4.40a}$$

$$\frac{dR}{dt} = (RS - 0.135 \times R) / PV \tag{4.42}$$

$$A = \frac{1785.0 \times R \times PV}{3.06} \tag{4.44}$$

$$\frac{dA}{dt} = (AS - 4.04 \times A) / PV \tag{4.45}$$

$$\left.\begin{aligned} ALSA &= A && \text{if } A < 18.0 \text{ ng./l.} \\ ALSA &= 4.43 \times A - 61.7 && \text{if } 18.0 \leq A < 34.0 \\ ALSA &= 0.78 \times A + 62.5 && \text{if } A \geq 34.0 \text{ ng./l.} \end{aligned}\right\} \tag{4.46}$$

$$ALSK = 21.64 \times PK - 55.5 \tag{4.47}$$

$$ALS = (ALSAx3.0 + ALSK) / 4.0 \tag{4.48}$$

$$\frac{d(ALD)}{dt} = (ALS - 0.62xALD) / PV \tag{4.49}$$

A2.5. Artificial Kidney Machine Model.

$$\left.\begin{aligned} ULTRF &= 0.0139xPCP + 0.7 \quad \text{if } PCP < 100.0 \text{ mm. Hg} \\ ULTRF &= 0.042xPCP - 2.1 \quad \text{if } PCP \geqslant 100.0 \text{ mm. Hg} \end{aligned}\right\} \tag{4.50}$$

$$\frac{d(C_{Bi} \times E)}{dt} = Q_B \times (C_{Bi} - C_{Di}) \times \left(\exp\left(-\frac{K.Ar}{Q_B}\right) - 1\right) \tag{4.54}$$

A2.6. Balance Equations.

$$\frac{d(TENA)}{dt} = SODMIN - UNA \quad \text{(dialysis machine off)} \tag{4.55}$$

$$\frac{d(TEK)}{dt} = POTMIN - UK \quad \text{(dialysis machine off)} \tag{4.56}$$

$$\frac{d(TENA)}{dt} = Q_b x(PNA-SODDIA) \times \left(\exp\left(-\frac{K_{sodium}{}^{xAr}}{Q_B}\right) - 1\right) + SODMIN - UNA \quad \text{(dialysis machine on)} \tag{4.57}$$

$$\frac{d(TEK)}{dt} = Q_B x(PK-POTDIA) x \left(\exp\left(-\frac{K_{potassium}{}^{xAr}}{Q_B}\right) - 1\right) + POTMIN - UK \quad \text{(dialysis machine on)} \tag{4.58}$$

$$PNA = TENA / E \tag{4.59}$$

$$PK = TEK / E \tag{4.60}$$

$$\frac{d(TINA)}{dt} = 0 \tag{4.61}$$

$$\frac{d(TIK)}{dt} = 0 \tag{4.62}$$

$$INA = TINA / I \tag{4.63}$$

$$IK = TIK / I \tag{4.64}$$

$$\frac{dE}{dt} = FLUMIN - UFL \qquad \text{(dialysis machine off)} \tag{4.65}$$

$$\frac{dE}{dt} = FLUMIN - UFL - ULTRF \qquad \text{(dialysis machine on)} \tag{4.66}$$

$$POS = PNA + PK + PC \tag{4.67}$$

$$IOS = INA + IK + IC \tag{4.68}$$

$$AVOS = \frac{POS \times E + IOS \times I}{E + I} \tag{4.69}$$

$$E = \frac{POS \times E}{AVOS} \tag{4.70}$$

$$I = \frac{IOS \times I}{AVOS} \tag{4.71}$$

$$PNA = \frac{PNA \times AVOS}{POS} \tag{4.72}$$

$$PK = \frac{PK \times AVOS}{POS} \tag{4.73}$$

$$INA = \frac{INA \times AVOS}{IOS} \tag{4.74}$$

$$IK = \frac{IK \times AVOS}{IOS} \tag{4.75}$$

$$\frac{d(C_I \times I)}{dt} = G - k_{I,E} \times (C_I - C_E) \tag{4.76}$$

$$\frac{d(C_E \times E)}{dt} = k_{I,E} \times (C_I - C_E) - K_r \times C_E \times FACT4 \qquad \text{(dialysis machine off)} \tag{4.77a}$$

$$\frac{d(C_E \times E)}{dt} = k_{I,E} x (C_I - C_E) - K_r x C_E x FACT4$$

$$Q_B x (C_E - C_{Di}) \times \left(\exp\left(- \frac{KxAr}{Q_B} \right) - 1 \right) \qquad (4.79a)$$

(dialysis machine on)

APPENDIX III

THE COMPUTER PROGRAMME.

Some of the symbols for the variables of the model in the computer programme are different from those given in Appendix I. These different symbols are listed in Table A3.

TABLE A3. Symbols For Variables Of The Model In The Computer Programme.

Variable in Appendix I	Variable in the computer programme
A	X(10)
ADH	X(12)
ALD	X(11)
DAP_o	APCONS
E	X(3)
ECRE	PCRE
EUR	PUR
I	X(6)
PCP	PCPR
Q_B	QB
R	X(9)
R_c	STPR
T_c	X(1)
T_s	X(2)
TEK	X(5)
TENA	X(4)
TIK	X(8)
TINA	X(7)

```
C
C         THIS PROGRAM REPRESENTS A MODEL OF THE PATIENT-
C       ARTIFICIAL KIDNEY MACHINE SYSTEM INCORPORATING
C       THE FOLLOWING SUBSYSTEMS:-
C       THERMOREGULATORY SYSTEM MODEL, CARDIOVASCULAR
C       SYSTEM MODEL,SODIUM AND POTASSIUM BALANCE,
C       A D H SYSTEM MODEL, ARTIFICIAL KIDNEY MACHINE,
C       RENIN -ANGIOTENSION -ALDOSTERONE SYSTEM MODEL
C       AND UREA AND CREATININE DYNAMICS
C       INCLUDING INTERACTION WITH CLINICIAN FOR INPUT OF DATA
C
        REAL INA,IK,IUR,ICRE,INASTO,IKSTO,IURSTO,ICREST
        DIMENSION XSTORE(50)
        COMMON /DE/ X(50),DX(50),N,T,DT,DTMIN,SBF,RS,KA,FACT1,FACT2
       1     ,FACT3,FACT4,ALS,UK,UNA,UFL,AS,TT,FLUMIN,SODMIN,POTMIN
       2      ,CO,AP,TPR,BV,GFR,FNA,SDTR,ULTRF,SODDIA,POTDIA,ADHS
       3      ,PNA,PK,INA,IK,PUR,PCRE,IUR,ICRE,RB
       4      ,IHF,W,PV
        COMMON /AI/ A1,CONS,APSTOR
        DATA K,EREL,ERAB/0,0.005,0.001/
        DTMIN = 0.001*DT
C
C        WRITE INTRODUCTION
C
        WRITE (4,10)
   10   FORMAT(1H0,40H THIS PROGRAM RUNS A MATHEMATICAL MODEL ,
       1     47HOF THE PATIENT-ARTIFICIAL KIDNEY MACHINE SYSTEM/
       2     46HTO GIVE PREDICTIONS FOR THE OUTCOMES OF DIALYSIS,
       3     46HTHERAPIES. THE USER WILL BE PROMPTED TO INPUT /
       4     33HDATA NEEDED FOR THE MODEL TO RUN.)
C
C        READ STATE OF PATIENT
C
  309   CALL READPA
C
C        READ INGESTION RATES
C
        CALL READIN
C
C        READ INITIAL CONDITIONS
C
        CALL READIC
C        CONVERT INITIAL CONDITIONS TO STATE VARIABLES
        X(4) = PNA * X(3)
        X(5) = PK * X(3)
        X(7) = INA * X(6)
        X(8) = IK * X(6)
        X(13) = IUR * X(6)
        X(14) = ICRE * X(6)
        X(15) = PUR * X(3)
        X(16) = PCRE * X(3)
```

```
C
C       STORE INITIAL CONDITIONS FOR POSSIBLE REUSE
C
      DO 20 I = 1,3
   20 XSTORE(I) = X(I)
      PNASTO = PNA
      PKSTO = PK
      XSTORE(6) = X(6)
      INASTO = INA
      IKSTO = IK
      XSTORE(9) = X(9)
      XSTORE(10) = X(10)
      XSTORE(11) = X(11)
      XSTORE(12) = X(12)
      PURSTO = PUR
      PCREST = PCRE
      IURSTO = IUR
      ICREST = ICRE
      AFSTOR = AF
C
C       READ PROPOSED THERAPY
C
   30 CALL READTH
      KA = 1
      DO 40 I=1,3
      X(I) = XSTORE(I)
   40 CONTINUE
      AF = AFSTOR
      PNA = PNASTO
      PK = PKSTO
      X(6) = XSTORE(6)
      INA = INASTO
      IK = IKSTO
      X(9) = XSTORE(9)
      X(10) = XSTORE(10)
      X(11) = XSTORE(11)
      X(12) = XSTORE(12)
      PUR = PURSTO
      PCRE = PCREST
      IUR = IURSTO
      ICRE = ICREST
C
C       START OF LOOP
C
   50 K = K + 1
C
C       APPLY CONTROLLER EQUATIONS
C
      CALL CONTRL
      HOUR = T/60.0
      IF (T.EQ.0.0) WRITE (4,70) HOUR,(X(I),I=1,3),CO,AF,
     1  X(6),PNA,PK,TPR,BV,INA,X(11),GFR,X(12),PUR,PCRE,UFL,UNA,X(10)
```

```
C
C        INTEGRATE
C
      ND = 0
      CALL INTEGR(EREL,ERAB,ND)
      PNA = X(4)/X(3)
      PK = X(5)/X(3)
      PUR = X(15)/X(3)
      PCRE = X(16)/X(3)
      INA = X(7)/X(6)
      IK = X(6)/X(6)
      IUR = X(13)/X(6)
      ICRE = X(14)/X(6)
C
C         OSMOSIS OF FLUID ACROSS CELL MEMBRANE
C
      CALL OSMOS
C
C        WRITE RESULTS
C
      IF (K.NE.30) GO TO 60
   53 WRITE (4,70) HOUR,(X(I),I=1,3),CO,AP,X(6),PNA,PK,
     1    TPR,BV,INA,X(11),GFR,X(12),PUR,PCRE,UFL,UNA,X(10)
   70 FORMAT(1X,4(F5.2,1X),F4.2,1X,F5.1,1X,F4.1,1X,F6.2,F4.1,1X,
     1      F5.1,1X,2(F4.1,1X),2(F5.1,1X),2(F5.2,1X),
     2      F5.3,1X,F5.2,1X,F5.3,1X,F5.1)
      K = 0
C
C        TEST FOR END OF TIME
C
   60 IF (T.LE.TT) GO TO 50
      K = 0
      T = 0.0
C
C        WRITE 'END OF PREDICTION TIME'
C
      IF (KA.EQ.1) GO TO 12
      WRITE (4,79)
   79 FORMAT(1H0,6X,18HEND OF PREDICTIONS)
      GO TO 13
   12 WRITE (4,81)
   81 FORMAT(1H0,6X,15HEND OF DIALYSIS)
C
C        TEST FOR REUSE WITH DIFFERENT THERAPY
C
   13 WRITE (4,80)
   80 FORMAT(1H0////6X,32HDO YOU WISH TO CHANGE ANY OF THE,
     1      35H VARIABLES OF THE DIALYSIS THERAPY?//
     2     16H 1.YES. 2.NO.   :)
      READ (4,82) IAC
   82 FORMAT(I1)
      IF (IAC.EQ.1) GO TO 30
```

```
C
C       TEST FOR USE FOR PREDICTION OF PATIENTS STATE AFTER DIALYSIS
C
      WRITE (4,64)
   64 FORMAT(1H0///6X,34HDO YOU WISH TO KNOW THE PREDICTION,
     1     22H OF THE PATIENTS STATE/16H AFTER DIALYSIS?//
     2     16H 1.YES. 2.NO.   :)
      READ (4,62)  IAF
      IF (IAF.EQ.2) GO TO 70
      KA = 0
C
C       ANY CHANGE IN STATE OF PATIEET AFTER DIALYSIS?
C
      WRITE (4,66)
   66  FORMAT(1H0//6X,36HANY ALTERATION IN PATIENTS REMAINING,
     1     17H KIDNEY FUNCTION?/16H 1.YES. 2.NO.   :)
      READ (4,62) IAR
      IF (IAR.EQ.2) GO TO 68
      CALL READFA
C
C       CHANGE IN INGESTION RATES?
C
   68  WRITE (4,69)
   69  FORMAT(1H0//6X,39HINGESTION RATES OF SUBSTANCES TO BE THE/
     1     31H SAME AFTER DIALYSIS AS BEFORE?/
     2     16H 1.YES. 2.NO.   :)
      READ (4,62) IAI
      IF (IAI.EQ.1) GO TO 92
      CALL READIN
C
C       POST-DIALYSIS PREDICTION FOR HOW LONG?
C
   92  WRITE (4,93)
   93  FORMAT(1H0//6X,42HPREDICTION OF VALUES OF VARIABLES UPTO HOW,
     1     17H MANY HOURS AFTER/13H DIALYSIS?  :)
      READ (4,94) TH
   94 FORMAT (F6.1)
      TT = TH + 60.0
C
C
      WRITE (4,21)
   21  FORMAT(1H0//47H THE PREDICTION OF THE VARIABLES AFTER DIALYSIS,
     1     16H IS AS FOLLOWS:-///31H HOURS C TEMP S TEMP ECFV CO   ,
     2     36HAP   ICFV  PNA   PK    TPR  BV   INA  ,
     3     45HALDO  GFR   ADH   UREA  CREA  UFL    UNA  AII)
C
C       GO BACK TO START OF LOOP
C
      GO TO 50
   90  STOP
      END
```

```
      SUBROUTINE CONTRL
      REAL INA,IK,IUR,ICRE,IHF,MSP
      COMMON /DE/ X(50),DX(50),N,T,DT,DTMIN,SBF,RS,KA,FACT1,FACT2
     1    ,FACT3,FACT4,ALS,DK,UNA,UFL,AS,TT,FLUMIN,SODMIN,POTMIN
     2     ,CO,AP,TPR,BV,QFR,FNA,SDTR,ULTRF,SODDIA,POTDIA,ADHS
     3     ,PNA,PK,INA,IK,PUR,PCRE,IUR,ICRE,RB
     4     ,IHF,W,PV
      COMMON /AI/ A1,CONS,APSTDR
C
C     TRS CONTROLLER
C
      IF (X(1).LT.35.0) STPR = 4484.3
      IF (X(1).GE.35.0 .AND. X(1).LT.36.4)
     1   STPR = -2662.8+X(1) +105362.0
      IF (X(1).GE.36.4 .AND. X(1).LT.37.0) GO TO 99
      IF (X(1).GE.37.0 .AND. X(1).LT.38.5)
     1    STPR = -256.2+X(1) + 9927.8
      IF (X(1).GE.38.5) STPR =64.1
      GO TO 100
   99 IF (X(2).LE.34.1) STPR = 17.3+X(2) - 209.8
      IF (X(2).GT.34.1) STPR = 36.9+X(2) - 809.9
  100 SBF = AP/STPR
      TPR = (STPR +20.934) / (STPR + 20.934)
C
C       CVS CONTROLLER
C
C       PRESSOR EFFECT OF ANGIO II
C
      IF (X(10).GE.27.0) GO TO 7
      DTPR = 0.037+X(10)-1.0
      GO TO 8
    7 DTPR = 5.44+ALOG10(X(10)) - 7.8
    8 TPR = TPR + DTPR
      CENA = 1.0
      CEK = 1.0
      IF (PNA.GT.148.0) CENA =-0.0125+PNA + 2.85
      IF (PK.GT.6.5) CEK = -0.065+PK+ 1.43
      CE = (CENA + CEK) + 0.5
      IF (X(3).GE.21.0) GO TO 20
      BV=0.33+X(3)
      GO TO 304
   20 BV=0.0156+X(3)+6.6
  304 PV = 0.6+BV
      MSP = 3.5+BV - 10.5
C  CARDIAC FUNCTION CURVES FOR NORMAL OR HYPOEFFECTIVE HEART
      IF (CE.LE.0.65.AND.CE.GE.0.62) IHF = IHF + 1.0
      IF (CE.LT.0.62) IHF = IHF + 2.0
      IF (IHF.GE.3.0) IHF = 3.0
      IIHF = IHF
      GO TO (501,502,503) IIHF
  501 C1 = 3.0
      C2 = 5.25
      GO TO 505
  502 C1 = 2.5
      C2 = 3.75
      GO TO 505
  503 C1 = 1.7
      C2 = 2.125
  505 C3 = (-1.0/(0.07+TPR))
      C4 = MSP/(0.07+TPR)
```

```
      CO = (C1*C4 - C2*C3)/(C1 -C3)
      RAF = (CO - C2)/C1
      IF (RAF.LE.2.0) GO TO 504
      GO TO (511,512,513) IIHF
  511 C1 = 0.875
      C2 =   9.5
      GO TO 515
  512 C1 = 0.625
      C2 = 7.5
      GO TO 515
  513 C1 = 0.375
      C2 = 4.75
  515 CO = (C1*C4 - C2*C3)/(C1 - C3)
      RAF = (CO - C2)/C1
      IF (RAF.LE.4.0) GO TO 504
      GO TO (521,522,523) IIHF
  521 CO = 13.0
      GO TO 525
  522 CO =  6.75
      GO TO 525
  523 CO = 6.25
  525 RAF = (CO - C4)/C3
  504 AF = CO*TFR
      IF (T.NE.0.0) GO TO 600
      AFCONS = AFSTOR - AF
  600 AF = AF + AFCONS
C
C     KIDNEY FUNCTION
C
      IF (AF.LE.20.0) GFR = 0.0
      IF (AF.LE.75.0.AND.AF.GT.20.0) GFR=1.72*AF-36.4
      IF (AF.LE.120.0.AND.AF.GT.75.0)
     1    GFR = -0.00808*AF**2.0 + 2.195*AF -13.6
      IF (AF.GT.120.0) GFR = 0.035*AF + 127.2
      GFR = GFR * FACT1
      FNA = GFR*FNA/1000.0
C  PROXIMAL REABSORPTION
      GTB = -0.0357*FNA + 5.813
      IF (GTB.GT.1.0) GTB = 1.0
      IF (GTB.LE.0.75) GTB = 0.75
      EFTR = GTB*GFR
      SFTR = GTB*FNA
C    LOOP OF HENLE
      EFLH = GFR -EFTR
      SFLH = FNA - SFTR
      IF (FACT1.GT.0.0)
     1    EBLH = -0.01 + EFLH/FACT1 + 0.65
      IF (FACT1.EQ.0.0) EBLH = 0.0
      ELHR = EBLH + EFLH
      SLHR = 0.8 + SFLH
      EFDT = EFLH - ELHR
      SFDT = SFLH - SLHR
```

```
C       RENIN - ANGIO - ALDO  SECRETION
        IF (FACT1.GT.0.0)
       1      RS = (0.01635 -0.00932*SFDT/FACT1)+FACT2
        IF (FACT1.EQ.0.0) RS = 0.0
        IF (RS.LT.0.0) RS = 0.0
        AS = 1765.0+X(9)+FV/3.06
        IF (X(10).LT.16.0) GO TO 201
        IF (X(10).GE.16.0.AND.X(10).LT.36.0) GO TO 202
        IF (X(10).GE.36.0) GO TO 203
  201   ALS = (3.0*X(10) + 21.64*FK - 55.5)/4.0
        GO TO 204
  202   ALS = (3.0*(4.43*X(10)-61.7) + 21.64*FK-55.5)/4.0
        GO TO 204
  203   ALS = (3.0*(0.76*X(10)+62.5)+ 21.64*FK-55.5)/4.0
  204   IF (ALS.LT.0.0) ALS = 0.0
C     SODIUM EXCRETION
        IF (X(11).LE.0.0) SDTR = 0.6 * SFDT
        IF (X(11).GT.0.0.AND.X(11).LE.65.0)
       1    SDTR =(0.003*X(11) + 0.596) * SFDT
        IF (X(11).GT.65.0.AND.X(11).LE.600.0)
       1    SDTR =(0.00021*X(11) + 0.633)* SFDT
        IF (X(11).GT.600.0) SDTR = SFDT
        UNA = SFDT - SDTR
C     A.D.H. RELEASE
        POS = PNA*2.11
        DWV = X(3) - 15.0
        IF (POS.GE.299.5) ADHSP = 0.346*POS -103.43
        IF (POS.LT.299.5) ADHSP = 0.0265*POS - 8.04
        IF (ADHSP.LT.0.0) ADHSP = 0.0
        IF (DWV.GE.1.6) ADHSV = 0.0
        IF (DWV.LT.1.6.AND.DWV.GE.1.0)
       1      ADHSV =(-0.063*DWV + 0.15)
        IF (DWV.LT.1.0.AND.DWV.GE.-1.2)
       1      ADHSV =(-0.75*DWV + 0.613)
        IF (DWV.LT.-1.2) ADHSV = 1.71
        IF (POS.GT.299.62.AND.DWV.GE.1.0) GO TO 560
        ADHS = (ADHSP + ADHSV) * 0.5
        GO TO 34
  560   IF (DWV.GE.2.0) GO TO 570
        ADHS = ((33.0*DWV-32.0) * ADHSV + ADHSP)
       1      / ((33.0*DWV-32.0) + 1.0)
        GO TO 34
  570   ADHS = (DWV*17.0*ADHSV + ADHSP)/(DWV*17.0 + 1.0)
C     FLUID EXCRETION
   34   IF (X(12).LE.0.756) EDOT = 0.0
        IF (X(12).GT.0.765.AND.X(12).LE.3.0)
       1   EDOT = 0.363* X(12) - 0.273
        IF (X(12).GT.3.0.AND.X(12).LE.5.0)
       1   EDOT = -0.0363*X(12)**2.0 + 0.364*X(12) + 0.109
        IF (X(12).GT.5.0) EDOT = 0.0012*X(12) + 0.9653
        EDTR = EDOT * EFDT
        UFL = EFDT - EDTR
C        EXCRETION  OF  POTASSIUM
        IF(X(11).LE.65.0) UKAL = (0.00026*X(11) + 0.0062)
        IF (X(11).GT.65.0) UKAL = (0.00009*X(11) + 0.0224)
        UKH = (0.107 * FK - 0.505)
        UK = (UKAL + UKH) * FACT3
        IF (UK.LE.0.0) UK = 0.0
        RETURN
        END
```

```
      SUBROUTINE INTEGR(EREL,ERAB,ND)
      REAL K1
      DIMENSION K1(50),XS(50),XZ(50),OLD(50)
      COMMON /DE/ X(50),DX(50),N,T,DT,DTMIN,SBF,RS,KA,FACT1,FACT2
     1     ,FACT3,FACT4,ALS,DK,UNA,UFL,AS,TT,FLUMIN,SDOMIN,POTMIN
     2      ,CO,AF,TPR,BV,OFR,FNA,SDTR,ULTRF,SDODIA,POTDIA,ADHS
     3      ,FNA,FK,INA,IK,PUR,PCRE,IUR,ICRE,RB
     4     ,IHF,W,FV
      DO 60 I=1,N
60    XS(I)=X(I)
      TO=T
      N1=1
      ND=MAXO(1,ND/4)
      H=DT/FLOAT(ND)
5     DO 2 J=1,ND
      CALL MODEL
      DO 10 I=1,N
10    XZ(I)=X(I)
      T=T+0.5*H
      DO 20 I=1,N
      K1(I)=DX(I)
      CALL MODEL
20    X(I)=XZ(I)+0.5*K1(I)*H
      DO 30 I=1,N
      K1(I)=DX(I)*2.0+K1(I)
30    X(I)=XZ(I)+0.5*DX(I)*H
      CALL MODEL
      DO 40 I=1,N
      K1(I)=DX(I)*2.0+K1(I)
40    X(I)=XZ(I)+DX(I)*H
      T=T+0.5*H
      CALL MODEL
      DO 2 I=1,N
      DX(I)=(DX(I)+K1(I))/6.0
2     X(I)=XZ(I)+DX(I)*H
      IF(N1.EQ.1)GO TO 3
      DO 50 I=1,N
      IF(ABS(OLD(I)-X(I)).GT.(ABS(EREL*X(I))+ERAB)) GO TO 3
50    CONTINUE
      GO TO 4
3     H=H*0.5
      IF(H.LT.DTMIN) GO TO 6
      DO 70 I=1,N
      OLD(I)=X(I)
70    X(I)=XS(I)
      N1=0
      T=TO
      ND=ND*2
      GO TO 5
6     WRITE(4,7)T
7     FORMAT(27H CONVERGENCE FAILURE AT T = ,F10.4)
4     RETURN
      END
```

```
      SUBROUTINE MODEL
      REAL INA,IK,IUR,ICRE
      COMMON /DE/ X(50),DX(50),N,T,DT,DTMIN,SBF,RS,KA,FACT1,FACT2
     1    ,FACT3,FACT4,ALS,DK,UNA,UFL,AS,TT,FLUMIN,SODMIN,POTMIN
     2     ,CO,AF,TPR,BV,GFR,FNA,SDTR,ULTRF,SODDIA,POTDIA,ADHS
     3     ,PNA,PK,INA,IK,PUR,PCRE,IUR,ICRE,RB
     4    ,IHF,W,PV
C
C     TRS MODEL
C
      DX(1)=(1366.0-405.6+(X(1)-X(2))-SBF+920.0+(X(1)-X(2))
     1      )/(766.7606 +W)
      DX(2)=(405.6+(X(1)-X(2))+SBF+920.0+(X(1)-X(2))
     1      -120.2+(X(2)-22.0)-127.6)/(42.6761+W)
      IF(KA.EQ.1) GO TO 10
C
C     CVS MODEL, UREA AND CREATININE
C
      DX(3)=(FLUMIN-UFL)/1000.0
      DX(4)=(SODMIN-UNA)
      DX(5)=(POTMIN- UK)
      DX(6)=0.0
      DX(15)=(0.7+(IUR-PUR)-0.139+FACT4+PUR)
      DX(16)=(0.4+(ICRE-PCRE)-0.0139+FACT4+PCRE)
      GO  TO 101
C
C      CVS MODEL, UREA AND CREATININE, MACHINE ON
C
   10 DX(3)=(FLUMIN-UFL-ULTRF)/1000.0
      DX(4)=(RB+(PNA-SODDIA)+(EXP(-0.150/RB)-1.0))
     1      +(SODMIN - UNA)
      DX(5)=(RB+( PK-POTDIA)+(EXP(-0.075/RB)-1.0))
     1      +(POTMIN - UK)
      DX(6)=0.0
      DX(15)=(RB+PUR+(EXP(-0.105/RB)-1.0)
     1    +0.7+(IUR-PUR)-0.139+PUR+FACT4)
      DX(16)=(RB+PCRE+(EXP(-0.090/RB)-1.0)
     1    +0.4+(ICRE-PCRE)-0.0139+PCRE+FACT4)
C
C       INTRACELLULAR SODIUM, POTASSIUM, UREA AND CREATININE
C
  101 DX(7)=0.0
      DX(8)=0.0
      DX(13)=(0.0064-0.7+(IUR-PUR))
      DX(14)=(0.00014-0.4+(ICRE-PCRE))
C
C      RENIN - ANGIO - ALDO AND A.D.H.  BALANCE
C
      DX(9) = (RS - 0.135+X(9))/PV
      DX(10)= (AS - 4.04+X(10))/PV
      DX(11) = (ALS - 0.62+X(11))/PV
      IF (X(12).LE.4.0)
     1   DADH = - 0.042+X(12) + 0.374
      IF (X(12).GT.4.0) DADH = 0.206
      DX(12) = (ADHS - DADH+X(12))/PV
      RETURN
      END
```

```
      SUBROUTINE READFA
      REAL IHF
       COMMON /DE/ X(50),DX(50),N,T,DT,DTMIN,SBF,RS,KA,FACT1,FACT2
     1    ,FACT3,FACT4,ALS,UK,UNA,UFL,AS,TT,FLUMIN,SODMIN,POTMIN
     2     ,CO,AP,TPR,BV,GFR,FNA,SDTR,ULTRF,SODDIA,POTDIA,ADHS
     3     ,PNA,PK,INA,IK,PUR,PCRE,IUR,ICRE,QB
     4   ,IHF,W
       WRITE (4,10)
   10 FORMAT(1H0///6X,36HTHE PATIENT IS SUFFERRING FROM RENAL,
     1    29H FAILURE. THE SYSTEM REQUIRES/19H INFORMATION ON THE,
     2    34H EXTENT TO WHICH THE NORMAL KIDNEY FUNCTIONS HAVE BEEN/
     3    10H IMPAIRED.//4X,31HHOW MUCH OF THE KIDNEY FUNCTION,
     4    44H TO EXCRETE SODIUM AND WATER REMAINS INTACT?)
   20 FORMAT (F4.2)
       READ (4,20) FACT1
       WRITE (4,30)
   30 FORMAT(1H0,4X,42HHOW MUCH OF THE KIDNEY FUNCTION TO SECRETE,
     1    22H RENIN REMAINS INTACT?)
       READ (4,20)FACT2
       WRITE (4,70)
   70 FORMAT(1H0,4X,42HHOW MUCH OF THE KIDNEY FUNCTION TO EXCRETE,
     1    26H POTASSIUM REMAINS INTACT?)
       READ (4,20) FACT3
       WRITE (4,90)
   90 FORMAT(1H0,4X,34HHOW MUCH OF THE KIDNEY FUNCTION TO,
     1    44H EXCRETE UREA AND CREATININE REMAINS INTACT?)
       READ (4,20)FACT4
   22 FORMAT  (F3.1)
       WRITE (4,140)
  140 FORMAT (1H0,4X,36H IS HEART PUMPING ABILITY DECREASED?/
     1    26H 1.NO. 2.BY 25%. 3.BY 50%. :)
       READ(4,22)IHF
       WRITE (4,150)
  150 FORMAT (1H0,4X,27H WEIGHT OF PATIENT IN KGS.:)
       READ(4,20) W
       RETURN
       END
```

```
      SUBROUTINE READIN
      COMMON /DE/ X(30),DX(30),N,T,DT,DTMIN,SBF,RS,KA,FACT1,FACT2,
     1     FACT3,FACT4,ALS,UK,UNA,UFL,AS,TT,FLUMIN,SODMIN,POTMIN
     2     ,CO,AF,TPR,BV,GFR,FNA,SDTR,ULTRF,SODDIA,POTDIA,ADHS
     3     ,PNA,PK,INA,IK,PUR,PCRE,IUR,ICRE,RB
     4  ,IHF,W
       WRITE (4,10)
   10 FORMAT(1H0///6X,37HTHE SYSTEM WILL NOW ASK FOR THE DAILY,
     1    19H INGESTION RATES OF/30H SUBSTANCES IN THE DIET OF THE,
     2    9H PATIENT.//4X,35HHOW MUCH FLUID HAS THE PATIENT BEEN,
     3    31H TAKING IN MILLILITRES PER DAY?)
   20 FORMAT (F7.1)
      READ (4,20) FLUDIN
      WRITE (4,30)
   30  FORMAT(1H0,4X,44HHOW MUCH SODIUM IN MILLIEQUIVALENTS PER DAY?)
      READ (4,20) SODIN
      WRITE (4,40)
   40 FORMAT(1H0,4X,36HHOW MUCH POTASSIUM IN MILLIEQUIVALENTS,
     1    9H PER DAY?)
      READ (4,20) PODIN
      FLUMIN = FLUDIN/(60.0*24.0)
      SODMIN = SODIN/(60.0*24.0)
      POTMIN = PODIN/(60.0*24.0)
      RETURN
      END
```

```
      SUBROUTINE READIC
      REAL INA,IK,IUR,ICRE
      COMMON /DE/ X(50),DX(50),N,T,DT,DTMIN,SBF,RS,KA,FACT1,FACT2
     1    ,FACT3,FACT4,ALS,UK,UNA,UFL,AS,TT,FLUMIN,SODMIN,POTMIN
     2     ,CO,AP,TPR,BV,GFR,FNA,SDTR,ULTRF,SODDIA,POTDIA,ADHS
     3     ,PNA,PK,INA,IK,PUR,PCRE,IUR,ICRE,RB
     4  ,IHF,W
      COMMON/AI/A1,CONS
      WRITE (4,10)
   10 FORMAT(1H0///6X,42HTHE MODEL REQUIRES INITIAL VALUES TO START,
     1    6H IT OFF.//25H TYPE CORE TEMPERATURE  :)
   20 FORMAT (F6.3)
      READ (4,20) X(1)
      WRITE (4,30)
   30 FORMAT(1X,24HTYPE SKIN TEMPERATURE  :)
      READ (4,20) X(2)
      WRITE (4,40)
   40 FORMAT(1X,34HTYPE EXTRACELLULAR FLUID VOLUME  :)
      READ (4,20) X(3)
      WRITE (4,50)
   50 FORMAT(1X,35HTYPE PLASMA SODIUM CONCENTRATION  :)
      READ (4,20) PNA
      WRITE (4,60)
   60 FORMAT(1X,36HTYPE PLASMA POTASSIUM CONCENTRATION  :)
      READ (4,20)PK
      WRITE (4,70)
   70 FORMAT(1X,34HTYPE INTRACELLULAR FLUID VOLUME  :)
      READ (4,20) X(6)
      WRITE (4,80)
   80 FORMAT(1X,42HTYPE INTRACELLULAR SODIUM CONCENTRATION  :)
      READ (4,20) INA
      WRITE (4,90)
   90 FORMAT(1X,43HTYPE INTRACELLULAR POTASSIUM CONCENTRATION  :)
      READ (4,20) IK
      WRITE (4,91)
   91 FORMAT(1X,27HTYPE RENIN CONCENTRATION  :)
      READ (4,20) X(9)
      WRITE (4,92)
   92 FORMAT(1X,36HTYPE ANGIOTENSIN II CONCENTRATION  :)
      READ (4,20) X(10)
      WRITE (4,93)
   93 FORMAT(1X,33HTYPE ALDOSTERONE CONCENTRATION  :)
      READ (4,20) X(11)
      WRITE (4,94)
   94 FORMAT(1X,25HTYPE ARTERIAL PRESSURE  :)
      READ(4,20) AP
      WRITE (4,95)
   95 FORMAT(1X,26HTYPE A.D.H. CONCENTRATION  :)
      READ (4,20) X(12)
      WRITE (4,96)
   96 FORMAT(1X,26HTYPE UREA CONCENTRATION  :)
      READ (4,20) PUR
      IUR =PUR
      CONS = PNA + PK - INA - IK - 5.0
      WRITE (4,97)
   97 FORMAT(1X,32HTYPE CREATININE CONCENTRATION  :)
      READ (4,20) PCRE
      ICRE = PCRE
      WRITE (4,98) CONS
   98 FORMAT(1X,47HCONSTANT FACTOR FOR INTRACELLULAR-EXTRACELLULAR,
     2    16H EQUILIBRIUM IS  :,F7.2)
      RETURN
      END
```

```
      SUBROUTINE READTH
      COMMON /DE/ X(30),DX(30),N,T,DT,DTMIN,SBF,RS,KA,FACT1,FACT2
     1     ,FACT3,FACT4,ALS,UK,UNA,UFL,AS,TT,FLUMIN,SODMIN,POTMIN
     2      ,CO,AF,TPR,BV,QFR,FNA,SDTR,ULTRF,SODDIA,POTDIA,ADHS
     3      ,PNA,PK,INA,IK,PUR,PCRE,IUR,ICRE,QB
     4   ,IHF,W
      WRITE (4,10)
   10 FORMAT(1H0///6X,
     1     16H SYSTEM REQUIRES/36H INFORMATION CONCERNING THE PROPOSED
     2     9H THERAPY.//36H TYPE CONCENTRATION OF SODIUM IN THE,
     3     13H DIALYSATE  :)
   15 FORMAT (F7.2)
      READ (4,15) SODDIA
      WRITE (4,20)
   20 FORMAT(1X,31HTYPE CONCENTRATION OF POTASSIUM IN THE DIALYSATE
      READ (4,15) POTDIA
      WRITE (4,30)
   30 FORMAT(1X,45HTYPE PROPOSED TIME IN MINUTES FOR DIALYSIS  :)
      READ (4,15) TT
      WRITE (4,60)
   60 FORMAT(1X,26HTYPE POST COIL PRESSURE  :)
      READ (4,15) PCPR
      IF (PCPR.GE.100.0) GO TO 61
      ULTRF = 0.013667 * PCPR + 0.6944
      GO TO 62
   61 ULTRF = 0.04167 * PCPR - 2.0833
   62 WRITE (4,130)
  130 FORMAT(1X,41H TYPE BLOOD FLOW RATE THROUGH MACHINE IN ,
     1     10HMLS/MIN  :)
      READ (4,15) QBM
      QB = QBM/1000.0
      WRITE (4,200)
  200 FORMAT(1H0//48H THE PREDICTION OF THE VARIABLES DURING DIALYSIS
     1     16H IS AS FOLLOWS:-///33H HOURS  C TEMP  S TEMP  ECFV  CO   AF,
     2     34H   ICFV  PNA    PK   TPR   BV  INA
     3     47H  ALBO  QFR   ADH   UREA  CREA  UFL    UNA  AII)
      RETURN
      END
```

```
      SUBROUTINE OSMOS
      REAL INA,IK
      COMMON /DE/ X(50),DX(50),N,T,DT,DTMIN,SSF,RS,KA,FACT1,FACT2
     1     ,FACT3,FACT4,ALS,UK,UNA,UFL,AS,TT,FLUMIN,SDOMIN,FOTMIN
     2      ,CO,AF,TFR,BV,GFR,FNA,SDTR,ULTRF,SDDDIA,FDTDIA,ADHS
     3      ,PNA,PK,INA,IK,FUR,FCRE,IUR,ICRE,RB
     4      ,IHF,W,FV
      COMMON /AI/ A1,CONS,APSTOR
C
C       OSMOSIS OF FLUID ACROSS CELL MEMBRANE
C
      OSME = PNA + PK + 156.2 - CONS/2.0
      OSMI = INA + IK + 161.2 + CONS/2.0
      TBW = X(3) + X(6)
      TOSM = X(3)*OSME + X(6)*OSMI
      TCONC = TOSM/TBW
      X(3) = X(3)*OSME/TCONC
      X(6) = X(6)*OSMI/TCONC
      PNA = PNA * TCONC/OSME
      PK = PK * TCONC/OSME
      INA=INA*TCONC/OSMI
      IK = IK*TCONC/OSMI
      RETURN
      END
```

```
      BLOCK DATA
      COMMON /DE/ X(50),DX(50),N,T,DT,DTMIN,SSF,RS,KA,FACT1,FACT2
     1     ,FACT3,FACT4,ALS,UK,UNA,UFL,AS,TT,FLUMIN,SDOMIN,FOTMIN
     2      ,CO,AF,TFR,BV,GFR,FNA,SDTR,ULTRF,SDDDIA,FDTDIA,ADHS
     3      ,PNA,PK,INA,IK,FUR,FCRE,IUR,ICRE,RB
     4      ,IHF,W,FV
      DATA N,T,DT/16,0.0,1.0/
      END
```